Coordination scientifique
Robert JOUMARD

Transports et pollution de l'air
Transport and Air Pollution

12e colloque / *12th Symposium*
Avignon, 16-18 juin / *June* 2003

Actes INRETS n°92 - Vol. 1
Juin 2003

Coordinateur scientifique / *editor*:

Robert JOUMARD est directeur de recherche au Laboratoire Transports et Environnement (LTE)
Robert JOUMARD is a Senior Researcher at the Laboratory Transport and Environment (LTE)

L'unité de recherche :

LTE : Laboratoire Transports et Environnement, INRETS, case 24, 69675 Bron cedex, France
Téléphone : +33 (0)4 72 14 23 00 - Télécopie : +33 (0)4 72 37 68 37
Email : joumard@inrets.fr

Comité scientifique / *Scientific Committee*:

Michel	André	INRETS, F
Richard	Ballaman	OFEFP, CH
Kevin	Bennett	Univ. Cape Town, SA
Mireille	Chiron	INRETS, F
Walter F.	Dabberdt	Vaisala, USA
Asif	Faiz	The World Bank, Nepal
Alan W.	Gertler	Desert Research Inst., USA
Ron	Hamilton	Middlesex Univ., UK
Robert	Joumard	INRETS, F
Sasha	Madronich	NCAR, USA
Tamás	Merétei	KTI, H
Patrice	Mestayer	École Centrale de Nantes, F
Suzana K.	Ribeiro	Federal Univ. Rio de Janeiro, BR
Christian	Sacré	CSTB, F
Zissis	Samaras	Lab. Applied Thermodynamics, GR
Johannes	Staehelin	ETH Zurich, CH
Peter	Sturm	Technical Univ. Graz, A

N°ISBN : 2-85782-588-9 N°ISSN : 0769-0266

© Les collections de l'INRETS
PRIX : 15,24 € TTC (TVA 5,5 %)

Les commandes doivent être adressées à l'INRETS - services publications - 2, av. du Général Malleret-Joinville - 94114 ARCUEIL CEDEX, et être accompagnées d'un chèque bancaire ou postal à l'ordre de : l'Agent Comptable de l'INRETS. Déduire la TVA pour l'étranger hors Union Européenne. Pour les pays de l'Union Européenne se reporter à la réglementation intercommunautaire en matière de TVA.

Fiche bibliographique

1 UR (1er auteur) INRETS-LTE		2 Projet n°	3 Actes INRETS n°92 - vol. 1
4 Titre 12e colloque "Transports et pollution de l'air"			
5 Sous-titre			6 Langue F/E
7 Auteur(s) JOUMARD Robert			8 Rattachement ext.
9 Nom adresse financeur, co-éditeur			10 N° contrat, conv.
			11 Date de publication juin 2003
12 Remarques			
13 Résumé Ces actes du 12e colloque organisé par l'INRETS, l'Université de Graz et le National Center for Atmospheric Research à Avignon du 16 au 18 juin 2003 regroupent les communications orales (tome 1) ou sous forme d'affiches (tome 2) sur des sujets aussi variés et complémentaires que les mesures de la qualité de l'air, les effets sur la santé, les modèles de dispersion physico-chimiques, les émissions unitaires, les inventaires d'émissions, les émissions des transports non-routiers, les coûts externes, les nouveaux carburants et technologies véhicule, la gestion des transports urbains, et les politiques de transport.			
14 Mots clés Transports, pollution atmosphérique, impacts, santé, modèles, émissions, technologie, politique de transport		15 Diffusion libre	
16 Nombre de pages 240	17 Prix 15,24 €	18 Confidentiel jusqu'au	19 Bibliographie oui

Publication data form

1 Unit (1st author) INRETS-LTE	2 Project n°	3 INRETS proceedings n°92 - vol. 1
4 Title 12th Symposium "Transport and Air Pollution"		
5 Subtitle		6 Language E / F
7 Author(s) JOUMARD Robert		8 Affiliation INRETS
9 Sponsor, co-editor, name and address		10 Contract, conv. n° 11 Publication date June 2003
12 Notes		

13 Summary

These proceedings of the the 12th symposium organised by INRETS, the Technical University of Graz and the National Center for Atmospheric Research in Avignon from 16 to 18 June, 2003, include the oral communications (Vol. 1) and posters (Vol. 2) presented and cover a great variety of items such as air quality measurements, health effects, physico-chemical dispersion models, unit emissions, emission inventories, non-road transport emissions, external costs, new fuels and vehicle technologies, urban traffic management, and transport policies.

14 Key Words Transport, atmospheric pollution, impacts, health effect, models, emissions, technology, transport policies		15 Distribution statement free	
16 Nb of pages 240	17 Price 15.24 €	18 Declassification date	19 Bibliography yes

Table des matières / *Content*

Introduction 7

Fine particulate (PM2.5 - PM1) at urban sites with different traffic exposure 9
M. Giugliano, G. Lonati, P. Butelli, L. Romele & R. Tardivo - Politecnico Milano (I)

Dispersion de la pollution à la sortie d'un tunnel autoroutier urbain 19
G. Goupil, R. Alary, C. Bugajny, C. Ribière, B. Brousse & B. Vidal - LCPP, Cetu (F)

Establishing an air pollution monitoring network for intra-urban population exposure assessment: a location-allocation approach 27
P.S. Kanaroglou, M. Jerrett, J. Morrison, B. Beckerman, M.A. Arain, N.L. Gilbert & J. Brook - McMaster Univ., Carleton Univ., Health Canada, Met. Sce Canada (CDN)

A study of trace metal concentration of urban airborne particulate matter and its role in free radical activity as measured by plasmid strand break assay 35
JJN. Lingard, A.S. Tomlin, A.G. Clarke, K. Healey, AWM. Hay, CP. Wild & MN. Routledge - Univ. Leeds (UK)

Distribution de l'exposition de la population urbaine à des polluants particulaires et gazeux génotoxiques et évaluation du risque de cancer - Étude GENOTOX'ER 43
É. Nerrière, D. Zmirou-Navier, O. Blanchard, I. Momas, Y. Le Moullec, J. Ladner, H. Guegan & M. Joyeux - IVS, Inserm, Ineris, Univ. Paris 5, LHVP, CHU Rouen, CENBG (F)

Effect of Vehicle Characteristics on Unpaved Road Dust Emissions 51
J.A. Gillies, V. Etyemezian , H. Kuhns, D. Nikolic & D.A. Gillette - DRI & NOAA (USA)

Chemical Characterization of Emissions from Advanced Technology Light Duty Vehicles 59
L. Graham - Environment Canada (CDN)

Vehicle Emissions of Speciated Carbonyls 67
D. Grosjean - DGA Inc. (USA)

Modelling vehicles kinematics relevance in network based urban emissions inventories 73
E. Negrenti & A. Parenti - Enea & Astran (I)

Conditions de fonctionnement des autobus parisiens en exploitation pour l'évaluation des émissions polluantes 81
M. André, B. Garrot, Y. Roynard, R. Vidon, P. Tassel & P. Perret - Inrets, RATP (F)

The dispersion of a traffic-related pollutant in two urban street canyons 89
J.W.D. Boddy, R. J. Smalley, J.E. Tate & A. S. Tomlin - Univ. Leeds (UK)

Influence of Gotthard Tunnel Shutdown on Aerosol, Nitrogen Oxide and Carbon Monoxide Concentrations in Alpine Valleys 97
A.S.H. Prevot, J. Thudium, S. Henne, J. Dommen, N. Bukowiecki & U. Baltensperger - PSI, Oekoscience (CH)

Air pollution mapping : relationship between satellite- made observations and air quality parameters 105
A. Ung, L. Wald, T. Ranchin, C. Weber, J. Hirsch, G. Perron & J. Kleinpeter - Univ. Pasteur, ENSMP, Univ. Strasbourg, ASPA (F)

Impact of Ecodriving on Emissions 113
H. Johansson, P. Gustafsson, M. Henke & M. Rosengren - TFK, SNRA, MTC AB (S)

Measurements and Analysis of Real-World Driving Behavior of Urban Buses 121
L. Tartakovsky, Y. Zvirin, M. Motzkau, M. Van Poppel, I. Riemersma, M. Veinblat, V. Baybikov, Y. Aleinikov & M. Gutman – Technion, RWTÜV, Vito, TNO (Israel, D, B, NL)

Regulated and nonregulated diesel and gasoline cold start emissions at different temperatures 129
M. Weilenmann, P. Soltic, C. Saxer, A.-M. Forss & N. Heeb - EMPA (CH)

Towards accurate instantaneous emission models 137
D. Ajtay, M. Weilenmann & P. Soltic - EMPA (CH)

PM regulation for 2-Stroke two-wheelers: Necessity or haphazard legislation? 145
R. Rijkeboer, D.A. Bremmers, Z. Samaras & L. Ntziachristos - TNO (NL), Aristotle Univ. (GR)

N2O-emissions of LD and HD vehicles 153
I. Riemersma, R. Vermeulen, R. Gense & R. Smokers - TNO Automotive (NL)

Towards meaningful real-world emissions factors for motorcycles: An evaluation of several recent TNO projects 161
R. Gense & D. Elst - TNO Automotive (NL)

Statistical analysis of road tunnel studies performed in the EU-project ARTEMIS 169
J. Staehelin, C. San Giorgio, B. Tona, G. Catone, W. K. Stahel, C. Colberg & P. Sturm - ETH (CH), TUG (A)

The Importance of the Road Transport Sector in the Global Warming - the Case of the City of Rio de Janeiro 177
L. B. Rego de Mattos & S.K. Ribeiro - Fed. Univ. Rio de Janeiro (BR)

Diesel vs. Gasoline Emissions: Does PM from Diesel or Gasoline Dominate in the U.S.? 185
A.W. Gertler - DRI (USA)

Transport and Environment Database System (TRENDS): Maritime Air Pollutant Emission Modelling 193
A. Georgakaki, R.A. Coffey, G. Lock & S.C. Sorenson - DTU (DK), Eurostat (L)

Estimation of the Cost due to Air Pollution of Transport in Sweden. 201
L. Nerhagen & H. Johansson - TFK, VTI (S)

10 ans de monétarisation des effets locaux de la pollution atmosphérique : des évaluations scientifiques aux décisions politiques 209
JP. Nicolas, F. Duprez, S. Durand, F. Poisson, PL. Aubert, M. Chiron, Y. Crozet & J. Lambert - LET, Inrets, Certu (F)

Real Life Evaluation of the Emission Reduction Potential of a City Bus Retrofitted with a Continuous Regenerating Trap 217
G. Lenaers & M. Van Poppel - Vito (B)

Transport Policies in Relation to Congestion and Air Quality in Seven European Cities 225
M. Haakana, M. Kauhaniemi, J. Kukkonen, S. Sihto, S. Neville, I. Myrtveit, B. Martin, P. Boulter, P. Segaar, T. Maggos, J. Bartzis, L. Luhana & R. S. Sokhi - FMI, YTV (FIN), Westminster (UK), ODPH (N), SICE (E), Utrecht (NL), NCSR Democritos (GR), TRL, Univ. Hertfordshire (UK)

Les enjeux de la pollution de l'air des transports 233
R. Joumard - Inrets (F)

Introduction

Robert Joumard

Ce douzième colloque, dans la lignée de ceux organisés depuis 1986 à Avignon, à Graz en Autriche et à Boulder aux États-Unis a pour objectif d'établir un bilan des connaissances scientifiques sur la pollution de l'air liée aux transports. Tous les modes de transports sont couverts (route, fer, air, mer), ainsi que l'ensemble des impacts de la pollution de l'air sur l'environnement. Les thèmes suivants sont traités :

- impacts de la pollution de l'air : études biologiques ou épidémiologiques des effets sur la santé des différents polluants, enquêtes sur la pollution sensible (odeurs, fumées, salissures), évolution des effets sur les écosystèmes, responsabilité des différentes sources, modèles de dispersion en zones urbaines et rurales, modèles physico-chimiques, qualité de l'air, ...
- émissions de polluants : caractéristiques des trafics, mobilité, comportements, émissions unitaires des moteurs et des véhicules, inventaires d'émissions des différents modes de transports aux niveaux local, régional et global, ...
- moyens de contrôle et de réduction : coûts externes, évolution des carburants, des moteurs, gestion des transports urbains, politiques de transport, réglementation, ...

Following the meetings held since 1986 in Avignon, Graz, Austria and Boulder, USA, this 12th symposium is aimed at assessing scientific knowledge in the field of air pollution due to transport. All transport modes are studied (road, railways, air, sea), as well as the effects of air pollution on the environment (health effects, dispersion, acid rain, greenhouse effect, etc...). The scope is:

- *Effects of air pollution: biological and epidemiological studies of different pollutants, surveys relating to perceived pollution (odours, fumes, soiling), effects on the ecosystems, part played by the different pollution sources, dispersion models in urban and rural areas, physico-chemical models, air quality, etc...*
- *Pollutant emissions: traffic characteristics, mobility, unit emissions for engines and vehicles, emission inventories for various transport modes at a local, regional, global scale, etc...*
- *Control and reduction methods: external costs, evolution of fuel and engine development, urban traffic management, transport policies, regulations, etc...*

12th International Symposium "Transport and Air Pollution" / 12e Colloque international "Transports et pollution de l'air", Avignon, 16 -18 *June* / juin 2003
proceedings / actes, n°92, tome / Vol. 1, Inrets ed., Arcueil, France, 2003, p. 9-17

Fine particulate ($PM_{2.5}$ - PM_1) at urban sites with different traffic exposure

Michele Giugliano, Giovanni Lonati, Paola Butelli, Laura Romele, Ruggero Tardivo
Dipartimento di Ingegneria Idraulica, Ambientale, Infrastrutture viarie, Rilevamento
Sezione Ambientale
Politecnico di Milano - P.zza L. da Vinci, 32 - 20133 Milano - Italy
Fax +39 02 23 99 64 99 - email: giovanni.lonati@polimi.it

Abstract
Fine particulate concentration data resulting from several monitoring campaigns performed in Milan at urban sites with different exposure to the emission sources are presented. Low volume $PM_{2.5}$ and PM_1 samplers are utilised together with a low volume optical analyser, enabling the intercomparison between the measurements obtained by the gravimetrical and the optical method. The concentration levels observed at the different sites are compared in order to point out intra-site seasonal differences and the inter-site differences for corresponding seasons of the year. These different concentration levels are analysed and explained considering the exposure to the primary emissions and accounting for the role of meteorology. PM_{10}, $PM_{2.5}$ and PM_1 are described in terms of the distribution of 1-hour concentration data and their relative mass fractions are determined.
Keys-words*: fine particulate, gravimetric measurements, optical measurements, urban area, traffic.*

Résumé
Dans cet article, les résultats de la surveillance des particules atmosphériques pour différents sites à Milan sont présentés. Deux capteurs de poussières pour $PM_{2.5}$ and PM_1 et un analyseur optique ont été utilisés. Les concentrations observées aux points de mesure ont été confrontées et la variabilité saisonnière dans chacun pointe a été evaluée. Les résultats ont été interpretés selon l'exposition des points de mesure au trafic vehiculaire, compte tenu des effects de la météorologie.
Mots-clefs : *poussières fines, analyseur gravimétrique, analyseur optique, zone urbaine, trafic.*

Introduction

Atmospheric pollution due to airborne fine particles is an environmental issue of increasing concern in Lombardy, Italy's most industrialised region, and in particular in the metropolitan area of Milan. The long-term (40 μg m^{-3} as annual average concentration) and short-term (no more than 35 exceedances per year of 50 μg m^{-3} for the daily average) standard for PM_{10} established by EU Directive (EU, 1999) are both largely not attained: out of the 40 stations of the regional air quality monitoring network operating in Lombardy during 2001, the long-term standard was not respected at 19 sites and the short-term standard at 37 sites. Warning episodes, as defined by the regional authorities (daily average concentrations simultaneously exceeding 50 μg m^{-3} at 2 or more monitoring sites of the area), frequently occur during the winter period. Moreover, the processes of secondary photochemical production of fine particles seem to play a significant role during summertime, when peak concentration events are observed too. The apportionment of the contribution of the stationary sources, mainly domestic heating, and of the mobile sources has a very important role for the definition of long-term control strategies and of the interventions to be taken when the warning episodes occur. These latter almost exclusively consist in the restriction of the circulation for some categories of vehicles during weekdays and in the prohibition of the circulation extended to all vehicles on Sundays. In order to asses the contribution of traffic to the observed concentration levels of fine particulate, several monitoring campaigns have been performed at 4

urban sites characterised by different exposure to the traffic sources: an urban background site, 2 kerbside sites and a tunnel site, all located in the city of Milan. A $PM_{2.5}$ and a PM_1 low volume sampler together with a low volume optical analyser have been simultaneously utilised during all the campaigns, which took place in spring, autumn and in the summer holiday period in August. Particulate matter samples obtained by the $PM_{2.5}$ and PM_1 samplers have been analysed for mass concentrations, allowing the intercomparison between the gravimetrical measurements and those performed by the optical analyser. The observed intra-site seasonal differences of concentration levels, as well as the inter-site differences for corresponding seasons of the year, have been explained considering the exposure to the primary emissions and accounting for the role of meteorology. The mass contribution of both $PM_{2.5}$ and PM_1 to PM_{10} concentration levels are evaluated and the distributions of PM_{10}, $PM_{2.5}$ and PM_1 concentration data are analysed.

1 – Methods

Monitoring sites

The monitoring campaigns have been performed between April 2001 and December 2002 at 4 sites in the city of Milan characterised by a different exposure to the mobile sources. A short description of each site and of its exposure to the traffic emissions, the duration and the period when the campaigns took place are reported in Table 1.

Site	Site Description	Site exposure to traffic	Monitoring campaign period and duration
UB	Urban background site in the city centre.	Not directly exposed to traffic emission since located in a walled yard	Spring: 18 days Summer: 40 days Autumn: 16 days
KR	Kerbside site in a residential area	Directly exposed to traffic emissions of a two-way, single carriageway street	Spring: 6 days Autumn: 8days
KS	Kerbside site in a suburban area	Directly exposed to traffic emissions of a two-way, double carriageway main street entering the city	Spring: 16 days
TU	Tunnel site in the city centre	Directly exposed to traffic emissions in a two-way, double carriageway tunnel	Autumn: 5 days

Table 1: Monitoring sites description

Tableau 1: Description des sites de mesure.

At the 2 kerbside sites the instruments were located immediately beside the pavement, while at the TU site they were located in the traffic divider half-way the 250 m long tunnel. At both the ends of the tunnel there are traffic lights that frequently cause queues of idling vehicles.

Instruments

Gravimetric samplers

The sampling of $PM_{2.5}$ has been carried out by means of a low-volume automatic sequential sampler (1 m^3 h^{-1} flowrate) equipped with $PM_{2.5}$ cut-off inlet and 47 mm PTFE filter (Manufacturer: TCR Tecora). The cartridge of filters are manually changed every 2 days without interruption of sampling. The weighing operation follows an internal procedure based on blank filters pre-conditioning at controlled relative humidity (in silica gel drier) for at least 48 hour and triple weighing of each filter by means of a balance with 10 μg resolution; the dust-loaded filters are equilibrated under the same conditions before weighing.

The sampling of PM_1 has been carried out with a low-volume IND LVS3 sampler (1 m^3 h^{-1} flowrate) with PM_1 sampling inlet and 47 mm PTFE filters (Manufacturer: Ingenieurbüro Norbert Derenda). Each sampling session lasts 24 hour (from midnight to midnight): since the dust-loaded filters are manually substituted, consecutive daily measurements are not available. The weighing procedure for PM_1 filters follows the European Standard EN 12341 for PM_{10} (CEN, 1998): 48-hours equilibration of the filter in an air-conditioned weighing room at (20 ± 1)°C and (50 ± 5)% relative humidity, triple weighing by means of a balance with 1 μg resolution. The same procedure is applied to each filter both before and after the sampling. All the data measured by the gravimetric samplers are presented in terms of daily average mass concentrations (μg m^{-3}) referred at 25°C and 1013 hPa.

Laser analyser

For simultaneous monitoring of PM_{10}, $PM_{2.5}$ and PM_1 a Grimm model 1107 particle size analyser has been used during all the campaigns (Grimm, 2002). This optical analyser uses light-scattering technology for single-particle counts, whereby a semiconductor laser serves as the light source. The scattered signal from the particle passing through the laser beam is collected at approximately 90° by a mirror and transferred to a recipient photo diode. After reinforcement, the signal passes a multi-channel signal analyser and is finally classified in the corresponding size range, where the incoming signal is counted. These counts are then converted to mass distribution and in particular into the mass cuts of PM_{10}, $PM_{2.5}$ and PM_1, based on an empirical density-factor suitable for the urban suspended particulate. The ambient air to be analysed is drawn into the measurement cell by means of an inhalable sampling head, connected to a internal volume-controlled pump at a flowrate of 1.2 liters per minute; the particles passed through the measurement cell are collected onto a 47 mm PTFE filter, thus enabling for gravimetrical verification of the particles mass reported by the optical analysis. During the monitoring campaigns 1-minute average concentrations of PM_{10}, $PM_{2.5}$ and PM_1 have been recorded on a data storage card: 1-hour and daily average concentrations have been subsequently calculated based on the recorded data and normalised to 25 °C and 1013 hPa, in order to allow the comparison to the corresponding gravimetric data.

2 – Results and discussion

Instruments comparison tests

Environmental field tests running parallel the $PM_{2.5}$ gravimetric sampler and the laser analyser have been performed at the UB Site. The accuracy of the laser analyser is checked by comparing the simultaneous daily average concentration data obtained with the gravimetric methodology. The scatter plot of all $PM_{2.5}$ data, separately collected during the three campaigns and pooled together, is presented in Figure 1. For PM_1, field tests running parallel the gravimetric sampler and the laser analyser have been performed at the UB (summer) and KR (spring) sites: the scatter plot of the 2 observed data sets is presented in Figure 2. The linear regression lines (solid), the perfect equivalence lines and its 20 μg m^{-3} two-sided envelope (dashed lines) are plotted too, in order to test the laser analyser for comparability with the gravimetric samplers, according to the procedure indicated by European Standard EN 12341.

The accuracy of the laser analyser when measuring $PM_{2.5}$ is confirmed by the high value of the correlation coefficient R^2, by the few data outside the acceptance region and by the regression line bounded within the limits of the acceptance envelope over the entire concentration ranges. For PM_1, even though the linear regression curve lays in the acceptance region, the data sets are less correlated

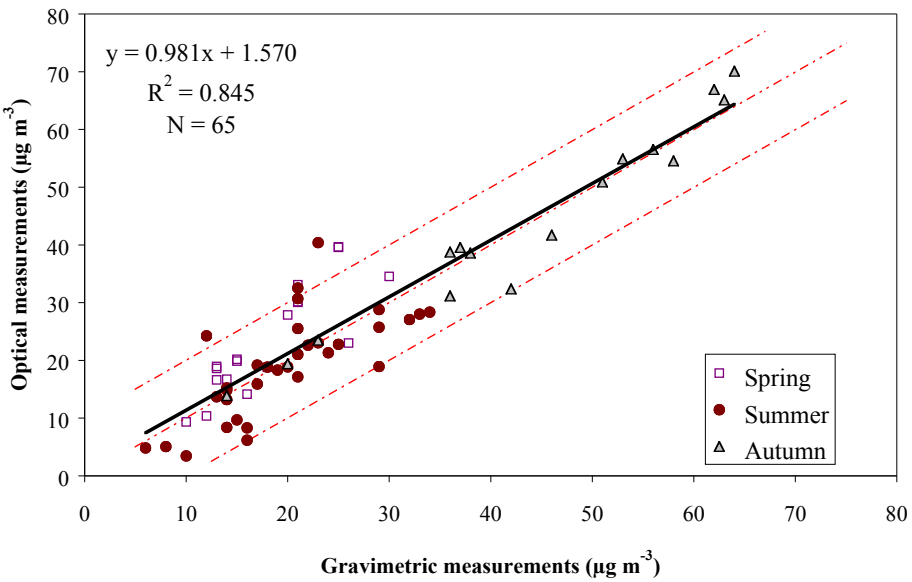

Figure 1: Scatter plot of daily average $PM_{2.5}$ concentrations observed by the gravimetric sampler and the laser analyser.

Figure 1: Diagramme de dispersion des concentrations moyennes sur 24 heures en $PM_{2.5}$.

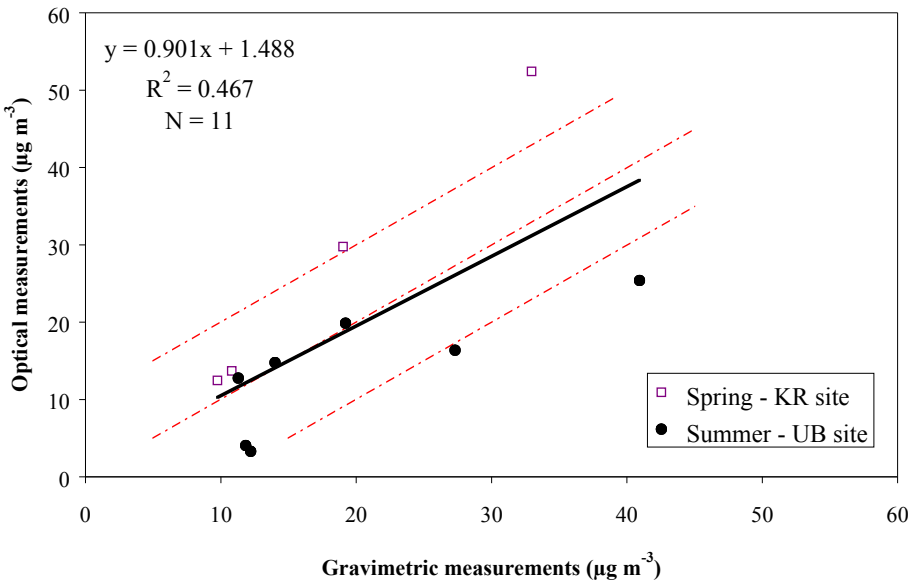

Figure 2: Scatter plot of daily average PM_1 concentrations observed by the gravimetric sampler and the laser analyser.

Figure 2: Diagramme de dispersion des concentrations moyennes sur 24 heures en PM_1.

and show a larger dispersion, with 5 out of the 11 data close to the border or clearly out of the acceptance region. Some of the larger departures from the perfect equivalence could depend on the inherent difficulties of weighing the small quantities of collected fine dust and on the possible variation of the average density of the analysed particles, not taken in account by the laser instrument when converting from particle counts to mass concentration. In fact, the empirical density-factor adopted for this conversion could be not always appropriate for the finer cuts of the atmospheric particulate, especially when the prevailing contribution of primary rather than secondary fine particulate to the observed concentrations, the primary component being characterised by a higher density, results in a variation of the average density.

Comparison between monitoring sites

Based on the data sets of daily PM average concentrations obtained by the laser analyser, a statistical analysis was performed in order to compare the observed concentration levels at the different sites. In particular, the analysis considers both the intra-site seasonal differences and the inter-site differences for corresponding seasons of the year: the former essentially depending on the activity of the emission sources and on the typical meteorological conditions of each season, the latter almost exclusively associated to the exposure to the emission sources, for the local meterological effects can be neglected at the urban scale. During each season the measurements were not performed simoultaneously: similar meteorological conditions occurred during the spring campaigns, while very different conditions occurred for the autumn campaigns. In fact at the UB site the autumn campaign took place in a period characterised by stable anticyclonic meteorological conditions whilst at the KR site the campaign occurred with adverse meteorological conditions, when prolonged heavy showers resulted in the wash-out of all the pollutants from the lower atmosphere. The intra-site and inter-site differences are thus explained taking into account the different meteorological conditions of each period. Box and whiskers plots summarizing the distributions of the daily average concentrations are reported in Figure 3-5, respectively for PM_{10}, $PM_{2.5}$ and PM_1: for each monitoring site and period the minimum and maximum values, the mean value and the range of two standard deviations around this latter are presented. In Figure 4-5, the distributions of the daily average concentrations measured by the gravimetric samplers at the TU site during a 6-days campaign for $PM_{2.5}$ and a 9-days campaign for PM_1 are reported too.

The daily average concentrations are in the 27.5÷55.9 μg m^{-3} range for PM_{10}, in the 18.2÷43.6 μg m^{-3} range for $PM_{2.5}$ and in the 15.3÷39.8 μg m^{-3} range for PM_1, with the lowest and the highest values always observed at the UB site in summer and autumn. For all the 3 granulometric cuts considered, the daily average concentration observed at the UB site in autumn is significantly higher than all the other corresponding values. $PM_{2.5}$ and PM_1 data from gravimetric samplers at the TU site are largely higher than the open-air optical measurements: the daily average values for $PM_{2.5}$ and PM_1 are 194.1 μg m^{-3} and 143.8 μg m^{-3}, that is, respectively, from 4 to 10 and from 4 to 8 times greater.

Seasonal intra-site differences in concentration levels result for the UB site: while the data distributions of spring and summer do not show relevant differences, in autumn the distribution is clearly shifted towards higher values, with a doubling of its central value with respect to the other seasons. On the contrary, at the KR site there are no statistically significant differences between the spring and autumn data sets: this fact is due to the very particular and unusual meteorological conditions in the autumn period, as already pointed out.

Inter-site differences have been evaluated at the UB, KR and KS sites in spring and at the UB and KR sites in autumn. In spring, when comparable meterological conditions occured during the 3 campaigns, the observed concentrations are very similar and there is neither a significant difference between the UB site and the 2 kerbside sites, nor between these latter. The meteorological effect of mixing in the lower atmosphere, typical for the area during this period of the year, is thus prevailing on the local effect associated to the exposition to the emission sources: the concentration levels, quite uniform in the whole urban area of Milan, are about 32 μg m^{-3} for PM_{10}, 24 μg m^{-3} for $PM_{2.5}$ and 21 μg m^{-3} for PM_1. In autumn the concentration levels at the UB site are higher than at KR site reasonably as a consequence of the great difference of meteorological conditions.

PM_{10}, $PM_{2.5}$ and PM_1 relative fractions

The mass contribution of $PM_{2.5}$ and PM_1 to PM_{10} concentration levels has been evaluated on daily and hourly average concentration data recorded by the laser analyser. For each site and for each monitoring campaign the $PM_{2.5}/PM_{10}$ and PM_1/PM_{10} ratios, as well as the $PM_1/PM_{2.5}$ ratio, have been estimated in terms of the slope of the linear regression model, for a better description of the ratios themselves over the entire range of concentrations observed, and reported in Table 2. Similar values for the PM ratios have been obtained for the 24-hour and 1-hour integration time. The role of traffic as a

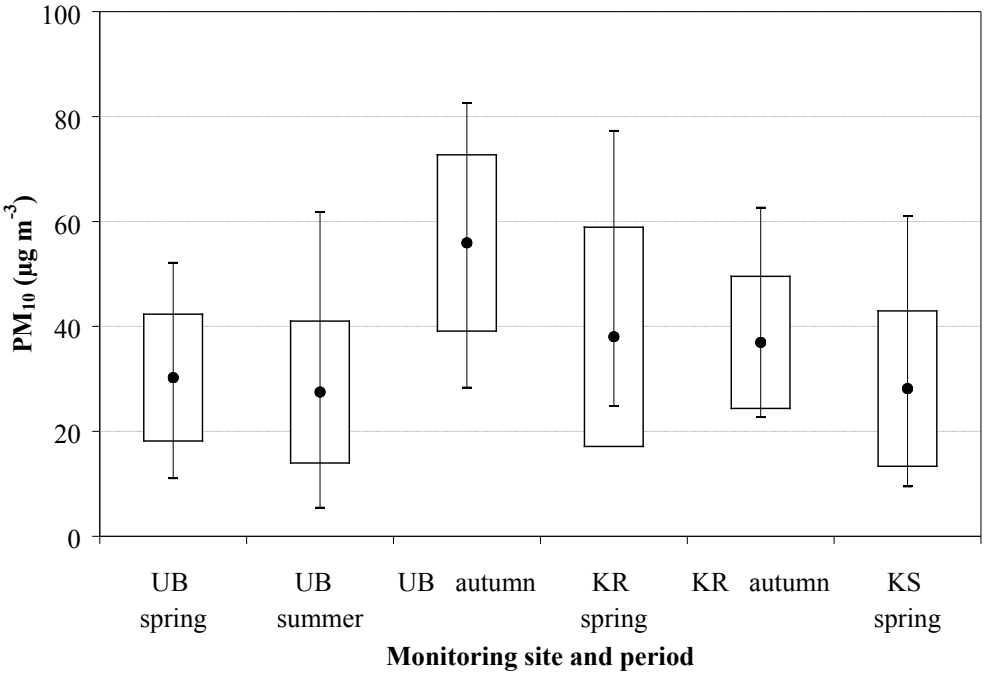

Figure 3: Distribution of daily average PM_{10} concentrations observed by the laser analyser.

Figure 3: French translation: Distribution des concentrations moyennes sur 24 heures en PM_{10} mesureés par l'analyseur optique.

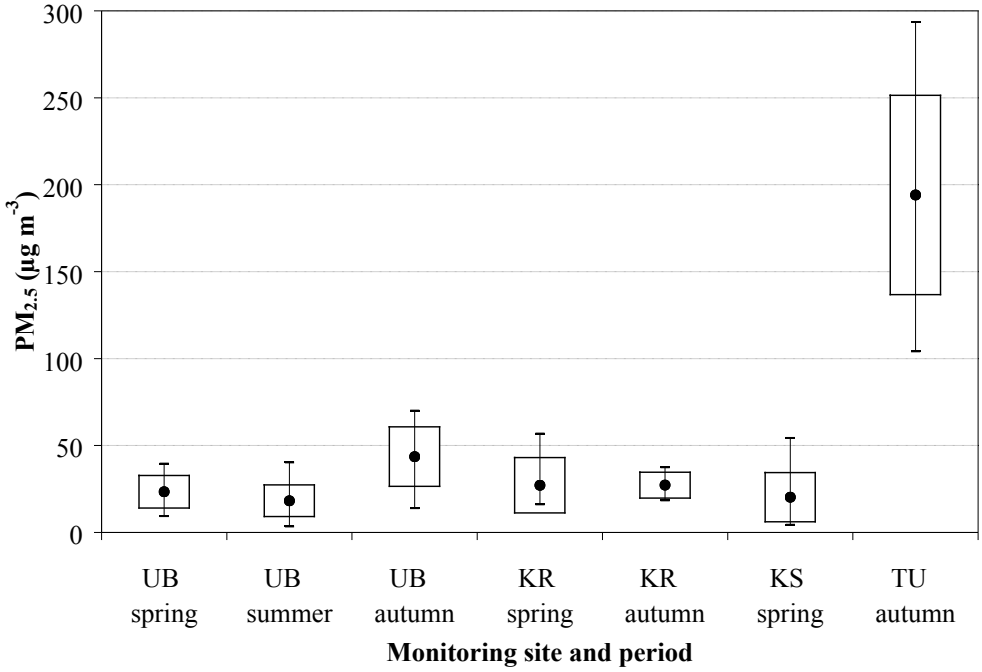

Figure 4: Distribution of daily average $PM_{2.5}$ concentrations observed by the laser analyser.

Figure 4: French translation: Distribution des concentrations moyennes sur 24 heures en $PM_{2.5}$ mesureés par l'analyseur optique.

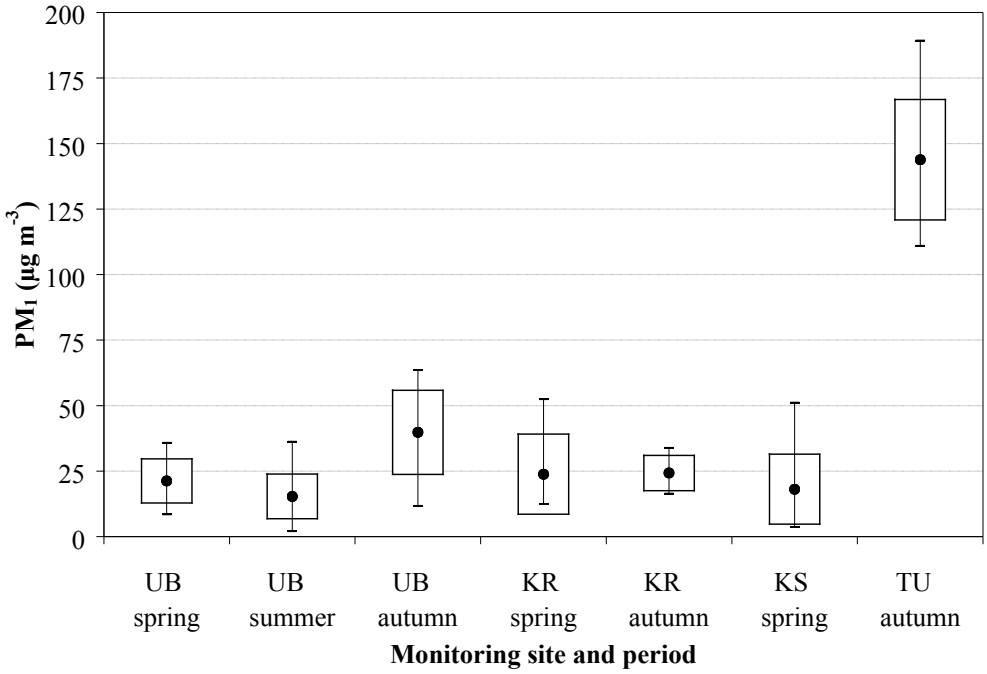

Figure 5: Distribution of daily average PM_1 concentrations observed by the laser analyser.

Figure 5: Distribution des concentrations moyennes sur 24 heures en PM_1 mesureés par l'analyseur optique.

primary source of the finest fractions of particulate is stated by the lowest values of the $PM_{2.5}/PM_{10}$ and PM_1/PM_{10} ratio observed in the summer holiday period at the UB site, when traffic is very reduced. At the other sites, all the values are very close, averaging respectively 0.74 and 0.67, with the highest values at the UB site in autumn, when very unfavourable meterorological conditions occurred, as already pointed out. However, when concentration levels are not very high the effect of the primary emissions is more appreciable as confirmed by the high contribution of $PM_{2.5}$ to PM_{10} concentrations at the heavy trafficated KS site in spring. The estimated values for the $PM_1/PM_{2.5}$ ratio show a lesser dispersion than the other ratios: on average the fraction of PM_1 is about the 90% of the $PM_{2.5}$, regardless of the site and the period of the year. The $PM_1/PM_{2.5}$ ratio was evaluated at the TU site too, based on the daily average data from 2 parallel gravimetric sampling: the low values of the ratio (0.59 and 0.76) suggest that the tunnel is a completely mixed and confined volume where the wake effects of the vehicles result in the resuspension of the particulate matter with larger size.

The evaluation of PM_{10}, $PM_{2.5}$ and PM_1 relative fractions has been completed by the analyses of the distribution of 1-hour average concentrations. As shown in Figure 6, where PM_{10}, $PM_{2.5}$, and PM_1 distributions of hourly average concentrations observed by the laser analyser at the UB site in summer are reported, the percentage contribution of $PM_{2.5}$ and PM_1 to PM_{10} mass concentration is almost the same in the whole data range: only for the lowest percentiles of the PM_{10} distribution a reduced contribution of the finest fractions, and in particular of PM_1, is observed. This fact suggests that the crustal fraction, essentially consisting of coarse particulate, is the prevailing PM_{10} constituent when the concentration levels are very low and that the increase of PM_{10} levels is mainly due to the primary and secondary emissions of the finest fractions from human activities.

Ratio	Range	Site of range minimum	*Site of range maximum*
$PM_{2.5}/PM_{10}$	0,64 – 0,77	UB Site – summer	UB Site – autumn KS site – spring
PM_1/PM_{10}	0,56 – 0,71	UB Site – summer	UB Site – autumn
$PM_1/PM_{2.5}$	0,87 – 0,92	UB Site – summer	UB Site – autumn

Table 2: $PM_{2.5}/PM_{10}$, PM_1/PM_{10} and $PM_1/PM_{2.5}$ ratios of daily average concentrations.

Tableau 2: Rapports des concentrations moyennes sur 24 heures: $PM_{2.5}/PM_{10}$, PM_1/PM_{10} et $PM_1/PM_{2.5}$.

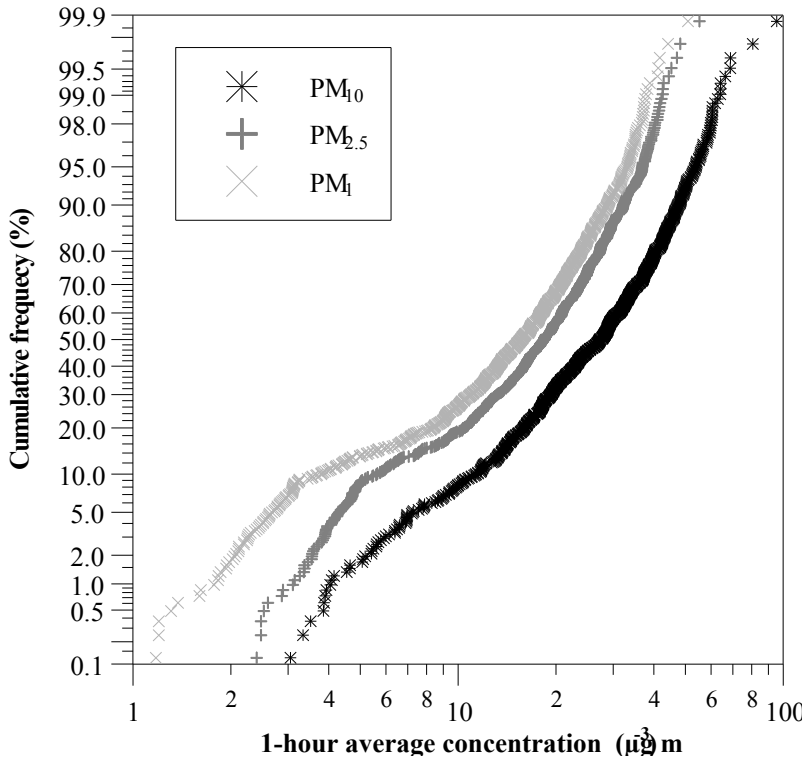

Figure 6: PM_{10}, $PM_{2.5}$, and PM_1 distributions of hourly average concentrations observed by the laser analyser at the UB site in summer.

Figure 6: French translation: Distributions des concentrations moyennes sur 1 heure mesureés par l'analyseur optique au site UB in été

Conclusion

The monitoring campaigns performed by means of both the particulate samplers and the optical analyser have provided sets of concentration data for PM_{10}, $PM_{2.5}$ and PM_1. In particular, these are the first data recorded in the area for the finest fractions of the particulate matter and allow for the description of the ambient concentration ratios between $PM_{2.5}/PM_{10}$, PM_1/ PM_{10} and $PM_1/PM_{2.5}$. Moreover, the simultaneous recording of data obtained by instruments operating with different measuring principles has confirmed of the accuracy of the optical measurements with respect to the gravimetrical ones when measuring $PM_{2.5}$. For PM_1, the equivalence between the measurements appears more questionable as a consequence of both the inherent difficulties of weighing small quantities of collected fine dust and the possible variation of the average density of the analysed particles, not taken in account when converting from particle counts to PM_1 mass concentration. This variation is probably associated to the prevailing contribution of primary rather than secondary

fine particulate to the observed concentrations. The comparison of the concentration levels at the different sites points out that the highest values are observed at the urban background in autumn, when meterorological conditions very unfavourable for the atmospheric dispersion occurred, and the lowest ones at the same site in summer, when the activity of the emission sources is reduced. At the tunnel site $PM_{2.5}$ and PM_1 concentration levels are 8 and 6 times higher than at open-air sites. The analyses of both the intra-site seasonal differences and the inter-site differences for corresponding seasons of the year point out the relevant role of meteorological conditions and of secondary sources, which are responsible for a diffused background concentration level and are even prevailing on the local effect of the exposition to the emission sources. In fact, when the meteorological conditions favour the mixing of the lower atmosphere, the concentration levels are quite uniform in the whole urban area, regardless of the site exposition to primary sources and to the traffic in particular. However, the role of the traffic as the main primary source of the finest factions of the particulate matter clearly appears when considering the relative mass contribution of $PM_{2.5}$ and PM_1 to PM_{10} concentrations: in the summer holiday period, when traffic is very reduced, these contributions are at their lowest, while in conditions of well-mixed atmosphere they are at their highest values in the site exposed to heavy traffic. This role is also confirmed by the analysis of the PM_1 contribution to $PM_{2.5}$ concentrations, estimated in about the 90% regardless of the site and the period of the year.

Acknowledgments

The authors wish to thank the Regione Lombardia for funding this research and the Regional Environmental Agency for the contribution to data acquisition.

References

CEN (1998): Air quality – Determination of the PM_{10} fraction of suspended particulate matter – Reference method and field test procedure to demonstrate reference equivalence of measurement methods. European Standard EN 12341

European Union (1999): Council Directive 1999/30/EC of 22 April 1999 relating to limit values for sulphur dioxide, nitrogen dioxide and oxides of nitrogen, particulate matter and lead in ambient air. EU Official Journal L 163 , 29/06/1999, p 41-60.

Grimm H. (2002): New portable environmental fine dust analyser for simultaneous monitoring of PM_{10}, $PM_{2.5}$ and PM_1. Proc. 11th Int. Conf. "Transport and air pollution", Graz, Austria, 19-21 June, 2002

12th International Symposium "Transport and Air Pollution" / 12e Colloque international "Transports et pollution de l'air", Avignon, 16 -18 *June* / juin 2003
proceedings / actes, n°92, tome / Vol. 1, Inrets ed., Arcueil, France, 2003, p. 19-26

Dispersion de la pollution à la sortie d'un tunnel autoroutier urbain

Ghislaine Goupil*, René Alary*, Christine Bugajny*, Catherine Ribière*, Bruno Brousse, Bruno Vidal****
*Laboratoire Central de la Préfecture de Police, 39bis rue de Dantzig 75015, PARIS, France
Fax + 33 1 55 76 27 05 – email : prefpol.dlc-dpn-pollutions@interieur.gouv.fr
** Centre d'Étude des Tunnels (CETU), 25 avenue François Mitterrand, 69674 BRON, France
Fax + 33 4 72 14 34 70 – email : Ventilation-Environnement.CETU@equipement.gouv.fr

Résumé
L'impact du trafic automobile du tunnel du Landy sur la qualité de l'air a fait l'objet de deux types d'études. En 1995, avant réalisation de la couverture, une prévision de l'impact des rejets a été réalisée à partir de données trafic et d'émissions unitaires d'une part, et d'autre part par une simulation sur maquette en canal hydraulique. En 2002, l'ouvrage étant terminé, une nouvelle étude d'impact a été effectuée à partir de mesure de CO, NOx et PM_{10} à proximité des immeubles environnants et en tête du tunnel. Cette communication présente les niveaux de pollution observés pendant les trois mois de mesure avec comparaison aux seuils réglementaires et aux niveaux relevés par des stations du réseau de surveillance ; puis compare les valeurs mesurées avec les études théoriques de 1995 et finalement propose une estimation de l'impact du rejet du tunnel sur la qualité de l'air.
Mots clés : *mesures, oxydes d'azote, PM_{10}, opacité, monoxyde de carbone, émissions, dispersion, maquette hydraulique, qualité de l'air, tunnel.*

Abstract
The dispersion of pollution at the portal of an highway tunnel in an urban area.
Two kinds of air quality studies were conducted on the south portal of the Landy tunnel on the A1 motorway, north to Paris (France). In 1995, before starting the construction works, a prediction of the exhaust impact was made based on traffic data. The dispersion in the atmosphere was studied using a small scale model in a water flume (see Fig.1 & Fig.2). Meteorological and background levels were also considered. The study concluded that the air quality will comply with the regulatory conditions valid at that time and dismissed the need of the construction of an exhaust chimney in altitude. In 2002 two field experiment campaigns (winter/summer) were organised to measure the CO, NO_x and PM_{10} levels near buildings (point O and S Fig.3), and the exhaust levels at the tunnel portal – CO, NO_x, opacity (point R Fig.3).
This paper shows the pollution levels observed during the three months of field experiment (see table 2). It demonstrates that point S showed higher levels than point O, whilst the tunnel exhaust levels are 5 to 10 times higher. The comparison with the levels registered by the survey network stations shows that pollution levels at point S are close to "traffic-station" levels, and that CO and PM_{10} levels comply with the regulatory thresholds, but not the NO_2. The contribution of the tunnel was observed to be about 20% of the total outside air pollution measurements (see table 3 & table 4). The field experiment demonstrated that the 1995 theoretical study was rather correct (see Fig.4 & Fig.5).
Key-words: measurements, nitrogen oxides, PM_{10}, opacity, carbon monoxide, emissions, dispersion,hydraulic model, air quality, tunnel.

Introduction

Le tunnel du Landy de l'autoroute A1 au Nord de Paris mesure 1,6 km avec un trafic journalier global de 200 000 véhicules auquel se rajoute le trafic contigu de la Route Nationale RN1 de 30 000 véhicules/jour. Lors de la couverture de la tranchée en 1995, une étude a déterminé par calcul sur la base d'émissions unitaires et par simulation sur maquette, la dispersion des polluants à la tête Sud du tunnel du Landy (Saint Denis – Département de Seine Saint Denis – France). Cette étude préconisait la mise en œuvre d'une extraction massive avec rejet en altitude par cheminée qui n'a ensuite pas été réalisée compte tenu de la diminution régulière des émissions en polluants des véhicules. Cette simulation montrait que les niveaux de pollution estimés aux horizons 2005 permettraient de satisfaire la réglementation en vigueur à la date des études de 1995, et dès 1997 en augmentant le débit de ventilation.

Deux campagnes de mesure ont été réalisées en 2002 afin de vérifier sur le terrain les estimations de 1995. Des indicateurs spécifiques de la pollution automobile présentant un intérêt sanitaire ont été choisis : le monoxyde de carbone (CO), les oxydes d'azote NO et NO_2 regroupés sous la terminologie générale NO_x et les particules fines de diamètre inférieur à 10 μm (PM10) sauf à la sortie du tunnel où ce dernier paramètre a été remplacé par l'opacité mesurée usuellement en tunnel.

1 - Étude sur maquette et modélisation (1995) [Brousse & Moret - 1995]

Phase de préparation des données

Des simulations numériques d'écoulement et de pollution de l'air en tunnel s'appuyant sur les comptages de trafic, les émissions unitaires des véhicules, et sur le fonctionnement de la ventilation mécanique, ont d'abord permis de définir la panoplie des rejets types à tester avec leurs vitesses et la concentration en polluants. Les données d'émissions ont été estimées pour 1997, date de fin de travaux de couverture de l'autoroute A1, ainsi que pour les horizons 2000 et 2005 avec des valeurs en baisse.

Les vitesses et directions de vent affectées d'une probabilité d'apparition ont été calculées à partir des données issues de la station météorologique voisine représentative du Bourget. Les mesures de pollution du réseau de surveillance AIRPARIF sur le site "urbain" d'Aubervilliers ont permis d'estimer la pollution de fond à prendre en compte.

Phase d'essais sur maquette

Sur la base des différentes combinaisons de classes de vents et de valeurs de rejets calculées auparavant, le taux de dispersion du rejet et l'exposition à la pollution d'une vingtaine de points sensibles sélectionnés et répartis dans l'environnement proche de la tête (voir Fig. 1) ont été déterminés à l'aide d'une maquette réalisée à l'échelle 1/140ième en canal hydraulique au laboratoire ACB-GEC ALSTHOM de Grenoble.

Approche statistique des niveaux de pollution

Par un calcul de probabilités, une courbe de concentrations en polluants classées en fonction de la fréquence d'occurrence a été établie pour chaque point choisi du site à laquelle a été superposé le niveau de pollution de fond, donnant le niveau final d'exposition.

L'étude a permis de chiffrer différentes configurations : a) extraction massive de tête limitant le rejet donc son impact sur l'environnement b) réduction des émissions unitaires des véhicules.

L'étude a par ailleurs servi à étudier l'insertion éventuelle d'une cheminée d'extraction et d'optimiser sa hauteur en fonction de la dispersion de son panache au-dessus du bâti.

Résultats de l'étude de 1995

Selon l'hypothèse des émissions unitaires évaluées pour 1997, le rejet tunnel exposerait seulement deux points du site (5 et 6) à un niveau de pollution légèrement supérieur au seuil fixé par le décret de 1991 [Décret n° 91-1122]. L'étude a permis d'établir le classement des points du site selon leur niveau d'exposition décroissant en NO_2 : 5, 6, 12, 4, 13-14, 1-10-11, 7, 17-18, 9-19, 8-15, 16, 3 (voir emplacements des points sur la figure 3).

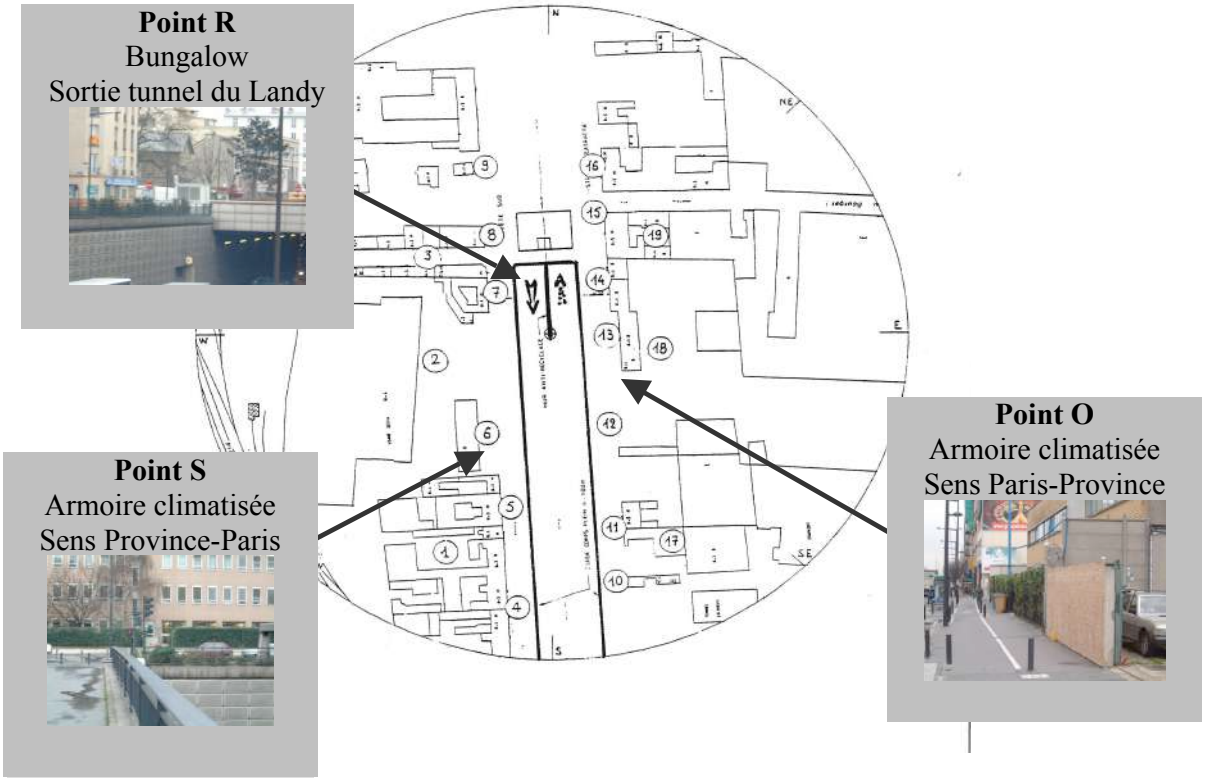

Figure 1 : Emplacements des points de mesure

Figure 1 : Measurements sites

2 - Étude 2002 et comparaison avec l'étude sur maquette de 1995

Méthodologie

Deux campagnes ont été menées, l'une en période hivernale et l'autre en période estivale, afin d'évaluer la pollution dans différentes configurations météorologiques. Trois points fixes équipés de matériel de mesure automatique ont été choisis :

Un point situé à la sortie du tunnel représentant les niveaux de pollution du rejet du tube Province-Paris (point R).

Deux points situés dans les zones les plus exposées selon la modélisation de 1995 : point O proche des points 12-13 sens Paris-Province et point S proche des points 5-6 sens Province-Paris.

Une cartographie du quartier par tubes à diffusion NO2 a permis de valider le choix de ces points. Le tableau 1 ci-après, regroupe les moyens de mesure mis en œuvre lors de ces deux campagnes.

Ces données de pollution ont été complétées par des comptages routiers et les données météorologiques issues de la station du réseau régional AIRPARIF de surveillance de la qualité de l'air à Paris 11ème.

Teneurs de référence et sites de comparaison

Les teneurs relevées dans l'air ambiant extérieur sont rapprochées des textes de référence en vigueur qui visent la population générale : les recommandations de l'O.M.S.1999 [OMS 1999] et le décret n°2002-213 du 15 février 2002 [Décret n°2002-213] .

Les résultats des mesures obtenus sur les différents sites sont également comparés à ceux de plusieurs stations AIRPARIF pendant la même période.

TYPE DE MESURE	**Polluants**	*MOYENS MIS EN ŒUVRE*	*DUREE*
Mesures automatiques			
Point O **Sens Paris Province** 76 avenue du Président Wilson 93210 La Plaine Saint Denis	CO NO_X PM10	Armoire mobile de mesure	Campagne hivernale : 4 semaines Du 15 janvier au 26 février 2002 Campagne estivale : 8 semaines Du 28 mai au 02 août 2002
Point S **Sens Province Paris** 85 avenue du Président Wilson 93210 La Plaine Saint Denis	CO NO_X PM10	Armoire mobile de mesure	
Point R **Tunnel du Landy** Tête Sud du tunnel Tube sens Province-Paris	CO NO_X Opacité Anémomètrie	Analyseurs dans bungalow Prise d'air en sortie de tunnel Opacimètre en tunnel Anémomètre en tunnel	
Mesures par prélèvements passifs			
12 points répartis dans le quartier : Sur la couverture de l'A1 En doublon des points O,S et R En doublon des sites de comparaison	NO_2	Tubes Passam	Campagne hivernale : 3 prélèvements successifs de 2 semaines Campagne estivale : 3 prélèvements successifs de 2 semaines

Tableau 1 : Moyens de mesure mis en œuvre

Table 1 : Measurements apparatus

3 - Résultats et discussion

Pendant les campagnes de mesure d'hiver et d'été, il a été observé une variabilité météorologique permettant de valider les travaux effectués.

Résultats généraux

Le tableau 2 ci-après présente les résultats statistiques des quatre polluants étudiés lors de l'étude 2002 aux différents points (point R, point O et point S) et aux stations AIRPARIF prises en référence. Ces résultats ont été calculés à partir des données horaires obtenues pour tous les polluants sauf pour les particules PM10 où le calcul a été réalisé à partir des données journalières.

Au regard des résultats, globalement, les niveaux en CO sont faibles. Les niveaux relevés sur le point S (sens Province-Paris) sont supérieurs à ceux relevés sur le point O.

Les niveaux à l'intérieur du tunnel juste avant la sortie sont de 5 fois (NO_2) à 10 fois (CO, NO) plus élevés que ceux mesurés dans l'air extérieur environnant. En raison de la présence quasi permanente d'un courant d'air de l'entrée vers la sortie du tunnel (effet de pistonnement des véhicules) la tête Sud est en principe la zone la plus polluée du tube. Le tunnel du Landy est équipé de capteurs CO et d'opacité permettant d'assurer le pilotage de la ventilation mécanique. En raison de concentrations élevées mesurées en NO_2 et de la toxicité de ce polluant, sa prise en compte pour gérer la ventilation est à considérer conformément aux recommandations du CHSPF [CSHPF 1998].

Comparaison aux sites du réseau AIRPARIF et aux teneurs de référence

Les moyennes, les maxima et les percentiles du point S (sens Province-Paris), sauf pour le CO, sont supérieurs à ceux obtenus pendant les mêmes périodes sur les 2 sites trafic du réseau AIRPARIF pris en référence. Les résultats statistiques du point O (sens Paris-Province) sont inférieurs à ceux obtenus sur les sites trafic du réseau mais supérieurs à ceux obtenus sur les sites urbains.

	Tunnel du Landy (Point R)	Sens Paris-Province (Point O)	Sens Province-Paris (Point S)	A1 Site trafic Réseau AIRPARIF	Périphérique Auteuil Site trafic Réseau AIRPARIF	Saint Denis Site urbain Réseau AIRPARIF	Paris 18ème Site urbain Réseau AIRPARIF
CO (mg/m³)							
Moyenne / Average	13	0,59	1,1	1,3	1,5	/	/
Maximum horaire	65	2,9	4,7	3,7	6,4	/	/
NO (µg/m³)							
Moyenne /	2900	86	230	160	200	8,1	/
Maximum horaire	8600	550	920	730	830	260	/
P50	2300	71	190	150	180	3,0	/
P98	7200	260	640	390	490	74	/
NO_2 (µg/m³)							
Moyenne / Average	450	71	99	84	92	31	/
Maximum horaire	1900	190	270	210	230	120	/
P50	330	70	98	85	91	26	/
P98	1300	130	190	140	160	75	/
P99,8	-	160	220	190	220	96	/
Tunnel : Opacité (km-1) – Points de mesure et stations AIRPARIF : PM10 (µg/m³)							
Moyenne / Average	1,9	23	45	/	42	/	21
Maximum	6,5	39	85	/	67	/	42
P50	1,5	23	43	/	41	/	20
P90,4	-	32	62	/	54	/	30
P98	4,5	38	75	/	65	/	38

Tableau 2 : Résultats statistiques en tunnel et en air ambiant extérieur

Table 2 : Statistical results in tunnel and in exterior ambient air

La comparaison des résultats obtenus sur les sites de l'étude avec les teneurs de référence demande certaines précautions relatives à leur interprétation. Les normes font parfois obligation d'une durée d'observation de un an alors que l'étude n'a duré que 11 semaines.

Sur tous les sites, aucun dépassement concernant le CO n'est observé. Pour le NO_2, l'objectif de qualité (40 μg/m^3) n'est pas atteint ; la valeur limite annuelle 2002 (56 μg/m^3) pour la protection de la santé n'est pas respectée sur les deux sites de l'étude et sur les sites trafic ainsi que pour les NO_x concernant la valeur limite annuelle 2002 (30 μg/m^3) pour la protection de la végétation. Le seuil de recommandation et d'information (200 μg/m^3) a été dépassé sur le point S (Sens Province-Paris) et les 2 sites trafic du réseau. Pour les PM10, toutes les références réglementaires sont respectées sur le point O (Sens Paris-Province) ; sur le point S (Sens Province-Paris), seule la valeur limite annuelle 2002 (Percentile 90.4=65μg/m^3) est respectée.

Influence des paramètres météorologiques

Il est observé des niveaux de pollution plus élevés avec les vents dominants (Sud-Ouest et Ouest) au point O (sens Paris-Province) en conformité avec son emplacement par rapport à l'autoroute A1. Ce sont les vents de secteur Sud-Est, Sud et Sud-Ouest qui entraînent des niveaux plus élevés au point S (sens Province-Paris) pour lequel, entre autre, la présence de bâtiments plus élevés nuit probablement à la bonne dispersion des polluants comme le montre les figures 2 et 3.

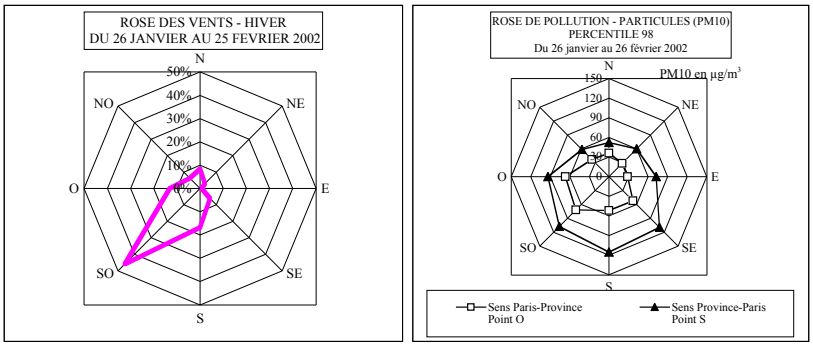

Figure 2 : Roses des vents et Roses de pollution pour les PM10 (Hiver)

Figure 2 : Compass card and PM10 versus wind direction charts (winter)

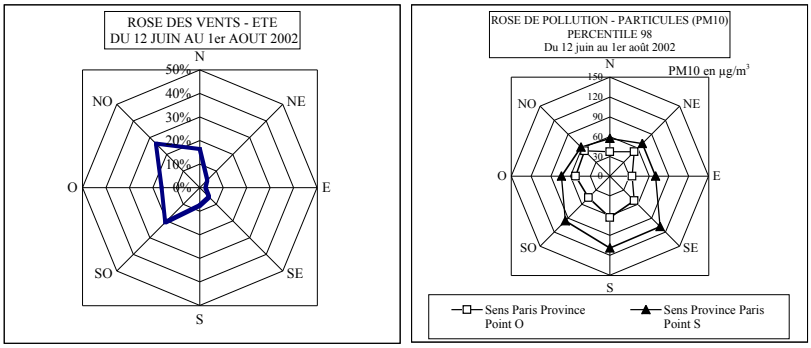

Figure 3 : Roses des vents et Roses de pollution pour les PM10 (Eté)

Figure 3 : Compass card and PM10 versus wind direction charts (summer)

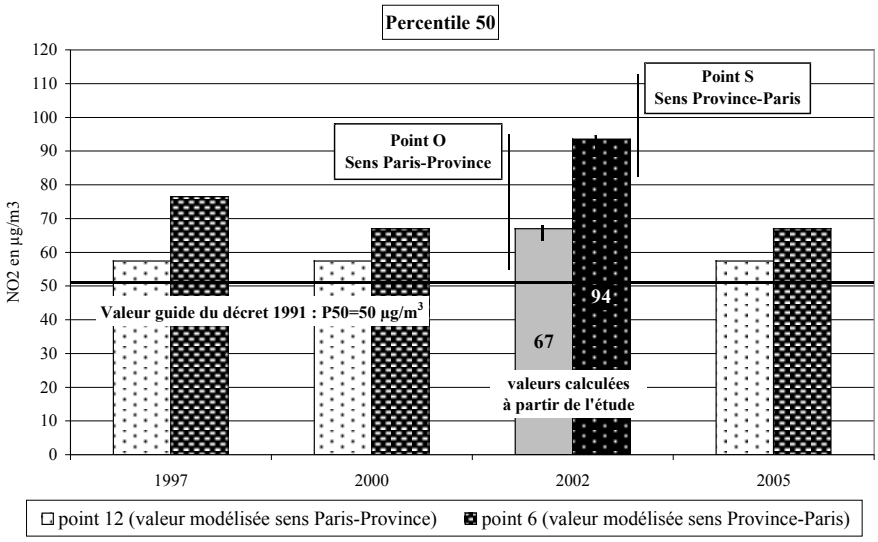

Figure 4 : Résultats de modélisation et de l'étude pour le percentile 50

Figure 4 : Simulation and 2002 study results for percentile 50

Comparaison de l'étude 1995 avec l'étude 2002

Les percentiles 50 et 98 en NO_2 dans la zone environnante de la couverture de l'A1 extrapolés sur l'année 2002 ont été comparés à ceux de la modélisation de 1995. La figure 4 présente les résultats de la modélisation pour 1997, 2000 et 2005 –aux points 12 et 6 (voir figure 1) - et ceux de l'étude 2002 pour le percentile 50.

Pour la valeur guide du décret de 1991 (P50=50μg/m^3 des teneurs moyennes horaires en NO_2), les valeurs calculées à partir des mesures 2002 dépassent les valeurs estimées par modélisation.

Pour la valeur limite du décret de 1991 (P98=200μg/m^3 des teneurs moyennes horaires en NO_2) non

représentée, les valeurs calculées à partir des mesures 2002 sont inférieures aux valeurs estimées par modélisation.

4 - Évaluation de l'impact du tunnel sur la qualité de l'air

Corrélation niveau tunnel et niveau air extérieur

Afin de montrer l'impact du tunnel sur l'environnement extérieur, le tableau 4 présente les coefficients de détermination R^2 (%),significatifs avec un seuil de probabilité supérieur à 95% entre chaque paire de variable.

Polluant tunnel		NO point R		NO2 point R		Opacité point R	
		hiver	été	hiver	été	hiver	été
Polluant extérieur	NO point O	35	20				
	NO point S	4.8	9.0				
	NO2 point O			31	17		
	NO2 point S			8.4	16		
	PM10 point O					20	17
	PM10 point S					6.3	7.8

Tableau 4: R^2 en % polluants tunnel/polluants air ambiant extérieur

Table 4 : Correlation between tunnel pollutants and exterior ambient air pollutants

Le tableau montre que les teneurs en NO mesurées au point O s'expliquent à 35% par le NO issu du tunnel l'hiver et 20% l'été. Pour le point S, la corrélation est nettement plus faible (inférieure à 10%). La différence entre les 2 points résulte de l'interaction des paramètres météorologiques et topographiques des 2 points de mesure (voir §2.2 : influence des paramètres météorologiques).

En ce qui concerne NO_2 au point O, les corrélations sont voisines de celles observées pour NO à ce même point (31% l'hiver et 17% l'été). La corrélation des teneurs NO_2 mesurées au point S est meilleure que pour NO. Le point O présente des corrélations moins bonnes l'été que l'hiver pour NO et NO_2. Au point S, c'est l'inverse : la corrélation est meilleure l'été que l'hiver. Cette différence peut s'expliquer par les phénomènes de photochimie atmosphérique qui affecte l'air ambiant extérieur en relation avec la variation du rapport NO/NO_2 (tableau 5). Le point O est plus influencé par les polluants provenant de l'autoroute et donc la photochimie a une contribution moins importante.

La corrélation réalisée entre opacité mesurée dans le tunnel et particules PM10 mesurées dans l'air ambiant extérieur est également meilleure au point O (environ 20%) par rapport au point S (inférieur à 10%).

Corrélation trafic et niveaux de polluant

Des calculs de coefficients de corrélation ont été réalisés entre les données de comptage (débit véhiculaire et taux d'occupation) et les données de pollution tunnel et air ambiant extérieur. Les teneurs en NO, NO_2 et Opacité du tunnel sont expliquées à 80% par le taux d'occupation du tube Province-Paris. La corrélation avec le débit véhiculaire est nettement moins bonne de l'ordre de 10% pour l'opacité à 25% pour le NO du tunnel. En ce qui concerne les polluants de l'air ambiant extérieur, cette corrélation est encore moins évidente.

		Moy. NO en µg/m^3	Moy. NO_2 en µg/m^3	Rapport NO/NO_2
Point O	Hiver	91	74	1.7
	Été	83	69	1.7
Point S	Hiver	281	94	4.2
	Été	200	100	2.8

Tableau 5 : Moyennes NO et NO_2 et rapport NO/NO_2 hiver et été

Table 5 : Average values NO and NO_2 and NO/NO_2 ratio

Conclusion

L'étude a montré que les niveaux de polluants sont généralement plus élevés dans le sens Province-Paris (point S) par rapport à l'autre côté de la voie, en conformité avec les résultats de la modélisation de 1995. Les teneurs observées côté sens Province-Paris (point S) sont proches de celles mesurées pour les stations « trafic » du réseau de surveillance de la qualité de l'air à Paris. Les niveaux de pollution relevés côté sens Paris-Province (Point O) sont supérieurs (NO, NO_2) ou proche (PM10) des stations de type « urbain ». La comparaison des données obtenues pendant les deux campagnes de mesures dans l'air ambiant extérieur avec les références réglementaires est satisfaisante pour CO et PM10 au point O (Paris-Province). Par contre, les deux sites de l'étude ne respectent pas la plupart des références réglementaires (objectif de qualité et valeur limite annuelle 2002) pour NO_2, comme les deux stations trafic du réseau prises à titre de comparaison. Concernant les PM10, le sens Province-Paris (point S), seule la valeur limite annuelle 2002 est respectée.

Les résultats de pollution dans le tunnel sont de 5 à 10 fois plus élevés selon le polluant considéré. Le profil journalier des polluants obtenu dans le tunnel présente une bonne corrélation avec le taux d'occupation relevé dans le sens de circulation Province-Paris.

Les vents de secteur Ouest dominants ont une influence très importante sur les niveaux observés au point O (sens Paris-Province) entraînant ainsi une bonne dispersion des polluants dans cette zone de bâti moins dense. Ce sont les vents de secteur Sud (SE, S, SO) qui ont une importance non négligeable sur les niveaux de pollution du point S (sens Province-Paris), pour lequel entre autre la présence de bâtiments plus élevés nuit probablement à la bonne dispersion des polluants.

Les résultats de ces campagnes 2002 mettent en évidence le non-respect de la valeur guide du décret de 1991 (P50=50 μg/m^3) en NO_2, un dépassement des résultats des estimations réalisées en 1995 mais sont du même ordre de grandeur que les résultats des stations trafic du réseau AIRPARIF. Par rapport à la valeur limite de ce même décret (P98=200μg/m^3) en NO_2, les résultats obtenus sont inférieurs aux prévisions 2005.

Compte tenu des incertitudes liées à la prise en compte des nombreuses hypothèses nécessaires à l'étude prospective, les mesures réelles 2002 ont montré que les estimations théoriques de 1995 étaient aussi correctes que possibles.

Références

Brousse B., Moret C. (1995) : « Couverture de l'autoroute A1 à la plaine Saint Denis » (Étude principale - 1ère partie et étude complémentaire - 2ème partie)

CSHPF (1998) « Qualité de l'air dans les ouvrages souterrains ou couverts » - pages n°19-26 et pages n°35-36

Décret n° 91-1122 du 25 octobre 1991 relatif au contrôle des émissions polluantes dans l'atmosphère et à certaines utilisations de l'énergie thermique (Journal Officiel de la République Française du 23/10/91)

Décret n° 2002-213 du 15 février 2002 relatif à la surveillance de la qualité de l'air et de ses effets sur la santé et sur l'environnement, aux objectifs de qualité de l'air, aux seuils d'alerte et aux valeurs limites (Journal Officiel de la République Française du 19/02/02)

OMS (1999) - Who Air Quality Guidelines.

12th International Symposium "Transport and Air Pollution" / 12e Colloque international "Transports et pollution de l'air", Avignon, 16 -18 *June* / juin 2003
proceedings / actes, n°92, tome / Vol. 1, Inrets ed., Arcueil, France, 2003, p. 27-34

Establishing an air pollution monitoring network for intra-urban population exposure assessment: a location-allocation approach

Pavlos S. Kanaroglou*, Michael Jerrett (Cor. Author), Jason Morrison*** Bernardo Beckerman** M. Altaf Arain** Nicolas L. Gilbert**** & Jeff Brook*******
* Canada Research Chair in Spatial Analysis, School of Geography and Geology, McMaster University, Hamilton, Ontario, Canada, L8S 4K1
** School of Geography and Geology and McMaster Institute of Environment and Health, McMaster University Hamilton, Ontario, Canada, L8S 4K1, Tel: 905-525-9140, x27317 Fax: 905-546-0463 - email : jerrettm@mcmaster.ca
*** School of Computer Science, Carleton University, Ottawa, Ontario, Canada
**** Health Canada, Air Health Effects Section, Ottawa, Ontario, Canada
*****Meteorological Service of Canada, Toronto, Ontario, Canada

Abstract
The purpose of this study is to develop a formal methodology for optimally locating air pollution monitors within an urban area. We apply our methodology in locating 100 nitrogen dioxide monitors in Toronto, Canada. Locations identified by the method represent land use, transportation infrastructure and the distribution of at-risk populations. The developed method may have widespread applicability for the design of pollution monitoring networks, particularly for measuring traffic pollutants with fine-scale spatial variability.
Keywords: air pollution, traffic emissions, monitoring networks, location-allocation models

Résumé
L'objectif de cette étude est de développer une méthodologie formelle permettant de déterminer la répartition géographique optimale d'un nombre donné d'appareils de mesure de la pollution atmosphérique à l'intérieur d'une zone urbaine. Nous avons utilisé notre méthode pour choisir l'emplacement de 100 échantillonneurs de dioxyde d'azote à Toronto (Canada). Les sites ont été sélectionnés en fonction de l'utilisation du territoire, des infrastructures de transport et de la distribution des populations à risque. Cette méthode pourrait s'avérer d'une grande utilité pour la conception de réseaux de surveillance de la pollution atmosphérique, particulièrement pour les polluants d'origine automobile présentant une grande variabilité spatiale.
Mots clés : pollution atmosphérique, réseaux de surveillance, modèles d'allocation des sites

Introduction

Policymakers and scientists have shown growing interest in the health effects of chronic exposure to air pollution. Researchers now focus on associations between health outcomes and air pollution variation within communities. A recent cohort study (Hoek et al. 2002) reported a large association between cardiopulmonary mortality and living near a major road (Relative Risk = 1.95, 95% CI: 1.09 - 3.51). Traffic-related air pollution is of particular interest from a regulatory perspective because demand for transportation will outpace improvements in vehicle technologies over the next decade (Mohammadian, 2002). Yet uncertainties in exposure assessment methodologies continue to raise questions about the reliability and accuracy of risk estimates from intra-urban air pollution studies (Briggs et al. 2000).

This paper describes a formal methodology for locating a fixed number of air pollution monitors in

Toronto, Canada. Previous studies have located monitors in an ad-hoc fashion, favouring the placement of monitors in traffic "hot spots" or in areas deemed subjectively to be of interest for land use and population characteristics (Lebret et al, 2000; Kukkonen et al., 2001; Goswami et al, 2002). We thus aim to make best use of costly air quality monitoring in the study area using a formal method to achieve optimal locations based on specified criteria.

1 - Methods

Conceptual Framework for Locating Monitoring Stations

The approach we use consists of two stages. First, based on specified criteria, we determine a continuous surface over the study area, which we term "the demand surface". Higher values of the surface correspond to increased need for monitoring. Second, we use the demand surface as an input to an algorithm that solves a constrained optimization problem in the general family of location-allocation (L-A) problems. The algorithm will identify the optimal locations for a predefined number of samplers.

We use two criteria for the determination of the demand surface. The first postulates that a larger number of monitors should be located where the pollution surface is expected to exhibit higher spatial variability. To implement this criterion, we need an initial estimate of the pollution surface, which is the approximate surface we hope to obtain after monitoring is complete. Since such a surface is not generally available, we recommend obtaining a first estimate with available government monitoring data or a spatially sparse network of ground stations operated by the researchers. In our particular application, we estimated the pollution surface through land use regression (LUR) with data from an area wider than the City of Toronto to encompass a large enough number of fixed-site monitoring stations (i.e., South-central Ontario). The process is described in more detail in the methodology implementation section below.

Spatial variability in pollution is determined by the semi-variance at a large number of locations in the study area. Usually a grid is imposed on the study area, and the semi-variance is determined at all the nodes of the grid. Mathematically, let $Z(\vec{x})$ represent a random variable of the pollution estimate at location $\vec{x}$, and $z(\vec{x})$ be a realization of this random variable. The spatial variability at location $\vec{x}$ then is provided by:

$$\gamma(\vec{x},\vec{x}+\vec{h}) = \tfrac{1}{2}\sum[\{z(\vec{x}) - z(\vec{x}+\vec{h})\}^2] \qquad \text{(Eq. 1)}$$

The right side summation occurs over all possible pairs of locations $\vec{x}$ and $\vec{x}+\vec{h}$, where $\vec{h}$ represents the lag distance between sets of points in the dataset. The determination of the semi-variance γ at all locations $\vec{x}$ will provide a surface of variability in the pollution surface. This creates the demand surface that satisfies the first criterion noted above.

To satisfy the second criterion, we modify appropriately the demand surface achieved through the semi-variance. Here, we intensify demand for pollution monitors in areas with high densities of at-risk populations. That population group might have demographic characteristics of importance for the intended health study, such as children or the elderly. To achieve this effect, a weighting scheme is implemented according to the equation:

$$W_x = \frac{P_x / P}{\gamma(\vec{x},\vec{x}+\vec{h}) / \sum_x \gamma(\vec{x},\vec{x}+\vec{h})} \qquad \text{(Eq. 2)}$$

Here P_x and P are the population strata of interest at location x and of the entire study area, respectively. This formulation resembles the location quotient representing the proportion of the population of interest at location x over the proportion of semi-variance at that same location.

The Study Area and Data

Monitoring data used to derive initial estimates were collected in major urban centres or suburbs of

South-central Ontario, a densely populated conurbation, extending from St. Catherines to Oshawa, roughly 200 km. For this study, we chose nitrogen dioxide (NO_2) as a proxy for traffic pollution because it is relatively inexpensive to measure and has been used widely as a metric of exposure to traffic emissions (Briggs et al. 1997). Independent variables were implemented with land use and transportation data acquired from a commercial source, DMTI Spatial Inc, Markham, ON, Canada.

Estimating the Pollution Surface

Mean NO_2 estimates at 16 Ontario Ministry of the Environment (MOE) locations served as the dependent variable in the LUR regression (Briggs et al. 1997). The 1999 NO_2 annual mean values at the 16 MOE air monitoring stations in the study area range between 12.4 to 28.4 parts per billion (ppb). Independent variables were obtained by measuring the respective area and length parameters within circular neighbourhood buffers centred on the MOE station position. Accurate geo-referencing was essential for the locations of pollution monitoring sites, roads and houses due to the highly localized nature of the estimates. We used a global position system to mark all the monitoring sites (ground-level accuracy of 7 m or less). Field validation of the DMTI land use coverage revealed high accuracy in attribute classification and spatial coordinates.

Land use variables were calculated in hectares and road lengths in kilometres. Land use parameters were measured under a circular buffer that extends from each monitoring location out to a radius of 100 m. Road length parameters were measured under two separate buffers. A first circular buffer extends from each monitoring point out to a radius of 50 m. A second buffer is in the shape of an annulus (donut), with the inner edge at a radius of 50 m and the outer at 200 m. All area and length calculations were performed using ArcView 3.2 software's Spatial Analyst extension (ESRI Corp., Redlands, CA).

In total, 16 land use and transportation variables were tested in a manual stepwise regression with S-Plus 6 software (Mathsoft, Cambridge, MA) to obtain a best estimate pollution model. A bivariate ordinary least-squares regression analysis was used in the initial step to develop a model that predicts the best pollution surface. The variable selection criterion was set at $p < 0.25$ statistical significance for the initial screening (Hosmer and Lemeshow 1989). The most statistically significant variables were sequentially included until a parsimonious model was achieved.

Parameters from the LUR model were used to predict the NO_2 pollution surface based on significant land-use and transportation criteria via a focal sum statistic. The focal sum statistic computes the area or the length parameters of the land use or transportation criteria within a same neighbourhood used for measuring the independent variables in the regression analysis. This was computed for every 5 m grid cell in Toronto. The 5 m resolution was chosen to allow a reasonable approximation of the vector dataset into raster format.

Creating a Surface of Monitoring Demand

We assume that the air pollution to be measured is spatially continuous. Consistent with geostatistical modelling, any pollution measurement represents a specific instance of a random process at the sampling location. That is, we assign a random variable $Z(\vec{x})$, with an actual value $z(\vec{x})$, at a location $\vec{x}$. Since pollution concentrations are spatially continuous, the distance between two separate sampling locations correlates with their measurement of the pollutant. The measurement of the variation between values at the locations $\vec{x}$ and $\vec{x}+\vec{h}$ is denoted as the semi-variance modified from Equation 1. We calculate the sum of all pair-wise semi-variances within a 300 m radius of $\vec{x}$ as a determination of the size of the semi-variance at $\vec{x}$:

$$S_{300m}(\vec{x}) = \tfrac{1}{2} \sum_{|\vec{h}| \le 300m} (z(\vec{x}) - z(\vec{x}+\vec{h}))^2 \qquad \text{(Eq. 3)}$$

Drawing from concepts of regionalized variable theory (Webster and Oliver, 1990), we note that the correlation of a random variable between two locations is inversely proportional to the semi-variance of the variable at those locations. A region $\mathfrak{R}$ does not benefit from further monitoring stations if distance between stations and their neighbours is reasonably small compared to the semi-

variances within those same neighbours.

Using previous results on NO_2 (Hewitt, 1991; Gilbert et al., 2002) we assume that little correlation exists (and hence maximal semi-variance) if $|\vec{h}|$ is "sufficiently large". While this correlation varies according to topography and meteorology, evidence suggests that 80-90% of traffic related effects come from less than 150m to 300 m away (English et al., 1999; Briggs et al., 2000). This suggests that locally, the semi-variance depends on $\vec{h}$, and we achieve a model with quasi-stationarity at the 300 m lag. We can then estimate the semi-variances between all points in a region $\mathfrak{R}$ by summing $S_{300m}(\vec{x})$ across all $\vec{\mathbf{x}} \in \mathfrak{R}$.

Augmenting Demand for Socio-Demographics

The demand intended for sampling stations computed via $S_{300m}(\vec{x})$ accounts for the need to represent pollution variability. When conducting a pollution exposure assessment, however, it*IIIF* may be desirable to measure pollution exposures more accurately, specifically in areas with particular socio-demographic (SD) characteristics. To achieve area specific weighting of the sampling network, we increase demand in areas with high target populations.

When employing SD in some spatial studies, the issue of the "Modifiable Area Unit Problem" becomes apparent (Fotheringham et al. 2000). The weighting process produces SD surfaces with coarse resolution, which must be taken into account when selecting the aggregation unit resolution of the SD dataset. We chose the census tract (CT) level because it provides a compromise between spatial detail and area homogeneity. Statistics Canada's CTs are equal in size to neighbourhood-like areas, approximately 2,500 to 8,000 people (the average population is about 4000). CT boundaries generally follow permanent physical features, such as major streets and railway tracks, and attempt to approximate cohesive socio-economic areas, but may not do so because of subjectivity in unit selection or neighbourhood change over time.

The population surface was aggregated at a 2500 m resolution to account for the spatial subjectivity built into the CT unit. This yields a surface with each grid cell containing the total population inside the cell boundary. The advantage of re-aggregating the CT-derived SD surface arises because the weighted surface is unlikely to have gaps in areas where the SD population is low. Gaps in the SD variable population inexorably reduce demand as clusters, generated via the pollution semi-variance. The re-aggregation thus ensures that the final demand surface represents both the population density and pollution variability. The weighting was implemented as a bivariate linear rescaling of the pollution semi-variance. This process conserved the total amount of demand in the unmodified semi-variance dataset, as per a slightly modified form of equation 2. In subsequent health studies this exposure assessment will assist with testing the association between onset of childhood asthma and traffic pollution in a case-control design. Consequently we augmented demand with populations of children six years of age or younger.

Computing Locations Using Demand

The discussion of computing demand does not address the issues of calibration, reliability or validation of the NO_2 predictions. For purposes of reliability, it is advisable to deploy two or more samplers at a single location; the measured value at a location is taken to be an average of the measurements at that location. A further level of accuracy is added to our network by calibrating the measurements against the collected MOE data. However, this also entails that the MOE stations must also be used as sampling locations in our network.

The remainder of this section details a technique for computing the locations of n number of monitoring stations, assuming that n is a specified constant before the computation. The computation of the locations begins by calculating the locational demand via a grid at the 500 m resolution. For Toronto, the centroid of each of the grid cell results in a lattice of 2537 potential locations, which we refer to as "candidate locations".

The goal of our L-A procedure is to select n primary station locations, both with respect to MOE

sites and to demand locations. In formulating this problem as a classic facility location problem, we constrain ourselves to problems solved using the ESRI's ARC/INFO software. This software offers two options: the P-Median Problem or P-MP (ReVelle and Swain, 1970) and the Attendance Maximizing Problem or AMP (Holmes et al., 1972).

The P-MP tries to place the n primary stations such that the sum of the demand times the distance from the demand location to its nearest monitoring station is minimized. The AMP is best described by analogy. We assume that the monitoring sites are stadiums. Each of the candidate locations contains the number of people equal to the "demand" at that location. In this analogy, the people travel to the closest stadium, but the probability of them attending a given event decreases linearly as the distance from the stadium increases. The essence of AMP is to maximize the total attendance of all stadiums (i.e., monitoring stations). Analogously, we seek to maximize attendance of pollution variability at our 100 sampling stations.

The AMP appears better suited for selecting sampling locations because of the decay rate in concentrations of NO_2 and other pollutants with distance from traffic source (English et al., 1999; Gilbert et al., 2002). We assume the demand at arbitrary locations j, farther away from the sampling location i, is less satisfied than the demand from a closer location k. This model also allows us to specify the maximum distance beyond which the monitoring station cannot measure. We posited, based on recent Canadian studies (Gilbert et al., 2002), that the correlation (i.e., semi-variance) is largely explained by values within the 300 m of location i. This was extended to assume that beyond 1.5 km there is a negligible correlation between any two points. The validation for this assumption is the measured decay rate of NO_2 around a major Canadian highway (Gilbert et al., 2002). This assumption was implemented in the AMP by setting the distance, at which demand or pollution semi-variance will "attend" a sampling location, to 1500 m.

The balance of the computation is performed using the L-A functionality of ESRI's ArcPlot module of ArcGIS. Specifically, we set the demand locations as the locations of the MOE stations that are assigned to the closest 500 x 500 m grid cell centroid and the candidates for n sampling locations. Each 500 x 500 m grid cell represents the sum of the 5 m resolution demand surface that intersects the 500 x 500 m cell area.

We set the optimization criteria to be the "Maximum Attendance (MaxAttend)" problem, and then ran the L-A function. Near-optimal or "heuristically optimal" solutions to these types of computationally intensive problems can be found in a reasonable amount of time using proven heuristic techniques. The Global Regional Interchange Algorithm (GRIA) (Murray and Church, 1994) is appropriate for large datasets because running time is linear with respect to n, which allows for computation with current desktop computing technology. The grid resolution affects the optimality of the solution. The use of a 500 m square grid of demand location was chosen as a problem of reasonable size for desktop computers given $n = 100$ and hence could be easily replicated by others.

2 - Results

Results of the LUR are displayed in Table 1. The Table shows that commercial, government and institutional, expressway (0-50 m), and expressway (50-200 m) are significant land-use and transportation variables in predicting NO_2 with the available dataset. Similar to other LUR results (Briggs et al. 2000), some coefficients take an unexpected sign (i.e., 0-50 is negative), but this appears to balance the other positive signs in the equation, and this model produced maximal prediction with mimimal bias (measured by the Mallaw's Cp statistic) compared to other models we tested. The pollution surface generated from this model had high pollution concentrations predicted in the vicinity of the expressways and relatively low pollution predictions in other areas.

Variable	Coefficient	Std. Error	t-value	Prob.>t	VIF
Constant	18.058	1.353	13.348	0.000	—
Commercial	5.223	2.080	2.511	0.029	1.0
Government/Institutional	1.748	1.065	1.641	0.129	1.1
Expressway (0-50m)	-592.725	228.883	-2.590	0.025	2.3
Expressway (50-200m)	253.155	68.532	3.694	0.004	2.4
	R-Sq 62.1%	Adj R-Sq 48.3%			

Table 1: Regression Results from Southern Ontario Data

Pollution values near expressways ranged from 29.5 to 1502 ppb, while in other areas the pollution ranged from 18.1 to 34.5 ppb. Given the range of the MOE monitoring concentrations and those noted in other studies (Hewitt 1991), such high levels are unrealistic. Yet, independent of the actual values, an important characteristic was preserved in the surface, namely the simple relative pollution variability caused by the different land uses – an indication that some areas have higher pollution variability than others. The variability was measured by the semi-variance using the obtained pollution surface. The unmodified semi-variance appears to have much the same characteristics as the pollution surface, with high values near expressways and low values in other areas.

Proximity to expressway features dominated sampling locations selected by the L-A model with the unmodified semi-variance, as seen in figure 1. In this area, 95% of the locations were assigned to areas that coincided with expressway features in the pollution model. The other 5% of the locations satisfied the attendance demand created by the surrounding expressways and consequently were located centrally.

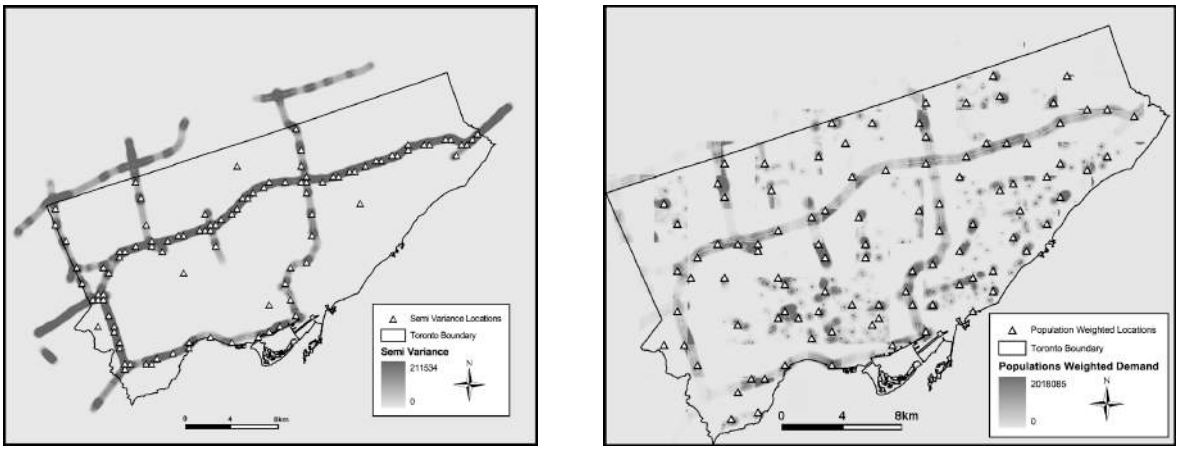

Figure 1: Comparison of Unmodified Sampling Locations to Population Weighted Locations

In contrast, the population weighting method (PWM) produced well-distributed monitoring network, as shown. There is a low-level clustering in the central west part of the city, an area with the highest aggregation of child populations.

It was necessary to ascertain the monitoring networks' capacity to represent key land use and transportation criteria once the L-A procedure was complete and alternative monitoring networks were configured. Measuring the representative capability of the network was performed with a simple pair-wise comparison of the land use, shown in figure 2, and transportation criteria (not shown) that intersect the initial buffer schema applied to the configured monitoring network.

Comparison values for locations produced from the unmodified semi-variance and PWM reveals that the PWM best represented the land use and transportation characteristics of all candidate sites. Not shown, the difference of means tests revealed significant differences between the candidates and monitoring locations in 6 of 10 land use and transporation categories for the unmodified demand, while only two categories were significantly different than the candidates for the PWM.

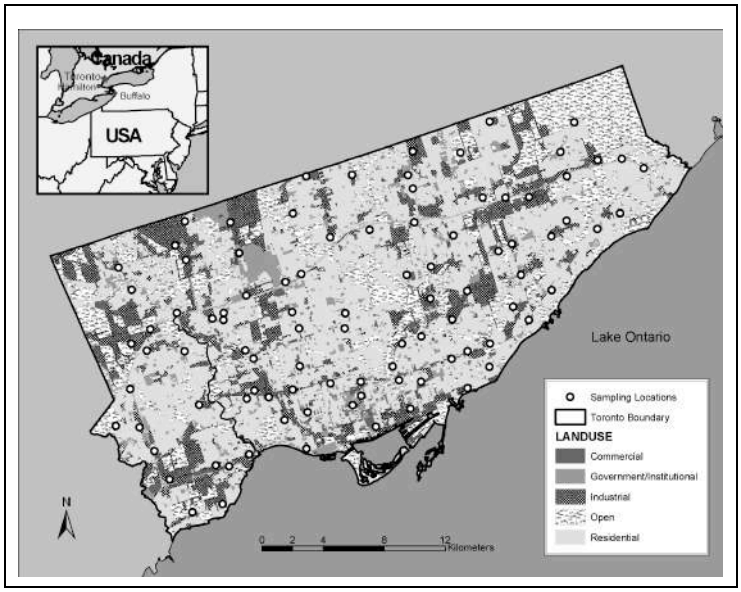

Figure 2: Sampling Locations in Toronto in Relation to Land Use

Conclusion

With the increasing need to understand the spatial distributions of air pollution at the intra-urban scale, the outlined method of locating air pollution monitors has proven to be an effective and systematic technique to maximize sampling coverage. The method offers flexibility to integrate an assortment of variables into the demand surface that can reconfigure the resulting monitoring network. In this application, the above-mentioned variable integration has been implemented with a socio-demographic weighting of children six years of age and under. As well, where we had to rely on sparse initial pollution data, the PWM ensured that the subsequent sampling locations would still be useful for human exposure assessment.

A total of 202 monitors have now been deployed in Toronto and in the neighbouring City of Hamilton. To further validate this method, we will replicate this process using these spatially extensive measured NO_2 data. We have implemented a similar procedure in Vancouver and will soon select locations for Montreal. This will allow for comparison of modelled results from a number of Canadian cities and will enable national-level health studies to be based on standardized procedures for establishing the monitoring network.

Acknowledgments

We are grateful to Health Canada and the Canadian Institutes of Health Research for funding this work. The first author is grateful to the Canada Research Chairs Program for supporting his research. We also thank Pat De Luca, Dan Crouse, Norm Finkelstein, and Chris Giovis for assistance with the GIS modelling.

References

Briggs D, Collins S, Elliott P, Fischer P, Kingham S, Lebret E et al. (1997): Mapping urban air pollution GIS: a regression-based approach. Int J Geographical Information Science, vol. 11, p 699-718.

Briggs D, de Hoogh C, Gulliver J, Wills J, Elliott P, Kingham S et al. (2000): A regression-based method for mapping traffic-related air pollution: application and testing in four contrasting urban environments. Sci Total Environ, vol. 253, p 151-167.

English P, Neutra R, Scalf R, Sullivan M, Waller L, Zhu L. (1999): Examining associations between childhood asthma and traffic flow using a geographic information system. Environ Health Perspect, vol 107, p 761-767.

Fotheringham AS, Brunsdon C, Charlton M. (2000): Quantitative Geography: Perspectives on Spatial Data Analysis, London, SAGE publications, 270 p.

Gilbert NL, Steib DM, Woodhouse S, Brook JR. (2002): Ambient nitrogen dioxide monitoring near a major highway using passive diffusion samplers. Epidemiology, vol. 13, p 5146-5147.

Goswami E, Larson T, Lumley T, Liu L-J S. (2002): Spatial characteristics of fine particulate matter: identifying representative monitoring locations in Seattle, Washington. J Air & Waste Management Assoc, vol. 52, p 324-33.

Hewitt CN. (1991): Spatial variations in nitrogen dioxide concentrations in an urban area. Atmospheric Environment, vol. 25B, p 429-434.

Hoek G, Brunekreef B, Goldbohm S, Fischer P, van den Brandt PA. (2002): Association between mortality and indicators of traffic-related air pollution in the Netherlands: a cohort study. Lancet, vol 360, n° 9341, p 1203-1209.

Holmes J, Williams FB, Brown LA. (1972): Facility location under maximum travel restriction: an example using daycare facilities. Geographical Analysis, vol 4, p 258-266.

Hosmer W, and Lemeshow S. (1989): Appiled Logistic Regression. New York: Wiley and Sons, 307 p.

Kukkonen J, Harkonen J, Karppinen A, Pohjola M, Pietarila H, Koskentalo T. (2001): A semi-empirical model for urban PM10 concentrations, and its evaluation against data from an urban measurement network. Atmos Environ 2001, vol 35, p 4433-4442.

Lebret E, Briggs D, van Reeuwijk H, Fischer P, Smallbone K, Harsemma H, Kriz, B, Gorynski P, Elliott P. (2002): Small area variations in ambient NO2 concentrations in four European areas. Atmospheric Environment, vol 34, p 177-85.

Mohammadian, A. (2002): Dynamic modelling of household automobile transactions within a microsimulation framework. Doctoral Dissertation, Department of Civil Engineering, University of Toronto, 174p.

Murray A, Church RL. (1994): Expanding spatial detail and restrictions in public sector location models. Paper presented at The Regional Science Association International, 41st North American Meetings, Ontario: Niagara Falls. 42 p.

ReVelle CS, Swain RW. (1970): Central facilities location. Geographical Analysis, vol 2, p 30-42.

Webster R, Oliver M. (1990) Statistical Methods in Soil and Land Resource Survey. Oxford University Press, Oxford. 316 p.

12th International Symposium "Transport and Air Pollution" / 12e Colloque international "Transports et pollution de l'air", Avignon, 16 -18 *June* / juin 2003
proceedings / actes, n°92, tome / Vol. 1, Inrets ed., Arcueil, France, 2003, p. 35-42

A study of trace metal concentration of urban airborne particulate matter and its role in free radical activity as measured by plasmid strand break assay

Justin Lingard*, Alison Tomlin *, Andrew Clarke*, Kate Healey, Alistair Hay**, Christopher Wild** & Michael Routledge****
*Energy and Resources Research Institute, University of Leeds, Leeds, LS2 9JT, UK
Fax + 44 113 256 7310 – email: fueast@leeds.ac.uk
**Molecular Epidemiology Unit, Academic Unit of Epidemiology & HSR, Algernon Firth Building, University of Leeds, Leeds, LS2 9JT, UK

Abstract
Epidemiological studies report a correlation between PM_{10} concentration and exacerbation of health effects. No clear evidence exists as to whether chemical toxicity, particle-size, or a combination of the two is responsible. This study aims to assess the influence of these factors on DNA strand breakage utilising size-fractionated roadside particulate samples. Samples were collected at two busy roadside and one urban background site. The concentrations of: Cr, Cu, Fe, Mn, Ni and Zn, were analysed by atomic absorption spectrometry. Based on average concentrations, Fe was found to be the most abundant element, predominantly concentrated in the coarser size range of 4.7-5.8μm. The other elements, present at much lower concentrations, were dominant in the smaller size fractions. Aqueous extracts of these size-segregated samples were used to measure the genotoxic effect of PM_{10} on DNA by plasmid strand break assay, showing that strand breaks were induced. PM_{10} in the smaller size fractions induced the highest levels of damage.
Keywords: *PM_{10}, urban particulates, size-fractionated, trace metals, DNA, plasmid strand break.*

Introduction

Elevated levels of roadside particulate matter due to transport sources are of concern due to its ability to penetrate deep into the lung and deliver variable concentrations of potentially harmful compounds to the site of gas-blood exchange. Although air quality standards are based on PM_{10} (particulate matter (PM) with a mass median aerodynamic diameter less than 10 μm) mass concentrations, research shows that exhaust PM consists of between 70-90% of particles, by number, with an aerodynamic diameter of <1 μm (Williams et al., 1989). These smaller particles can remain airborne for 10 days or longer (QUARG, 1996). Additionally, coarse particles generally deposit in the upper airways, whereas PM of <0.5 μm has the ability to pass and deposit in the respiratory tract (QUARG, 1996). Recently concern has also grown over the role of ultrafine particles, those with a diameter <50 nm, which are believed to provoke alveolar inflammation in susceptible individuals. Li et al. (1996), demonstrated that PM_{10} particles exhibit free radical activity that can cause DNA damage in vitro and inflammatory response in vivo. No clear evidence has yet emerged as to whether chemical toxicity, particle-size distribution, or a combination of the two is responsible for observed effects.

Trace metals are one source of chemical toxicity within PM. Their concentration in ambient air can be attributed to both natural and anthroprogenic processes and studies show that the concentrations of elements vary greatly (Lee et al., 1994). Naturally occurring elements typically occur in the coarser modes of urban PM_{10}. Metals can also be attributed to anthroprogenic activities and are typically found at elevated concentrations in urban areas, especially in the fine modes. Fe and Mn are both crustally and anthroprogenically derived and in urban areas can be attributed to soil, re-

suspended road dust, mechanical wear and combustion. Because of the range of sources, additional Fe and Mn may be found in both the fine and coarse modes of urban particles. Mn compounds have been used as lube oil and fuel additives (Pfeifer et al., 1999). Cr, Cu, Ni and Zn are principally anthroprogenically derived, although they do occur naturally in low concentrations. Ni and V are associated with fossil fuel combustion. Cu and Zn are released from both tyre and brake pad wear of automobiles. Other sources of Zn include coal combustion, smelting operations, paint, incineration and wood burning (Var et al., 2000).

Due to their anthroprogenic sources, there has been much interest generated in the potential deleterious effects of the trace metal component of respirable particles. Researchers have been keen to identify which metals are important with respect to the observed health effects. Numerous comparative studies exist of the effects of ultrafine (Uf) particles comprised of distinct elements. The instillation of Ag, Al_2O_3 & TiO_2 into the alveolar space of rats showed no effect for Ag, but similar inflammatory response for the latter two (Oberdöster et al., 1992). Acid washing to remove surface Fe has been demonstrated to reduce the inflammation and airway hyper-reactivity of particles (Tepper et al., 1994). Normal human bronchial epithelial (NHBE) exposed to residual oil fly ash (ROFA) containing Fe, Ni & V caused the release of inflammatory mediator proteins: IL-6, IL-8 and TNF-α. It is hypothesised that the release of these inflammatory mediators, coupled with trace metals, may further contribute to the toxic effects of ROFA (Carter et al., 1997). This is reinforced by studies conducted by Murphy et al., 1998, which concluded that the surface chemistry of a particle is more important than the ultrafine size in explaining its biological reactivity. On the other hand, work undertaken by Donaldson et al, (2000), found that Uf particles comprised of classically low-toxicity, low-solubility materials such as carbon black (CB) and titanium oxide (TiO_2) are more inflammogenic than their larger but still respirable counterparts. The cut-off size for this increased toxicity lay somewhere between 65 and 202 nm. The addition of soluble transition metals to the surface of UfCB, namely $FeSO_4$ and $CuSO_4$, showed that although they were not necessarily involved in the initiation of inflammation, oxidative stress was important. Their role could be additive or synergistic when found within Uf. It has been suggested that Uf particles present a relatively large particle number and surface area to the lung per unit of deposited mass of particles compared to larger respirable particles. This provides the opportunity for surface chemistry to have a profound effect, particularly free radical or transition metal-mediated Fenton chemistry, leading to the generation of oxidants (Donaldson et al., 1998). Additional to the inflammatory responses observed in the airway, Uf particles may be able to translocate about the human body, possessing the ability to cross the air-blood barrier. Uf ^{99m}Technetium labelled carbon particles (<100 nm) have been shown to diffuse rapidly into the systemic circulation, exerting a direct influence on the heart and vessels, providing further explanation of the observed cardio-vascular morbidity and mortality corresponding to ambient particulate matter (Nemmar et al., 2002). This previous work points to the need for ambient air studies resolving both particle size and possible toxic compound concentrations to study the role of particle size and metal-mediated DNA damage.

The aims of this study are two-fold: firstly, to collect and analyse the concentration of six trace metals, namely: Cr, Cu, Fe, Mn, Ni and Zn in size-fractionated samples (0.1-10 μm) of urban PM_{10} from typical urban roadside and a background sites. This allows an assessment of the size fractions in which these metals are predominantly found. The second aim is to link these studies to genotoxic effects in order to determine the factors influencing certain health impacts. This is achieved by assessing the ability of PM_{10} to induce DNA strand breakage (a measure of oxidative DNA damage) using the plasmid strand break assay.

1. Method

In this study the investigation of six trace, transition metals: Cr, Cu, Fe, Mn, Ni, and Zn was undertaken using atomic absorption spectrometry (AAS) in size fractionated samples of urban PM_{10} collected at three sites in and around Leeds City Centre, UK. The practical and extraction methodology follows that laid out in Clarke et al. (1996b & 1999). Three sites were established;

two sites were UK urban roadside, the further at an urban background site. At each site a Graseby-Andersen Mark II 1 ACFM Non-Viable Ambient Particle Sizing Sampler, allowed the size-fractionated collection of PM_{10}. At the roadside sites the impactors were situated at a distance of 1 m from the road and at an elevation of 2 m. The two roadside sites were chosen as they have a high traffic density, carrying >25,000 vehicles per day. The first site at Vicar Lane (Grid Ref. SE303334) is part of an open plaza and forms part of the Public Transport Box in Leeds City Centre. The traffic is therefore dominated by diesel fuelled buses, and to a lesser extent, through traffic with gasoline SI engines. Two impactors were sited at this location and run in tandem. The first was used to collect samples for trace metal analysis, the second to collect gravimetric samples, which were subsequently used, for the plasmid strand break assay. The second site, situated in Headingley (Grid Ref. SE279360), adjacent to the A660 (Otley Road) is one of the main arterial routes into the City with peak rush hour flows of over 3000 vehicles per hour of which 7% are estimated to be diesel (Clarke et al., 1996a). The site is enclosed on both sides by two-storey buildings. Traffic flow for the rest of the day is in the region of 1700 vehicles per hour with 9% estimated to be diesel (Clarke et al., 1996a). Both buses and heavy goods vehicles constitute the diesel vehicles found at this site. The third impactor was sited on the fifth floor of the Houldsworth School of Applied Science building at the University of Leeds at an elevation of about 25 m (Grid Ref. SE292350). This acts as a measure of background concentration of trace metals found in urban PM_{10}.

The size-fractionated samples of PM_{10} were collected onto a PTFE (Teflon) substrate, which was placed on top of the stage collection plates and used for the trace metal analysis. Quartz fibre filters (Whatman Filters) were employed to collect gravimetric samples of PM_{10}, due to their lower mass, and were subsequently used in the biochemical experiments. The back-up filters (BF) are cellulose nitrate substrate (Whatman Filters). Three sites were operated simultaneously during the period of July 2001 to November 2002, allowing 11 (3 x 14 days and 8 x 28 days) sets of samples to be collected at the roadside and 8 (8 x 28 days) at the background. The flow rate through the pumps was 1 cubic foot per minute (25.47 $lmin^{-1}$). The impactors were operated at ambient temperature, meaning that the reported size distributions for particles are as they exist in the atmosphere, i.e. either solid particles or droplets. The concentrations reported are based on gas flow at ambient temperature and are not corrected to a reference temperature (Clarke et al., 1999). Batch extractions were performed on the sets of disks from each site via acid digestion following the method laid-out in Clarke et al. (1996b). A control solution was prepared for every set of samples. Graphite furnace atomic absorption spectrometry (GFAAS) was employed in the case of Cr, Cu, Mn, and Ni utilising the Varian AA10 coupled with a GTA97. A Varian AA10 provided flame analysis of Fe and Zn.

Six batches of gravimetric samples were used in plasmid strand break assay, with three experiments performed for each batch. This assay detects the induction of DNA strand breaks by measuring the conversion of supercoiled plasmid DNA to the relaxed form produced when the DNA is nicked. Particulates were extracted from the filters in a final volume of 50 µl water and 5 µl was incubated with 2 µg plasmid DNA for 60 hours. Plasmid DNA was visualised by agarose gel electrophoresis with ethidium bromide staining. Supercoiled and relaxed DNA was quantified using BioRad QuantityOne Software.

2. Results and Discussion

Roadside sampling: The mean, minimum and maximum concentrations of six transition metals: Cr, Cu, Fe, Mn, Ni and Zn, across all samples for each site are shown in table 1.

Transition metal	Site	Minimum concentration (ngm^{-3})	Maximum concentration (ngm^{-3})	Average concentration (ngm^{-3})	50th percentile size range (µm)
Cr	OR	2	82	15	1.1
	VL	2	55	13	2.1
	HS	1	6	4	1.1
Cu	OR	3	59	26	4.7
	VL	4	105	29	4.7
	HS	1	12	7	3.3
Fe	OR	200	733	344	5.8
	VL	288	586	416	5.8
	HS	67	675	196	4.7
Mn	OR	3	32	12	3.3
	VL	6	19	12	4.7
	HS	1	10	4	3.3
Ni	OR	1	62	12	1.1
	VL	2	24	6	2.1
	HS	2	3	2	2.1
Zn	OR	28	247	103	3.3
	VL	32	252	106	2.1
	HS	49	120	83	3.3

Table 1: Minimum, maximum, average concentrations and 50th percentiles of six transition metals found in urban PM_{10} at three sites in Leeds, UK

The table shows that significant enhancement in both mean and maximum concentrations occurs for all metals at the two roadside sampling sites Otley Road (OR) and Vicar Lane (VL) compared to those at the urban background site, the Houldsworth School (HS). This suggests roadside contributions from traffic-related sources and re-suspended particles due to ground level winds and traffic movements. This is confirmed for three of the trace metals in figure 2, where their presence in the coarse modes is shown to be much higher at the two roadside sites than for the background site which is at roof-top level. Despite the difference in the traffic profiles of the two roadside sites, there is little difference in their average concentrations of trace metals. Similarly, the 50th percentile size range (i.e. the diameter below which 50% of the total PM_{10} mass exists) of the trace metals is in good agreement with Cr, Ni, and Zn found to be dominant in the finer size fractions and Mn, Cu and Fe, in the coarser ranges. The only slight differences are that Ni is found to be higher at OR where petrol vehicle sources are dominant, possibly due to the presence of Ni-based catalysts used with SI engines. Calculation of the percentage of trace metal in each size stage was achieved by normalising the concentration for a particular stage against the total concentration of the element found in the PM_{10}. Figure 1 shows the percentage cumulative distributions for the trace metals by site allowing examination of the predominance of specific elements within distinct size ranges. Based on average concentrations, Fe is found to be the most abundant element, typically 196-416 ngm^{-3}. In a review of European urban trace metal concentrations in PM_{10} presented in Lee et al. (1994), concentrations of Fe ranged from 92.5 to 1430 ngm^{-3}, with elevated concentrations due to enhancements from localised industrial sources. Figures 1 and 2 show that, by mass, Fe is predominantly concentrated in the coarser size range, above 4.7-5.8 µm, at the background site, reinforcing the theory that it derives from crustal sources. The placing of Fe in the coarser size range concurs with the work of Clarke et al., 1996b & 1999, who carried out similar measurements at sites around Leeds. Enhancements in the concentration of Fe at the two roadside sites occur in both the coarse and fine modes compared to the urban background site, with Fe showing high concentrations in the finer modes compared to other compounds, see figure 2. The sources may be ascribed to mechanical wear and grinding in engines, the coarse mode, and inherent Fe compounds found in engine fuel which may be released through exhaust gas emissions, the finer modes.

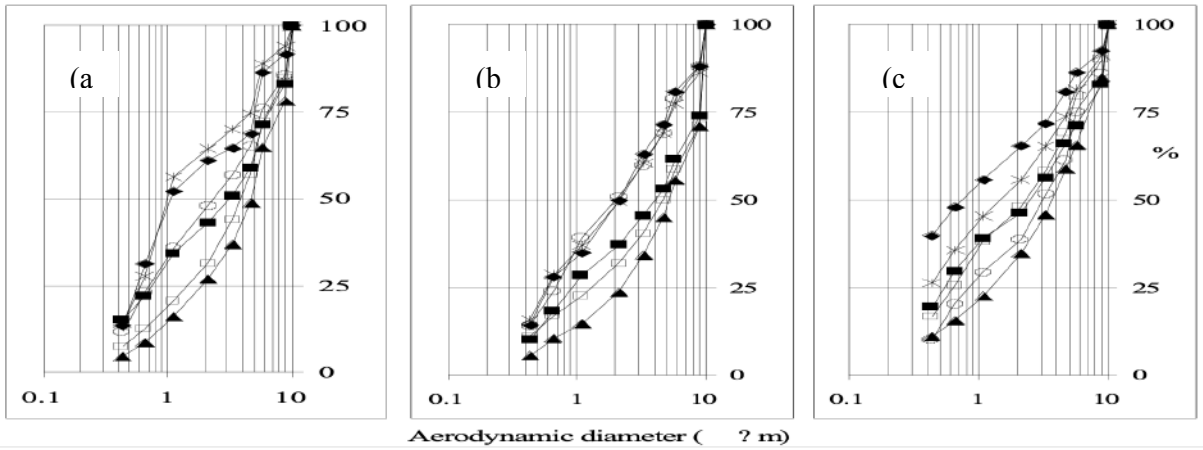

Figure 1: The average % cumulative distribution of trace metals by mass with aerodynamic diameter at (a) OR, (b) VL, (c) HS (—♦— Cr, —□— Cu, —▲— Fe, —■— Mn, —○— Ni, —x— Zn)

Both Cr and Ni are dominant in the finer modes, with all three sites showing that 50% by mass was found in the size fraction smaller than 1.1-2.1 μm. The OR site shows a particularly steep increase in both these metals in the finest three modes (<1.1 μm), which could be attributed to engine emissions from local traffic sources. The elevation in Cr concentration at the roadside sites persists throughout the size-fractionated samples of PM_{10} as shown in figure 2. The literature offers no specific engine combustion source and previous localised enhancements have been due to industrial processes. On the otherhand, Ni is typically derived from catalysts and continuously regenerating particle traps (CRT) used in SI and diesel vehicles respectively, to control engine emissions. Furthermore, organo-metallic compounds of Fe and Ni are used as fuel and lube oil additives, though not extensively (Richards, 2001). The mean concentration of Mn at OR is the same as that at VL, although the maximum is higher. The concentration is elevated at the roadside throughout the size ranges, although in the last three stages (5.8-10 μm), the roadside sites show a much higher level of enhancement over the HS site. Mn is typically compounded with Fe to produce steel, and used as an oil additive $Mn_3(PO_4)_2$, corresponding to possible enhancement in the both the coarse and fine modes. The profile for Mn is similar to that for Fe and Cr with higher average levels in the larger size fractions at VL compared to OR. This suggests possible sources from road-dust re-suspension. The Vicar Lane site is near an open junction and so may experience higher wind-speeds and therefore turbulence, than at the Otley road site which lies within a fairly narrow street. The proximity to the junction and to a bus terminal may also increase the level of particle re-suspension due to vehicle movements at the VL site. Elevated levels of Mn in the smallest size fraction at OR suggest engine emission sources due to local traffic, which consists of predominantly petrol vehicles. The enhancement of Zn at the roadside sites, shown by the greater maximum concentrations, is possibly due to tyre wear. This arises from the Zn content of the tyre rubber, which is approximately 2% ZnO by weight (UK NAEI, 2002). The high minimum concentration for Zn at HS was believed to be to the presence of Zn based paint used to waterproof and seal the building roof. The average concentrations of Cu at both OR and VL are similar, 26 and 29 ngm^{-3} respectively. The greatest maximum concentration of 105 ngm^{-3} was measured at VL. Comparatively high concentrations were observed in both the smallest and largest size fractions for Cu at VL. Elevated concentrations of Cu at roadside sites are typically associated with brake pad wear (Var et al., 2000). The site at Vicar Lane was situated close to one of the main bus boarding and alighting stops, around the City centre, hence the constant start-stop of vehicles may account for the observed elevated concentrations.

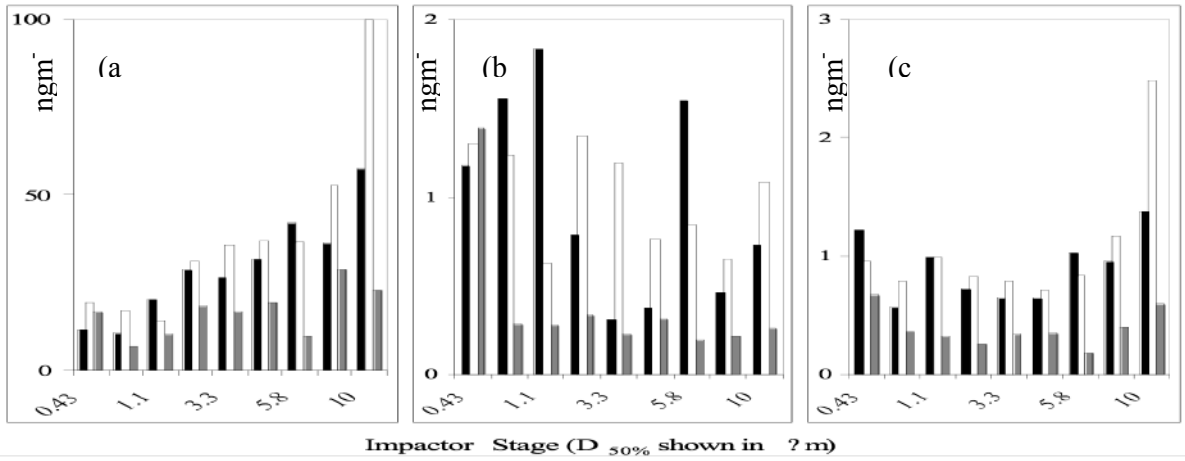

Figure 2: The average concentration (ngm^{-3}) of trace metals within each size stage at ▇ OR, □ VL, ▒ HS for (a) Fe, (b) Cr ,(c) Mn

Particle mediated free radical damage to plasmid DNA: Aqueous extracts of these size-segregated samples were used to measure the genotoxic effect of PM on DNA in a plasmid strand break assay. Oxygen radicals generated in solution can damage DNA to induce, among other lesions, single strand breaks. When a single strand break is introduced into supercoiled plasmid DNA, the DNA relaxes. This change in form of plasmid DNA is easily detected by gel electrophoresis as relaxed form plasmid migrates more slowly through the agarose gel than does supercoiled plasmid. Figure 3a shows that PM collected in the smaller size range caused the greatest depletion of supercoiled DNA. One problem that we recognise with these experiments is the difficulty in assessing the efficiency of extracting the PM from different filters. The data presented in figure 3a assumes an extraction efficiency of about 40%. Attempts were made to assess the extraction efficiency by measurement of the extracted mass. However, these measurements were affected by the presence of filter fibres in the extracted material. Consequently, it was not possible to accurately determine the extraction efficiency for the PM samples. Assuming that the extraction efficiency between filters was similar, then figure 3a shows that the greatest level of DNA breakage was induced by the finest fraction of PM collected. This is in agreement with previous work (Donaldson et al., 2000). The damage caused by the particles on the BF ($D_{50\%}$=0.43 µm) appears to be more than 50% the amount caused by those collected on stage 7 ($D_{50\%}$=0.65 µm) and three to five times the levels observed in stages 0 to 6. The error bars highlight some variation, derived from the repetitions of the DNA plasmid strand break assay experiments.

Several explanations may exist to explain how particle size may influence the observed damage. Firstly, as shown in figures 1 and 2, several of the transition metals were concentrated in the smaller size fractions and therefore may form a larger fraction of the total particle mass for small particles. Additionally, as pointed out by Murphy et al. (1998), the surface chemistry of particles may be more important than the Uf size in explaining its biological activity. Sub-micron particles have a larger surface area to mass ratio than coarse particles, with the surface area to mass ratio proportional to 1/r. This would allow for a greater surface of contact for any compound adsorbed on the particle for it to interact with a biological surface. In the case of the present study this would allow any metals present adsorbed on the finer particles a greater opportunity to pass into the extract solution. In order to test this hypothesis, the concentration of Fe in the extracted samples was analysed by AAS and compared with that from the original samples. The influence of possible traces of Fe in the filter itself was accounted for by analysing a set of similarly extracted blank filters. Figure 3b shows the extraction efficiency of Fe for each stage. The figure shows a higher efficiency for the smaller size stages, supporting the theory that available surface area plays an important role. The increase in metals in solution associated with finer particles may offer an explanation to the observed increase in damage to DNA. Similar work conducted by Donaldson et al., (1996) with PM_{10} extracts from tapered element oscillating microbalance (TEOM) from an urban site in Edinburgh, UK, showed PM_{10} mediated damage of supercoiled DNA. This was ascribed to the hydroxyl radical, as inhibition

was achieved by the addition of mannitol, a hydroxyl radical scavenger. The work also showed that the samples of PM_{10} contained substantial amounts of Fe^{3+} as measured spectrophotometrically, and that the inclusion in the assay of desferrioxamine-B (DSF-B), an effective iron chelator was effective in protecting against particulate induced plasmid damage.

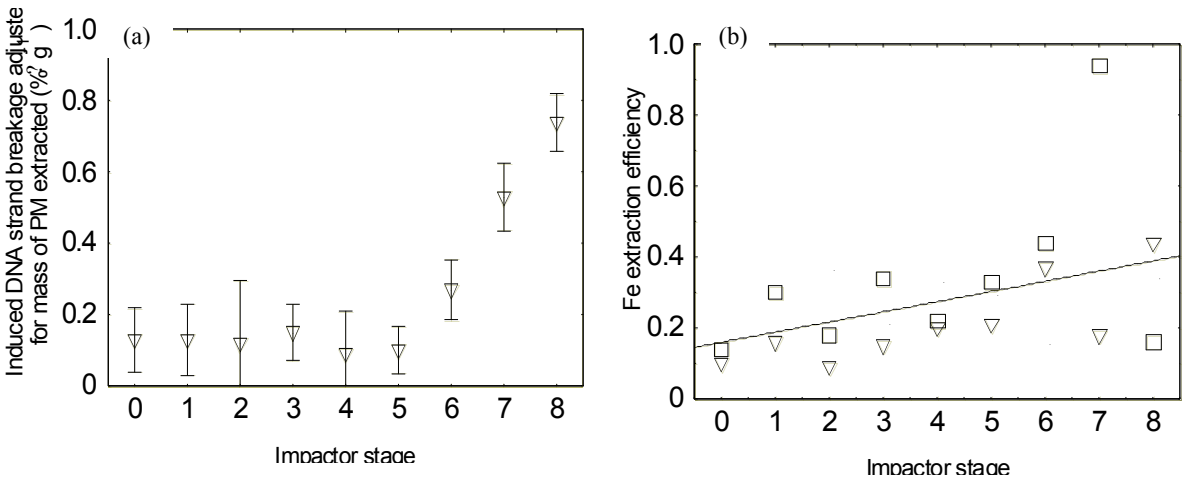

Figure 3: (a) the amount of induced DNA strand breaks for the mass of PM extracted, (b) extraction efficiency for Fe vs. impactor stage

Conclusions

The study has shown that at urban roadside sites there is a marked increase in the concentration of the trace metals studied: Cr, Cu, Fe, Mn, Ni, and Zn when compared to an urban background site. Fe is found at higher concentrations and predominantly found in the coarse mode. The other elements are typically found in the finer fractions, but at lower concentrations. Their presence in the finer mode at the roadside locations would suggest significant transport sources. Aqueous extracts of size-fractionated samples of urban PM_{10} have been shown to induce strand breakage in plasmid DNA, with the greatest damage caused by the sub-micron particles. In this assay DNA damage is almost certainly due to oxygen radicals generated in the aqueous solution, with metal ions being the most likely mediator of oxygen radical formation. Having controlled for mass, the damage is believed to be a function of the greater available surface area of the smaller particles and subsequent effects on surface chemistry.

Acknowledgements

The authors would like to thank Dave Cherry and Richard Crowther of the West Yorkshire Highways Department and Christopher Hill of Leeds City Council's Department of the Environment for their permission and assistance with the establishment of the roadside sites. JL & KH are funded by EPSRC & MRC PhD studentships respectively. Work presented here was supported by an EPSRC JIF award to the LANTERN consortium.

References

Clarke, A. G., Chen, J. –M., Pipitsangchand, S., & Azadi-Bougar, G. A. (1996a): Vehicular particulate emissions and roadside air pollution. Sc of the Tot Env, vol. 189/190, p. 417-422.

Clarke, A. G., Andrews, G. E., Azadi-Boogar, G. A., Bartle, K. D., Talebi, S. M., & Askey, S. A. (1996b): Final report to the DoE on the sources and chemistry of atmospheric particles. EPG/1/5/44, November 1996.

Clarke, A. G., Azadi-Boogar, G. A., & Andrews, G. E. (1999): Particle size and chemical composition of urban aerosols. Sc of the Tot Env, vol. 235, p. 15-24.

Donaldson, K., Li, X. Y., & MacNee, W. (1998): Ultrafine particle mediated lung injury. J Aero Sc, vol. 5/6, p. 553-560.

Donaldson, K., Stone, V., Gilmour, P. S., Brown, D. M., & MacNee, W. (2000): Ultrafine particles: mechanisms of lung injury. Phil Trans of the Royal Soc (London), vol. A358, p. 2741-2749.

Graseby-Andersen (1985): Operating manual for Andersen 1 ACFM non-viable ambient particle sizing samplers. Graseby-Andersen, Atlanta.

Lee, D. S., Garland, J. A., & Fox, A. A. (1994): Atmospheric concentrations of trace elements in urban areas of the United Kingdom. Atm Env, vol. 28, p. 2691-2713.

Leeds City Council (2002): Air Quality Review and Assessment. http://www.leeds.gov.uk/downloads/2001727_89298648.pdf.

Li, X. Y., Gilmour, P. S., Donaldson, K., & MacNee, W. (1996): Free radical activity and pro-inflammatory effects of particulate air pollution (PM_{10}) in-vivo and in-vitro. Thorax, vol. 51, p. 1216-1222.

Murphy, S. A., BéruBé, K. A., Pooley, F. D., & Richards, R. J. (1998): The response of lung epithelium to well characterised fine particles. Life Sc, vol. 62, p. 1789-1799.

National Atmospheric Emission Inventory (NAEI) (2002), 'Actions on zinc emissions', http://www.naei.org.uk/pollutantdetail.php.

Nemmar, A., Hoet, P. H. M., Vanquickenborne, B., Dinsdale, D., Thomeer, M., Hoylaerts, M. F., Vanbilloen, H., Mortelmans, L., & Nemery, B. (2002): Passage of inhaled particles into the blood circulation in humans. Circulation, vol. 105, p. 411-414.

Oberdöster, G., Ferin, J., Gelein, R., Soderholm, S. C., & Finkelstein, J. (1992): Role of the alveolar macrophage in lung injury: studies with ultrafine particles. Environ Health Per, vol. 97, p. 193-199.

Pfeifer, G. D., Harrison, R. M., & Lynam, D. R. (1999): Personal exposure to airborne metals in London taxi drivers and office workers in 1995 and 1996. Sc of the Tot Env, vol. 235, p. 253-260.

Quality of Urban Air Review Group (QUARG), (1996): Airborne particulate matter in the United Kingdom 3rd Report. HMSO, London.

Richards, P. (2001): Fuel borne catalysts for DPF regeneration – In "University of Leeds short course notes - Diesel particulate and NOx emissions", Department of Fuel and Energy, University of Leeds.

Seaton, A. (1995): Particulate air pollution and acute health effects. Lancet, vol. 345, p. 176-178.

Talebi, S. M. (PhD Thesis 1996): Instrumental analysis of metals in the urban air. University of Leeds.

Tepper, J. S., Lehmann, J. R., Winsett, D. W., Costa, D. L., & Ghio, A. J. (1994): The role of surface-complexed iron in the development of acute lung inflammation and airway hyperresponsiveness. Am J Resp and Crit Care Med (Supp), vol. 149, nº 4, part 2.

Var, F., Narita, Y., Tanaka, S. (2000): The concentration, trend and seasonal variation of metal in the atmosphere in 16 Japanese cities shown by the results of National Air Surveillance Network (NASN) from 1974 to 1996. Atm Env, vol. 34, p. 2755-2770.

Williams, D. J., Milne, J. W., Roberts, D. B. (1989): Particulate emissions form 'In-Use' vehicles, Part I – spark ignition engines. Atm Env, vol. 23, p. 2639-2645.

12th International Symposium "Transport and Air Pollution" / 12e Colloque international "Transports et pollution de l'air", Avignon, 16 -18 *June* / juin 2003
proceedings / actes, n°92, tome / Vol. 1, Inrets ed., Arcueil, France, 2003, p. 43-50

Distribution de l'exposition de la population urbaine à des polluants particulaires et gazeux génotoxiques et évaluation du risque de cancer - Étude GENOTOX'ER –

Éléna Nerrière[1], Denis Zmirou-Navier[2], Olivier Blanchard[3], Isabelle Momas[4], Yvon Le Moullec[5], Joël Ladner[6], Hervé Guegan[7], Michel Joyeux[8]
[1] Institut de veille sanitaire, DSE, 8 quai Bir Hakeim, 94 415 Saint Maurice,France
[2] INSERM U420, Fac de médecine, 9 avenue de la Forêt de Haye, 54 505 Nancy, France
[3] INERIS, Parc Technologique ALATA, 60 550 Verneuil-en-Halatte, France
[4] Faculté de pharmacie Paris 5, 4 avenue de l'observatoire, 75 006 Paris, France
[5] Laboratoire d'Hygiène de la ville de Paris, 11 rue George Eastman, 75 013 Paris, France
[6] Département Epidémiologie et Santé Publique, CHU, Rouen, France
[7] ARCANE-CENBG, Le Haut-Vigneau, BP 120 33 175 Gradignan cedex, France
[8] Ecole Pratique des Hautes Etudes et INSERM, 9 av de la Forêt de Haye, 54 500 Nancy.

Résumé
Le programme Genotox'er est conduit dans quatre agglomérations urbaines françaises (Paris, Rouen et Strasbourg, après une étude pilote à Grenoble en 2001) en collaboration avec les réseaux de surveillance de la qualité de l'air (Airparif, Air Normand, Aspa et Ascoparg). Dans chaque site, 60 à 90 volontaires enfants et adultes, portent pendant 48 heures un appareillage multipolluants (Chempass modèle 3400) au cours de deux saisons différentes. Dans chaque agglomération, les volontaires vivent dans 3 différents secteurs contrastés en terme de pollution (proximité au trafic automobile, fond urbain et secteur industriel). Le dispositif prélève simultanément NO_x, benzène, $PM_{2.5}$ et PM_{10} dont les constituants cancérogènes sont analysés : les métaux par la technique PIXE et les HAP par CHPL. Le test des comètes est utilisé pour quantifier le potentiel génotoxique d'extraits organiques issus des particules collectées. Les résultats descriptifs préliminaires semblent montrer des réponses plus fortes aux tests dans les secteurs exposés au trafic automobile.
Mots-clés : *pollution atmosphérique urbaine, exposition personnelle, $PM_{2.5}$ et PM_{10}, NO_2, NO_x, benzène, métaux, HAP, génotoxicité.*

Abstract
Several recent epidemiological studies suggest that the risk of cancer is increased for people who live in geographical areas affected by atmospheric pollution. The Genotox'er programme is intended to characterise the exposure to the fine particles incriminated in these effects. The work is carried out in four French cities (Paris, Rouen and Strasbourg, after a pilot study in Grenoble in 2001) with the co-operation of the air-quality monitoring networks (Airparif, Air Normand, Aspa and Ascoparg). At each site, 60 to 90 children and adults, all volunteers, carry a multi-pollutant system for 48 hours (Chempass model 3400). Each volunteer takes part twice in two different seasons (summer /winter). In each center, the volunteers live (home and work/school) in 3 different sectors contrasted in terms of pollution (the first highly exposed to motor traffic, the second of basic urban type, the third more industrial). This system allows simultaneous sampling of NO_x, benzene, $PM_{2.5}$ and PM_{10}. The particles carcinogenic components are analysed: the metals by the PIXE technique and the PAHs by HPLC. The comet test is used to quantify the genotoxic potential of organic extracts obtained from the particles collected. This research protocol will make it possible to evaluate how the quantity and the chemical composition of the particles vary between the subjects according to the collection sector and to their exposure to automobile pollution. The preliminary

descriptive results seem to show stronger test answers in sectors exposed to motor traffic. The results of the Grenoble and Paris campaigns, the Rouen summer phase, will be presented at the conference, including a total of 210 subjects.
Key-words: *urban air pollution, personal exposure, $PM_{2.5}$ and PM_{10}, NO_2, NOx, benzene, metals, PAHs, genotoxicity.*

Introduction

Plusieurs études épidémiologiques suggèrent que le risque de cancer, en particulier du poumon, est accru pour les personnes résidant dans des zones géographiques affectées par la pollution atmosphérique (Barbone et coll 1995, Beeson et coll 1998, Laden et coll 2001, Nyberg et coll 2000, Pope et coll 2002). Le rôle cancérogène de la pollution atmosphérique, et notamment des particules, est sans doute pour partie associé aux composés génotoxiques véhiculés, tels que certains métaux particulaires (Fernandez et coll 2001, 2002) et les Hydrocarbures Aromatiques Polycycliques (HAP) (Ares et coll 2000, Burgaz et coll 2002, Spinosa et coll 1999, Iwai et coll 2000, Kyrtopoulos et coll 2001). Les émissions de particules ultra-fines par les moteurs de type diesel pourraient jouer un rôle dans cet excès de risque en population générale, si peuvent être extrapolés les résultats des travaux toxicologiques et épidémiologiques en milieu professionnel (Bhatia et coll 1998), mais les composés métalliques et organiques liés au chauffage urbain et aux activités industrielles sont également incriminés.

L'étude Genotox'er se propose de caractériser la distribution des expositions personnelles de populations urbaines françaises à certains métaux et composés organiques cancérigènes particulaires ou gazeux (benzène) selon les caractères des lieux de vie (sites industriels, présence de sources mobiles proches, situations de pollution urbaine de fond...). Ce travail permet une analyse du potentiel génotoxique des particules atmosphériques prélevées en fonction des caractéristiques des lieux de leur collecte et de leur composition chimique.

1 - Méthodes

L'étude multicentrique est réalisée dans différents sites urbains et industriels, contrastés en termes de qualité de l'air et de sources d'émission. Ces sites ont été retenus en fonction du programme pilote de l'ADEME (Agence De l'Environnement et de la Maîtrise de l'Energie) sur les nouveaux polluants à surveiller d'après la Directive cadre de l'Union Européenne de 1996. Chacun fait l'objet de 2 campagnes de mesures : de février à mars et de mai à juillet. Il s'agit des agglomérations de Grenoble (étude pilote en 2001), Paris (2002), Rouen (2002 et 2003) et Strasbourg (2003). L'étude porte sur des enfants de 6 à 12 ans non exposés au tabagisme passif au domicile, ainsi que sur des adultes non-fumeurs non exposés professionnellement. Trois zones sont déterminées a priori, dans chaque agglomération : (i) « l'hyper-centre », fortement marqué par le trafic automobile ; (ii) une zone représentative du fond urbain ; (iii) une zone influencée par des émissions industrielles. Les profils d'activité industrielle des sites sont différents : pétrochimie à Grenoble, stockage d'hydrocarbures à Paris et industries lourdes à Rouen. Dix enfants et dix adultes (15 à Paris) sont recrutés par zone, avec le souci de minimiser la variance des expositions au sein de chaque strate (zone au sein de l'agglomération), tout en la maximisant entre strates. Le recrutement des 60 (90 à Paris) sujets se fait sur la base du volontariat, par le biais notamment des écoles.

La mesure de l'exposition personnelle aux polluants, réalisée pendant 48 heures, utilise le dispositif développé par le département des sciences de l'environnement de l'Ecole de Santé Publique de Harvard : le modèle Chempass 3400® (Demokritou et coll 2001), permettant de prélever en parallèle $PM_{2.5}$, PM_{10}, benzène, NO_2 et NO_x. L'appareillage, installé dans un sac à dos, comporte une pompe portative BGI® (modèle 400) fournissant un débit en chaque tête de prélèvement de 1,8 L/mn. Les particules sont prélevées sur filtres Téflon (Gelman®, diamètre 37mm, porosité 2 μm). Les pesées des filtres vierges et échantillonnés sont réalisées après déionisation (type Multistat EI-RN®) et sont suivies d'une mesure réflectométrique (indice de fumée noire) indicatrice de la teneur en suies de combustion des particules (Kinney et al 2000, Roemer et van Wijnen 2001). Le benzène est prélevé

par diffusion passive au moyen d'un tube Radiello Perkin Elmer (Gonzales-Flesca et coll 1999) et les NO_x par badges passifs Ogawa®.

Les teneurs en éléments minéraux, notamment en métaux cancérigènes, sont analysées par la technique physique PIXE (Particle Induced X-ray Emission) par le laboratoire ARCANE-CENBG (Guégan et coll 2000). Les teneurs en HAP sont déterminées par l'INERIS (méthode de référence du NIOSH) après extraction aux ultra-sons par acétonitrile et analyse par chromatographie liquide à haute performance (CLHP). La moitié de chaque extrait, après évaporation et reprise au DMSO, est envoyée à l'équipe INSERM de Nancy, chargée de l'analyse de la génotoxicité par le test des comètes. Ce test d'altération primaire de l'ADN (avec blocage enzymatique et temps d'incubation de 24 heures) permet donc de caractériser le potentiel génotoxique des extraits organiques des particules. En parallèle des campagnes de métrologie personnelle sur chacun des sites, les trois stations fixes de surveillance de la qualité d'air correspondant aux secteurs d'étude sont équipées de façon à mesurer les mêmes polluants : $PM_{2.5}$, $PM_{10,}$ NO_x et benzène.

2 – Résultats

Le tableau 1 donne les expositions personnelles moyennes en $PM_{2.5}$ et PM_{10} et les pourcentages de réflectance associés pour chacun des sites d'étude et de leurs sous secteurs lors 2 saisons. Le nombre total d'individus explorés est précisé dans la 1ère colonne. Les valeurs les plus fortes en particules sont obtenues dans le secteur industriel pour les 2 saisons à Grenoble, dans le secteur industriel en hiver et dans le secteur de proximité au trafic en été pour l'Ile de France, et, paradoxalement, dans le secteur de fond pour Rouen. Pour les 3 secteurs confondus, elles sont légèrement plus élevées en hiver qu'en été pour les 2 sites Grenoble et Ile de France, et surtout en zone industrielle. Les pourcentages de réflectance, permettent d'apprécier la noirceur d'un filtre, associée plus spécifiquement aux suies de combustion. La réflectance d'un filtre vierge est de 100 %, celle d'un filtre empoussiéré est d'autant plus faible que sa teinte se rapproche du noir absolu dont la réflectance est nulle. Les résultats montrent que les filtres à particules les plus noires sont quasiment toujours ceux portés par les volontaires des secteurs de proximité au trafic automobile.

Les expositions personnelles en benzène (tab. 2) les plus élevées concernent les secteurs industriels pour Grenoble (2 saisons), l'Ile de France (été), et le secteur de proximité au trafic pour la phase hivernale en Ile de France. Les valeurs pour le NO_2 sont systématiquement plus élevées dans le secteur de proximité au trafic automobile.

Pour les teneurs en minéraux des particules, trois sont présentés ici : nickel, arsenic et plomb dont deux sont cancérigènes (Ni et As). Il convient de préciser que sur l'ensemble des prélèvements effectués aucun n'a dépassé en ng/m^3 les futurs seuils réglementaires pour le Ni, l'As et le Pb. Les pourcentages massiques (figure 1) des PM_{10} les plus élevés correspondent pour le nickel à la zone industrielle à Grenoble, et à celle de proximité au trafic en Ile de France. En Ile de France, les pourcentages des teneurs en plomb sont plus élevés en proximité au trafic, alors qu'à Grenoble il s'agit du secteur de fond urbain, témoignant que le trafic n'a plus d'influence sur les teneurs en plomb. On retrouve des faibles traces d'arsenic à Grenoble dans les 3 secteurs excepté en fond en hiver et de manière moins importante en zones de proximité et industrielle en Ile de France.

La fig. 2 est une illustration des résultats du dosage des HAP extraits à partir des échantillons $PM_{2.5}$ collectés pendant la phase hivernale en Ile de France. Les expositions personnelles aux HAP apparaissent supérieures dans les secteurs industriel et de proximité au trafic automobile.

		$PM_{2.5}$			*PM_{10}*		
		PROXIMITE	*FOND*	*INDUSTRIEL*	*PROXIMITE*	*FOND*	*INDUSTRIEL*
GRENOBLE HIVER N=58	Teneur Reflectance	22,8 (7,7) 74 (13)	28,3 (13,1) 72 (17)	33,6 (15,3) 79 (12)	29,2 (10,2) 66 (9)	33,4 (13,6) 71 (19)	41,5 (16,9) 77 (19)
GRENOBLE ÉTÉ N=56	Teneur Reflectance	23,7 (9,3) 65 (8)	23,1 (9,3) 73 (12)	24,2 (8,6) 82 (11)	29,5 (7,4) 63 (10)	30,8 (14,9) 70 (12)	31,7 (9,7) 77 (11)
ILE DE FRANCE HIVER N=87	Teneur Reflectance	29,6 (12,3) 65 (9)	20,2 (8,9) 85 (10)	32,7 (13,5) 71 (16)	51,5 (16,5) 65 (7)	41,5 (16,1) 81 (12)	55,0 (21,8) 71 (15)
ILE DE FRANCE ETE N=79	Teneur Reflectance	24,0 (7,2) 67 (9)	18,0 (4,8) 78 (12)	22,2 (6,8) 74 (12)	50,4 (18,7) 63 (7)	37,1 (8,8) 79 (13)	40,1 (11,2) 67 (11)
ROUEN ETE N=50	Teneur Reflectance	22,3 (8,6) 72 (9)	24,5 (13,4) 77 (9)	19,9 (6,2) 84 (10)	44,6 (17,8) 72 (10)	51,2 (21,5) 81 (12)	36,2 (11,9) 88 (9)

Tableau 1 : Expositions personnelles moyennes en particules (teneur en µg/m^3 et écart-type) et pourcentages moyens de réflectance en lumière verte (pourcentage et écart-type).

Table 1: Average Particles exposures (content in µg/m^3 and standard deviation) and average percentages of reflectometry of the particles filters by green light (percentage and standard deviation) among the three sectors.

	BENZENE			*NO_2*		
	PROXIMITÉ	*FOND*	*INDUSTRIEL*	*PROXIMITE*	*FOND*	*INDUSTRIEL*
GRENOBLE HIVER N=56/57	8,0 (6,5)	7,5 (3,5)	9,5 (3,5)	28,5 (13,0)	27,5 (9,0)	22,5 (9,5)
GRENOBLE ETE N=52/52	5,7 (2,1)	6,7 (4,5)	7,8 (5,4)	35,8 (8,3)	26,0 (8,6)	20,1 (5,0)
ILE DE FRANCE HIVER N=77/91	7,6 (6,1)	4,7 (1,7)	6,9 (7,0)	39,2 (13,4)	22,5 (17,3)	35,4 (11,8)
ILE DE FRANCE ETE N=68/82	6,3 (4,5)	4,1 (2,0)	7,8 (8,7)	41,7 (10,4)	21,3 (8,1)	37,0 (14)
ROUEN ÉTÉ N=0/39	Non mesuré	Non mesuré	Non mesuré	24,5 (13,3)	24,5 (7,5)	20,1 (7,1)

Tableau 2 : Expositions personnelles moyennes en benzène et NO_2 (teneur en µg/m^3 et écart-type).

Table 2: Benzene and NO_2 average exposures (content in µg/m^3 and standard deviation) among the three sectors.

S'agissant des tests de genotoxicité, la figure 3 fait état d'un des paramètres du test des comètes (« moment de la comète ») mesurés auprès des mêmes échantillons franciliens. La réponse à ce test appréciant le potentiel génotoxique des extraits organiques est plus marquée dans le groupe de population se situant dans le secteur de proximité au trafic, les résultats pour le groupe industriel se situant au même niveau que ceux obtenus sur des échantillons témoins de laboratoire (non portés par les sujets).

3 - Discussion

Ces résultats descriptifs présentés ne sont pas exhaustifs, car ne sont pas encore disponibles les résultats des analyses chimiques des particules et du test génotoxique pour les échantillons franciliens et rouennais des campagnes estivales. Cependant, les tendances dégagées confortent l'hypothèse qu'il existerait une hétérogénéité des teneurs ou des compositions des particules du fait de la nature et de la proximité des sources ; les expositions aux agents gazeux mesurés diffèrent aussi selon les groupes des volontaires. Les résultats concernant les particules montrent, pour les deux fractions granulométriques, que les expositions les plus fortes sont obtenues auprès des volontaires vivant en secteurs industriel et de proximité au trafic, et plus en hiver qu'en été. En été, le trafic urbain et les activités industrielles sont les principales sources, auxquelles s'ajoutent les réactions de chimie atmosphérique et le transport des particules à longue distance. En hiver, d'autres sources interviennent, notamment le chauffage urbain, avec souvent des conditions dispersives moins favorables (The Quality of Urban Air Rewiew Group 1996). Les résultats de réflectométrie

confirment que c'est en proximité

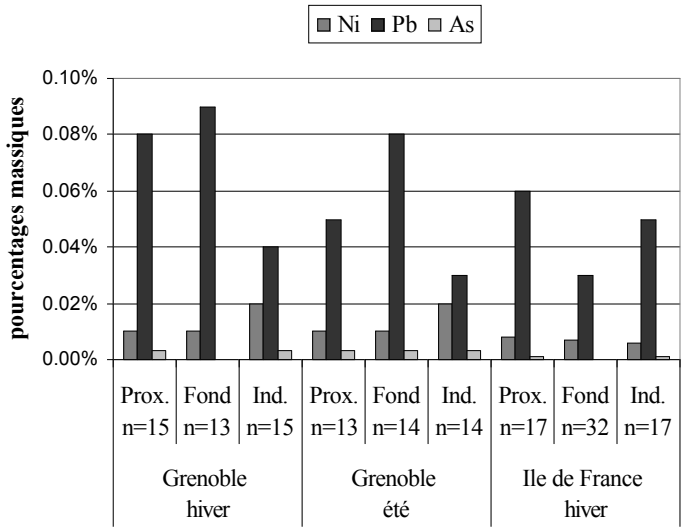

Figure 1 : Teneurs en arsenic, plomb et nickel des PM_{10} personnelles à Grenoble et en Ile de France (exprimées en % de la masse particulaire).

Figure 1: Concentrations (in terms of % particles mass) of arsenic, lead and nickel from PM_{10} in personal exposure samples in Ile de France and Grenoble.

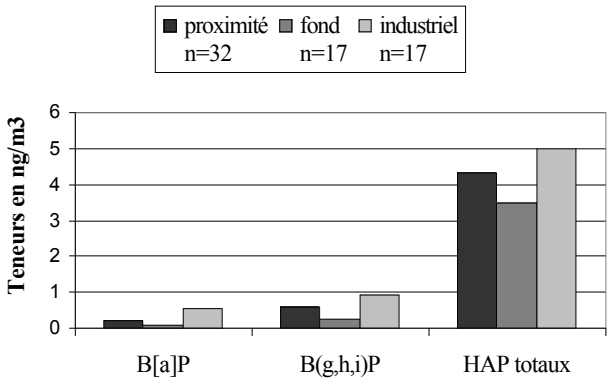

Figure 2: Expositions moyennes aux B[a]P, B(g,h,i)P et HAP totaux particulaires dans les filtres personnels $PM_{2.5}$ en Ile de France (hiver).

Figure 2: Average exposures to B(a)P, B(g,h,I)P and to total PAHs from $PM_{2.5}$ personal samples in Ile de France (winter).

au trafic automobile, que les filtres sont les plus noirs de par leur charge en carbone élémentaire (Roemer et van Wijnen 2001). En ce qui concerne le benzène, les concentrations semblent être plus élevées en zones industrielle et de proximité, avec cependant une grande variabilité inter-individuelle. L'exposition des personnes au benzène est augmentée en situation de plus forte pollution automobile, mais elle dépend aussi des activités individuelles et, de manière très importante, de la présence de sources intérieures (Gonzales-Flesca et coll 2000, Raaschou-Nielsen et coll 1997). Les concentrations en NO_2, composé reconnu comme provenant majoritairement des gaz d'échappement dans l'air urbain extérieur, sont également plus élevées en situation de proximité au trafic. Le classement des sujets en regard des émissions liées au trafic fera cependant l'objet d'analyses plus fines prenant en considération les configurations urbaines locales. Effectivement, une personne recrutée pour la proximité de ses lieux de vie (domicile et travail) à de grands axes de circulation, peut s'avérer en fait être protégée de la pollution automobile par une barrière d'immeubles. Le logiciel ExTra, développé par le CSTB de Nantes et l'INRETS sera appliqué à cet effet et permettra le calcul d'un indice d'exposition à la pollution atmosphérique d'origine automobile pour chacun des volontaires en fonction de ses lieux de vie (Sacré et coll 1993).

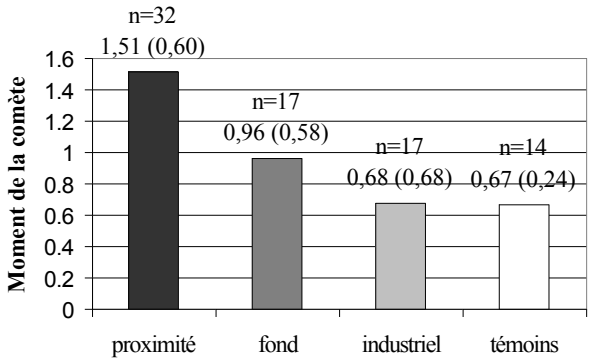

Figure 3: Résultats du test des comètes à partir d'extraits organiques de $PM_{2.5}$ d'Ile de France (hiver).

Figure 3: Comet test results from $PM_{2.5}$ organic extracts in Ile de France (winter).

Peu d'études nous permettent de comparer simultanément, en population générale, les expositions aux $PM_{2.5}$ et PM_{10} d'enfants et adultes non exposés à un environnement tabagique. Les expositions aux $PM_{2.5}$ observées tous secteurs confondus (de 18 à 33,6 $\mu g/m^3$) sont proches de celles de l'étude EXPOLIS à Grenoble variant en moyenne de 21,9 à 36,7 $\mu g/m^3$ (Boudet et coll 2000). Cette même étude a montré des niveaux d'exposition aux $PM_{2.5}$ beaucoup plus contrastés dans plusieurs villes européennes (de 10 à 72 $\mu g/m^3$) du fait notamment de la participation de fumeurs (Koistinen 2002). Une étude réalisée auprès de 62 employés de bureau parisiens (Mosqueron et coll 2002) a montré que les niveaux d'exposition personnelle aux $PM_{2.5}$ était de 30,4 $\mu g/m^3$, valeur légèrement supérieure à celle obtenue dans notre groupe de volontaires parisiens (29,6 $\mu g/m^3$ en hiver et 24 en été). De la même manière, l'exposition personnelle au NO_2 de ces employés s'élevait à 43,6 $\mu g/m^3$ contre 39,2 $\mu g/m^3$ en hiver et 41,7 en été dans notre groupe. Les expositions au benzène mesurées (de 4,1 à 9,5 $\mu g/m^3$) sont également inférieures à la valeur moyenne (10,3 $\mu g/m^3$) obtenue auprès de 50 sujets adultes non-fumeurs grâce au même dispositif de prélèvement lors du programme Macbeth (Gonzales-Flesca et coll 2000). Cette différence pourrait s'expliquer par la diminution des concentrations extérieures liées à la baisse du benzène dans l'essence. Dans l'ensemble, les expositions de nos volontaires semblent être plus faibles que celles des études référencées précédemment. Cette différence pourrait s'expliquer par la participation d'enfants qui sont, a priori, moins exposés au trafic que les adultes (cette hypothèse peut être rapidement testée puisque nous disposons des données enfants et adultes). Tous les sujets ont, de plus, été recrutés pour la faible distance qui sépare leur domicile de leur lieu professionnel ou scolaire, ce qui pourrait expliquer que leur exposition à la pollution automobile lors des déplacements est plus limitée que dans d'autres études. Ces hypothèses seront vérifiées lors de l'analyse des carnets budgets espace temps.

Si la technique analytique PIXE permet de mesurer un très grand nombre d'éléments minéraux (à l'exception du cadmium). L'expression des résultats en pourcentage de l'élément détecté par rapport à la masse recueillie va permettre de s'intéresser à la variation de la nature élémentaire de la particule, ce qui apporte une information qualitative sur son origine (Guégan et coll 2000). L'arsenic, émis lors d'activités industrielles lourdes et de combustion de charbon (Koistinen 2002), n'apparaît que sous forme de traces dans les trois secteurs de Grenoble (sauf l'hiver en fond) et en proximité et zone industrielle en Ile de France. Le nickel, traceur du pétrole brut en général et des fuels lourds en particulier (Guégan et coll 2000, Koistinen 2002), est effectivement en proportion plus importante en milieu industriel à Grenoble et, en Ile de France, dans le secteur de proximité au trafic. Conformément à sa proscription dans les carburants, nous constatons qu'à Grenoble, les teneurs en plomb ne sont pas plus élevées en secteur de proximité au trafic que dans les autres secteurs d'où la confirmation de l'existence d'autres sources émettrices (incinérateurs d'ordures ménagères, activités industrielles diverses…). Cependant, le plomb reste majoritairement présent dans la zone exposée à la pollution automobile à Paris, ce qui laisse supposer que le parc automobile des véhicules roulant à l'essence plombée n'est pas encore totalement renouvelé.

En milieu urbain ou suburbain, les sources d'HAP gazeux et particulaires, sont principalement les

sources mobiles, le chauffage domestique et l'incinération des déchets solides. Les expositions personnelles aux HAP sont fortement influencées par les activités impliquant une combustion : pollution automobile, environnement tabagique ou cuisine (Levy et coll 2002). Les résultats présentés ici concernent les fractions $PM_{2.5}$ pour le benzo[a]pyrène, le plus cancérogène des HAP, et le benzo(ghi)pérylène, connu comme traceur de la pollution par les véhicules essence (Boström et coll 2002). Les expositions des volontaires d'Ile de France dans les secteurs de trafic et industriel sont effectivement plus élevées qu'en zone de fond urbain. Les résultats du test des comètes, réalisé sur les mêmes échantillons, ne donnent pas exactement le même classement, puisque la réponse est plus forte en proximité au trafic puis en fond urbain. Cela laisse supposer que les extraits organiques mis en contact avec les cellules, contiennent des substances organiques capables d'altérer l'ADN autres que les 16 HAP dosés (liste US EPA). D'après une étude de Spinosa et coll (1999), utilisant le test d'Ames à partir de prélèvements de PM_{10} en milieu urbain, les fractions les plus mutagènes sont les cétones, les aldéhydes, les quinolones et les acides carboxyliques. Parce qu'elles ne sont pas mesurées dans ce travail, il n'est pas possible de relier leurs teneurs à la réponse des tests de génotoxicité.

Conclusion

Ces résultats préliminaires confortent l'hypothèse d'une hétérogénéité des niveaux d'exposition des habitants des villes à différents polluants de l'air, selon leurs lieux de vie, et en relation avec la proximité de sources locales de pollution. Les premiers résultats des tests génotoxiques suggèrent qu'à cette hétérogénéité de la qualité de l'air répond une inégalité du risque d'atteinte du matériel génétique, et donc du risque de cancer. Ces résultats devront être vérifiés sur l'ensemble des sites d'étude pour pouvoir tirer des conclusions plus fortes. Seront aussi comparées les expositions personnelles avec les mesures de la surveillance de la qualité de l'air.

Remerciements

Ce programme bénéficie d'une bourse de thèse ADEME co-financée par l'INERIS et l'Institut de Veille Sanitaire, d'un financement PRIMEQUAL-PREDIT 2, du PRQA Rhônes-Alpes et de la Fondation de France. Nous remercions également les réseaux de surveillance de la qualité de l'air des villes de Grenoble, Paris, Rouen et Strasbourg pour leur participation active.

Références

Ares A., Eckl PM. & I. Raffelsberger (2000): Genotoxicity at low-level dose of inspirable urban ambient air particulate in a semiarid regime. Environ. Monitoring and Assesment, vol 63, p 389-408.

Barbone F., M. Bovenzi, F.Cavallieri & G. Stanta (1995): Air pollution and lung cancer in Trieste, Italy. Am. J. Epidemiol., vol 141, n° 12,p 1161-9.

Bhatia R., P. Lopipero & AH. Smith (1998): Diesel exhaust exposure and lung cancer. Epidemiology, vol 9, p 84-91.

Beeson WL., DE. Abbey & SF. Knutsen (1998): Long term concentrations of ambient air pollutants and incident lung cancer in California adults: results from the ASMOGH study. Environ. Health. Perspect., vol 106, n° 12, p 813-22.

Boström CE., P. Gerde, A. Hanberg & coll (2002). Cancer risk assessment, indicators, and guidelines for Polycyclic Aromatic Hydrocarbons in the ambient air. Environ Health Perspect., vol 110 (suppl. 3), p 451-88.

Boudet C., D. Zmirou & J. Déchenaux (2000). Exposition personnelle aux particules fines ($PM_{2.5}$) de la population grenobloise : l'étude européenne EXPOLIS. Rev Epidemiol Sante Publique, vol 48, n° 4, p 341-50.

Burgaz S., GC. Demercigil, B. Karahalil & AE. Karakaya (2002): Chromosomal damage in peripheral blood lymphocytes of traffic policemen and taxi drivers exposed to urban air pollution. Chemosphere, vol 47, p 57-64.

Demokritou P., IG. Kavouras, ST. Ferguson & P. Koutrakis (2001): Development and laboratory performance evaluation of a personal multipollutant sampler for simultaneous measurements of particulate and gaseous pollutants. Aerosol Sci. Technol., vol 35, p 741-752.

Fernandez AJ., M. Ternero, FJ. Barragan & JC. Jimenez (2001): Size distribution of metals in urban aerosols in Seville (Spain). Atmos. Environ., vol 35, p 2595-601.

Fernandez AJ., M. Ternero, FJ. Barragan & JC. Jimenez (2002): A chemical speciation of trace metals for fine urban particles. Atmos. Environ., vol 36, p 773-80.

Gonzales-Flesca N., MS. Bates, V. Delmas & V. Cocheo (2000): Benzene exposure assessment at indoor, outdoor and personal levels. The French contribution to the life Macbeth programme. Environ. Monitoral & Assess., vol 65, n° 2, p 59-67.

Guégan H., A. Fleury, JB. Demonthon & coll (2000) : Analyse multi-élémentaire par sonde PIXE des particules fines, recherche de la contribution respective des différentes sources. Colloque PRIMEQUAL, Toulouse, 29/11-1/12/2000.

Iwai K., S. Adachi, M. Takahashi, L. Möller, T. Udagawa, S. Mizuno & I. Sugawara (2000): Early oxidative DNA damage and late development of lung cancer in diesel exshaut-exposed rats. Environ. Res. Sect., vol 84, p 255-64.

Kinney PL., M. Aggarwal, ME. Northridge, N. Janssen & P. Shepard (2000): Airborne concentrations of $PM_{2.5}$ and diesel exhaust particles on Harlem sidewalks: a community-based pilot study. Environ. Health. Perspect., Vol 108, n° 3, p 213-8.

Koistinen K. (2002). Exposure of an urban adult population to PM2.5: methods, determinants and sources. Thesis. Publications of th National Public Health Institute, Finland, 81 p.

Krytopoulos SA., P. Georgiadis, H. Autrup & al (2001) : Biomarkers of genotoxicty of urban air pollution overview and descriptive data from a molecular epidemiology study on populations exposed to moderate-to-low levels of polycyclic aromatic hydrocarbons : the AULIS project. Mutat. Res., vol 496, p 207-28.

Laden F., J. Swartz, FE. Speizer, D. Dockery (2001): Air pollution and mortality: a continued follow-up in the Harvard six cities study. ISEE 2001 abstracts, Garmish-Partenkirchen, RFA, 2-5 sept 2001.

Levy JI., T. Dumyahn & JD. Spengler (2002): Particulate matter and polycyclic aromatic hydrocarbon concentrations in indoor and outdoor microenvironnements in Boston, Massachussetts. J. Expos. Anal. Environ. Epidemiol., vol 12, p 104-14.

Mosqueron L., I. Momas & Y. Le Moullec (2002). Personal exposure of Paris office workers to nitrogen dioxide and fine particles. Occup. Environ. Med., vol 59, n ° 8, p 550-5.

Nyberg F., P. Gustavsson, L. Järup, T. Bellander, N. Berglind, R. Jakobsson & G. Pershagen (2000): Urban air pollution and lung cancer in Stocklom. *Epidemiology*, vol 11, n° 5, p 487-95.

Pope CA., RT. Burnett, K. Ito, D. Krewski & GD. Thurston (2001): Mortality effects of long-term exposure to air pollution: analysis of extended follow-up of the ACS cohort. ISEE 2001 abstracts, Garmish-Partenkirchen, RFA, 2-5 sept 2001.

Pope CA., RT. Burnett, MJ. Thun, EE. Calle, D. Krewski, K. Ito & GD. Thurston (2002): Lung cancer, cardiopulmonary mortality and long term exposure to fine particulate air pollution. JAMA, vol 287, n° 9, p 1132-41.

Raaschou-Nielsen O., C. Lohse, BL. Thomsen, H. Skov & JH. Olsen (1997): Ambient air levels and exposure of children to benzene, toluene, and xylenes in Denmark. Environ. Res., vol 75, p 149-59.

Roemer WH. & JH. van Wijnen (2001): Differences among black smoke, PM_{10}, and $PM_{1.0}$ levels at urban measurement sites. Environ. Health. Perspect., vol 109, n° 2, p 151-4.

Sacré C., M. Chiron & JP. Flori (1993). Elaboration d'un indice d'exposition à la pollution atmosphérique d'origine automobile à l'usage des études épidémiologiques. Rapport INRETS et CSTB, 60 p.

Spinosa De Martinis B., NY. Kado, LRF. De Carvalho, RA. Okamoto & LA. Gundel (1999): Genotoxicy of fractioned organic material in airborne particles from São Paulo, Brazil. Mutat. Res., vol 446, p 83-94.

The Quality of Urban Air Review Group (1996): Airborne particulate matter in the United Kingdom. 3rd report of the Quality of Urban Air Review Group, Dept Environ., London, 176 p.

12th International Symposium "Transport and Air Pollution" / 12e Colloque international "Transports et pollution de l'air", Avignon, 16 -18 *June* / juin 2003
proceedings / actes, n°92, tome / Vol. 1, Inrets ed., Arcueil, France, 2003, p. 51-58

Effect of Vehicle Characteristics on Unpaved Road Dust Emissions

John A. Gillies, Vicken Etyemezian, Hampden Kuhns*, Djordge Nikolic** & Dale A. Gillette*****
*Desert Research Institute, 2215 Raggio Parkway, Reno, NV, USA 89512, Fax +011 775-674-7060 – e-mail: jackg@dri.
**Desert Research Institute, 775 E. Flamingo Road, Las Vegas, NV, 89119, USA
***National Oceanic and Atmospheric Administration, Research Triangle Park, NC, USA, 2771

Abstract
This paper presents PM_{10} fugitive dust emission factors for a range of vehicles types and examines the influence of vehicle and wake characteristics on the strength of emissions from an unpaved road. Vertical profile measurements of mass concentration of the passing plumes were carried out using a series of 3 instrumented towers. PM_{10} emission fluxes at each tower were calculated from knowledge of the vertical mass concentration profile, the ambient wind speed and direction, and the time the plume took to pass the towers. The emission factors showed a strong linear dependence on speed and vehicle weight. Emission factors (EF = grams of PM_{10} emitted per vehicle kilometer traveled) ranged from approximately EF=0.8×(km/hr) for a light (~1,200 kg) passenger car to EF=48×(km/hr) for large military vehicles (~18,000 kg). In comparison to emission estimates derived using U.S. EPA AP-42 methods the measured emission factors indicate larger than estimated contributions for speeds generally > 10-20 km/hr and for vehicle weights > 3000 kg. The size of a wake created by a vehicle was observed to be dependent on the size of the vehicle, increasing roughly linearly with vehicle height. Injection height of the dust plume is least important to long-range transport of PM_{10} under unstable conditions and most important under stable atmospheric conditions.
***Keys-words**: PM_{10}, fugitive emissions, unpaved roads.*

Introduction

Most unpaved roads consist of a graded and compacted roadbed usually created from the parent soil-material. The rolling wheels of the vehicles impart a force to the surface that pulverizes the roadbed material and ejects particles from the shearing force as well as by the turbulent vehicle wakes (Nicholson et al., 1989). Studies have found that dust emission rates depend on the fine particle content of the road (Cowherd et al., 1999; MRI 2001), soil moisture content, vehicle speed (Nicholson et al., 1989), and vehicle weight (U.S. EPA, 1996; MRI, 2001). As part of a study to understand the contributions of military testing and training activities to regional particulate matter in the western U.S. (Gillies et al., 2002), a study was undertaken to measure unpaved road dust emissions from wheeled vehicles and characterize their wakes and dust injection heights. These tests were carried out at Ft. Bliss, TX. A mix of civilian and military vehicles covering a substantial range of weights, length and width dimensions, and number of wheels were used to understand how these properties relate to emissions of dust, specifically the PM_{10} component. The results of these measurements are compared with modeled results using earlier (U.S. EPA, 1996) and more recent (MRI, 2001) estimation methods.

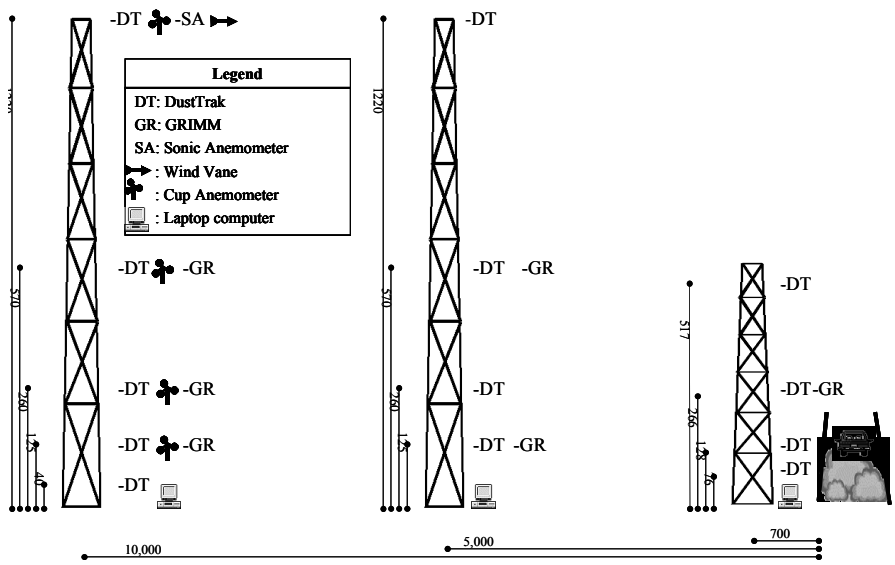

Figure 1: Schematic diagram of the 3-tower dust monitoring system. Units are shown in centimeters.

1 - Experimental Methods

From April 11 through 24, 2002, unpaved road emission flux experiments were conducted at Ft. Bliss, TX, using an upwind/downwind measurement technique similar to Gillies et al. (1999). Three towers were set up collinearly and perpendicular to a 1000 m section of unpaved road. The three towers were all downwind of the road at distances of 7 m, 50 m, and 100 m. A schematic diagram of the tower monitoring system is shown in Fig. 1. Each downwind tower was instrumented with four DustTraks (Model 8520, TSI Inc., St. Paul, MN) configured to measure PM_{10} that were spaced logarithmically (Fig. 1) in the vertical direction. The DustTrak is a portable, battery-operated, laser-photometer that uses light scattering technology to determine mass concentration in real-time.

The tower at 7 m downwind (DT_1) had measurement positions at 0.76, 1.28, 2.66, and 5.18 m above ground level (AGL). The second tower (DT_2) at 50 m had measurement positions at 1.25, 2.6, 5.7, and 12.2 m AGL. The third tower at 100 m (DT_3) had the same measurement positions as DT_2 with an additional sampling location at 0.4 m AGL. Five anemometers, one wind vane, and one temperature probe were mounted on DT_3 in order to characterize the local meteorological conditions. Dust concentration and meteorological data were collected and stored on PCs located at each tower running a custom-designed LabView data acquisition program.

Road dust PM_{10} emissions were created by having a test vehicle travel back and forth along the roadway for a number of passes. The test vehicles traveled at set speeds of 16, 24, 32, 40, 48, 56, 64, 72, and 81 km/hr. After two passes at the same speed, the vehicle speed was increased incrementally to the maximum and then decreased incrementally to the slowest speed. Vehicles paused between passes to allow a plume to move by all three towers. Test vehicle descriptions and physical characteristics are presented in Table 1.

A three-dimensional sonic anemometer (Applied Technologies Inc., Boulder, CO) was used to assess the magnitude of the turbulent wake behind vehicles and assess its effect on the initial distribution of the vehicle-generated dust plume. The tests were carried out at night because under stable atmospheric conditions, the turbulence generated by a vehicle can be more readily identified with a sonic anemometer than when the atmosphere is unstable and the background turbulence level is much higher. Three vehicles with considerably different profiles were tested: a Dodge Neon, a 1979 GMC van, and a GMC C5500 truck. The sonic anemometer was mounted on the tower at a height of 0.9 meters above ground level (AGL) and extended 1.1 meters towards the road. Each vehicle was driven past the tower once heading north and once heading south at 16, 32, 48, and 64 km/hr for a total of eight passes per vehicle. After all three vehicles completed this cycle the sonic

anemometer was moved to 2.4 meters and then to 5.5 meters AGL. The driving pattern (three vehicles, four speeds, two passes at each speed) was repeated at each of those two heights.

Bulk surface samples were collected at the beginning and end of the testing to determine the percent silt content of the road material.

VEHICLE Type	Model Year	Vehicle Specifications Weight (kg)	Length (m)	Width (m)	Height (m)	Under-carriage Area (m^2)	Number of Wheels
Dodge Neon	2002	1176	4.34	1.71	1.42	7.43	4
Dodge Caravan	2002	1759	5.09	1.83	**1.76**	9.31	4
Ford Taurus	2002	1516	5.08	1.83	1.41	9.30	4
GMC G20 Van	1979	3100	5.1	1.85	2.00	9.44	4
HMMWV	n/a[1]	2445	4.57	2.16	1.83	9.87	4
GMC C5500	1999	5227	9.04	2.29	3.30	20.67	6
M977 HEMTT	n/a	17727	9.96	2.44	2.85	24.29	8
M923A2 (5-ton)	n/a	14318	8.74	2.44	3.07	21.32	6
M1078 LMTV	n/a	8060	6.43	2.44	2.69	15.69	4

[1]n/a: data not available

Table 1: Test Vehicle Characteristics.

2 - Results

PM_{10} emissions fluxes were calculated for each downwind tower using the assumption that each DustTrak represented the PM_{10} concentration over a height that spanned half the distance to the next lowest monitor to half the distance to the next highest monitor (Fig. 1). The time series of PM_{10} concentrations were examined for each DustTrak at each location. Each peak in concentration was associated with an individual vehicle pass and each pass was assigned a start and stop time. The emissions factor per vehicle pass for each downwind tower was calculated using the sum of the 1-second PM_{10} fluxes with the equation:

$$EF = \sum_{\text{start time of peak}}^{\text{end time of peak}} \left\{ \cos(\theta) \sum_{4}^{4} u_i \, C_i \, \Delta z_i \, \Delta t_i \right\} (1)$$

where the outer summation is over the period of plume impact, EF is the estimated emissions factor of PM in grams per vehicle kilometer traveled (g-PM vkt^{-1}), θ is the angle of the 5-min. average wind direction relative to the flux plane, i is monitor position on the tower, u_i is the 5-min. average wind speed (m s^{-1}) over the height interval represented by the ith monitor, C_i is 1-s PM concentration (mg m^{-3}) as measured by the ith monitor, Δz (m) is the vertical interval represented by the ith monitor, and Δt (s) is the duration that the plume impacts the tower. For all emission factor calculations only the concentration data associated with wind approach angles of $\leq 45°$ with respect to the tower line were used. Winds speeds and directions measured on the third downwind tower were assumed to be representative of the speeds at the other towers.

For the period of the testing the moisture content of the roadbed material was <0.5% and the silt content of the road changed from 4 to 7%.

Examples of the emission of PM_{10} per vehicle kilometer traveled as a function of vehicle speed (E_s, g-PM_{10}/vkt) for the light (<4000 kg) and the heavier (>4000 kg) vehicles are shown in Fig. 2 and 3. The emission factor value for each speed category is based on the average from multiple passes for all three towers and the error bars represent the standard deviation of the three-tower average. From the relationships depicted in these figures it is apparent that vehicle speed and size play important roles in the magnitude of the emissions.

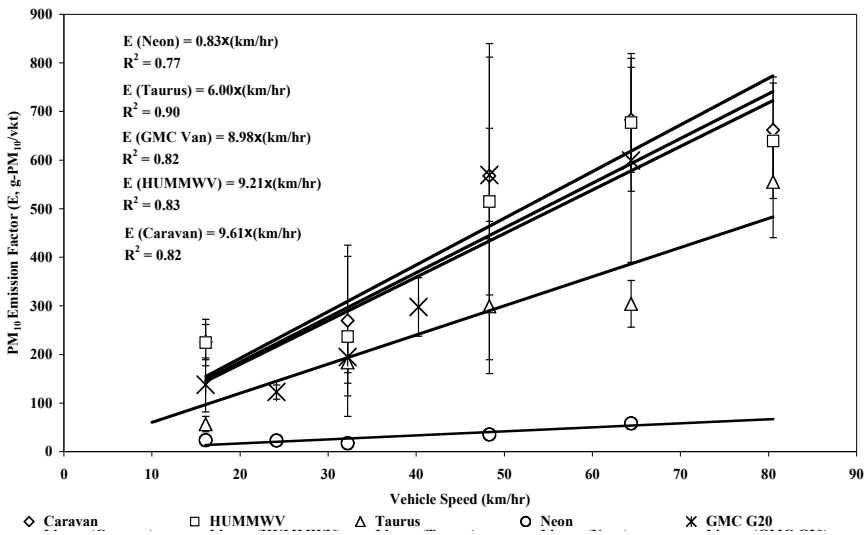

Figure 2 : Emission factors as a function of speed for vehicles <4000 kg. Error bars represent the standard deviation of the mean value for that speed based on multiple vehicle passes, and for all three towers combined.

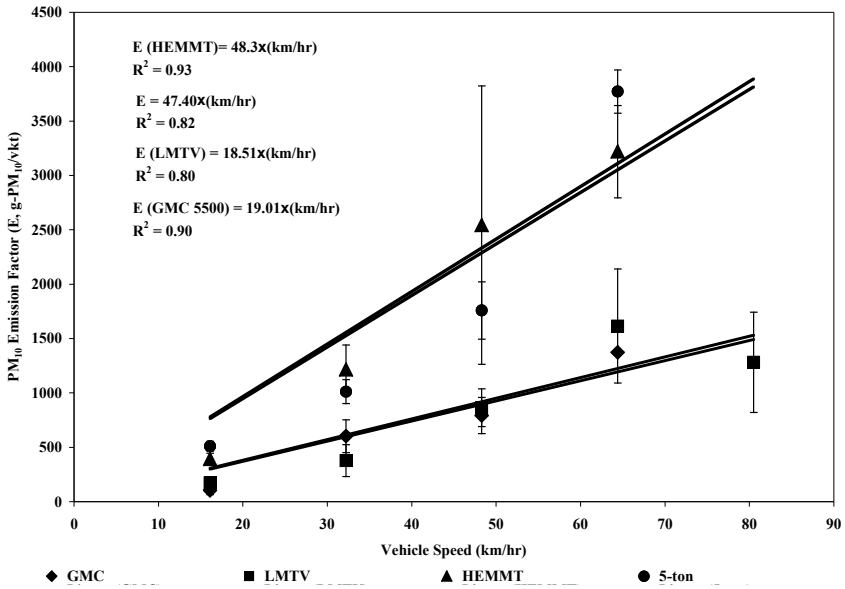

Figure 3 : Emission factors as a function of speed for vehicles >4000 kg. Error bars represent the standard deviation of the mean value for that speed based on multiple vehicle passes, and for all three towers combined.

The results of the nighttime wake turbulence tests are shown in Fig. 4, which illustrates that the size of the turbulent wake behind a vehicle increases with physical size. The GMC C5500 creates a measurable wake up to a height of approximately 6 m. The GMC G20 wake only goes up to about 2.5 m. The Dodge Neon is apparently too small to cause a measurable wake, even at the minimum anemometer height setting of 0.9 m. The dotted line drawn for the compact car is based on a linear fit of the wake heights of the box truck and the cargo van vs. their physical heights (3.2 and 2.0 m, respectively). The height of the compact car at the rear of the vehicle is 1 m giving an approximate wake height of 1.7 m according to this regression (see Fig. 5). The wake height is important because it gives an indication of the height to which the dust plume is mixed behind the vehicle. As a first approximation, we may assume that the dust emitted behind a vehicle is well-mixed up to the height of the turbulent wake (approximately 1.7 times the height of the vehicle). This "injection" height may play an important role when determining the fraction of particulate matter that deposits close to the road vs. the fraction that is transportable; as a rule, the further a particle is from the

ground initially, the less likely it is to deposit in a given period of time.

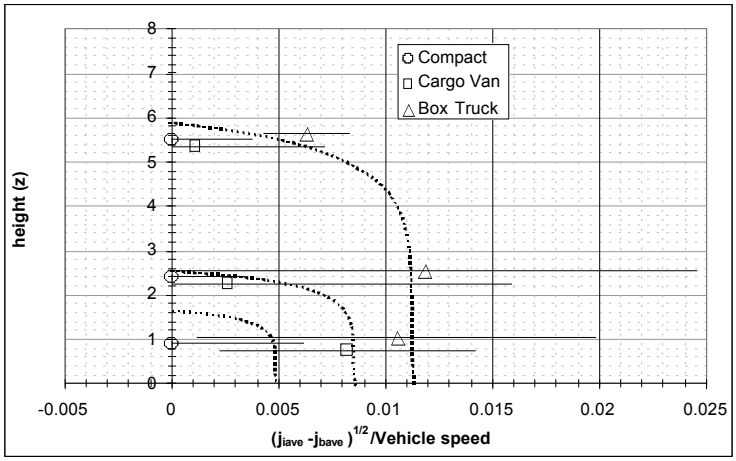

Figure 4: Turbulence generated vs. height above ground for three vehicle types. The x-axis represents the difference between the vertical component of vehicle turbulence and the background fluctuations in vertical velocity normalized by the speed of the vehicle. The terms j_{iave} and j_{bave} represent the average value of the squared difference between the average vertical velocity component and its fluctuating component during the presence and absence (i.e., background), respectively of the vehicle wake. The horizontal lines represent the background turbulence standard deviation. The dotted lines represent hand drawn curves to fit the data. The dotted line corresponding to the compact car was drawn based on the assumption that the height of the wake plume is proportional to the height of the vehicle (see Fig. 5).

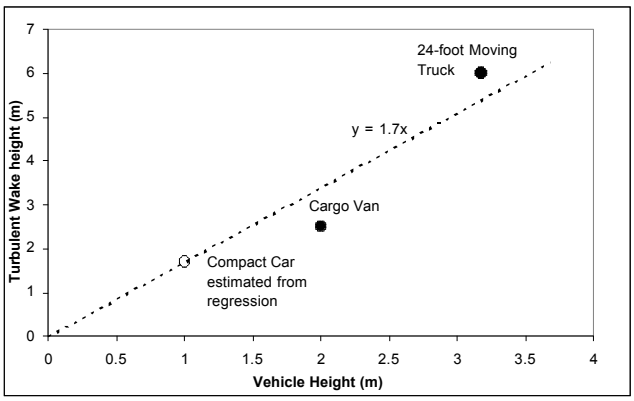

Figure 5: Estimate of turbulent wake height vs. physical vehicle height. The dotted line represents a zero-intercept regression on the data from the GMC G20 and GMC C5500. The hollow circle is an estimate of the wake height for the Neon based on the regression.

The approximation for the injection height suggested here is simplistic. This height is likely to depend on a number of parameters, most notably, the atmospheric stability, the shape of the vehicle, and the angle of the ambient wind with respect to the direction of vehicle travel. The analysis here is based on data obtained under stable conditions. Under unstable conditions, turbulent mixing is not inhibited by buoyancy forces and therefore, it is likely that the effective injection height will be larger because of this. For the present purpose, it is sufficient to note that the height to which a dust plume is thoroughly mixed in the wake of a vehicle is dependent on the size of the vehicle, increasing in a roughly linear relationship with height.

3 - Discussion

Fig. 2 and 3 demonstrate that vehicle speed is an important factor with respect to unpaved roadway PM_{10} emissions for the tested vehicles. The effect of speed on emissions is linear and relatively invariant with vehicle type as shown in Fig. 6. This figure shows the emissions normalized to the fastest speed obtained for each test vehicle. Regardless of test vehicle type the emissions from the roadway increase at a constant rate with increasing speed. MRI (2001) also reported for other

unpaved roadways that emissions vary with speed raised to a power typically between 1 and 1.5. This suggests that physical characteristics of the vehicles such as shape and number of tires and tread pattern may have only a minor influence on the emissions. There is however, a discernable effect of vehicle weight on the emissions from the unpaved road. A plot of the emission factors as a function of speed from the regression-derived equations presented in Fig. 3 and 4 are plotted against the weights of the vehicles in Fig. 7.

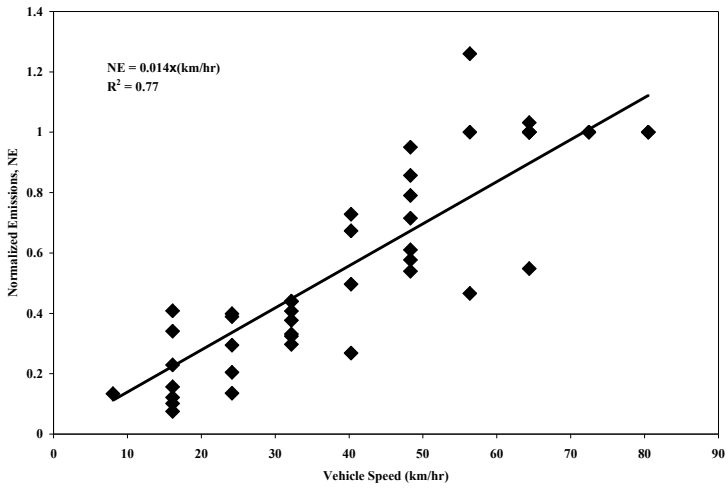

Figure 6: The effect of vehicle speed on emissions independent of vehicle weight.

In earlier emission factor estimation methodologies the effect of vehicle weight on PM_{10} emissions was treated as a power function with the weight being raised to the 0.7 or 0.45 power. The Ft. Bliss data show a strong linear relationship between weight and emissions (Fig. 7). The vehicle undercarriage area and the number of wheels have weak and no discernable relationships with emission factors, respectively, as indicated by low correlation coefficients.

In comparing the measured emission factors from the vehicles tested at Ft. Bliss with other estimation methods several differences are clear. Using a U.S. EPA method published in AP-42 in 1996 (U.S. EPA, 1996) it was observed that on average this method under-predicted the emissions from each test vehicle by a factor of 2.4 (±0.9) for roads of 4% silt content and 1.4 (±0.5) for roads of 7% silt content over the range of vehicle speeds tested. More recent estimation methods offer two options for public roads and a separate method for industrial roads. Comparing the measured emission factors at Ft. Bliss with the MRI (2001) approaches shows that for the MRI option 1 emission model, which is: E (lb- PM_{10}/vmt)=$1.8(s/12)^{0.97}(S/30)^{0.46}/(M/0.5)^{0.23}$, where s represents silt content (%), S is mean vehicle speed (mph), and M is surface moisture content, the Ft. Bliss emissions for individual vehicles are under-predicted due to the difference between speed expressed as a power function in the model and the linear dependence observed in the data. The option 2 emission model, which is E (lb-PM_{10}/vmt) = $1.7(s/12)^{0.95}(S/30)^{1}/(M/0.5)^{0.23}$ differs for an individual vehicle from the measured values by a factor of ~0.3, which reflects the effect of the denominator on the speed term in the second model.

The major difference between the modeled and measured values is caused by the observed effect of vehicle weight on emissions (Fig. 7). For the Ft. Bliss data the model over-predicts emissions for vehicles <~1250 kg for a 4% silt content and <~2000 kg for a 7% road silt content and under-predicts for heavier vehicles. For lighter vehicles (~1250 kg) the measured to predicted value is ~0.6 to 1 for silt contents of 4 and 7%, respectively. At the heavy end (~18000kg) the measured emissions are ~8 to ~14 times greater than the modeled values, for 4 and 7% silt contents, respectively.

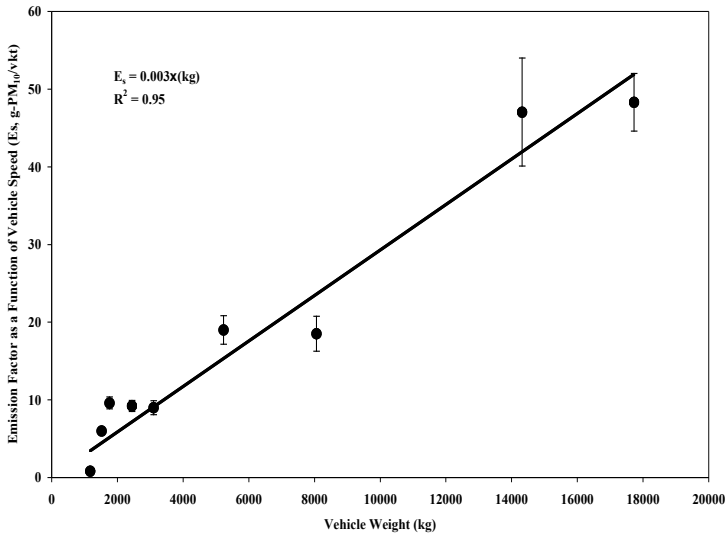

Figure 7: The relationship between emission factor (as a function of vehicle speed) and vehicle weight. The error bars represent the standard error of E_s.

The movement of the heavy military vehicles at Ft. Bliss can be compared to the movement of industrial vehicles on haul roads. For this case MRI proposed the emission model: E (lb-PM_{10}/vmt) = $1.5(s/12)^{0.87}(W/3)^{0.45}$ where W represents the mean vehicle weight in tons. Using the industrial road model neglects the speed effect that was observed in the Ft. Bliss data. The result is that the model over-predicts emissions for speeds less than ~10 km/hr for 4% silt content roads and ~18 km/hr for 7% silt content roads and under-predicts emissions at faster speeds. At ~80 km/hr the model under-predicts heavy vehicle (> 5000 kg) emissions by a factor of 5 to 8 times for 7 and 4% silt contents, respectively.

The effect of injection height on emissions was assessed using the ISC3 model (U.S. EPA, 1995) to model changes in the concentration profile downwind of a ground-level source (Etyemezian et al., 2003). The initial dispersion parameter (σ_z) was assumed to equal one-half of the injection height. The modeling results indicated that the injection height for the dust plume is least important under unstable atmospheric conditions, and most important under stable atmospheric conditions. This is because under unstable conditions, the dust plume is lofted up high quickly anyway, more or less regardless of the starting height. Under stable conditions, the extent of vertical mixing is retarded by buoyancy, and a lower injection height allows the particles to be closer to the ground for a longer period of time, thereby enhancing deposition.

Comparison of downwind removal rates indicates that for unstable conditions, the injection height has a non-trivial, but small effect. For very stable conditions, the injection height has a large effect, approaching a factor of two difference in estimated removal rates at 1,000 m downwind of the source. The difference between the removal of particles for two plumes with different injection heights is confined to the near-source region. That is, the difference does not continue to grow past about 1,000 meters downwind. With this in mind, and noting as before that most unpaved road dust emissions are likely to occur in the daytime, when conditions are neutral to unstable, the effect of the injection height is secondary to the uncertainties associated with deposition velocities and dispersion parameters.

Conclusions

As part of a larger study to assess the contributions of military training and testing to fugitive dust levels emission factors for a range of vehicles types for unpaved roads were measured at Ft. Bliss, TX in April 2002. A downwind array of three instrumented towers were used to measure the mass concentration of dust in the advecting plumes created by the vehicles traveling on the roadway. The magnitude of the emissions was controlled primarily by vehicle speed and vehicle weight, both of

which had linear effects on the emissions. Other physical characteristics of the vehicles (e.g., # wheels, undercarriage, area, height) did not appear to heavily influence the emissions. The effect of the injection height of the dust as a function of vehicle wake size was found to be minimal in neutral and stable conditions, becoming important only in very stable conditions. In comparison with U.S. EPA methodologies for determining contributions of fugitive dust from unpaved roads the Ft. Bliss emission factors would generally under-predict the emissions from vehicles traveling within the testing and training range of this military post by a factor of 2 using the AP-42 (1996) methods. An important question still remains to be resolved, which is "what is the eventual fate of these emissions"? There is still considerable discrepancy between the inventory-derived amounts of unpaved road dust contributions and the amount of mineral-type fugitive dust observed in the ambient air.

Acknowledgements

Our research team would like to acknowledge the support of the Strategic Environ. Res. & Develop. Program (SERDP) and Ft. Bliss for supplying military vehicles and personnel to this project. The support of the Directorate of the Environment at Ft. Bliss has been invaluable and the work of Mr. Clyde Durham (formerly of the DoE) on our behalf has been instrumental in our success.

References

Cowherd, C., P. Englehart, G.E. Muleski, J.S. Kinsey, & K.D. Rosbury (1999): Control of Fugitive and Hazardous Dusts, Noyes Data Corp., Park Ridge, NJ.

Etyemezian V., H. Kuhns, J. Gillies, J. Chow, M. Green, K. Hendrickson, M. McGown, & M. Pitchford (2003a): Vehicle based road dust emissions measurement (III): effect of speed, traffic volume, location, and season on PM_{10} road dust emissions. Atmospheric Environment (submitted).

Etyemezian V., H. Kuhns, J. Gillies, M. Green, M. Pitchford, & J. Watson (2003b): Vehicle based road dust emissions measurements (I): Methods and Calibration. Atmospheric Environment (submitted).

Etyemzian, V., J.A. Gillies, H. Kuhns, D. Nikolic, J. Watson, J. Veranth, R. Laban, G. Seshadri, & D. Gillette (2003c): Field Testing and Evaluation of Dust Deposition and Removal mechanisms. Final Report, technical report prepared for The WESTAR Council.

Gillies, J.A., J.G. Watson, C.F. Rogers, D. DuBois, J.C. Chow, R. Langston, & J. Sweet, 1999, Long term efficiencies of dust suppressants to reduce PM_{10} emissions from unpaved roads. The Journal of the Air & Waste Management Association, vol.49, p 3-16.

Gillies, J.A., P. Arnott, V. Etyemezian, D.A. Gillette, H. Kuhns, E. McDonald, H. Moosmüller, W. G. Nickling, G. Schwemmer, T. Wilkerson, & K. J. Thome (2002): Characterizing and Quantifying Local and Regional Particulate Matter Emissions from Department of Defense Installations. Annual Report 2002, technical report prepared for Strategic Environ. Res. & Develop. (SERDP), Arlington, VA, 22203-1821.

Kuhns, H., V. Etyemezian, D. Landwehr, C. MacDougall, M. Pitchford, & M. Green (2001): Testing Re-entrained Aerosol kinetic Emissions from Roads (TRAKER): a new approach to infer silt loading on roadways. Atmospheric Environment, vol. 35, p 2815-2825.

Midwest Research Institute (2001): Revisions to AP-42 Section 13.2.2 "Unpaved Roads". Technical Memorandum prepared for the U.S. EPA.

Nicholson, K.W., J.R. Branson, P. Geiss, & R.J. Cannel (1989): The effects of vehicle activity on particle resuspension. Journal of Aerosol Science, vol. 20, p 1425-1428.

U.S. EPA (1995): User's Guide for the Industrial Source Complex (ISC3) Dispersion Models Volume II: Description of Model Algorithms. US Environmental Protection Agency, Office of Air Quality Planning and Standards: Emissions, Monitoring, and Analysis Division, RTP, NC.

U.S. EPA (1996): Compilation of Air Pollutant Emission Factors. Vol. 1: Stationary Point and Area Sources, U.S. EPA Office of Air and Radiation, Office Air Quality Planning and Standards, RTP, NC.

12th International Symposium "Transport and Air Pollution" / 12e Colloque international "Transports et pollution de l'air", Avignon, 16 -18 *June* / juin 2003
proceedings / actes, n°92, tome / Vol. 1, Inrets ed., Arcueil, France, 2003, p. 59-66

Chemical Characterization of Emissions from Advanced Technology Light Duty Vehicles

Lisa Graham
Environment Canada, Emissions Research and Measurement Division, 335 River Road, Ottawa, Ontario, Canada, K1A 0H3, Lisa.Graham@ec.gc.ca

Abstract
Results of detailed emissions measurements of seven advanced technology vehicles are reported. Six of the seven vehicles were imported from Europe and Japan and are not available for sale in Canada. Three of the vehicles were direct injection diesel technology, three were gasoline direct injection (GDI) technology and one vehicle was a gasoline-electric hybrid. The emissions were characterized over four test cycles representing different driving conditions. Samples of the exhaust were collected for determining methane, non-methane hydrocarbons and carbonyl compounds for the purposes of comparing ozone forming potential of the emissions. The diesel fuelled vehicles had emissions with both the highest specific reactivity and ozone forming potential.
Keys-words*: emissions characterization, Diesel Direct Injection, Gasoline Direct Injection, Gasoline-Electric Hybrid, non-methane hydrocarbons, carbonyl compounds, ground level ozone forming potential.*

Résumé
Voici la présentation de l'analyse détaillée des émissions de sept véhicules de haute technologie. Six des sept véhicules importés d'Europe et du Japon ne sont pas en vente sur le marché canadien. De ces derniers, trois sont munis d'un moteur diesel à injection directe; trois autres d'un moteur à essence à injection directe et le dernier d'un moteur hybride électrique-gazoline. Quatre protocoles d'essai furent utilisés pour caractériser les émissions dans diverses situations de conduite routières. Pour comparer le potentiel de formation d'ozone des émissions, des échantillons des gaz d'échappement de ces véhicules furent analysés. Les concentrations de méthane, d'hydrocarbures autres que le méthane et des composés carbonylés furent mesurées. Des émissions ayant des taux plus élevés de réactivité spécifique et de potentiel de formation d'ozone furent observées pour les véhicules à moteur diesel.
Mots-clés*: caractérisation des émissions, moteur diesel à injection directe, moteur à essence à injection directe, moteur hybride électrique-gazoline, hydrocarbures autres que le méthane, composés carbonylés, potentiel de formation d'ozone troposphérique.*

Introduction

Recent advances in both diesel and gasoline engine technologies have resulted in a selection of advanced technology vehicles appearing on the market in Europe and Japan. These technologies require high quality, low sulphur fuels readily available in these regions, but not yet widely available in North America. As fuel quality improves in North America, these vehicles may be offered for sale here.

Gasoline direct injection technology offers the greater fuel economy characteristic of a diesel engine in a gasoline-fuelled engine. Environment Canada is interested in comparing the emissions of vehicles equipped with these engines to the conventional gasoline vehicles (multiport fuel injection – MPFI) and to vehicles equipped with advanced direct injection diesel engines.

Policy decisions with regard to fuel mix require the careful balancing of improvements in fuel economy (and hence a reduction in greenhouse gas emissions) with a variety of competing emissions characteristics such as ground level ozone forming potential, toxicity, primary particulate matter emissions, and emissions of gases that react in the atmosphere to form secondary particulate matter. It is therefore in Canada's best interest to understand the composition of the emissions produced by new technology options before accepting or rejecting these options.

In a co-operative study between Transport Canada and Environment Canada, vehicles representing these new technology options were acquired and evaluated for driveability, safety, fuel economy and emissions. The project report presents details of all emissions measurements [Graham (2000)]. Only the results of the gaseous emissions chemical characterization are presented in this paper.

1 – Measurement Method

Specifications of the seven test vehicles are given in Table 1.

	Curb Weight (kg)	Engine	Transmission	Fuel Economy (L/100 km)	Emissions Controls
Diesel Direct Injection					
2000 Mercedes A170	1095	1.7L turbocharged inline 4 cylinder 66 kW @ 4200 rpm 180 Nm @ 1600-3200 rpm	5 speed manual, automatic clutch	5.6 city 4.2 hwy	Oxidation catalyst
2000 MicroCompact SmartCar	730	0.8L turbocharged inline 3 cylinder 30 kW @ 4200 rpm 100 Nm @ 1800-2800 rpm	6 speed automatic, sequential gearbox	3.6 city 3.2 hwy	Oxidation catalyst
2000 Volkswagen Lupo		1.2L turbocharged inline 3 cylinder 45 kW @ 4000 rpm 140 Nm @ 1800-2400 rpm	5 speed automatic, sequential gearbox	3.4 city 2.7 hwy	EGR Oxidation catalyst
Gasoline Direct Injection					
2000 Nissan Gloria	1628	3.0L V6 177 kW	4 speed automatic	Not available	3-way catalyst
2000 Renault Megane	1135	2.0L inline 4 cylinder 103 kW @ 5500 rpm 200 Nm @ 4250 rpm	5 speed manual	8.7 city 6.1 hwy	3-way catalyst
2000 Mitsubishi Dion	1390	2.0L inline 4 cylinder 99 kW	4 speed automatic	Not available	3-way catalyst
Gasoline-Electric Hybrid					
2000 Toyota Prius	1254	1.5L inline 4 cylinder 52 kW @ 4500 rpm 111 Nm @ 4200 rpm **Electric motor:** Permanent magnet 33 kW @ 1040-5600 rpm 350 Nm @ 0-400 rpm **Batteries:** NiMH, 228 cells @ 1.2V each	Electronically controlled continuously variable	4.5 city 4.6 hwy	3-way catalyst

Table 1: Specifications for test vehicles.

Tableau 1: Description des véhicules testés.

Tailpipe emissions were determined in the laboratory using a chassis dynamometer to simulate vehicle inertia and road load and a constant volume sampling system to obtain emissions samples for analysis. The Canadian emissions certification fuels (Tier 1 gasoline, low sulphur diesel) were used in all testing. Two repeats of each test cycle were completed. Reported emissions are an average of the two repeats.

The vehicles were tested over several driving cycles to investigate the response of the technology to different driving styles. The Federal Test Procedure (FTP) allowed examination of cold and hot

start emissions, a non-demanding driving style and city fuel economy. The FTP was implemented using the older four-phase version of test rather than the current three-phase test to facilitate particulate matter sample collection [Whitney (1998)]. The Highway Fuel Economy Test (HWFET) was performed to complete the fuel economy evaluation and to examine how high-speed highway driving affects the emissions from the vehicle. It has been recognized that low power, long idling periods common to congested urban driving are not well represented by the FTP, so the New York City Cycle (NYCC) was used to capture this style of driving. Aggressive driving habits such as hard accelerations and decelerations coupled with high speed driving are reflected in the US06 test.

Emissions of the gaseous criteria pollutants: carbon monoxide (CO), oxides of nitrogen (NO_X) and total hydrocarbons (THC); and of carbon dioxide (CO_2) were determined for each phase of a test or each test as applicable. Samples were also collected for determining carbonyl compound emissions and for determining methane and detailed characterization of non-methane hydrocarbons. Particulate matter ($PM_{2.5}$) mass emission rates were determined over each test and samples for characterization of carbon composition the particulate matter were collected.

Dilute exhaust samples for methane and non-methane hydrocarbon analysis were collected in separate Tedlar™ bags for each phase or test cycle. Approximately 165 volatile organic compounds were determined by cryogenic preconcentration gas chromatography with flame ionization detection (GC-FID). The detection limits expressed in mass emission rate units are given in Table 2.

Samples for carbonyl compound analysis were collected by drawing dilute exhaust through silica gel Sep-Pak cartridges coated with 2,4-dinitrophenylhydrazine (2,4-DNPH). The hydrazones were removed from the cartridge using a solvent and the liquid sample that resulted was analysed by reverse phase high performance liquid chromatography (HPLC) with UV-Visible diode array detection. Detection limits for the target carbonyl compounds are given in Table 2.

	FTP Phases 1&3	FTP Phases 2&4	FTP Comp	HWFET	NYCC	US06
methane	0.08	0.09	0.08	0.05	0.1	0.07
NMHCs	0.0002	0.0002	0.0002	0.0001	0.0003	0.0001
Formaldehyde	0.004	0.003	0.003	0.002	0.006	0.003
Acetaldehyde	0.005	0.004	0.004	0.002	0.008	0.004
Acrolein	0.007	0.004	0.005	0.003	0.01	0.005
Acetone	0.007	0.005	0.005	0.003	0.01	0.005
Propionaldehyde	0.006	0.004	0.005	0.003	0.009	0.005

Table 2: Organic compound detection limits in mg/km.

Tableau 2: Limite de détection des composés organiques en mg/km.

2 – Results

Non-methane Organic Gases

Methane and non-methane hydrocarbons were determined for all vehicles (except the Nissan Gloria) over each test phase. The complete set of results is available in the project report [Graham (2000)]. The discussion below focuses on the emissions of toxic hydrocarbons.

Emission rates for selected toxic hydrocarbons are presented in Table 3. The cold start (Phase 1) produced the highest emission rates of the FTP test cycle, though the increase as compared to the hot start (Phase 3) emissions seen with the diesel fuelled vehicles was not as great as would be seen with traditional MPFI gasoline vehicles. This increase is greater for the GDI vehicles than for the diesel vehicles indicating significant enrichment is still required on engine start. The cold start emissions for the Prius are not significantly different from those observed in the other phases of the FTP indicating that the emissions control technology is able to deal effectively with the cold start emissions. The Prius emission rates are also very low and show more variation than seen with other vehicles, due to the correction for dilution air composition.

	FTP Phase 1	FTP Phase 2	FTP Phase 3	FTP Phase 4	HWFET	NYCC	US06
Mercedes A170							
1,3-butadiene	0.662	0.470	0.530	0.510		0.429	0.011
benzene	0.873	0.844	0.641	0.804	0.038	1.67	0.094
toluene	0.382	0.347	0.191	0.130	0.019	0.580	
ethylbenzene	0.135		0.080			0.124	
m&p-xylene	0.339	0.088	0.110			0.227	
o-xylene	0.188	0.160	0.096	0.084		0.303	
1.1.1.1.1.1 MicroCompact SmartCar							
1,3-butadiene	0.879		0.337			0.470	0.066
benzene	0.572	0.036	0.255	0.024	0.018	0.497	0.134
toluene	0.267	0.007	0.131	0.026	0.035	0.131	0.096
ethylbenzene	0.084						
m&p-xylene	0.205						
o-xylene	0.117						
Volkswagen Lupo							
1,3-butadiene	0.344		0.126	0.027		0.228	
benzene	0.507	0.094	0.257	0.079	0.001	0.429	0.041
toluene		0.123	0.246	0.069		0.013	0.111
ethylbenzene							
m&p-xylene	0.144						
o-xylene	0.076		0.032				
Mitsubishi Dion							
1,3-butadiene	0.529						
benzene	4.59	0.022	0.007			0.072	0.832
toluene	38.8	0.126	0.018			1.29	1.36
ethylbenzene	1.10					0.119	0.071
m&p-xylene	1.15					0.311	0.186
o-xylene	0.637					0.123	0.064
Renault Megane							
1,3-butadiene	0.803						0.017
benzene	5.20	0.045	0.088	0.005	0.003	0.071	0.260
toluene	29.2	0.314	1.97	0.592	0.320		0.989
ethylbenzene	1.30						0.050
m&p-xylene	1.40						0.099
o-xylene	0.721		0.042				0.033
Toyota Prius							
1,3-butadiene			0.020	0.035			
benzene	0.025	0.002	0.033	0.044		0.010	0.005
toluene	0.205	0.019	0.203	0.523	0.020	0.026	0.058
ethylbenzene							
m&p-xylene	0.011		0.014	0.026			
o-xylene			0.030	0.053			

Table 3: Emission rates of selected toxic hydrocarbons (mg/km). Missing values are below detection limits.

Tableau 3: Taux d'émission de certains hydrocarbures toxiques (mg/km). Les données manquantes sont inférieures aux limites de détection.

The high speed driving of the HWFET and US06 tests produce lower emission rates due to the high temperature of the exhaust and the efficient operation of the oxidation catalyst. Only modest increases in the diesel vehicle emissions are seen in the US06 over the HWFET due to aggressive driving. Significant increases in emissions for the GDI vehicles are seen in the US06 over the HWFET due to aggressive driving. Aggressive and high speed driving do not increase the emissions from the Prius as compared to the FTP results.

The emission rates for the NYCC cycle are slightly higher than those observed over the FTP phases (other than phase 1) for all vehicles. This is due in part to the short distance travelled during the test (much of the test time is spent idling). For the Prius, the NYCC emissions are also very low, likely due to the hybrid design that allows the engine to shut off when the electrical side of the powerplant is able to provide the required power.

It should be noted that the dominance of toluene in the emission profile of the gasoline fuelled vehicles is due to the composition of the test fuel (Tier 1 certification) and is not typical of commercially available fuels.

	FTP Phase 1	FTP Phase 2	FTP Phase 3	FTP Phase 4	HWFET	NYCC	US06
Mercedes A170							
Formaldehyde	17.7	12.8	12.7	14.0	0.78	27.6	2.06
Acetaldehyde	9.85	5.96	6.48	5.65	0.41	12.6	1.23
Acrolein	1.30	0.90	1.36	0.71			
Acetone	4.96	3.00	3.41	2.55	0.46	3.22	1.40
Propionaldehyde	1.81		1.04	0.65		1.01	
SmartCar							
Formaldehyde	15.7	0.75	6.59	0.62	0.33	12.5	4.30
Acetaldehyde	7.42	0.24	3.03	0.11	0.15	5.66	1.90
Acrolein	1.17						0.37
Acetone	3.67	0.38	1.41	0.31	0.11	3.75	0.94
Propionaldehyde	1.54		0.34				0.39
Volkswagen Lupo							
Formaldehyde	5.10	0.97	3.18	1.26	0.01	7.93	0.64
Acetaldehyde	3.72	0.73	1.92	0.71	0.13	4.32	0.48
Acrolein							
Acetone	1.84	1.26	1.03	1.36		3.99	0.44
Propionaldehyde	0.34						
Mitsubishi Dion							
Formaldehyde	0.35	0.07		0.15	0.20	0.19	
Acetaldehyde	0.58	0.08	0.07	0.16	0.20	0.81	0.14
Acrolein							
Acetone	0.43	0.03		0.05	0.03		
Propionaldehyde							
Renault Megane							
Formaldehyde	0.81	0.26	0.09	0.27	0.03	0.68	0.02
Acetaldehyde	0.72	0.10			0.01	0.65	
Acrolein							
Acetone	0.44	0.15	0.02	0.05	0.01	0.93	0.02
Propionaldehyde							
Toyota Prius							
Formaldehyde	0.12	0.07	0.17	0.22	0.07	0.39	0.08
Acetaldehyde				0.36	0.06	0.20	
Acrolein							
Acetone							
Propionaldehyde							

Table 4: Emission rates of selected carbonyl compounds (mg/km). Missing values are below detection limits.

Tableau 4: Taux d'émission de certains composés carbonylés (mg/km). Les données manquantes sont inférieures aux limites de détection.

Emission rates for selected carbonyl compounds are presented in Table 4. Carbonyl compound emission rates for diesel fuelled vehicles have historically been greater than for conventional gasoline vehicles. This trend is observed to continue in that the emissions remain lower for the GDI vehicles as compared to the DDI vehicles.

Carbonyl compounds emissions from the diesel vehicles are dominated by formaldehyde. Acetaldehyde is the next most abundant carbonyl. Cold start emissions produce larger number of detected carbonyl species. For all vehicles, NYCC emission rates are greater than the FTP composite emission rates. HWFET emission rates are the lowest. The US06 emission rates are greater than the HWFET emission rates due to the aggressive driving characteristics of the cycle.

For the GDI vehicles, NYCC emission rates are greater than the FTP composite emission rates but also show significant variability. This variability is more likely due to the variation in combustion conditions and catalyst temperatures than due to analysis sensitivity. Carbonyl compounds appear in

the exhaust due to incomplete combustion and at the low power demand and low exhaust temperatures of this cycle, the combustion conditions and catalyst temperatures have a large potential for variation. The US06 emission rates are the lowest, followed by the HWFET and FTP composite emission rates. The emissions from the Prius are not much lower than for the other gasoline fuelled vehicles.

3 - Discussion

All vehicles meet the gaseous emissions standards currently applicable in Canada. All vehicles except the Mercedes A170 meet the PM emission rate standards. This result may be due more to the quality of the test fuel used (higher sulphur and lower cetane as compared to the European test fuel) than to the vehicle technology.

The motivation for performing detailed analysis on the hydrocarbon composition of the exhaust is to understand the photochemical reactivity and ozone forming potential of the vehicle/fuel combination. Different organic compounds have different reactivities towards forming ground level ozone when emitted into an airshed. One such scale for measuring these relative reactivities is the Carter Maximum Incremental Reactivity scale (MIR) [CARB(1999)]. Methane is generally considered unreactive towards forming ground level ozone and the discussion is therefore usually limited to non-methane organic gases (non-methane hydrocarbons, carbonyl compounds and alcohols or ethers if present in the fuel). The mass emission rate for each compound is multiplied by its corresponding MIR value to obtain an estimate of how much ozone might be generated photochemically if that amount of the compound were introduced into the atmosphere. The specific reactivity of the exhaust is defined as the total amount of ozone produced divided by the total non-methane organic gas (NMOG) emission rate. The ozone forming potential is defined as the amount of ozone per mile of travel the vehicle would be expected to contribute to the airshed. Fig. 1 compares the specific reactivities of the emissions over each test for each vehicle. Fig. 2 compares the ozone forming potential over each test for each vehicle.

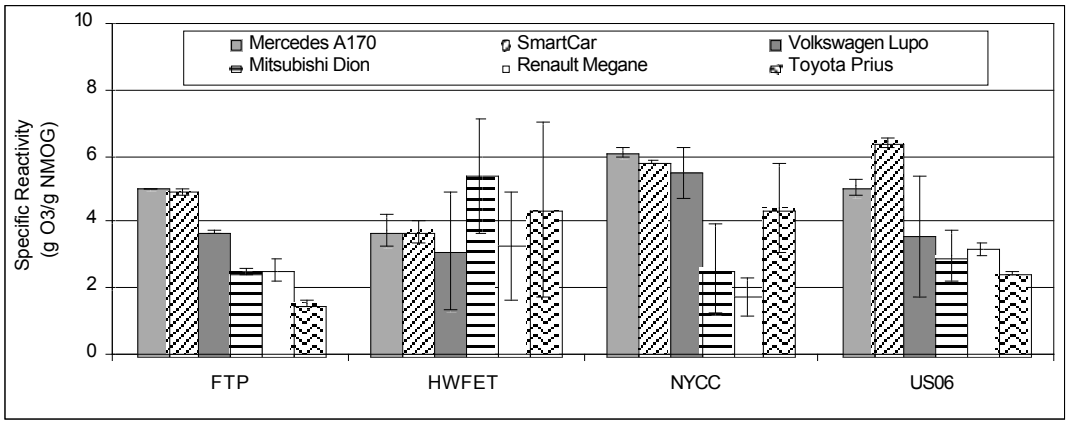

Figure 1: Comparison of NMOG specific reactivity for all vehicles and driving cycles.

Figure 1: Comparaison du taux de réaction spécifique des gaz organiques autres que le méthane pour tout les véhicules et les protocoles d'essai.

The diesel fuelled vehicles tend to have higher specific reactivities than the GDI vehicles and the gasoline-electric hybrid for the FTP, NYCC and US06 driving cycles. There are smaller differences among the vehicles for the HWFET cycle. Factoring in the mass emission rates for these vehicles, the ozone forming potential of the diesel fuelled vehicles is generally greater than that of the GDI vehicles, especially for the congested urban driving of the NYCC. The ozone potential of the gasoline-electric hybrid is very low due to the very low emission rates, despite sometimes having higher specific reactivity than other vehicles.

Figure 3 shows the relative contributions of hydrocarbons and carbonyl compounds to the NMOG emission rates and to the ozone forming potential for the FTP test. The diesel emissions show a

significant contribution from carbonyl compounds to both the emission rate and the ozone forming potential while the gasoline emissions show very small contribution from carbonyl compounds.

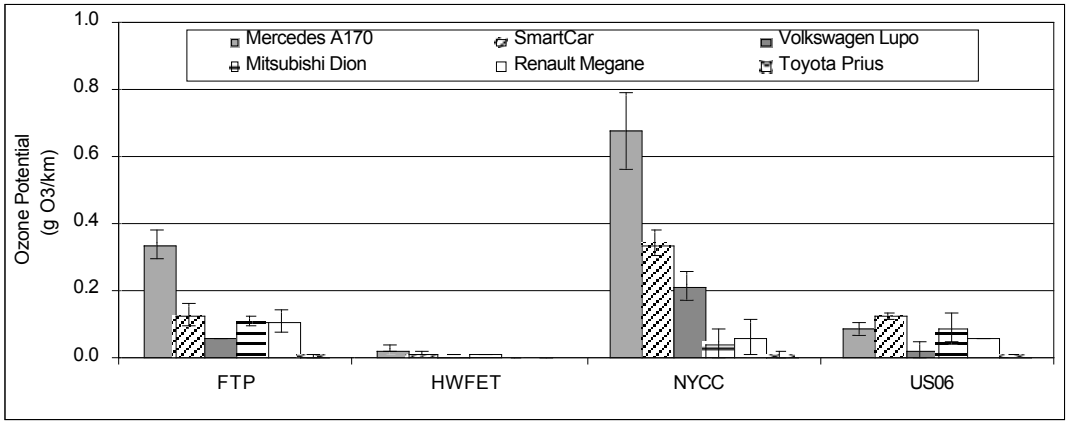

Figure 2: Comparison of ozone forming potential for all vehicles and driving cycles.

Figure 2: Comparaison des taux de formation d'ozone pour tout les véhicules et les protocoles d'essai.

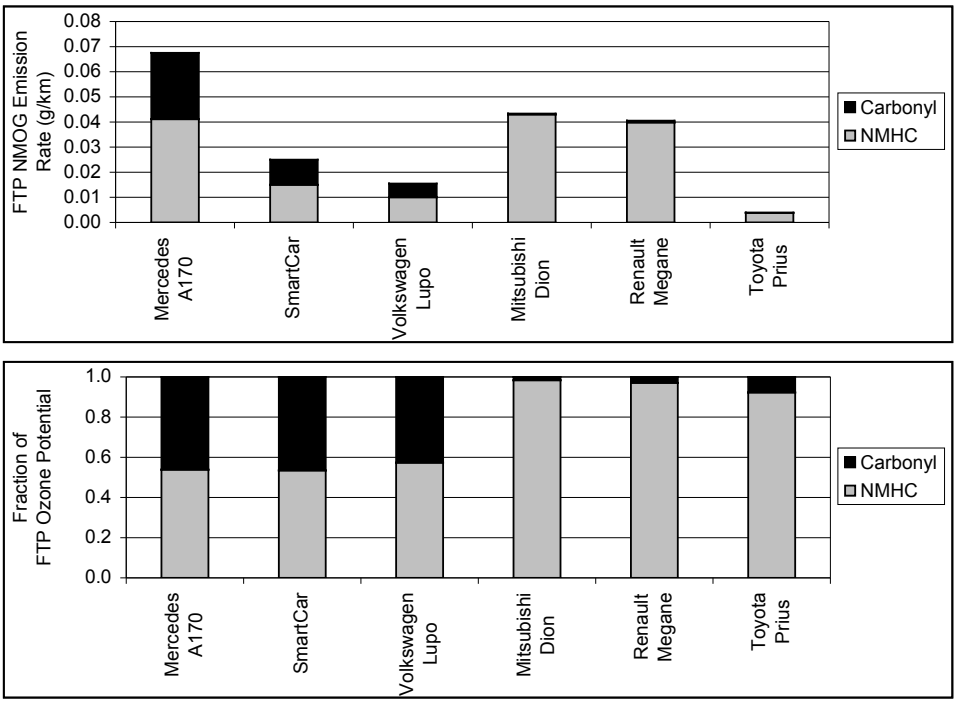

Figure 3: Distribution of NMOG emission rate and ozone forming potential.

Figure 3 : Distribution des taux d'émission de gaz organiques autres que le méthane et des potentiels de formation d'ozone.

Conclusion

Advanced technology vehicles (European and Japanese imports) vehicles were tested as received using emissions testing procedures that are standard in Canada. It is recognized that these vehicles were not specifically designed to meet Canadian emissions standards. Our interest was in conducting an initial evaluation of these vehicles in the context of them being offered for sale in their present configurations.

The three direct injection diesel vehicles all met the current Canadian LDDV Tier 1 emissions standards for CO, NO_X and THC. The Lupo and SmartCar also met the current PM standard while the A170 did not. The three GDI vehicles tested met the current Canadian Tier 1 and LEV

emissions standards for CO, NO_X and NMHC/NMOG. Two of the vehicles (the Dion and Megane) also met the ULEV standards for CO and NO_X but not NMOG. The Gloria met the ULEV NO_X emission standard but not the CO standard. The Toyota Prius met quite easily the ULEV standards for all pollutants.

The advantages of the GDI technology were observed in substantially lower NO_X and PM emissions as compared to the diesel vehicles, but as compared to the conventional MPFI vehicles, PM emissions were significantly greater.

The reactivity of the exhaust towards forming ground level ozone was evaluated. Under all operating conditions, the diesel vehicles had substantially higher ozone forming potentials than the GDI vehicles. Under some conditions the diesel vehicles showed up to an order of magnitude greater ozone forming potential. This was attributed to higher emissions of the highly reactive carbonyl compounds.

Acknowledgments

The author wishes to thank

- Transport Canada (Motor Vehicle and Standards Research – Energy and Emissions Engineering) and specifically Mr. John Thorpe for making the vehicles available for emissions testing;
- The staff of Environment Canada – Emissions Research and Measurement Division for technical support during emissions testing;
- Natural Resources Canada for research funding through their Program for Energy Research and Development.

References

CARB (1999) California Air Resources Board, "California Non-Methane Organic Gas Test Procedures", Amended 5 August 1999, Appendix 1, p 1-1 – 1-5.

Graham (2000) Graham, L.A.; Characterization of Emissions from Advanced Technology Vehicles, Environment Canada, ERMD Internal Report #00-63, 2000, 120 p.

Whitney (1998) Whitney, K.A., M. Bergin; Composition of Primary Particulate Exhaust Emissions from Alternative Fuels, Proceedings of the International Specialty Conference "$PM_{2.5}$ – A Fine Particle Standard", Long Beach, California, January 28-30, 1998, Air and Waste Management Association, p 590-604

12th International Symposium "Transport and Air Pollution" / 12e Colloque international "Transports et pollution de l'air", Avignon, 16 -18 *June* / juin 2003
proceedings / actes, n°92, tome / Vol. 1, Inrets ed., Arcueil, France, 2003, p. 67-72

Vehicle emissions of speciated carbonyls

Daniel Grosjean

DGA, Inc., 4526 Telephone Road, Suite 205, Ventura, CA 93003, USA
Fax 1-805-644-0142 - email: danieldga@aol.com

Abstract
Speciated carbonyls (up to ca. 120 aldehydes and ketones) have been measured in vehicle emissions using liquid chromatography-atmospheric pressure negative chemical ionization mass spectrometry. Examples discussed here include on-road carbonyl emissions measured in a U. S. highway tunnel and emission factors measured in dynamometer tests carried out in Brazil using the Brazilian high oxygen content gasoline-ethanol blend. Other dynamometer and highway tunnel results obtained in Brazil and in the U. S. will be included in the oral presentation along with a discussion of exhaust carbonyls vs. fuel hydrocarbons.
Key-words: *speciated carbonyls, emission factors, dynamometer tests, highway tunnels, Brazilian gasoline-ethanol blend.*

Introduction and Study Rationale

Carbonyls (aldehydes and ketones) continue to receive scientific and regulatory attention as toxic air contaminants, mutagens and carcinogens. Motor vehicles are a major source of carbonyls in urban air. Detailed information on vehicle emissions of carbonyls is necessary to assess the contribution of vehicles to ambient levels of carbonyls, to estimate population exposure and possible adverse health effects, and to examine the importance of vehicle- emitted carbonyls in the formation of ozone, peroxyacyl nitrates ($RC(O)OONO_2$) and other toxic photochemical products. The composition and the reactivity of vehicle-emitted carbonyls vary with fuel composition (e.g., oxygenated gasolines that contain MTBE or ethanol; CNG; LPG; low-sulfur diesel fuel; biodiesel), engine and exhaust control technology (e.g. catalytic converter) and the overall characteristics of the vehicle fleet in a given urban area (e.g., age, maintenance, driving patterns, number of light-duty (LD) vehicles vs. number of trucks and public transportation buses and vans). As fuel composition, vehicle technology and vehicle fleet continue to evolve in urban areas throughout the world, it is important to characterize current vehicle emissions of carbonyls, to examine the air quality benefits of regulatory decisions regarding vehicle fuels and emission controls, and to provide baseline data for future studies.

Past studies of vehicle emissions of carbonyls have been limited to formaldehyde, acetaldehyde and, less frequently, several other low molecular weight (MW) carbonyls. A new analytical method has been introduced (Grosjean, et al., 1999) that involves liquid chromatography separation of carbonyls as their DNPH derivatives and detection by diode array uv-visible spectroscopy and by atmospheric pressure negative chemical ionization mass spectrometry (LC-DAD-APNCI-MS). This method, combined with the collection of airborne carbonyls on DNPH-coated silica gel cartridges downstream of KI oxidant scrubbers, has been applied to the identification of vehicle-emitted carbonyls in two highway tunnels and to the measurement of the corresponding on-road emission factors (Grosjean, et al., 2001; Kean, et al., 2001). We describe here some recent results regarding vehicle emissions of carbonyls in dynamometer tests and highway tunnels. These two types of studies complement each other: dynamometer tests yield information for a given vehicle with well-documented engine technology, exhaust control technology, fuel composition and driving cycle, while highway tunnel studies yield information on emissions averaged over a large number of

vehicles (typically several thousands) under "real-world" conditions. The examples described here include data from two countries, Brazil and U.S.A. Due to space constraints, experimental methods are omitted here and additional examples of results will be included in the oral presentation.

1 - Carbonyls identified in vehicle emissions

Gasoline and diesel fuel contain hundreds of hydrocarbons, whose oxidation (incomplete combustion) leads to many carbonyls in vehicle exhaust. In its present (2002-2003) stage of application, the LC-DAD-APNCI-MS method may yield data for ca. 100-120 carbonyls, depending on the complexity of the sample studied, the volume of air sampled and the desired level of detail for data acquisition. Given in Table 1 are concentrations for 128 carbonyls measured in a sample collected in a highway tunnel in Madison, Wisconsin, U.S.A., during winter 2001. The volume of air sampled was ca. 0.4 m^3. The carbonyls identified are listed in order of elution (starting with the left-hand column) and ranged from C_1 (formaldehyde) to C_{14} (tetradecanal and isomers). Several polar carbonyls such as hydroxycarbonyls and oxoacids elute before formaldehyde. The total carbonyl concentration was ca. 12.1 μg/sample, and individual carbonyl concentrations ranged from 1-2 ng/sample for minor components to ca. 2-3 μg/sample for the most abundant components such as formaldehyde, acetaldehyde and acetone. Entries such as C7 ALP ISOM #5 (seven carbon atoms aliphatic carbonyl isomer) in Table 1 reflect the current limitations of our collection of reference compounds; that is, the MW and chemical functionality of the compound could be determined but no reference standard was available for positive identification of the isomer(s) present in the sample.

Glyoxylic acid	0.008	2-Oxohexanal	0.003
Pyruvic acid	0.025	C8 ALP ISM #5	0.002
3-Hydroxy-2-Butanone	0.025	C8 UNSAT ISM #1	0.000
Hydroxyacetaldehyde	0.016	C8 ALP ISM #6	0.015
Hydroxyacetone	0.047	C8 UNSAT ISM #2	0.002
5-Hydroxy-2-Pentanone	0.005	2,3-Hexanedione/ISM	0.002
Formaldehyde	2.973	C8 ALP ISM #7	0.024
2,4-Pentanedione		C8 ALP ISM #8	0.014
3-Oxobutanal		C8 ALP ISM #9	0.013
5-Hydroxy-methyl-furfural		Pinonaldehyde (TENT)	0.001
Acetaldehyde	2.292	3,4-Hexanedione/ISM	0.002
Succinnic dialdehyde		C8 ALP ISM #10	0.010
1,4-Benzoquinone (TENT)		Octanal	0.032
Acrolein	0.574	C9 ALP ISM #1	0.011
Acetone	2.268	2-Oxoheptanal/ISM	0.002
2-Furaldehyde	0.048	C9 ALP ISM #2	0.020
Propanal	0.189	Unknown #3 (MW=154, ARM)	
Crotonaldehyde	0.032	Unknown #4 (MW=234, ARM)	0.008
Methacrolein	0.079	C9 ALP ISM #3	0.003
2-Butanone (MEK)	0.431	C9 ALP ISM #4	0.002
Butanal/Isobutanal	0.095	trans-2-Nonenal/ISM	0.001
Cyclopentanone (TENT)		C9 ALP ISM #5	0.005
Methyl Vinyl Ketone	0.048	C9 ALP ISM #6	0.022
Benzaldehyde	0.296	C9 ALP ISM #7	0.012
o/m/p-Anisaldehyde		Nonanal	0.067
2-Pentenal/ ISM	0.010	C8 DICARB #1	
C5 ALP ISM #1	0.022	C10 ALP ISM #1	0.010
Cyclohexanone		C10 ALP ISM #2	0.007

Isopentanal	0.098	Unknown #5 (MW=202, ARM)	0.027
2-Pentanone	0.044	C10 ALP ISM #3	0.004
Glyoxal	0.017	trans-2-Decenal/ISM	0.005
Pentanal	0.044	C10 ALP ISM #4	0.011
Acetophenone	0.033	C10 ALP ISM #5	0.005
o-Tolualdehyde	0.067	2-Decanone	0.011
C6 ALP ISM #1	0.006	Decanal	0.020
m-Tolualdehyde	0.138	C9/C10 DICARB #1	0.013
p-Tolualdehyde	0.107	C11 ALP ISM #1	0.002
Indanone	0.004	Unknown #6 (MW=221, ARM)	0.003
Cinnamaldehyde		C9/C10 DICARB #2	
C6 ALP ISM #2	0.074	C11 ALP ISM #2	0.003
4-Methyl-2-Pentanone (MIBK)	0.035	Unknown #7 (MW=256, ALP)	0.015
C6 UNSAT ISM #1	0.004	Unknown #8 (MW=282, ARM)	0.015
Glutaraldehyde	0.008	trans-2-Undecenal/ISM	0.000
C6 ALP ISM #3	0.009	C11 ALP ISM #3	0.003
C6 ALP ISM #4	0.010	Unknown #9 (MW=282, ARM)	0.051
Methyl Glyoxal	0.309	Undecanal	0.010
C6 ALP ISM #5 (2-Hexanone)	0.037	C12 ALP ISM #1	0.005
Hexanal	0.103	C12 ALP ISM #2	0.002
DMBZ ISM #1	0.141	C12 ALP ISM #3	0.002
C7 ALP ISM #1	0.013	Unknown #10 (DICARB)	0.004
2,5-Dimethylbenzaldehyde	0.112	2-Dodecanone	0.005
C7 ALP ISM #2	0.014	C12 ALP ISM #4	0.006
2,4-Dimethylbenzaldehyde/ISM	0.070	Dodecanal	0.007
DMBZ ISM #2	0.033	C13 ALP ISM #1	0.005
C7 ALP ISM #3	0.038	C13 ALP ISM #2	0.002
C7 ALP ISM #4	0.002	Unknown #11 (MW=234, ARM)	0.028
2-Oxobutanal	0.054	C13 ALP ISM #3	0.001
C7 ALP ISM #5	0.013	Unknown #12 (MW=285, ALP)	0.007
C7 ALP ISM #6	0.011	Tridecanal	0.004
6-Methyl-5-Heptene-2-One	0.024	C14 ALP ISM #1	0.002
C7 UNSAT ISM #1	0.002	C14 ALP ISM #2	0.002
Biacetyl	0.053	C14 ALP ISM #3	0.002
C7 ALP ISM #7	0.010	C14 ALP ISM #4	0.002
2-Heptanone	0.035	C14 ALP ISM #5	0.002
Unknown #1 (MW=236, ALP)	0.022	Tetradecanal	0.002
C7 ALP ISM #8	0.018		
C7 UNSAT ISM #2			
2,4,6-Trimethylbenzaldehyde/ISM	0.101	Total Carbonyls, ug/sample	12.08
Heptanal	0.044	Count of Carbonyls	128
2-Oxopentanal	0.009	Count of Carbonyls Identified	117
C8 ALP ISM #1	0.003	Count of Carbonyls Unidentified	11
C8 ALP ISM #2	0.002	% Identified, mass basis	98
C8 ALP ISM #3	0.006		
2,3-Pentanedione	0.010	ISOM: isomer; ALP: saturated aliphatic;	
Unknown #2 (MW=226, ALP)	0.009	UNSAT: unsaturated aliphatic;	

C8 ALP ISM #4	0.019	AROM: aromatic; DICARB: aliphatic dicarbonyl; TENT: tentative structural assignment; U: unknown; MW: molecular weight; blank entry: below detection limit

Table 1: Concentrations of carbonyls (microgram per sample) in sample collected in a highway tunnel

2 - Emission factors for speciated carbonyls

The example given in Table 2 is for carbonyls measured in the exhaust of a Brazilian light-duty vehicle in Phase 2 (hot stabilized) of a dynamometer test (essentially the same as U. S. FTP 75). The vehicle fuel was a gasoline-ethanol blend (ca. 23 vol % ethanol). Brazil is unique in the world for its heavy reliance on ethanol, which is used as a LD vehicle fuel (currently ca 20% of the LD fleet) or as a component of gasoline-ethanol blends (ca. 80% of the LD fleet). The oxygen content of the Brazilian gasoline-ethanol blend is high, i.e., 8% by weight. Emission factors are given in Table 2 on a mass per unit fuel consumed basis. Since fuel sales are well documented in most countries, data of the type given in Table 2 can be readily used to construct carbonyl vehicle emission inventories for a given city, metropolitan area, state or country. The most abundant carbonyl in Table 2 is acetaldehyde, which results from incomplete combustion of hydrocarbons and ethanol. Exhaust emissions of acetaldehyde from LD vehicles fueled with the gasoline-ethanol blend, together with exhaust emissions of acetaldehyde from LD vehicles fueled with ethanol, contribute to the higher (than in most countries) levels of acetaldehyde measured in the ambient air of Brazilian cities (Grosjean, et al., 2002).

Formaldehyde	8103.41	2,4-Dimethylbenzaldehyde/ISM	1047.74
Acetaldehyde	11670.88	DMBZ ISM #2	1007.44
Acetone	7767.26	C7 ALP ISM #1	107.20
Acrolein	46.92	2-Oxobutanal	37.61
Propanal	650.85	ARM ISM #2	154.99
Crotonaldehyde	256.51	Biacetyl	223.88
Methacrolein	151.26	TMBZ ISM #1 (b)	116.01
2-Butanone (MEK)	287.84	Heptanal	9.71
Butanal	230.95	2,4,6-Trimethylbenzaldehyde/ISM	378.55
Benzaldehyde	4884.55	TMBZ ISM #2	464.03
o/m/p-Anisaldehyde	251.91	2-Oxopentanal	105.12
Isopentanal	195.38	C8 ALP ISM #1	197.01
2-Pentanone	85.48	2,3-pentanedione	29.20
C5 ALP ISM (b)	122.11	C8 ALP ISM #2	33.13
Glyoxal	59.21	C8 ALP ISM #3	143.28
Pentanal	118.21	Octanal	26.87
Acetophenone	335.81	C9 ALP ISM #1	107.46
o-Tolualdehyde	895.50	C4 SUB BENZ (b)	26.87
m-Tolualdehyde	4029.76	C8 DICARB	29.92
p-Tolualdehyde	2841.50	C9 ALP ISM #2	22.78
ARM ISM #1 (b)	149.25	C9 ALP ISM #3	18.56
C6 ALP ISM #1	223.88	Nonanal	295.31
trans-cinnamaldehyde	328.35	C10 ALP ISM #1	24.65
Indanone	262.12	2-Decanone	53.40
C6 ALP ISM #2	53.51	Decanal	180.74

4-Methyl-2-Pentanone (MIBK)	52.42	C10 DICARB (b)	33.29
Methyl Glyoxal	28.66	C11 ALP ISM #1	23.90
Hexanal	120.13	Undecanal	63.74
DMBZ ISM #1 (b)	295.52	C12 ALP ISM #1	39.51
2,5-Dimethylbenzaldehyde	2014.88	Dodecanal	4.47
		C13 ALP ISM #1	1.49

C5 = 5 carbon atoms, C6 = 6 carbon atoms, and so on; ALP = aliphatic; ISM = isomer; ARM = aromatic; DMBZ = dimethylbenzaldehyde; TMBZ = trimethybenzaldehyde; SUB BENZ = substituted benzaldehyde. Carbonyls are listed in order of elution, starting at the top of the left-hand column.

Phase 2 (hot stabilized) of dynamometer test. Vehicle and fuel information: Ford Mondeo 1995, 4 cylinders, engine displacement 2.0 L, multiple fuel injection, air/fuel ratio control, 3-way catalytic converter, manual transmission, odometer reading = 10,000 km. Measured fuel economy in test's Phase 2 = 9.2 km / L. Fuel: gasoline-ethanol blend, ethanol = 23 vol %, C = 78.2 weight %, H = 13.8 weight %, Oxygen = 8.8 weight %, fuel density = 0.765 kg / L.

Table 2: Emission factors (μg/L of fuel consumed) for carbonyls in exhaust of Brazilian light-duty vehicle fueled with a gasoline-ethanol blend (23 vol % ethanol)

Conclusion

Liquid chromatography-atmospheric pressure chemical ionization mass spectrometry has been used to measure speciated carbonyls (up to ca. 120 aldehydes and ketones) in vehicle emissions. Two examples of application are discussed here, one involving measurements of on-road emissions of carbonyls in a U.S. highway tunnel and the other involving dynamometer tests carried out in Brazil using the Brazilian gasoline-ethanol blend. Additional results to be discussed in the oral presentation will include work in progress regarding (a) speciated carbonyls in exhaust from diesel engines, (b) LD vehicle carbonyl emissions in cold start, hot stabilized and hot start phases of dynamometer tests, (c) the effect of catalytic converters on LD vehicle emissions of carbonyls, (d) relationships between carbonyl emissions and the fuel speciated hydrocarbon composition, and (e) "real-world" carbonyl emissions measured in a highway tunnel in Brazil.

Acknowledgements
Measurements of carbonyls in Wisconsin, U.S.A., were made as part of a larger study carried out by Dr. James J. Schauer and his group, Dept. of Civil and Environmental Engineering, U. of Wisconsin, Madison, WI. Measurements made in Brazil by D. Grosjean, E. Grosjean, A. Moreira, L. F. R. Moreira and J. C. S. Almeida are sponsored by PETROBRAS, Rio de Janeiro, Brazil, Contract CENPES 650 2038014.

References

Grosjean D., E. Grosjean and A. W. Gertler (2001): On-road emissions of carbonyls from light-duty and heavy-duty vehicles. Environ. Sci. Technol., vol. 35, nº 1, p 45-53.

Grosjean E., P. Green and D. Grosjean (1999): Liquid chromatography analysis of carbonyl 2,4-dinitrophenylhydrazones with detection by diode array ultraviolet spectroscopy and by atmospheric pressure negative chemical ionization mass spectrometry. Anal. Chem., vol. 71, p 1851-1861.

Kean A. J., E. Grosjean, D. Grosjean and R. A. Harley (2001): On-road measurements of carbonyls in California light-duty vehicles. Environ. Sci. Technol., vol. 35, nº 21, p 4198-4204.

Grosjean D., E. Grosjean and L. F. R. Moreira (2002): Speciated ambient carbonyls in Rio de Janeiro, Brazil. Environ. Sci. Technol., vol. 36, nº 7, p 1389-1395.

12th International Symposium "Transport and Air Pollution" / 12e Colloque international "Transports et pollution de l'air", Avignon, 16 -18 *June* / juin 2003
proceedings / actes, n°92, tome / Vol. 1, Inrets ed., Arcueil, France, 2003, p. 73-80

Modelling vehicles kinematics relevance in network based urban emissions inventories

Emanuele Negrenti*, Antonio Parenti**
*ENEA, Via Anguillarese n° 301, 00060, Rome – Italy - Fax. +39 06 3048 6611,
e-mail: negrenti@casaccia.enea.it
**ASTRAN S.r.l., Via Monfalcone n° 22, 01100, Viterbo – Italy, e-mail: a.parenti@astran.it

Abstract
An innovative approach has been developed during last four years for taking into account vehicles speed variability along links in urban networks on the basis of standard traffic information provided by widely used traffic models. The algorithms for fuel consumption and carbon monoxide emissions initially obtained during an EC funded project allowed the prediction of significant differences between smooth traffic and congested traffic flows having the same average vehicles speed. This line of research was continued in the framework of the Programme Agreement between ENEA and the Italian Ministry of Environment and the new model for describing the relevance of vehicles kinematics was applied also to Volatile Organic Compounds emissions. The combined use of speed profiles reconstruction, average speed emission functions and instantaneous emission data allows the definition of a corrective function – named the Kinematics Correction Factor – based on four parameters: average link speed, green time percentage at link end, link length and traffic linear density. The results show the improvement reachable in the prediction of the spatial and temporal distribution of emissions in an urban network and in the modelling of traffic emissions on a very local scale.
Keys-words *: models, emissions, kinematics, fuel consumption, traffic density*

Introduction

National and regional emissions inventories are usually based on emission functions depending on average speed. At the current level of knowledge of the traffic conditions on extra-urban networks this is probably the only practical solution. The situation in the urban context can be different. Traffic modelling techniques allow a link based description of vehicles behaviour. The adoption of the 'average speed approach' in the calculation of traffic emissions in urban networks implies significant limitations of sensitivity and low accuracy of results. The reason of this inaccuracy derives from the many different ways in which the same average speed can be obtained along a link in a network. Different combinations of the fundamental vehicle driving conditions (cruising, acceleration, deceleration and idling) can produce the same average speed on the link, but the vehicle emissions can vary significantly due to the very different emission rates during the different phases. Travelling at an average speed of 50 Km/hr during the night along a not congested urban street implies a very smooth speed cycle and low consumption and emission rates. On the opposite, travelling at the same average speed on a congested motorway where the speed limit is much higher implies frequent idling and acceleration events, causing consumption and emission rates three times higher or more. In order to have a realistic distribution of emissions over space and time, it is therefore necessary to represent the kinematics content of traffic data. Widely used traffic models provide several output data that can be used for defining this content. Classic assignment models give vehicles flows and average link speed from which traffic density can be derived: this quantity is a good indicator of traffic congestion. More dynamic traffic models provide partial information on

the speed cycle on the link, such as primary and secondary stops due to the presence of traffic ligths and queues. Advanced traffic simulators provide detailed speed profiles instant by instant. Each of these output data sets shows advantages and disadvantages for the modelling of kinematics effects on emissions. The work developed here refers to the first case and is based on the possibility of using traffic density information for estimating the fractions of time spent by a vehicle in the various kinematic phases and then to reconstruct the likely speed cycle on the link for given values of average speed, traffic density, green time at traffic light at link end, and link length.

1 - Methodology

Alternatives for describing vehicles kinematics in network analysis

The TEE (Traffic Energy and Emissions) model of ENEA (Negrenti (1999)) offers alternatives to the 'average speed approach' for the calculation of passenger cars hot emissions as a function of their kinematics. Such alternatives include : a) the detailed 'speed cycle' Model, extensively applied in the SAVE HESAID Project (Hoglund (1999)); b) the simplified 'reconstructed cycle' Model; c) and an innovative approach named 'Kinematics Correction Factor' that was developed in the first version, for CO emissions and fuel consumption, during the 4th Framework Programme DG XII ESTEEM Project (Vacca (1999)). The research on the latter was continued in the framework of the Programme Agreement between ENEA and the Italian Ministry of Environment in order to obtain also the VOC emission kinematics correction functions (Zanini(2003)).

One of the promising alternatives to the classic average speed emissions approach aims at obtaining a reasonably adequate kinematics description on the basis of an easily available input: an essential speed cycle is here 'reconstructed' by the model itself as a function of the average speed along the link, a congestion indicator such as the 'lane flow density' (flow to speed ratio in the link lanes), and the fraction of green time at the intersection at the end of the link. The information required is rather easily obtainable by the commonly used traffic models and the reconstructed cycle can be sophisticated enough for taking into account the essential characteristics of the different driving phases: time spent in acceleration and related acceleration rate, cruise speed, idling time.

The congestion level represented by traffic density is used for calculating the fractions of time spent during cruising, acceleration, deceleration and idling phases (see Fig. 1). This specific model describes the well known traffic conditions based on the traffic density. The model makes reference to a normalised density given by the ratio of lane density to its maximum value. For low densities, traffic is smooth, very limited interactions occur among vehicles and all the time is spent in the cruise phase. For higher normalised density values accelerations induced by interactions start, thus reducing time available for cruising. When normalised density exceeds a threshold value, spontaneous breakdown occurs and short idling events take place. When density approaches the limit value we observe a fast decline of cruise time, a progressive reduction of time spent in accelerations and the rise of idling time until traffic is blocked at the density saturation value.

The relationships between the traffic lane density and the time fractions spent in the kinematics phases clearly depends on the number of lanes. If only one lane is available for the traffic flow, the level of disturbance imposed by the presence of the other vehicles is higher and we can expect an anticipation of the congestion effects compared with the case of multiple lanes. This differentiation is qualitatively sketched in Figure 1 and represents one of the areas of current development of the methodology. This ongoing enhancement aims at taking into account additional traffic disturbances such as pedestrians, secondary intersections, and a significant fraction of heavy duty vehicles in the flow, and will be pursued in the frame of the ISHTAR Project (Negrenti(2001).

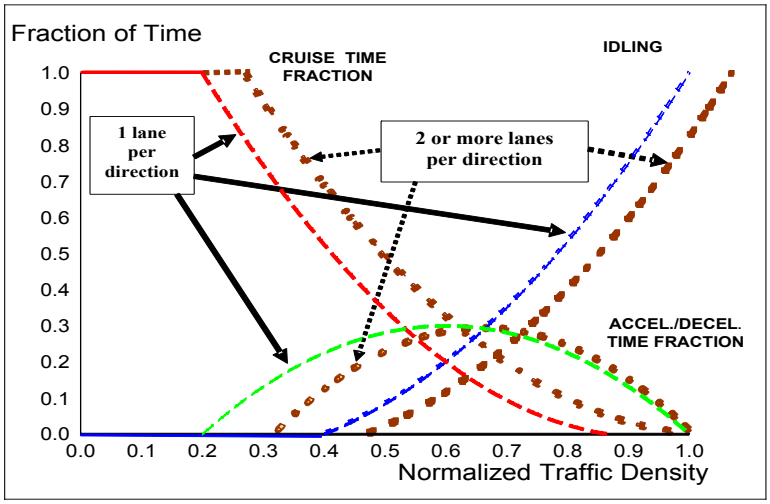

Figure 1: Qualitative Time Fractions spent in kinematics phases in free flow conditions, including the effect of lanes number (Source: ISHTAR Project – see Negrenti (2001))

Speed Cycle reconstruction from kinematics time fractions

The time spent during acceleration and deceleration is used to estimate the number of acceleration episodes on the basis of a driver behaviour hypothesis and acceleration rates derived from measured data. The acceleration rate is modelled as speed dependent, in order to take into account the power limitation of vehicles: the highest power levels are allowed at low speed, while acceleration rate tends to zero when speed rises. The minimum speed along the speed cycle can also be calculated from these data. The knowledge of the average speed and the time spent in cruising and in the other driving phases allows also the cycle cruising speed to be calculated.

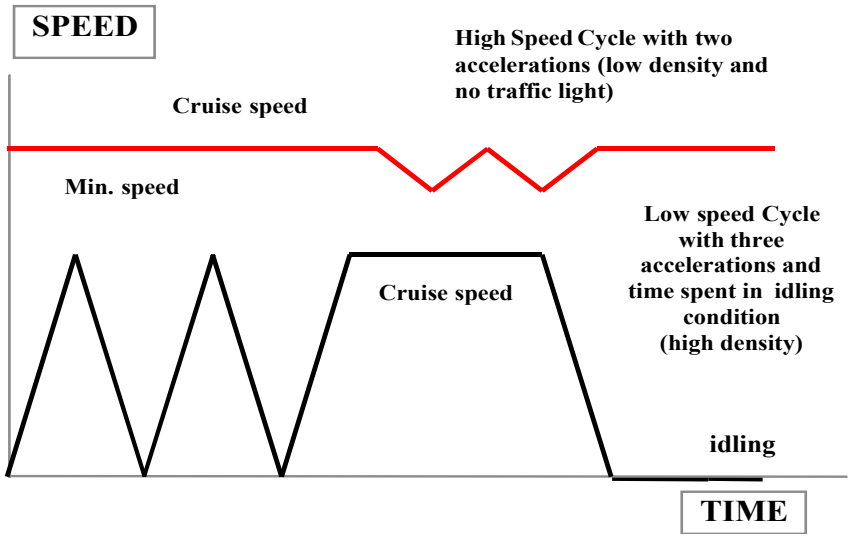

Figure 2: Two examples of reconstructed speed cycles having different average speed and different content of speed variability ((2002))

The overall result (see Figure 2) is a 'reconstructed' speed profile characterised by: a time interval spent in idling (only for high densities or presence of a traffic light), some accelerations and deceleration episodes between the minimum speed and the cruise speed, and a time interval spent at 'cruise' speed. This relatively simple solution describes the likely speed cycle far from the traffic light that is supposed (if any) at link end. The presence of a traffic light is simulated by a simple additional speed cycle formed by a deceleration interval, an idling phase and a final acceleration.

The overall result is the prediction of a speed cycle representative of traffic conditions on links with or without a traffic light. Based on these information the TEE model can calculate passenger cars emissions over the modelled speed cycle by using different instantaneous emission factors in each of the described kinematics phases. The four basic variables from which the speed cycle reconstruction depend are traffic density (affecting the time fractions), green time at traffic light (affecting the presence and the shape of the additional small cycle at link end), average speed (which affects primarily the cruise speed) and link length (which defines the importance of the undisturbed upstream speed cycle).

Calculation of the kinematics correction factor under the possible traffic conditions

The 'Kinematics Correction Factor' (KCF) Model makes extensive use of the 'reconstructed cycle' algorithm. The KCF approach assumes that the effect of speed variability can be expressed by means of a 'kinematics correction function', i.e. a multiplying variable coefficient of the classic hot emission term based on the average speed, representing the variability of emissions with the kinematics content of a given cycle. According to this approach, the 'corrected' emission 'E' is obtained as the product of the 'average' emission 'e', calculated from the average speed 'v', and the 'kinematics correction factor' KCF:

$$E = e(v) * KCF \qquad (1)$$

The KCF can be derived from a set of emission calculations in which both the 'reconstructed cycle' model and the average speed correlation are used. In order to derive a function of general applicability, the authors had to define a matrix of possible traffic conditions. By considering a discrete number of average speeds, of 'green time percent', of congestion levels represented by traffic density, and of different link lengths, it was possible to define a four-dimensional matrix of theoretical traffic situations for which the emissions of CO and VOC were calculated with both the approaches. This way the influence of the speed cycle can be quantified and the characterisation of the KCF as a function of speed, density, green time fraction and link length can be performed. The matrix used in the most recent recalculation of the KCF includes over 1300 traffic conditions.

For each of these test cases, the emissions and fuel consumption over the link were calculated with both the average speed emission functions and with instantaneous emissions (MODEM database, see: Sturm (1999)) over the reconstructed speed cycle. The ratios between the two sets of results provided the searched KCF values matrix. Starting from these values, functions were searched for describing the variability of the KCF with the four input parameters.

Deriving the kinematics correction correlation

The correlation between the KCF and the four input parameters was searched as the product of four independent functions (Negrenti (1999), Parenti (2002). This solution has the big advantage of greatly simplifying the form of the final correlation based on a high number of input variables. Such a correlation has the following shape:

$$KCF = K0 * d(D) * g(G) * l(L) * v(V) \qquad (2)$$

where d, g, l, and v are classic mathematical functions of the variables D (traffic lane density, in vehicles/Km), G (green time fraction), L (length, in Km) and V (Average Link Speed), and K0 represents the value of the KCF coefficient for 'central' values of the four input variables. The mathematical functions describing the sensitivity of the KCF functions identified for CO, VOC and fuel consumption to the four input variables are summarised in Table 1. The input parameters have a different relevance on the value of the KCF. The clearly most important sensitivity is given by traffic density. The reason of this has to be found in the dependence of accelerations content from the density value that is taken as the key input in the time fractions sub model. Typical profiles of sensitivity to traffic density are shown in Figure 3.

Function	Consumption functions	CO functions	VOC functions
d(D)	c1, for D < 30 c2*D+c3, for 30<D<90 c4-c5*D, for D>90	c1+c2*exp(d/c3), for D<90 c4-c5*D, for D>90	c1, for D<30 c2+c3*exp(d/c4), for D<90 -c5*d+c6, for D>90
g(G)	c6, for G<0.9 c7-c8*G, for .9<G<1.	C6+c7*exp(-G/c8)	c6*G+c7
l(L)	c9+c10*exp(-L/c11)	c9+c10*exp(-L/c11)	c8-c9*EXP(-L/c10)
v(V)	c12+c13*exp(-V/c14)	c12-c13*exp(-V/c14)	-c11*V + c12

Table 1: Functions of the KCF correlation for Fuel Consumption, CO and VOC

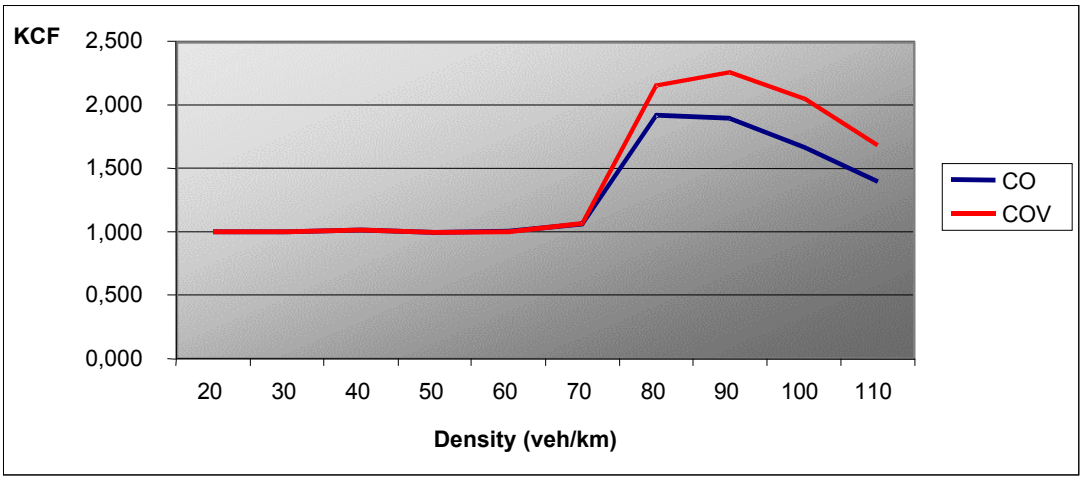

Figure 3 : Density sensitivity of KCF for CO (lower curve) and VOC (Parenti (2002)))

This sensitivity to density shows relevant characteristics: the similarity of trend between CO and VOC, the rapid increase of the corrective function for densities higher than 60 vehicles/Km, the relevant peak values and the decrease of the functions for very high density values, when idling is predicted to be more frequent than acceleration.

The coefficients included in the KCF correlation depend on the fleet composition, i.e. the mix of catalyst, not catalyst and diesel vehicles. The work performed so far by ENEA and ASTRAN assumed an Italian fleet composition. A further step under consideration is the possibility to derive a KCF correlation for various vehicles classes (e.g. diesel and gasoline passenger cars). This split would amplify the work for the derivation of the KCF correlation but would give results an enhanced applicability. It must be noted that differences of KCF among vehicle classes appear not to be particularly relevant: in other words the entity of the correction seems to be more linked to the kinematics effect than to the vehicle type. The documented activity was focussed on CO and VOC but the methodology is applicable to all the pollutants for which both average speed emission functions and instantaneous emissions data are available (e.g. NOx).

2 - Validation of the Kinematics Correction Function approach

Validation tests of the KCF methodology have been run in order to assess the absolute and differential accuracy. The relative accuracy was verified by comparing the measured ranges of variability of emissions with the changes predictable with the KCF correlation. The absolute

accuracy was mostly assessed by comparing the pollution levels predictable with and without the use of the KCF correlation, with the measured CO concentrations.

Relevant validation activities were performed on the basis of CO pollution levels measured in Rome (Vacca (1999)). The validation tests were organised in two sites (Corso Francia and Via Tiburtina), showing different architectural features conditioning the micro-scale dispersion process. The ADMS-Urban dispersion model (CERC Ltd - UK) was applied, and the results have been compared with measurements provided by two local monitoring stations. ADMS has a street canyon option (Hertel (1989)) and receives as main input the wind speed, angle and lateral spread, the local time, the cloud cover, the boundary layer height, the ground surface heat flux and temperature. The measurement positions are just a few meters from the road side. Buildings at Corso Francia site are 4 to 5 floors high and located a few tens of meters from the road edge. Buildings at Via Tiburtina are higher (around 10 floors) and closer to the road. The Tiburtina site is therefore closer to the street canyon concept. The dispersion model was applied using TEE emissions estimates for working days and Saturday. The traffic measurements and emission estimates referred to the morning peak between 8 and 9 a.m. The usage of the 'average speed' emission factors causes a high underestimate of the concentrations in both sites. Instead, by using the KCF, the simulated concentrations were satisfactory both in the case of Via Tiburtina, where they show (in the average) a light overestimation for both working day and Saturday, and the case of Corso Francia, where the canyon model is applied to a more complex topography and the absolute accuracy is lower (differences of 30 - 40 %), but still good, if we consider the uncertainty sources and the error coming from the use of the simple average speed approach (roughly 200 - 300 %). In differential terms, i.e. comparing the working day and the Saturday, the models chain correctly predicted a reduction of the pollution level around 40-50 %.

Following this positive experience and after having refined the algorithms for time fraction and speed cycle reconstruction, the KCF upgraded and extended correlation was assessed again both in differential and in absolute terms. A specific assessment was performed in 2002 in co-operation with STA SpA (the Mobility Agency of Rome) in the framework of the implementation and testing of the EC FP5 HEAVEN Project (Tomassini (2002)) System, aiming at calculating the pollutant concentrations in a large area in the north side of the city centre of Rome.

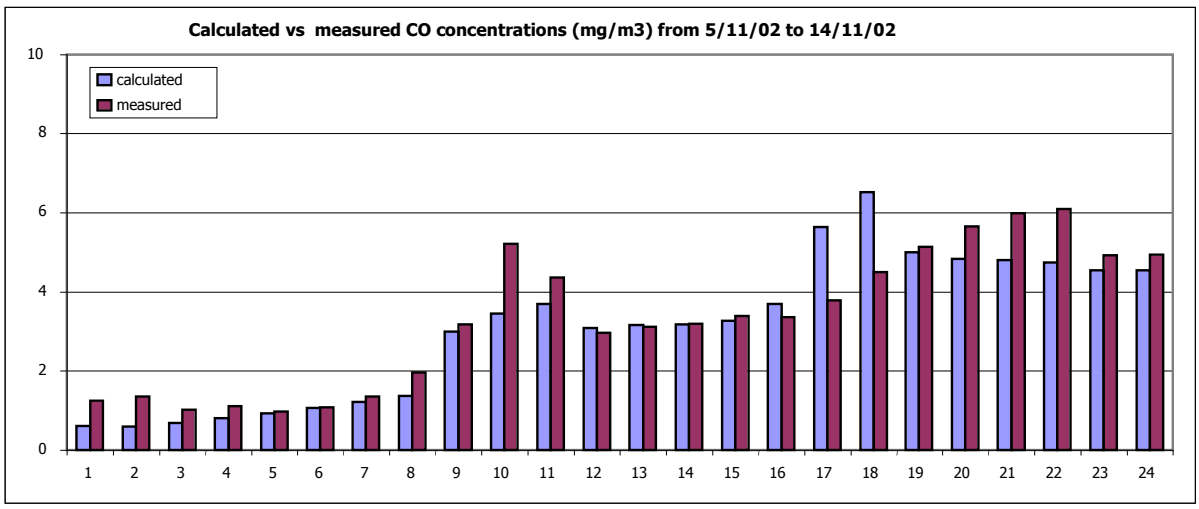

Figure 4 : Comparison of measured and calculated hourly CO concentrations (mg/m3) at Viale Libia (working days data between 5 and 14 November 2002 - Courtesy of STA SpA Rome – 2002)

Estimated CO levels were compared with the measured values in the Viale Libia monitoring station. Significant differences were found between the use of the KCF correction and the simple use of the COPERT III functions for hot emissions. The use of the correction largely provided the best results (see Fig 4 and 5)

The daily profiles are predicted with very good approximation. The correlation of data calculated and measured is remarkably high (0.85). The calculated CO level without the adoption of the KCF correlation would have been sensibly lower.

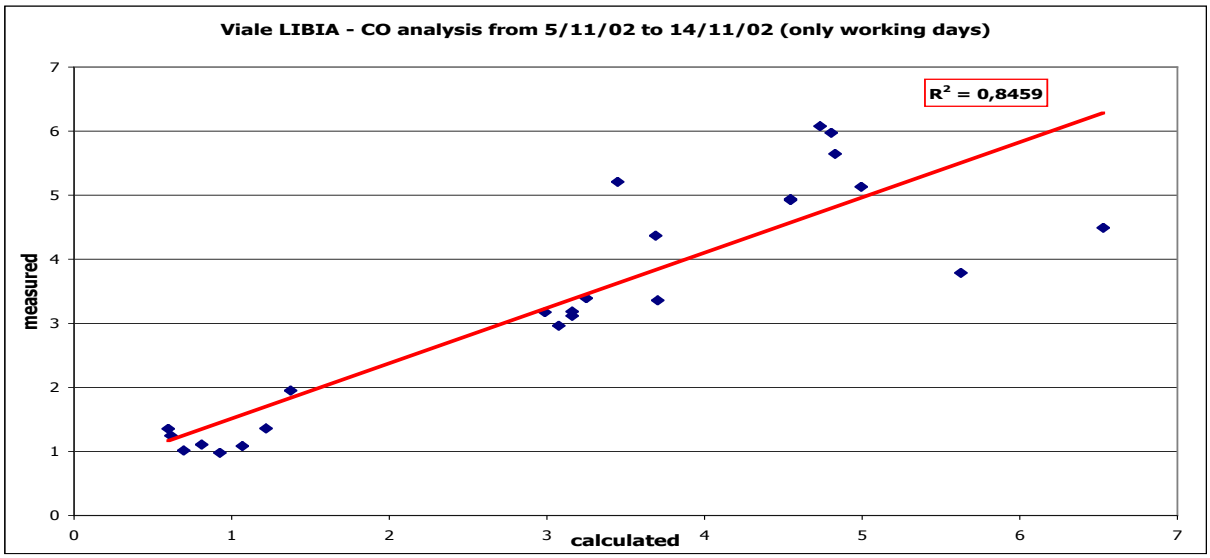

Figure 5 : Correlation of measured and calculated CO concentrations (mg/m3) at Viale Libia (working days data between 5 and 14 November 2002 – Courtesy of STA SpA Rome - 2002)

Conclusion

The developed approach offers a new solution to the problem of modelling the variability of consumption and emissions with vehicles kinematics in urban transport networks. The method and the software developed combine reconstructed speed cycles with average speed emission factors and instantaneous emissions data making the whole algorithm capable of describing the effects of driving patterns on the emission and consumption levels. The KCF approach was successfully applied and assessed with tests in Rome, in the framework of the EC ESTEEM Project (1999), further extended to VOC emissions in the framework of a contract between ENEA and the Italian Environment Ministry, and recently reassessed on the basis of CO measurements in Rome in the frame of the EC HEAVEN Project. The greater accuracy demonstrated at link level is a very good basis for further application and systematic assessment. This will be done in the framework of the EC FP5 ISHTAR Project.

Acknowledgements

The authors wish to thank M. Tomassini, F. Nussio and P. Aloja at STA SpA for their contribution of data made available through the HEAVEN System.

References

CERC Ltd (2002): ADMS – Urban Air Quality Management System – 3 King's Parade – Cambridge UK – http://www.cerc.co.uk

Heich H. (1998) : EC Project COMMUTE: Common Methodology for Multi-Modal Transport Environmental Impact Assessment, Deliv. 2: Methodology Report Volume 3: Commute Tool

Hertel O. (1989) : OSPM Operational Street Pollution Model – Danish NERI – DMU LUFT A 135

Hoglund P. (1999) : SAVE HESAID Project FINAL REPORT – edited by Prof. P. Hoglund – Royal Institute of Technology - Stockholm – 1999

Joumard R. (1998) EC DG VII MEET Project: Final Report (Del. 21) Emission Factors and Traffic Characteristics Data Set

Negrenti E. (1998) The 'corrected average speed' approach in ENEA's TEE model - ARRB Conference – Sydney – December 1998

Negrenti E. , Zanini G. (1999) 'Integrating Average Speed emissions and instantaneous emissions sensitivity' – Transport and Air Pollution Conference – Graz 1999 – Proceedings Edited by Graz Univ. of Technology

Negrenti E. (2001) ISHTAR Contract EVK4 – CT 00034 – 2001 – Description of work (Technical Annex) – issued by ENEA

Parenti A. (2002) ASTRAN srl -'Sviluppo ed applicazione di una versione aggiornata del codice TEE comprendente il calcolo delle emissioni di benzene e particolato' – Under contract to ENEA Environment. Dept. In the framework of the Agreement of Programme with the Environment Ministry – p. 27 - 40

Sturm P. (1999) Engine Maps and Vehicle Models – MEET Project Deliverable 6 – by Graz University of Technology

Tomassini M. (2002) : EC FP5 HEAVEN Project Final Conference – Prague – December 2002 (www.rec.org/HEAVEN)

Vacca R. (1999) : DG XII ESTEEM Project Final Report – issued by ISIS Rome.

Zanini G. (2003) : Final Report of the Task 'Prevenzione dell'Inquinamento da Benzene e Idrocarburi Policiclici Aromatici' – in the frame of the Agreement of Programme 1998-2002 between ENEA and the Environment Ministry – chapter 4.1, p. 125-163

12th International Symposium "Transport and Air Pollution" / 12e Colloque international "Transports et pollution de l'air", Avignon, 16 -18 *June* / juin 2003
proceedings / actes, n°92, tome / Vol. 1, Inrets ed., Arcueil, France, 2003, p. 81-88

Conditions de fonctionnement des autobus parisiens en exploitation pour l'évaluation des émissions polluantes

Michel André*, Bénédicte Garrot, Yves Roynard**, Robert Vidon*, Patrick Tassel*, Pascal Perret***
* INRETS, Lab. Transport et Environnement, Case 24, 69675 Bron cedex, France - email : michel.andre@inrets.fr
** RATP, Département Environnement et Sécurité, 13 rue Jules Vallès, 75547 Paris cedex 11, France - email : benedicte.garrot@ratp.fr

Résumé
A partir des caractéristiques urbaines (géographie, habitat, voirie, trafic) et des statistiques d'exploitation (vitesse, irrégularité, etc.), on décrit et caractérise le réseau d'autobus de la RATP en Ile-de-France. On définit ainsi une double typologie des lieux et des lignes de bus selon leurs itinéraires au travers de ces lieux. Quatre lignes représentatives sont sélectionnées, sur lesquelles un autobus est instrumenté. On mesure en exploitation le fonctionnement du moteur (couple, régime, températures), la vitesse et la localisation du véhicule, la charge en passagers, le profil routier et les sollicitations électriques et pneumatiques. Plus de 25000 km et 1600 heures de conduite sont enregistrés. On décrit les grandes lignes de l'approche méthodologique et le protocole expérimental. Les conditions de circulation des autobus sont analysées en fonction des lignes et des spécificités urbaines des zones traversées. On construit ensuite des cycles de conduite représentatifs des conditions réelles de circulation, qui permettront ainsi de relier les émissions polluantes des autobus aux conditions et lieux d'exploitation.
Mots-clefs : *autobus, émissions de polluant, SIG, exploitation, instrumentation, vitesse, cycle d'essai.*

Abstract
Operating conditions of Paris buses in use for evaluation of pollutant emissions.
This study is intended to link the pollutant emissions from buses to their driving conditions and to the urban context. Envisaged in the case of the Ile de France region, this procedure constitutes a methodological basis for the characterisation of bus networks using the geographical and/or operation tools and databases. Firstly, the bus routes are characterised by associating analysis of bus operating conditions (load, speed, irregularity) and the urban characteristics (geography, housing type, traffic, ...) collected and managed by a GIS (Geographical Information System). This multidimensional analysis gives access to bus-route profiles according to the types of zones travelled. Secondly, one vehicle of a route from each of the categories thus defined is instrumented in order to measure the parameters of operation in commercial use. The parameters measured concern engine operation (torque, engine load, temperatures) the speed and location of the vehicle (GPS, speed sensor), the passenger load (direct counting of passengers and measurement by inflation pressure of pneumatic springs), the load linked to the road profile (slope), and electrical and pneumatic loads. After an outline of the methodological approach of network characterisation, the instrumental protocol is described and the general result of the experiments is drawn up. In total, over 25,000 km were recorded over 1,600 hours of driving, for which the main operating parameters were measured at second time intervals. Preliminary analyses (characterisation of urban zones) and location of the recordings enable the bus operating conditions to be linked to local specificities. The bus operating conditions (speeds, congestions, load, etc.) are analysed in function of the routes and the geographical and urban specificities of the zones traversed and served. These

data are then analysed for the construction of driving cycles which are representative of real traffic conditions and which will serve as a basis for the measurement of real pollutant emissions of buses on a vehicle test bench. These driving cycles will then enable to associate pollutant emissions to the corresponding driving conditions and geographical areas.
***Keys-words**: bus, pollutant emissions, GIS, operating conditions, use, instrumentation, speed.*

Introduction

Les émissions de polluants des véhicules routiers sont fortement liées aux conditions d'utilisation et de fonctionnement de ces véhicules. Leur évaluation nécessite généralement l'analyse fine de ces conditions et le développement de méthodes représentatives de mesure (ou cycle d'essai).

Les conditions de fonctionnement des autobus sont d'abord liées au "contexte" urbain qu'ils traversent et à leurs conditions d'exploitation commerciale. Une caractérisation de ce contexte doit permettre d'identifier des conditions types d'exploitation, pour lesquelles il sera possible de mesurer les émissions réelles de polluants. Ultérieurement, ces informations devront permettre de prédire les conséquences énergétiques et environnementales liées à un contexte particulier, et d'optimiser des politiques de réduction énergétique et des nuisances par l'affectation pertinente de véhicules peu polluants sur les zones les plus défavorables, ou par l'optimisation des itinéraires.

C'est dans ce but qu'une recherche a été entreprise sur les lignes franciliennes de la RATP, en raison de la richesse des informations disponibles. La méthode est cependant applicable à l'étude d'autres réseaux sous réserve de disponibilité des données géographiques urbaines et d'exploitation des bus.

La description du milieu urbain traversé par les lignes de bus et de leurs conditions d'exploitation permet d'établir une typologie des lieux et des lignes. À partir de cette première étape, on sélectionne des lignes représentatives sur lesquelles sont instrumentés des autobus. On décrit le protocole expérimental et établit le bilan du suivi. L'analyse des conditions de fonctionnement des autobus selon les lignes et les contextes permet ensuite de construire des cycles d'essais représentatifs et décrivant l'ensemble de situations identifiées précédemment.

1 – Caractérisation du réseau et sélection de lignes de bus représentatives

On analyse le « contexte urbain » dans lequel évoluent les bus, au travers d'informations sur la population, l'emploi, l'habitat, le réseau routier, le trafic, les lieux desservis (écoles, gares, commerces, etc.) ou traversés (cf. André et. al. 2002a & 2002b). Ces données sont calculées sur la région Ile de France découpée en 225 000 cellules de 100 x 100 mètres et collectées dans un SIG (système d'information géographique). Elles sont complétées par les caractéristiques et statistiques d'exploitation des lignes de bus (couloirs réservés, nombre et types d'arrêts, vitesse commerciale, nombre de passagers, fluctuations liées à la congestion, accidents, particularités de la charge en passagers, dessertes et connections particulières, etc.).

L'analyse factorielle sur les cellules géographiques et la classification permettent d'établir une typologie des zones en 12 classes, les principaux paramètres de différenciation étant la densité et le type d'habitat, les types de voiries, et le niveau de trafic (Tableau 1). On réalise ainsi un "zonage" de l'agglomération en : des zones de très faible population, habitat individuel, éloignement maximal aux commodités, des zones intermédiaires d'habitat individuel isolé ou mixte ou concentré, des zones de proximité de grands axes routiers associant une forte densité d'habitat, les centres-villes concentrés parisiens ou de villes de banlieue.

Les lignes d'autobus traversent ou desservent ces différentes zones (Figure 1). Elles sont donc analysées suivant une démarche similaire selon leur itinéraire au travers des types de zones.

	%	Superficie et caractéristiques des zones géographiques	Répartition de l'habitat (en% de la surface) Collectif	Individuel	Population / km2	Emploi / km2	Indicateur d'éloignement (km)	Trafic nb veh/h /10^{-2} km^2
1	9.7	Très faible population, éloignement important	0.06	2.3	231	340	**9.5**	30
2	12.3	Faible population, pentes	0.6	2.8	1059	2444	4.8	30
3	4.1	Habitat individuel isolé, réseau secondaire	4.6	20.7	1638	1788	**5.9**	**300**
4	3.4	habitat mixte isolé, réseaux second. et tertiaires	10.3	27.5	4100	3080	4.0	**750**
5	9.4	Habitat individuel isolé, pentes	6.0	17.3	2008	1358	4.2	30
6	7.8	Habitat mixte dense, proximités	8.3	**61.7**	**5186**	1586	3.1	80
7	7.7	Habitat individuel concentré	1.4	**91.3**	4317	792	3.3	60
8	2.4	Routes principales, trafic élevé	2.6	3.9	2160	3156	4.2	**6630**
9	5.3	Forte population à proximité d'axes primaires	14.1	16.1	**6134**	**6441**	2.7	**1890**
10	8.1	Habitat mixte concentré, forte population	**30.5**	18.4	**12186**	4503	2.1	100
11	4.3	Habitat collect. concentré, forte popul. et emploi	**61.8**	2.3	**24182**	**24750**	1.5	510
	25.4	Zones inhabitées (non analysées)	NA	NA	NA	NA	**6.8**	NA
		Ensemble	10.6	24.6	4956	6101	5.0	350

Tableau 1: Caractéristiques des zones géographiques identifiées par classification

Table 1: Average housing, population and employment characteristics of the 11 geographical classes identified through statistical analysis and classification

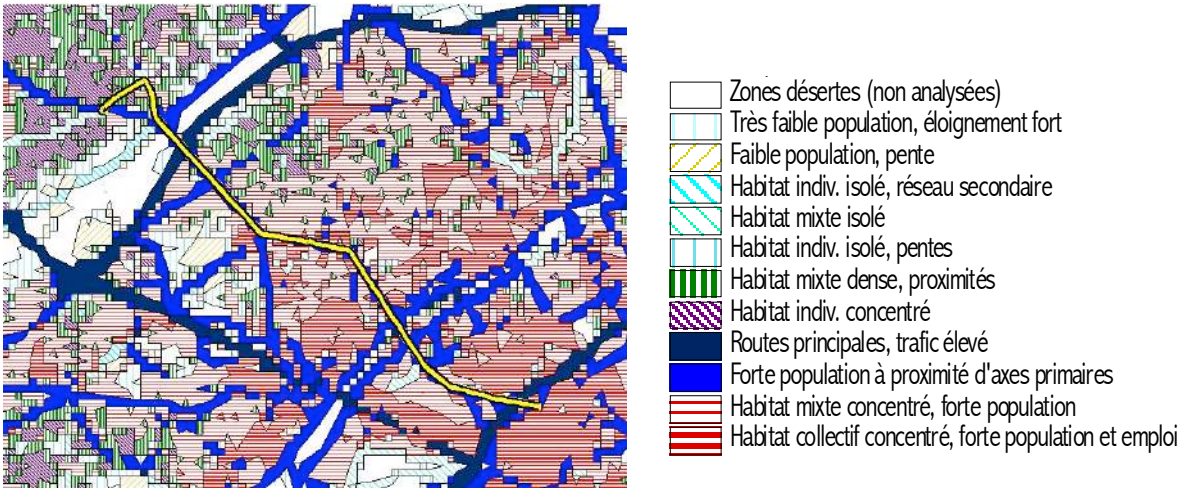

Figure 1 : Visualisation d'une ligne particulière (Ligne 163: Porte de Champerret – Grand Cerf de Paris vers la proche banlieue ouest) et du contexte urbain traversé par cette ligne

Figure 1 : Illustration of one typical bus line and of the urban context used by this line (line163: Porte de Champerret – Grand Cerf, from Paris to the near west suburbs)

On définit ainsi 5 grandes catégories de lignes, caractérisées par leur itinéraire mais aussi par leur conditions d'exploitation (cf. Tableau 2) :

- 73 lignes (34% du réseau en distance), qui empreintent le réseau routier principal avec des trafics élevés et desservent des centres-villes concentrés. Ces lignes circulent en moyenne à 14 km/h et présentent des taux d'irrégularité[1] de service assez élevés. La ligne 163 reliant Paris à la proche banlieue Nord-Ouest représentative de ce groupe sera sélectionnée pour les expérimentations.
- 32 lignes (15% du réseau) desservant les zones isolées d'habitat individuel ou mixte. La ligne mixte 206 et 207 (de Noisy-Le-Grand vers La Queue en Brie ou vers Pontault-Combault) desservant les banlieues éloignées de l'Est de Paris représente bien cette classe.
- 52 lignes (25% du réseau) desservant des zones d'habitat individuel ou mixte concentré. La ligne 319 reliant Massy Palaiseau RER à Rungis Marché international en banlieue Sud éloignée est caractéristique de cette catégorie.

[1] l'indice d'irrégularité est défini à partir des variations d'horaires de passage à différents points de la ligne

- 55 lignes (21% du réseau) desservant principalement Paris ou des zones de forte densité d'habitat. Ces lignes circulent en moyenne à 11 km/h et présentent les plus forts taux d'irrégularité de service et d'accidents. La ligne 47 (Gare du Nord – Arcueil) a été sélectionnée pour représenter cette classe.
- 6 lignes atypiques de dessertes des aéroports ou du RER, longues et rapides (28 km/h) et empreintant les autoroutes, et qui ne seront pas considérées pour la suite des travaux.

La sélection des lignes représentatives s'est appuyée sur les critères de représentativités au sein des classes et sur la couverture par ces lignes des zones géographiques identifiées précédemment.

Catégorie de lignes et caractéristiques d'itinéraires	Vitesse commerciale (km/h)	Indice d'irrégularité	Points de congestion (1/km)	*taux d'accidents ($1/10^5$km)*
1-Desserte de zones de forte densité, réseau primaire, trafic élevé	14.2	0.32	0.27	*8.6*
2-Desserte de zone d'habitat isolé	15.3	0.30	0.22	*7.8*
3-Desserte de zones d'habitat mixte concentré et isolé	15.2	0.29	0.24	*6.6*
4-Desserte de zone d'habitat collectif concentré (centres-villes)	10.5	0.46	0.61	*14.9*
5-Lignes rapides empreintant les autoroutes	27.6	0.23	0.12	*4.4*
Ensemble	*14.0*	*0.35*	*0.32*	*9.7*

Tableau 2: Caractéristiques moyennes d'exploitation des catégories de lignes identifiées.

Table 2: Average operation characteristics calculated over the 5 classes of bus lines identified through the automatic clustering as a function of their routes.

2 - Instrumentation

On souhaite mesurer en conditions réelles d'exploitation les paramètres ayant une incidence directe ou indirecte sur les émissions de polluants des bus : paramètres environnementaux (température, conditions climatiques), paramètres cinématiques (vitesse du véhicule et accélérations), arrêts (commerciaux ou dus aux intersections et à la congestion), charge du véhicule (nombre des passagers), fonctionnement du moteur (couple et régime de rotation, rapports de boîte de vitesse, température), fonctionnement des équipements auxiliaires électriques et pneumatiques.

Par ailleurs, la prise en compte du contexte urbain, qui est à la base de la démarche, implique de localiser précisément le bus et les données enregistrées. Sans détailler l'ensemble de l'instrumentation, on revient ci-après sur quelques fonctions et enseignements essentiels.

Charge du véhicule

La charge en passagers est mesurée au travers de la pression dans les coussins pneumatiques (suspension hydraulique du véhicule). Le signal enregistré est moyenné entre arrêts (et arrêts exclus, puisque c'est au cours des arrêts que montent ou descendent les passagers). Des comptages des passagers effectués sur quelques trajets enregistrés ont permis d'étalonner cette procédure. les corrélations obtenues entre nombres de passagers dans le bus et valeurs moyennes de la pression sont relativement satisfaisantes (R^2 de 0,7 à 0,9 selon les cas).

GPS, vitesse, altitude

Un GPS a été utilisé (conjointement à un capteur de distance) pour notamment mesurer la vitesse et l'altitude. On doit cependant constater les limites de ce système liées sans doute principalement à l'environnement urbain et analysées en (Hamelin, 2001). Des effets de masque (passage sous une trémie, un pont, entrée dans un centre routier) ou d'échos (sur les parois des immeubles) peuvent en effet causer soit la perte des signaux de localisation (on conserve alors les valeurs précédentes) soit des brutales fluctuations des valeurs. Les écarts observés entre la vitesse GPS (calculée à partir des informations de positionnement) et celle mesurée par un capteur de distance illustrent bien ces problèmes (Figure 2).

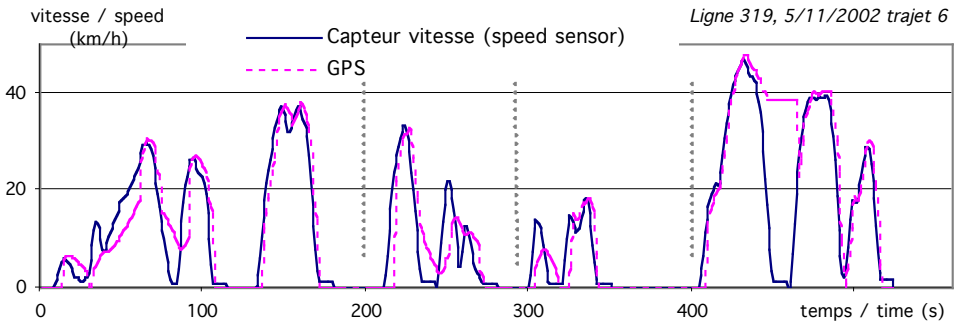

Figure 2 : Ecarts observés entre les vitesses mesurée par un GPS et l par un capteur de distance

Figure 2 : Gaps observed between the speed as measured by a GPS and the speed measured by a distance sensor (4 typical cases for illustration)

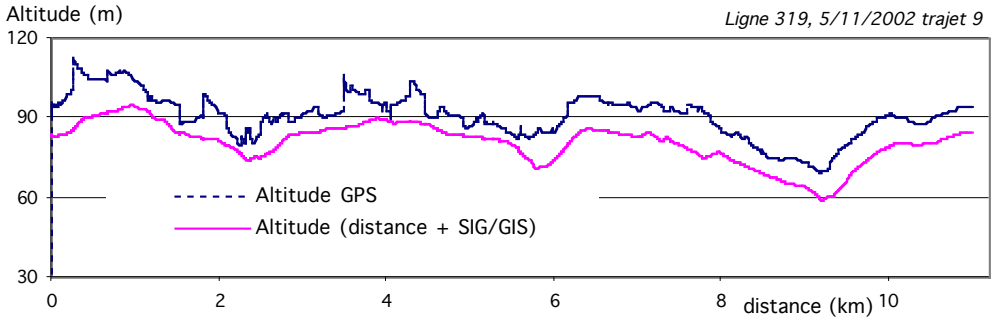

Figure 3 : Incertitudes observées sur l'altitude mesurée par un GPS

Figure 3 : Gaps observed between the altitude measured by a GPS and the longitudinal profile of the bus line according to the altitude level curves in the GIS

Les sauts observés sur l'altitude GPS (comparée avec le profil en long de la ligne calculé à partir des courbes de niveaux topographiques) sont également révélateurs de ces problèmes (Figure 3).

Localisation du véhicule et profils d'arrêts

La localisation des données est essentielle pour une démarche qui vise à associer conditions de circulation et spécificités locales. Deux méthodes originales ont été développées dans ce but.

La première s'appuie sur le GPS. Compte tenu des imprécisions constatées, il n'est pas possible d'associer en permanence les informations de localisation du GPS aux données enregistrées. On définit donc des points remarquables (terminus, dépôt, passage à un arrêt particulier), par une zone de tolérance autour des coordonnées les plus fréquemment observées, et des points de référence dont la distance aux terminus est connue avec précision. Le passage aux points remarquables et leur chronologie permet d'identifier le type de trajet (du dépôt vers le terminus 1, du terminus 1 vers le terminus 2, etc.). Une validation par les distances entre les points remarquables et aux passages des points de référence confirme cette identification (Figure 4). Connaissant les points de départs et d'arrivée ainsi identifiés, on associe l'altitude et les informations urbaines (type de zones traversée) tout au long du profil de la ligne.

La seconde méthode s'appuie sur le profil des arrêts commerciaux de la ligne. On définit les distances à l'origine des arrêts aller et retour de chacune des lignes, assorties d'une tolérance et on obtient ainsi une signature de chacun des itinéraires possibles (Figure 5). Les données enregistrées sont ensuite analysées à partir d'un arrêt quelconque, en comparant la suite chronologique des arrêts suivants aux différentes signatures. On comptabilise le nombre d'arrêts correspondants effectivement à ceux devant être observés, et on identifie ainsi efficacement les itinéraires et leurs points de départ et arrivée. L'affectation des informations urbaines et pentes se fait ensuite comme précédemment.

Les taux d'identification des trajets par les 2 méthodes varient de 60% (lignes 206-207) à 75-80% pour les autres lignes. Les distances non identifiées correspondent aux liaisons (vers le dépôt, etc.) et à des courses anormales ou interrompues. La méthode basée sur le GPS a été appliquée aux lignes

206-206 et 319 pour lesquelles les arrêts sont trop peu souvent observés. La méthode basée sur les profils d'arrêts s'est avérée très fiable pour les lignes 47 et 163 observant généralement un grand nombre des arrêts prévus.

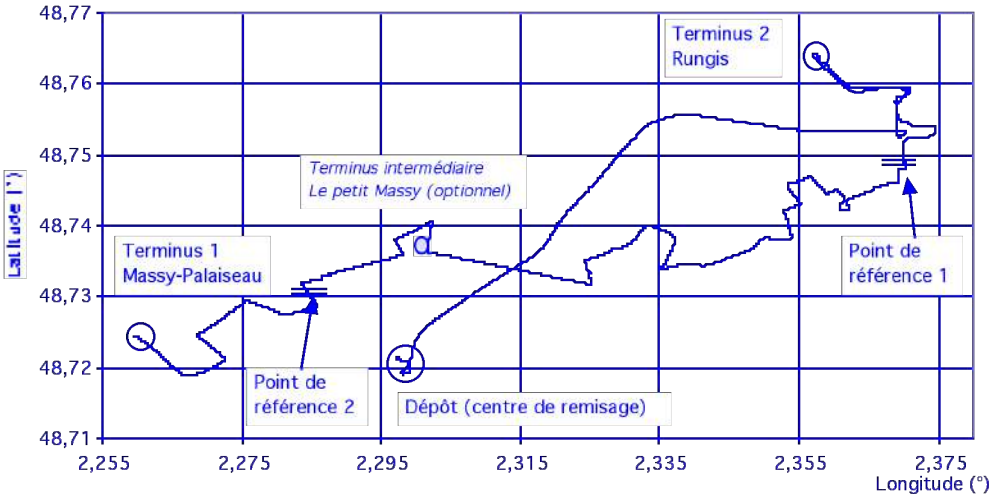

Figure 4 : Localisation et identification des trajets selon les informations GPS et le repérage préalable des points remarquables (Terminus, dépôt) et de référence.

Figure 4: Localisation and identification of the bus routes through the GPS information and the preliminary identification of remarkable and reference points (terminus, bus centre).

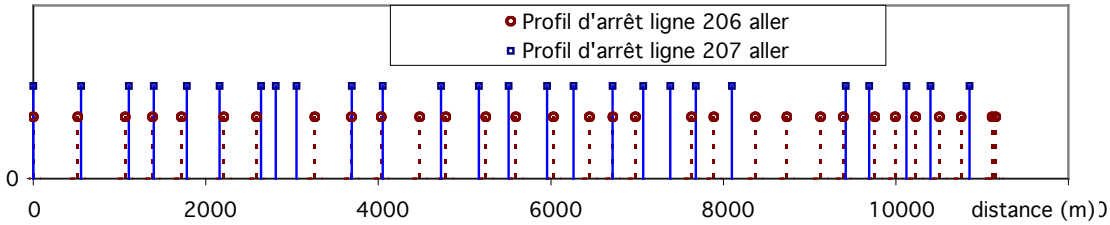

Figure 5 : Profils des arrêts des lignes 206 et 207 aller (en distance).

Figure 5: Stops profiles of the bus lines 206 and 207 (in distance). The first stops are shared.

Ligne bus line	distance (km)	durée duration (h)	vitesse moyenne et hors arrêts average and running speed (km/h)		durée d'arrêt stop duration (%)
47	4970	433	11,5	20,0	42,6
163	4985	359	13,9	23,3	40,5
206-207	9623	495	19,4	25,4	23,3
319	5419	280	19,3	24,8	22,0
Ensemble	25018	1567	16,0	23,6	32,4

Tableau 3: Bilan de l'expérimentation et conditions moyennes de circulation.

Table 3: Status of the experimentation and average driving characteristics.

3 - Protocole et bilan expérimentaux

Deux véhicules de types Renault R312 et Agora, les plus représentatifs du réseau RATP et de caractéristiques d'exploitation et performances très similaires hormis une motorisation plus récente sur l'Agora, ont été instrumentés. Chacun des véhicules a été affecté successivement sur 2 des lignes retenues, puis suivi en exploitation commerciale normale sur une durée minimale de 1 mois, avec les rotations habituelles des conducteurs, non informés de l'expérimentation.

Plus de 25000 km (1600 heures de conduite) ont ainsi été enregistrés en conditions réelles d'exploitation. La vitesse moyenne de circulation est de 16 km/h. Elle est beaucoup plus faible sur la ligne parisienne 47 (11 km/h) que sur les lignes de banlieue éloignées. Les durées relatives à l'arrêt dépassent 40% de la durée de trajet pour les lignes 47 et 163.

4 – Conditions de circulation et spécificités locales

L'analyse des données enregistrées selon les zones définies en section 1 permet de comparer les caractéristiques moyennes de circulation (Tableau 4). On repère des zones de circulation difficile (centre-ville mais aussi certaines zones d'habitat isolé) tandis que des conditions plus aisées sont rencontrées généralement dans les zones de faible population. Ces contrastes démontrent le pertinence d'une approche géographique de caractérisation des conditions de circulation et des émissions de polluants.

Zones géographiques Geographical area	distance covered (in %)	vitesses moyenne et hors arrêts average and running speed (km/h)		nb. et durée d'arrêt stop nb. and durat. (1/km)	(%)
Lieux non identifiés dont les liaisons	5,0	17	26	2,2	33,6
Très faible population, éloignement important	0,3	NA	NA	NA	NA
Faible population, pentes	0,3	31	36	0,6	14,6
Habitat individuel isolé, réseau secondaire	3,7	26	29	1,3	11,0
habitat mixte isolé, réseaux second. et tertiaires	7,3	16	23	2,9	29,4
Habitat individuel isolé, pentes	2,5	18	24	2,0	27,0
Habitat mixte dense, proximités	4,8	21	25	1,7	15,5
Habitat individuel concentré	2,8	25	27	0,9	8,4
Routes principales, trafic élevé	6,3	19	24	2,1	18,5
Forte population à proximité d'axes primaires	30,2	14	22	4,4	34,9
Habitat mixte concentré, forte population	13,6	17	23	2,6	26,7
Habitat collect. concentré, forte popul. et emploi	22,5	11	20	5,2	43,3
Zones inhabitées	0,8	19	22	1,6	13,3

Tableau 4: Caractéristiques moyennes de circulation selon les zones géographiques.

Table 4: Average driving characteristics according to the geographical areas.

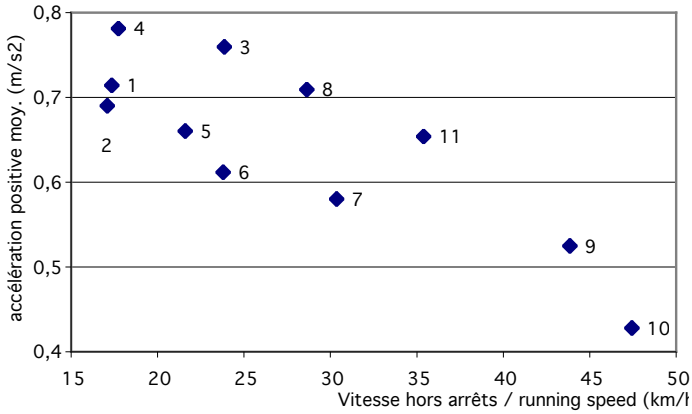

Figure 6 : Typologie en 11 classes des conditions de circulation des bus dans une représentation vitesse - accélération

Figure 6: Typology of the observed driving conditions into 11 classes, represented here as a function of the speed and acceleration.

5 – Typologie cinématique et construction de cycles de conduite

Les concepts développés en (André, 2002) ont été adaptés au cas des autobus pour l'analyse des cinématiques et la construction de cycles représentatifs. On analyse les sections de trajets enregistrées dans chacune des zones géographiques. Ces sections sont décrites par le profil de vitesse sous forme d'une distribution croisée des vitesses et accélérations instantanées, puis soumises à une analyse des correspondances. On établit une typologie des conditions de circulation par classification (Figure 6), c'est à dire une déclinaison dans un espace vitesses – accélérations.

Le croisement de cette typologie des conditions cinématiques avec les zones géographiques types permet d'établir une correspondances entre zones et conditions rencontrées les plus fréquemment (ou les plus caractéristiques). Cette correspondance est utilisée pour construire des cycles représentatifs (Figure 7) permettant de décrire la diversité des conditions cinématiques et associant ces conditions aux lieux sur lesquels elles sont rencontrées. Ces cycles permettront ainsi un re-localisation des

émissions de polluants.

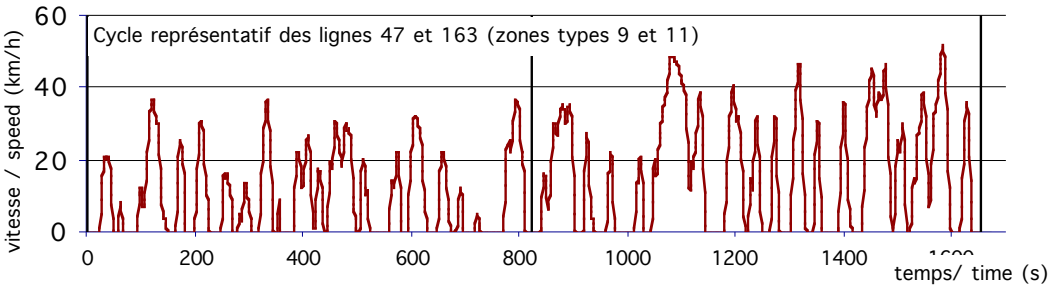

Figure 7 : Cycle de conduite représentatif des conditions de circulation en zones d'habitat collectif concentré (centre-ville, zone 11) et sur les axes primaires à fort trafic (zone 9).

Figure 7: A bus driving cycle, representative of the driving conditions observed in the concentrated group housing areas (town centre, area type 11) and on the primary road network with high traffic (area type 9)

Conclusion

Une démarche méthodologique complète, permettant de relier émissions de polluants des bus aux caractéristiques locales d'exploitation, a été développée et est décrite brièvement dans ce papier. Cette démarche inclut la description et la caractérisation des lignes d'un réseau de bus selon les spécificités des lieux desservis. La sélection de lignes représentatives et l'instrumentation complexe d'autobus ont permis d'enregistrer 25000 km en conditions de circulation et d'exploitation réelles. A partir de la caractérisation des conditions de conduite selon les zones géographiques on construit des cycles de conduite représentatifs qui permettront de lier les émissions de polluants au contexte urbain local et aux conditions d'exploitation.

Remerciements

Les auteurs remercient l'ADEME (Agence de l'environnement et de la Maîtrise de l'Energie) pour son aide financière, l'équipe de l'atelier Essais et Prototype de la RATP et l'IAURIF (Institut d'Aménagement et d'Urbanisme de la Région Ile de France) pour leurs contributions à ces travaux.

Références

André M.. (2002): The ARTEMIS European driving cycles for measuring car pollutant emissions. 7th International Symposium, Highway and Urban Pollution. Barcelona, 20-23 May 2002. To be published in The Science of the Total Environment, Special Issue.

André M. & Villanova A. (2002a): Caractérisation des lignes d'autobus d'un réseau selon les données d'exploitation et d'environnement urbain. Rapport INRETS-LTE 0201. Bron, France, 2002; 107 p.

André M. & Villanova A. (2002b): Characterisation of an urban bus network for environmental purposes. 7th International Symposium, Highway and Urban Pollution. Barcelona, 20-23 May 2002. To be published in The Science of the Total Environment, Special Issue.

Hamelin N. (2001): Localisation de véhicules à l'aide d'un système d'information géographique. Rapport INRETS-LTE0127, Bron, France. 65p.

12th International Symposium "Transport and Air Pollution" / 12e Colloque international "Transports et pollution de l'air", Avignon, 16 -18 *June* / juin 2003
proceedings / actes, n°92, tome / Vol. 1, Inrets ed., Arcueil, France, 2003, p. 89-96

The dispersion of a traffic-related pollutant in two urban street canyons

J.W.Douglas Boddy[*], Robert J. Smalley[*], James E. Tate[**] & Alison S. Tomlin[*]
[*]Energy and Resources Research Institute, University of Leeds, LS2 9JT, United Kingdom
Fax +44 113 343 2549 - Email: prejwb@leeds.ac.uk
[**]Institute for Transport Studies, University of Leeds, LS2 9JT, United Kingdom

Abstract
The dispersion of a traffic-related pollutant within city streets of differing geometries has been investigated experimentally. The influence of background wind direction, traffic conditions and street geometry on roadside carbon monoxide concentrations is demonstrated. Concentrations on the leeward side of narrow street canyons are shown to be substantially higher than on the windward side for even sided, step-down and step-up street canyons. Long-term averages of CO and traffic flow indicate a strong linear relationship when the flow is low. This relationship changes during periods of high flow, when concentrations are dependent upon the level of congestion present. Concentrations in the narrower street are influenced more strongly by traffic flow than in the wider one, indicating that understanding the combined influences of meteorology and building geometries on the dispersion of traffic-related pollutants, may have implications for the application of traffic management measures.
Keywords*: urban wind field, street canyon, dispersion, traffic-related pollutant, carbon monoxide.*

Introduction

Local authorities are required to meet air quality targets for urban areas and in order to do so many are considering the application of traffic demand management strategies for areas projected to exceed these targets. Examples of such measures include controlling traffic signalling, re-locating traffic queues during congested periods, and the introduction of vehicle restrictions such as low emission zones and congestion charging. Before applying such measures, planners aim to predict the possible influences on roadside pollutant concentrations using air quality dispersion models. Previous work indicates that urban areas with high pollution exhibit not just high traffic related emissions, but also air flow conditions that may affect the local dispersion of pollutants, thus influencing roadside concentrations (e.g. Vachon *et al*., 2000). The flow conditions are often dependant on the interaction between the background meteorology and the geometry of the surrounding streets. A successful model must be able to represent the combined influences of traffic emissions and dispersion within complex geometries. One example of conditions that may limit dispersion is the existence of an urban street canyon. A street canyon is defined as a street of high aspect ratio, which is the term used to describe the ratio of building height to street width (H/W). It has been demonstrated numerically (e.g. Sini *et al*., 1996; Leitl & Meroney, 1997), and by using wind tunnel modelling (Kastner-Klein, 1997, 2001; Rafailidis, 1997), that flow and dispersion within street canyons essentially depends on the aspect ratio, the street length and building roof geometry (Ketzel *et al*., 1999). Within street canyons of $H/W \approx 1$, Louka *et al*. (2000) suggest that pollutants released by vehicles at street level under certain background wind directions are transported by a recirculation vortex within the street canyon. The vortex may cause the build up of traffic-related pollutants on the leeward side of the canyon and may limit the escape of pollutants from the street. However, not all urban streets conform to this strict definition of a street canyon. Many streets have a non-uniform width or may have buildings that differ in height on either side. It

is important therefore that any model that is used to inform decisions on traffic management plans must be able to represent the influence of traffic on road-side concentrations for a range of street types and background meteorological conditions. Presently, many such numerical models are being developed (e.g. Boddy *et al*., 2003). However, very few data sets exist which provide simultaneous measurements of the key parameters required for model evaluation. In the present study, involving field experiments, an attempt is made to determine the influence of wind direction and vehicle traffic flow on the dispersion of a traffic-related pollutant within two urban streets of different geometry.

1 - Experimental methodology

This paper presents data from an on-going field campaign conducted in the city of York, UK. During part of the campaign, between 1 August and 9 December 2002, measurements of carbon monoxide (CO) concentrations and vehicle occupancy have been made within two perpendicular streets of slightly different geometry. The two streets chosen were Bootham and Gillygate, both situated within the inner ring road of the city, and are joined by a traffic-signal controlled T-intersection as depicted in Fig. 1a. Bootham is aligned at approximately 225° from N, while Gillygate is predominantly at 45°, although the end opposite to the intersection is at approximately 30° from N. The vehicle traffic flow characteristics for both streets are obtained as a by-product of the operation of the SCOOT (Split Cycle Offset Optimisation Technique) demand-responsive Urban Traffic Control system (Hunt et al., 1991). SCOOT provides a variety of traffic flow measures from piezo-electric loop detectors embedded close to the up-stream end of a link, or road section, between traffic signals. This study uses a traffic flow measure derived from the detector occupancy operating at a frequency of 4Hz. Marsden and Bell (1992) demonstrated that this measure of flow is reliable in urban traffic flow conditions. 15-minute averages of the vehicle flow and occupancy of the detector (%) were obtained in both directions for Bootham and in one direction for Gillygate for the campaign period. Simultaneous wind velocity data at 7 m are obtained from an automatic weather station located in a park approximately 500 m north of the intersection. 15-minute averages of CO concentrations are measured using electrochemical sensors, which are incorporated within Learian streetboxes attached to roadside lampposts within each street at 15 different locations. The locations of streetboxes discussed in this study are depicted in Fig. 1a. CO is used as it can be treated as a passive pollutant on urban time-scales, providing a degree of simplification for model evaluation when compared with secondary species like NO_2.

(a) (b)

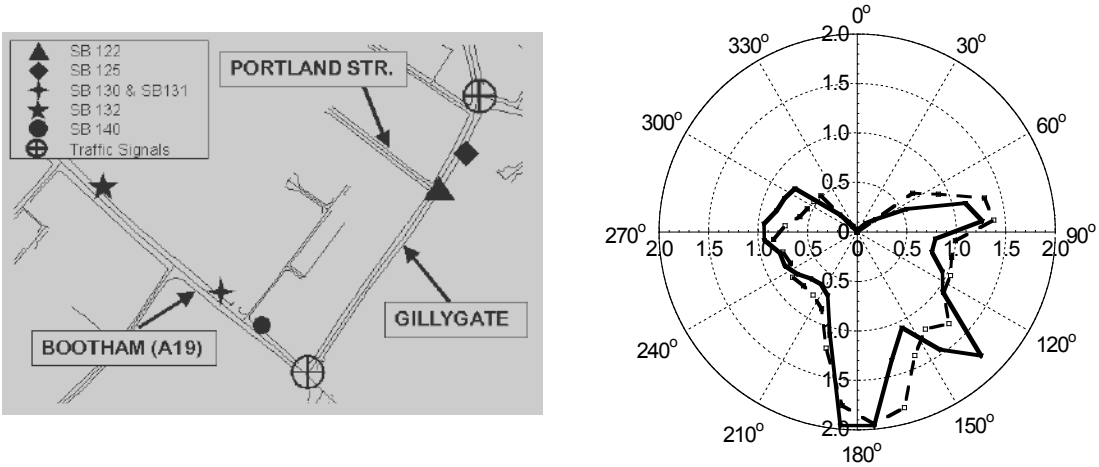

Figure 1: (a) Schematic diagram of the experimental site with location of streetboxes marked.
(b) — Mean wind direction frequency (percent/4); —□— mean wind speeds (ms^{-1}).

Co-location surveys utilising two streetboxes and a US EPA certified Gas Filter Correlation CO Analyser demonstrated the precision, repeatability and reliability of the streetbox measurement of CO over a one-month period. When compared with the reference analyser r^2 values of 0.95 and 0.96 were achieved.

Buildings of different heights surround both streets, which allows for a range of street canyon geometries to be studied within one experiment. Overall Gillygate is a relatively narrow street canyon, with *H/W* of approximately 0.75. The aspect ratio of Bootham, on the other hand, is approximately 0.65, and yet there are several sections with a much lower ratio. Both streets have high vehicle flows, with significant periods of congestion. In this paper, data from several of the streetboxes are compared with the aim of determining the influence of detector height and horizontal location, vehicle congestion, and surrounding building topology on long-term average concentrations. In Gillygate the selected streetboxes are on the leeward and windward sides of the street during background winds from the SE and NW, respectively. In addition, a further streetbox has been located in Portland Street which is a side street adjoining Gillygate aligned at approximately 315° from N as shown in Fig. 1a. In Bootham the geometry of the canyon is more complex, with the street separating a high building and a low wall, with a height ratio of 0.45. Therefore, the selected streetboxes are on the leeward and windward sides of the street for winds from the NE. For streetboxes 130 and 131 this forms a step-down canyon with $H/W = 0.57$ and the SW a step-up canyon, $H/W = 0.26$, respectively.

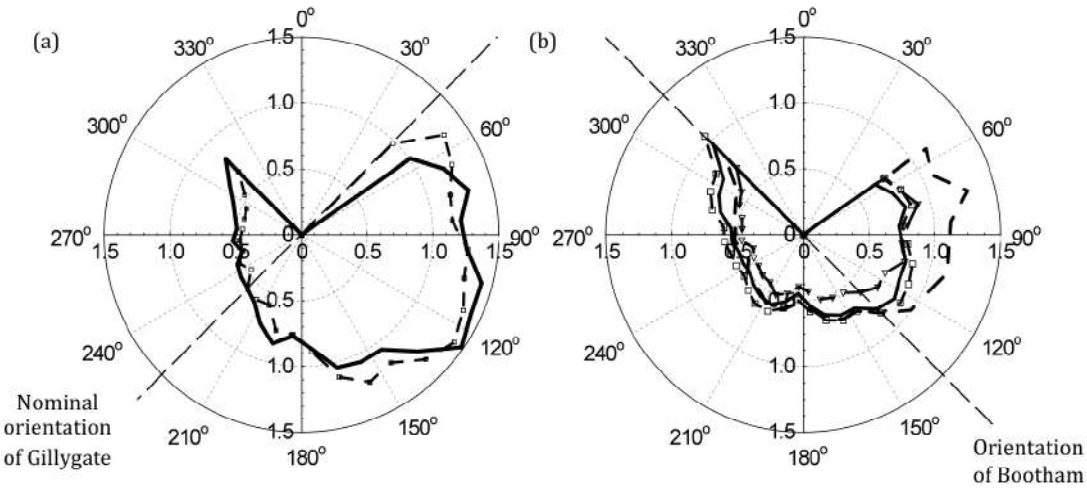

Figure 2: Sector averaged CO concentrations (ppm) in (a) Gillygate (Streetbox — 122 and —□— Streetbox 125). (b) Bootham (— Streetbox 130, —□— Streetbox 131, — ▼- Streetbox 132 and --- Streetbox 140).

2 - Results And Discussion

Fig. 1b shows the normalised wind-direction frequency distribution and wind speed rose from the background meteorological station for each 10°-wind direction sector during the monitoring period. Data has been excluded for wind speeds < 0.3 ms^{-1} due to the limited accuracy of the instrumentation in this range. The predominant direction and greatest wind speeds are from the S and to a lesser extent the SE, whereas the least frequent winds are from the NNW to NE. While the low frequency of these winds could be attributed to synoptic conditions, trees immediately N of the wind vane are likely to influence the data.

Fig. 2a and 2b present mean CO concentration roses for selected streetboxes in Gillygate and Bootham respectively. These are formed from the average of all 15-minute values within a 10° sector for the chosen period. Sectors with less than 0.5% of the total number of values are neglected since the averaging process for so few points may not be statistically significant. Low wind-speed conditions are also excluded as described above. One of the streetboxes had to be removed for maintenance between 10 October and 7 November and, therefore, these dates have been excluded from the data for all streetboxes in order to allow for equivalent comparison. The orientations of Gillygate and Bootham are indicated on the figures. The two streetboxes in Gillygate are located on the SE side of the canyon. Streetbox 125 is at a height of 4.5m and is surrounded on both sides by

high buildings with a local aspect ratio of 0.76. Streetbox 122 is at a height of 3.5m and is situated opposite Portland Street. Therefore high buildings exist on only one side, as shown in Fig. 1a. During SE winds, the mean concentration of CO is higher at both the Gillygate streetboxes than for SW winds, which are parallel to the canyon axis. This is likely to be due to the presence of a recirculation region on the leeward side of the buildings, effectively reversing the above roof flow at street level and leading to the transport of emissions towards the detector. Such a vortex flow regime has often been cited as a characteristic feature in street canyons with perpendicular wind flow (Berkowicz, 2000), but in this case there is also evidence of flow reversal occurring opposite the junction.

Parallel flow also has a significant role in the transport of CO. In Gillygate, SW winds have a 'flushing' effect, with some of the lowest CO concentrations occurring during these conditions. Streetbox 122 shows slightly higher concentrations for S, SW and W winds than streetbox 125. A possible explanation for this is that in such conditions, flow may be diverted from Gillygate into Portland Street, thus flushing out some pollutants before reaching streetbox 125. Conversely, for winds from the NE, streetbox 125 exhibits higher concentrations than streetbox 122. A likely reason for this is that in congested periods, idling traffic may occur on both sides of the street to the North East of the streetboxes, since the flow of both inbound and outbound traffic may become saturated. Under conditions of extreme congestion, traffic also queues in the streets leading up to the junction at the NE end of Gillygate (a further discussion of these conditions is given later). As a consequence, this region is likely to experience the influence of high upwind emissions and, additionally, any flushing of Portland street would only effect streetbox 122 for these wind directions. The influence from near-parallel flow should not be neglected either. During such conditions, above-roof flow is at a slight angle to the street axis and may induce a helical flow regime along the canyon (Nakamura and Oke, 1988). Further verification of the existence of a helical flow regime in these streets is necessary and will be investigated using street-level sonic anemometers in future field experiments. However, this type of flow regime may explain the higher than expected mean CO concentrations during near-parallel winds from the ENE in Gillygate.

In Bootham, the overall concentrations are lower than in Gillygate, perhaps reflecting the wider aspect ratio of this street. The chosen streetboxes, as shown in Fig. 1a, are on the leeward side during NE winds. Consequently, these winds may promote the development of a vortex flow regime, as indicated by the higher mean concentrations of CO in these wind sectors. In both streets the windward (i.e. winds from the NW and SW in Gillygate and Bootham, respectively) concentrations are significantly lower compared with those measured on the leeward side. The concentrations from streetboxes 130 and 131 located on the same lamppost at the respective heights 4.52m and 2.99m were compared to establish the influence of vertical displacement on concentrations. Their measurements followed a similar profile, with the lower streetbox recording slightly higher mean concentrations, due to the increased dispersion and diffusion of pollutants from the source at the upper streetbox. This has been confirmed by fitting a linear relationship between the two datasets, with a gradient of 1.08 and a regression coefficient of $r^2 = 0.91$. Data was compared from streetboxes 140, 130 and 132 (heights 4.5m, 4.52m and 3.83m respectively) in order to establish the variation with horizontal displacement along Bootham. Fig. 2b demonstrates that streetbox 140, the streetbox closest to the Bootham/Gillygate signalised intersection, recorded the highest mean concentrations, especially under Easterly winds. Concentrations then reduced with distance away from the intersection, with streetbox 130 recording levels higher than 132. This is not surprising, as the streetboxes closest to the traffic signals will have more frequent queuing traffic adjacent to them, with associated higher emission rates.

Fig. 3 shows how the 15-minute vehicle flow averages vary with vehicle occupancy for Bootham for inbound (towards the junction with Gillygate) and outbound flow directions. The occupancy is determined from the percentage time a vehicle spends over the sensor compared to the total sampling period. The figure shows that the inbound flow starts to become saturated above a certain level of occupancy (~12%) and congestion starts to occur due to the limited number of vehicles allowed to pass through the signal junction. From this point an increase in vehicle occupancy does

not lead to further increases in traffic flows. Instead, it often results in decreases in flow at very high occupancies. This decrease may be due to special events occurring in the street that further constrict the flow, although it should also be pointed out that the algorithm used to derive flow from occupancy is less accurate for high occupancy conditions. Outbound flow on Bootham, as shown in Fig. 3b, remains much more freely moving than the inbound flow, with very few data points above the 12% occupancy level. An almost linear relationship exists between flow and occupancy for most outbound flow conditions.

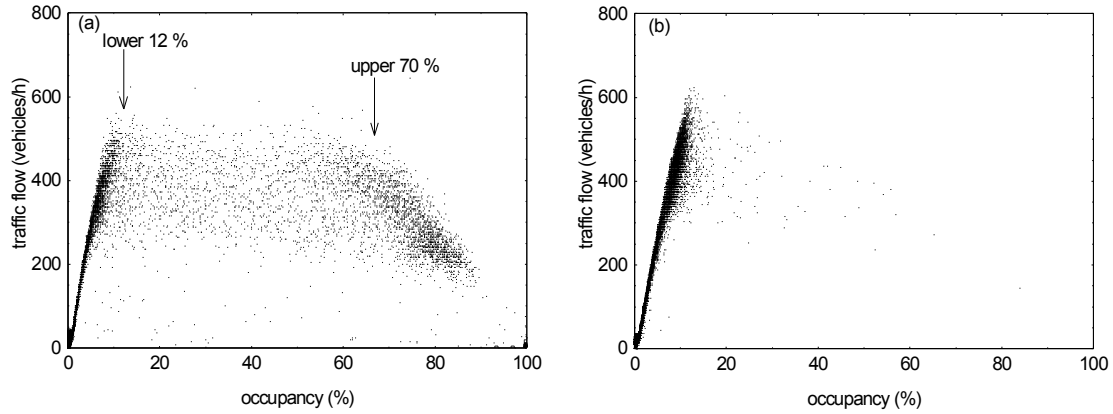

Figure 3: 15 minute averages of SCOOT traffic flow versus % occupancy for Bootham. (a) inbound traffic. Lower and upper occupancy limits are indicated. (b) outbound traffic.

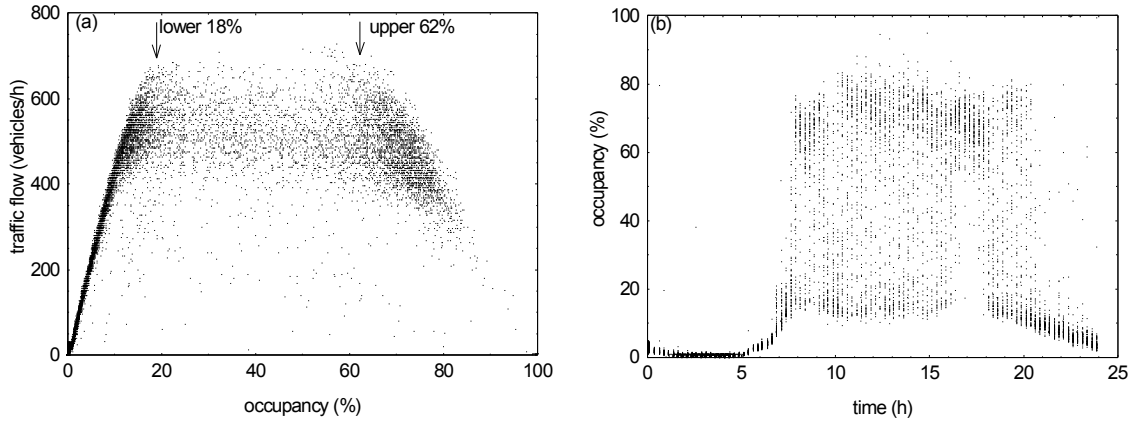

Figure 4: (a) 15 minute averages of SCOOT traffic flow versus occupancy for Gillygate inbound traffic. (b) Time series of 15 minute averages of SCOOT occupancy for whole monitoring period.

Fig. 4a shows the inbound flow for Gillygate, which exhibits similar levels of flow saturation to those seen in Bootham with a slightly higher maximum flow. Unfortunately SCOOT occupancy data was not available for outbound flow on Gillygate for the chosen monitoring period. However, manual traffic counts suggest that it is more congested than the outbound flow on Bootham. On certain parts of Gillygate queuing traffic may exist on both sides of the street during congested periods. Fig. 4b shows the 15-minute occupancy data against time of day for inbound flow on Gillygate for the total monitoring period. The figure indicates that periods of congestion exist for most of the day from between 07:30 and 19:00. For the majority of this time the flow flips between congested and non congested conditions as shown by the clustering of data points around low and high occupancies. The data also shows that for the afternoon rush-hour period between 16:30 and 18:30, congested flow and high occupancy conditions dominate.

The dependence of average CO concentrations on the inbound average traffic flow in Bootham and Gillygate is shown in Fig. 5. The figures were formed by first separating the raw data into low, medium and high occupancy traffic conditions as indicated in Fig. 4a and 5a and then, within each

condition, averaging the same daily 15-minute period between August and December. Although variation occurs in each quantity over short time scales a significant linear regression (r^2 = 0.93 for Gillygate and 0.97 for Bootham) exists between average traffic flow and CO concentrations when the traffic flow is relatively low. Slopes of 0.0023 and 0.0015 exist for Gillygate and Bootham, respectively. A minimum threshold of 20 vehicles has been used for the linear fit since below this the

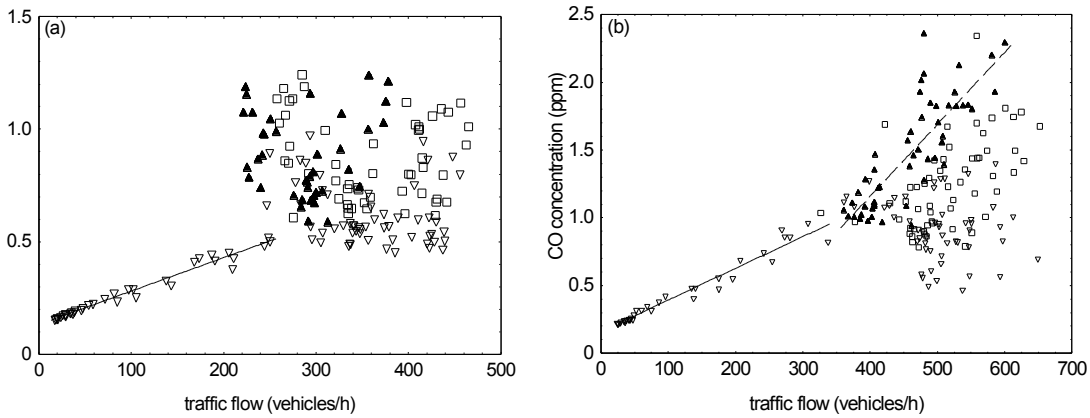

Figure 5: 15 minute daily averages of CO concentration against traffic flow, conditioned using 3 occupancy regimes. —— curve fit for low flow; – – – curve fit for high occupancy. (a) Gillygate, Streetbox 125: ∇, occupancy < 18%; □, 18%≤ occupancy ≤62%; ▲, occupancy > 62%; (a) Bootham, Streetbox 132: ∇, occupancy < 12%; □, 12%≤ occupancy ≤70%; ▲, occupancy > 70%.

CO concentration tends non-linearly to the seasonal nighttime background levels. The times corresponding to the linear fit are approximately between 05:30 – 07:15 and 21:30 – 03:00 in both streets. For high occupancy conditions a linear relationship also exists for Gillygate with r^2 = 0.68. A linear trend does not exist for Bootham during high occupancies and further investigation will be required to determine the reason for the higher degree of scatter. The influence of outbound flows in both streets is a possible reason for the difference between the two and will be investigated further during future experiments. The slope is much higher for high occupancy conditions than for low flows (i.e. 0.0053 for Gillygate compared to 0.0023 for low flows). Therefore the dependence of CO concentrations on traffic flow is much stronger for high flow and high occupancy conditions than for low flow conditions. The average CO levels are also elevated for high flow and high occupancy conditions when compared to high flow and low occupancy conditions for both streets. In fact, some very low concentrations are found for traffic flows of 500-600 vehicles/hr in Gillygate under low occupancy conditions. Therefore, for most of the day it is the level of congestion in the streets, rather than the overall level of traffic flow, that has the greatest influence on pollutant concentrations. During congested flow the number of stop-starts will be greater than for freely flowing traffic: leading to higher emissions levels during periods of acceleration and idling than would be found in free flow (Waters, 1992). Congestion has a significant impact on emissions and potential benefits in air quality could be achieved if traffic flow was maintained below saturation levels for longer periods.

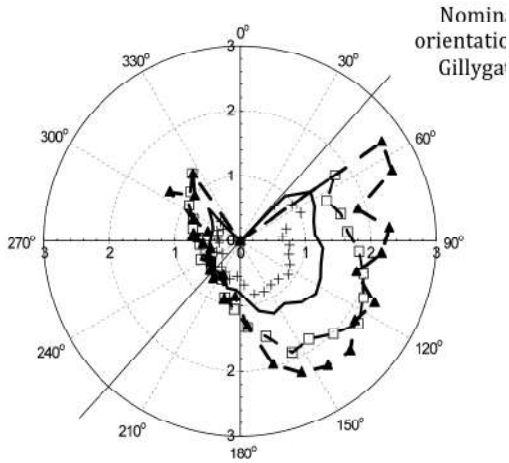

Figure 6: Concentration rose conditioned on occupancy for Streetbox 125 on Gillygate. —— all occupancy. +, low occupancy; ⊟, medium occupancy; –▲– high occupancy, as for Fig. 5.

The higher slopes for Gillygate shown in Fig. 5 suggest a stronger interdependence between CO concentration and traffic flow for this street when compared to Bootham. This could be for several reasons. Firstly, overall Gillygate has a narrower aspect ratio than Bootham, possibly promoting the existence of vortex flow regimes at more locations within the street and limiting the overall volume into which emissions are dispersed. Furthermore, Gillygate shows higher average concentrations from the S, SSW and SSE directions, as demonstrated in Fig. 2, which all have a contribution to perpendicular flow across the street. Fig. 1b suggests that these are high frequency sectors, which may contribute to a higher overall average for Gillygate. Fig. 6 presents the concentration roses for streetbox 125 on Gillygate where the data has first been separated into high, medium and low occupancy conditions before sector averaging. For high occupancy (i.e. congested) conditions, wind directions that are perpendicular to the street lead to higher mean leeward CO concentrations than wind directions that are parallel to the street. This would support the claim that limited ventilation of the street occurs under perpendicular background flows compared to parallel flows where the pollutants are effectively flushed down the street. The effect is more marked for high occupancy conditions than for low occupancy conditions. Additionally, under high occupancy conditions in Gillygate there are abnormally high average concentrations for winds from the NE direction. This feature is not present for lower occupancies and is probably due to the dispersion of emissions from congested streets entering Gillygate from its NE junction. These features confirm the importance of understanding the complex interactions between traffic conditions, emission levels, meteorology and local topology in determining mean roadside concentrations of traffic-related pollutants.

Conclusion

Concentrations of CO measured in two urban streets of different geometry indicate increased pollutant concentrations on the leeward side of the street for cross-canyon rooftop winds, corresponding to a possible vortex structure within the canyon. The pollution concentrations within each street and their dependence on overall traffic flows were found to vary for different street geometries with the narrower street demonstrating higher average CO levels. When traffic flow is relatively low, a strong linear relationship exists with the CO concentrations measured in each street. This relationship collapses under congested conditions where the mean CO levels depend not just on the traffic flow but also on the level of congestion within the street. Significant benefits in urban air quality may result from attempts to reduce the level of vehicle occupancy within narrow streets of the types presented in this paper. A further implication of the results from this study is the need for urban air quality models to represent both complex street geometries, which influence local dispersion conditions, and complex traffic conditions. The ability to represent the effect of congestion on emissions could significantly improve the predictive quality of urban air quality models and therefore their overall usefulness in assessing traffic management measures.

Acknowledgements

The authors gratefully acknowledge the assistance provided by Mr D. Young during the experimental campaign and meteorological and SCOOT data provided by the City of York Council. EPSRC JIF and PLATFORM awards to the LANTERN Consortium supported this work. RJS and JWDB gratefully acknowledge financial support from NERC.

References

Berkowicz, R. (2000), OPSM – A parameterised street pollution model. Environ. Monit. Assess. 65, 323 – 331.

Boddy, J.W.D., Dixon, N., Smalley, R.J., Tate, J.E and Tomlin, A.S. (2003) An intercomparison between road-side concentrations of traffic related pollutants in two urban streets, 4th International Conference on Urban Air Quality, 25 – 27 March, Prague.

Hunt P.B., Robertson D.I., Bretherton R.D., and Winton R. I. (1991), SCOOT - A traffic responsive method of co-ordinating signals, Laboratory Report 1014, TRRL, Crowthorne, Berkshire.

Kastner-Klein, P., Fedorovich, E. and Plate, E.J. (1997), Gaseous pollutant dispersion around urban-canopy elements: wind tunnel case studies, Int. J.Environ. Pollut. 8, 727 – 737.

Kastner-Klein, P., Fedorovich, E. and Rotach, M.W. (2001), A wind tunnel study of organised and turbulent air motions in urban street canyons, J. Wind Eng. Ind. Aerodyn. 89, 849 – 861.

Ketzel, M., Berkowicz, R., Müller, W. and Lohmeyer, A. (1999), Dependence of street canyon concentrations on above roof wind speed - implications for numerical modelling, Rouen, 11 - 14 October.

Leitl, B.M. and Meroney, R.N. (1997), Car exhaust dispersion in a street canyon: numerical critique of a wind tunnel experiment, J. Wind Eng. Ind. Aerodyn. 67&68, 293 – 304.

Louka, P. Belcher, S.E. and Harrison, R.G. (2000), Coupling between air flow in streets and the well-developed boundary layer aloft, Atmos. Environ.34, 2613 – 2621.

Marsden, G., Bell, M and Reynolds, R. (2001), Towards a real-time, microscopic emissions model, Transportation Research Part D. Vol 6 37-60.

Nakamura Y, and Oke T.R. (1988), Wind, temperature and stability conditions in an E-W oriented urban canyon. Atmos. Environ. 22, 2691 – 2700.

Rafailidis, S. (1997), Influence of building area density and roof shape on the wind characteristics above a town, Boundary-Layer Meteorol. 85, 255 – 271.

Sini, J-F., Anquetin, S. and Mestayer, P.G. (1996), Pollutant dispersion and thermal effects in urban street canyons, Atmos. Environ. 30, 2659 – 2677.

Vachon, G., and 14 others (2000), Experimental investigation of pollutant dispersion within a street in low wind conditions, 9th International Scientific Symposium Transport and Air Pollution, 5–8 June, Avignon, France, pp. 95 – 102.

Waters, M.H.L (1992) Road vehicle fuel economy: state-of-the art review, *HMSO*, London.

12th International Symposium "Transport and Air Pollution" / 12e Colloque international "Transports et pollution de l'air", Avignon, 16 -18 *June* / juin 2003
proceedings / actes, n°92, tome / Vol. 1, Inrets ed., Arcueil, France, 2003, p. 97-103

Influence of Gotthard Tunnel Shutdown on Aerosol, Nitrogen Oxide and Carbon Monoxide Concentrations in Alpine Valleys

A.S.H. Prevot*, J. Thudium, S. Henne*, J. Dommen*, N. Bukowiecki*, U. Baltensperger***
* Laboratory of Atmospheric chemistry, Paul Scherrer Institut, CH-5232 Villigen-PSI Switzerland - Fax: +41 56 3104525 - email: andre.prevot@psi.ch
** Oekoscience AG, Werkstr. 2, CH-7000 Chur, Switzerland

Abstract
Due to the tragic accident in the Gotthard road-tunnel, leading to a complete closing from 24 October - 21 December 2001, the trans-alpine traffic strongly decreased in the adjacent valleys, while traffic increased in the valleys of the alternative San Bernardino route. A strong effect of these traffic changes could be observed for nitrogen oxides (NO_x) concentrations where changes of more than a factor of three were observed. For the aerosol mass, the effects were less pronounced and often not significant. For the active aerosol surface, aerosol volume, as well as carbon monoxide, mobile measurements revealed that other emission sources, probably residential heating with a high fraction of wood burning, are important especially in the Mesolcina valley along the San Bernardino route. Near San Vittore, the concentrations of e.g. the active aerosol surface would increase from the highway toward the small village. The analysis of the PM10 (aerosol mass concentration of all particles of diameter D < 10 μm) monitoring data also suggests that other sources than the traffic explains most of the variance in the PM10 concentrations. However, nanoparticle (<50 nanometers) number concentrations, which hardly contribute to aerosol surface or mass, seemed to be dominated by the emissions of the highway.
Keywords*: aerosols, particulate matter, nitrogen oxide, traffic emissions, Gotthard tunnel*

Introduction

At the end of October 2001, the Gotthard road-tunnel was shut down after a terrible accident for around two months. This shutdown influenced the traffic through the Swiss Alps significantly. A major fraction (around 65%) of the traffic usually passing along the Gotthard route then used the San Bernardino route instead. This situation yielded a unique opportunity to study the influence of this trans-Alpine traffic on the air quality within the Alpine valleys along these routes. It is possible to compare the air quality before and after the shutdown and as well the air quality to the year before. In addition to these statistical analyses, measurements were performed using a mobile laboratory allowing to measure trace gases and aerosol properties while driving. This van and the equipment was described in detail by Bukowiecki et ali (2002). Data included in this paper were measured by a scanning mobility particle sizer (SMPS, DMA TSI 3071 and CPC TSI 3010) for aerosol size distributions (7<D<310 nm), a diffusion charging sensor (DC, Matter Engineering LQ1-DC) for the active aerosol surface area concentration, a home built NO_2 luminol chemiluminescence instrument with chromium trioxide (CrO_3) converters for NO_x and a resonance fluorescence carbon monoxide (CO) instrument (Aerolaser AL-5002, Gerbig et ali, 1999). In Fig. 1, one can see the mobile van in the Mesolcina valley near San Vittore. With these high time resolution measurements spatial distributions of pollutant concentrations on the valley floor were determined on 6 days south and 4 days north of the Alps. In addition, measurements along the slope allowed for the determination of the air quality conditions at around 300 meters higher altitude. In this paper, only mobile measurements of south of the Alps will be shown. Several monitoring station data of NO_x

and PM10 were used for statistical analysis.

Figure 1: Mobile laboratory of the Paul Scherrer Institute. The inlet of the trace gases is made out of Teflon (PFA) where the air is first passing through a large Teflon filter. The aerosol inlet is made out of stainless steel and allows for isokinetic sampling at around 50 km/h (see also Bukowiecki et ali (2002).

1 – Results and discussion

Figure 2 shows an example of how the pollutant levels were influenced by the tunnel shutdown. The NO_x concentrations at Erstfeld (at the Gotthard route in the Reuss valley North of the Alps) dropped to much lower values after the tunnel accident and significantly increased again after the tunnel was opened again. Before and after the tunnel shutdown, the heavy-duty vehicles are responsible for more than half of the NO_x emissions. Thus, the traffic density of heavy-duty vehicles per day does generally correlate rather well with the observed NO_x concentrations (Figure 2). After the tunnel shutdown, the heavy-duty traffic was lower. Nevertheless, the NO_x concentrations were similarly high as before the tunnel shutdown due to stronger temperature inversions inducing less dilution in January than in October. This shows that an accurate determination of the effect of the emission changes on the air quality needs to take the meteorology into account. Fortunately, the weather conditions during the tunnel shutdown were comparable to the conditions during the same months of the previous years and in January/February after the tunnel shutdown.

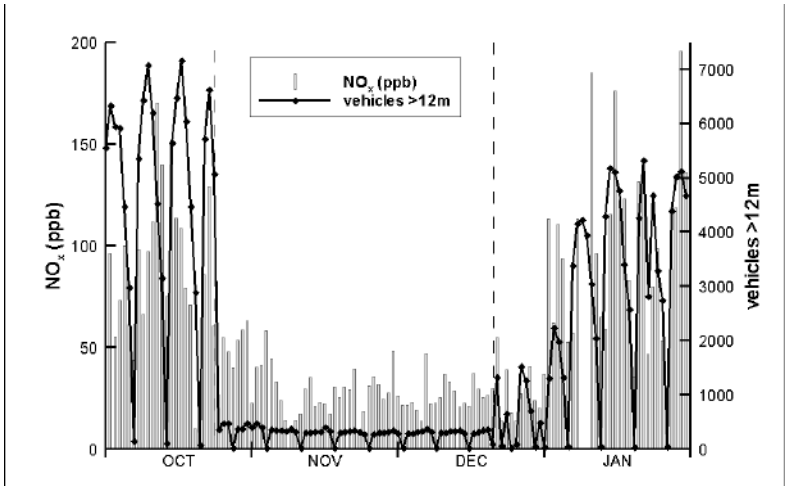

Figure 2: Daily average NO_x, concentrations and long vehicles (>12.5 meters, mostly heavy duty vehicles) traffic density in Erstfeld (8 meters from highway). The dashed vertical lines indicate the time period of the tunnel shutdown.

The weather was dominated by stagnant high-pressure conditions with strong temperature inversions formed during the nights. The average diurnal patterns of the temperature inversion occurrences, determined from temperature measurements along the slopes of the different valleys, were nearly identical (differences mostly lower than 5%) in 2000 and 2001 (Figure 4).

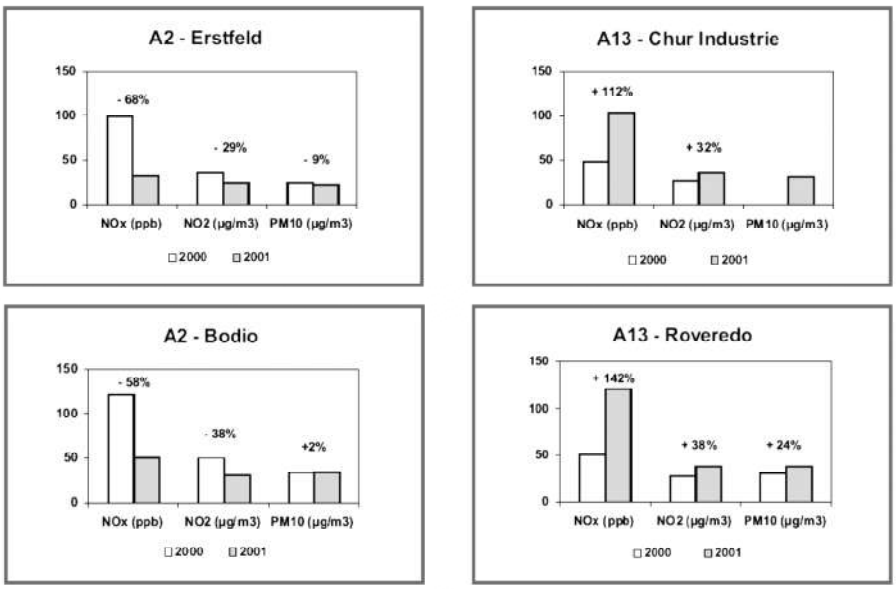

Figure 3: NO_x, NO_2 and PM10 concentration differences in 2001 during the tunnel shutdown compared to 2000 along the Gotthard route (A2) and the alternative San Bernardino route (A13). The stations Erstfeld, Chur Industrie and Roveredo are around 10 meters from the respective highways and the station Bodio is in a small village around 300 meters from the highway.

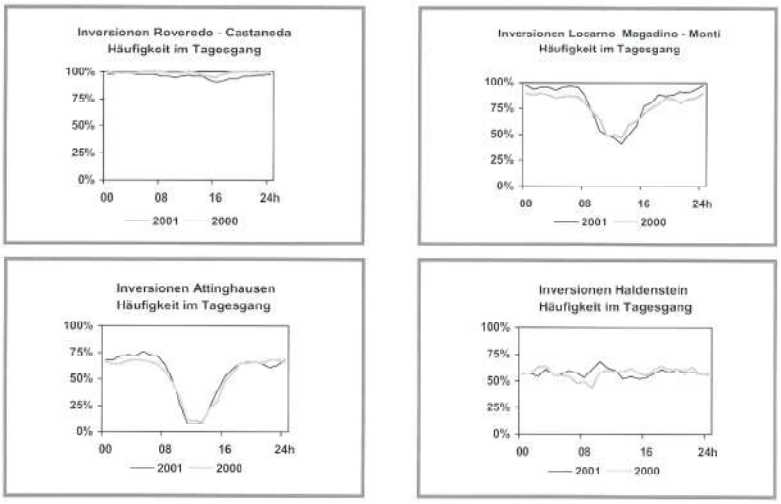

Figure 4: Average diurnal patterns of the temperature inversion occurrences during the tunnel shutdown in 2001 and the same period in 2000. Locarno is located around 25 kilometers away from Bodio and Roveredo.

In Figure 3 the concentrations during the tunnel shutdown are compared to measurements in the previous year. The NO_x concentrations decreased along the Gotthard route by 58% and 68% respectively for Erstfeld (North of the Alpine ridge) and Bodio (South of the Alpine ridge). In contrast, concentrations on the alternative route increased in Chur (North of the Alpine ridge) and Roveredo (South of the Alpine ridge) by 112% and 142% respectively. These changes are very significant and show that the NO_x emissions of the transalpine traffic are to a large extent responsible for the NO_x concentrations observed in the Alpine transit valleys. For PM10, the concentrations are not as strongly changed, and the differences are often not significant. This means that either the local traffic emissions do not contribute as much to the already existing background as for NO_x or other PM10 emission sources than the traffic play an important role.

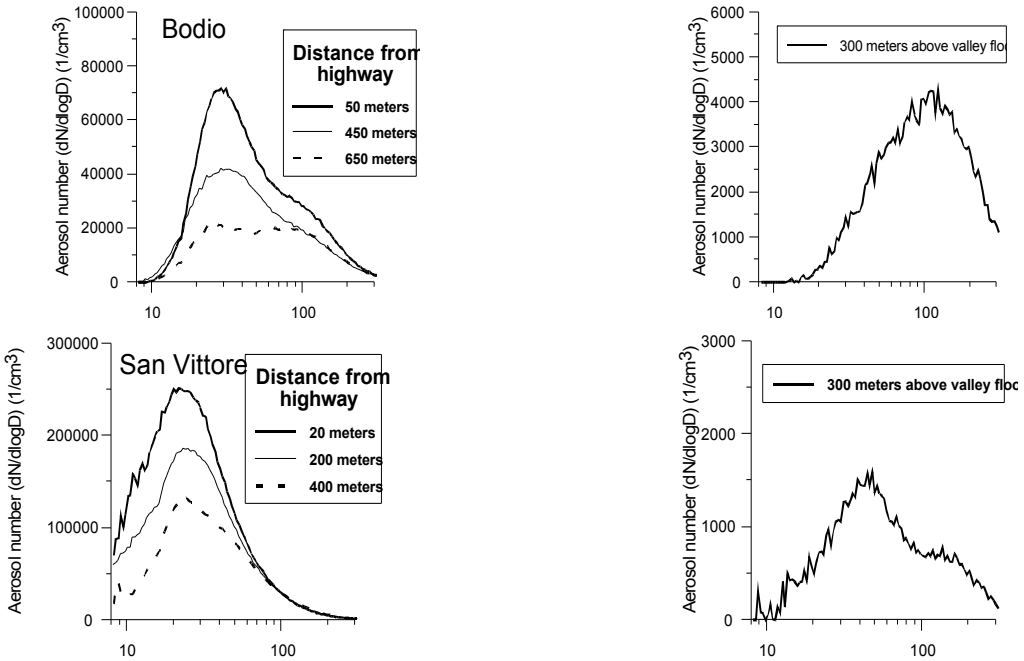

Figure 5: Aerosol number size distributions on December 10 near Bodio (Gotthard) (upper panels) and on January 9 near San Vittore (San Bernardino) (lower panels) at different distances from the highway and 300 meters above the valley floor.

Beside the statistical analyses of the monitoring stations, mobile measurements were performed on six and four days south and north of the Alpine ridge, respectively. In Figure 5, examples of aerosol number size distributions near Bodio at the Gotthard route and near San Vittore along the San Bernardino route (both locations south of the Alpine ridge) are shown. In these examples, the nanoparticle (diameter D < 50 nanometers) concentrations were much higher close to the highway than further away. This strong decrease is mainly caused by the short lifetime (typically around 10 minutes) of these small particles due to rapid coagulation. It is important to note that the nanoparticles are very important for the aerosol number concentration but are negligible for the total aerosol mass. The particle concentrations with diameters in the range of 80-140 nanometers (typical size of directly emitted soot particles) were nearly constant at San Vittore with increasing distance to the highway, whereas the concentrations were highest near the highway in Bodio. At both locations, aerosol size distributions were also measured 300 meters above the valley floor. The concentrations were a factor of 10 to 100 lower at these altitudes compared to the valley bottom. This shows that the pollutants are very efficiently trapped by the inversions close to the valley floor.

The average concentrations of NO_x, carbon monoxide, aerosol nanoparticle number (10<D<30 nanometers), aerosol volume (80<D<140 nanometers) and active aerosol surface areas as a function of the distance to the road are shown for the afternoons of all six measuring days south of the Alps near Bodio and San Vittore in Figure 6. In general, the concentrations of all trace gases and aerosol properties are higher close to the highway than further away near Bodio. However in San Vittore, this can only be observed for NO_x and the nanoparticles. The active aerosol surface area, the aerosol volume of particles with a diameter of around 100 nanometers and the carbon monoxide tends to increase with distance to the highway. The area further away from the highway was closer to the village San Vittore.

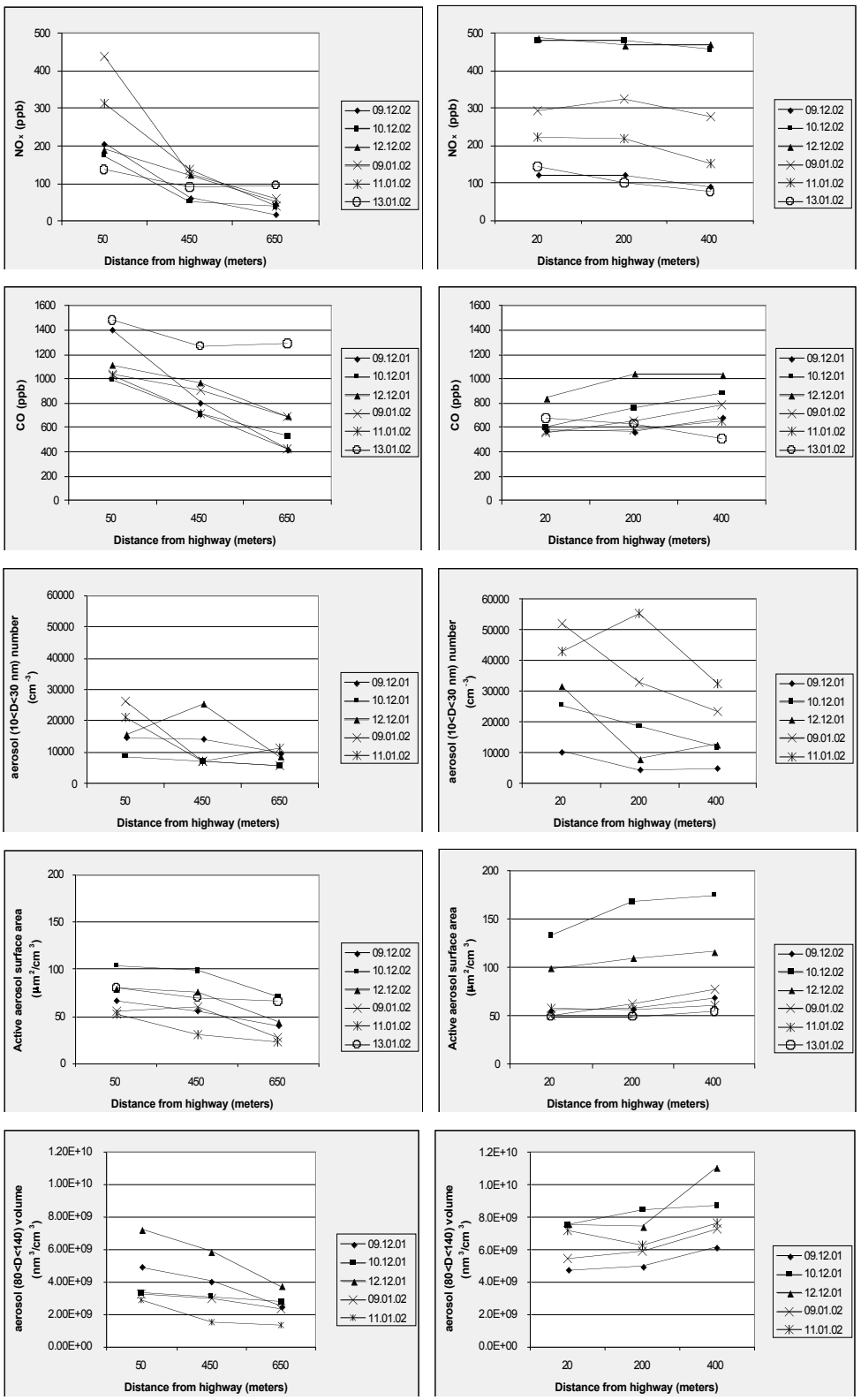

Figure 6: NO_x, carbon monoxide, aerosol number (10<D<30 nanometers), active surface areas and aerosol volume (80<D<140 nanometers) as a function of the distance to the road measured in the afternoons in Bodio (left figures) and San Vittore (right figures).

This leads to the hypothesis that there is a significant aerosol and carbon monoxide source in the village. Measurements in the village itself were a factor of 2-5 higher than the concentrations found close to the highway for those days. A likely emission source is wood burning that includes significant amounts of carbon monoxide and particles (e.g. Khalil and Rasmussen, 2003). Wood

burning is often used for heating in this Alpine valley.

The monitoring data of Roveredo (close to San Vittore) is used in the following to substantiate the importance of other sources than the traffic for the particulate pollution level in this area (Figure 7). At Roveredo, the NO_x concentrations were considerably enhanced during the tunnel shutdown as already shown in Figure 3. Right after the tunnel reopening, the concentrations were considerably lower because of very low traffic density between Christmas and New Year's Day. The PM10 concentrations were not significantly increased during the tunnel shutdown although diesel trucks are the major traffic source of NO_x and particulate matter. This observation is further evidence that for this region the traffic emissions are not responsible for most of the variance observed in the PM10 data. The PM10 concentrations seem to rather depend on the ambient temperature (Figure 7). At lower temperatures, more emissions due to residential heating occur. Temperature measurements at different altitudes along the valley slope showed that the inversion strength was not significantly correlated with the temperature so that more emissions rather than less mixing is the likely reason for the concentration increase in December. Between Christmas and New Year's Day, the PM10 concentrations are not at all dropping as the NO_x concentrations but are as high as in the week before. All these observations comprise more evidence that probably residential heating emissions are very important for the particulate pollutant levels in this area. At days with increased wind speeds and more vertical dilution, both NO_x and PM10 concentrations are usually substantially lower (Figure 7).

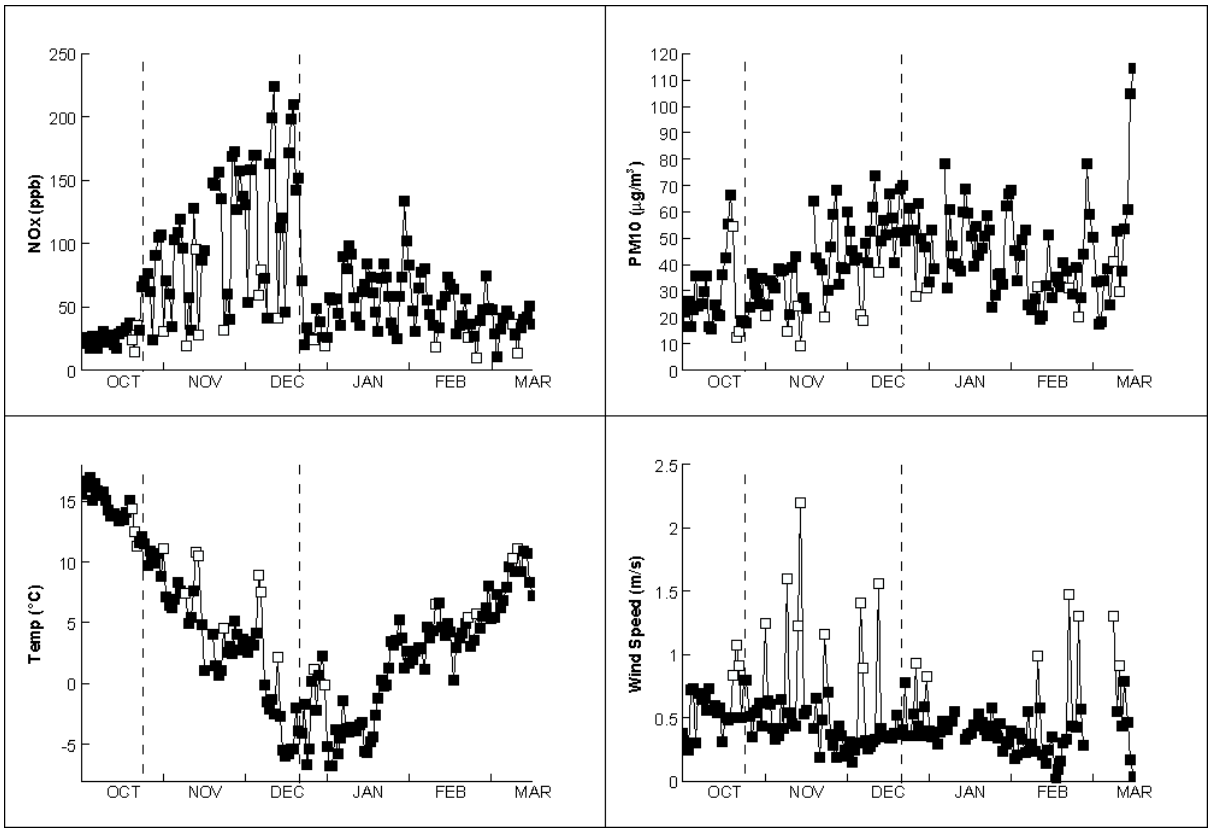

Figure 7: Daily averages of NO_x, PM10, temperature and wind speed in Roveredo at the San Bernardino route. The dashed vertical lines indicate the time period of the tunnel shutdown. The open rectangles indicate the days with windspeeds larger than 0.8 m/s.

Conclusions

The Gotthard road-tunnel shutdown led to considerably lower NO_x concentrations along the Gotthard route and higher NO_x concentrations along the San Bernardino route. Concerning aerosols, the analysis proved to be more complex. The traffic is the most important source of nanoparticles but the aerosol volume, active aerosol surface and aerosol mass seem to be influenced by other important emission sources, at least in the valleys along the San Bernardino route south of the Alpine ridge. There is some evidence that this emission source is residential heating by wood burning. The influence of these additional sources and the high background concentrations of PM10 render the precise analysis of the tunnel shutdown influence on the particulate concentration level difficult and the calculated changes are thus often not significant. One also needs to emphasize that finally the health impacts of the aerosols are decisive. The chemical composition of the aerosols of the different sources is significantly different and has likely different impacts on health. But not only the chemical composition, also the size of the aerosols might cause different effects. Epidemiological studies have mostly shown significant correlation of health impacts with particulate matter (Dockery et ali, 1993; Laden et ali, 2001), but other studies also indicate that the nanoparticles, which are negligible in mass, might have considerable effects as well (Donaldson et ali, 1998). Future concurrent measurements of wood burning tracers and traffic tracers could be used to better quantify the contributions of these emission sources to the particulate matter concentration levels in different regions (e.g. Khalil and Rasmussen, 2003).

Acknowledgements

We would like to thank the BUWAL and the Cantons Graubünden, Ticino, and Uri for the financial support of this study. We appreciated the good local support in Ticino during the campaigns. We also thank René Richter and Hans Meier for their patience while driving day after day on the same routes.

References

Bukowiecki, N., J. Dommen, A.S.H. Prévôt, R. Richter, E. Weingartner, & U. Baltensperger (2002): A mobile Pollutant Measurement Laboratory - Measuring Gas Phase and Aerosol Ambient Concentrations with High Spatial and Temporal Resolution, Atmos. Environ., 36, 5569-5579.

Dockery, D.W., C.A. Pope, X.P. Xu, J.D. Spengler, J.H. Ware, M.E. Fay, B.G. Ferris & F.E. Speizer (1993): An Association between Air-Pollution and Mortality in 6 United- States Cities, N. Engl. J. Med., 329, 1753-1759.

Donaldson, K., X.Y. Li & W. MacNee (1998): Ultrafine (nanometre) particle mediated lung injury, J. Aerosol. Sci., 29, 553-560.

Gerbig, C., S. Schmitgen, D. Kley, A. Volz-Thomas, K. Dewey & D. Haaks (1999): An improved fast-response vacuum-UV resonance fluorescence CO instrument, J. Geophys. Res., 104, 1699-1704.

Khalil, M.A.K. & R.A. Rasmussen (2003): Tracers of wood smoke, Atmos. Environ., 37, 1211-1222.

Laden, F., J. Schwartz, F.E. Speizer & D.W. Dockery (2001): Air pollution and mortality: A continued follow-up in the Harvard six cities study, Epidemiology, 12, 437.

12th International Symposium "Transport and Air Pollution" / 12e Colloque international "Transports et pollution de l'air", Avignon, 16 -18 *June* / juin 2003
proceedings / actes, n°92, tome / Vol. 1, Inrets ed., Arcueil, France, 2003, p. 105-112

Air pollution mapping: relationship between satellite- made observations and air quality parameters

Anthony Ung*, Lucien Wald*, Thierry Ranchin*, Christiane Weber, Jacky Hirsch**, Gilles Perron***, Joseph Kleinpeter*****
*Remote Sensing & Modelling Group, Ctre for Energy Studies, Ecole des Mines de Paris, B.P.207, 06904 Sophia Antipolis cedex, France - Fax +33 493 95 75 35 - email: Anthony.ung@ensmp.fr
** Lab. Image et Ville, Louis Pasteur University, Strasbourg, France
*** ASPA (Association pour la Surveillance et l'étude de la Pollution Atmosphérique en Alsace), Schiltigheim, France

Résumé
Les villes ne peuvent se permettre d'équiper tous les quartiers, les rues et les places d'un dispositif de surveillance de la qualité de l'air. Dans les articles précédents, nous avons présenté une méthodologie de densification du nombre de points de mesures permettant une nouvelle cartographie des concentrations des polluants. Une des étapes concerne l'établissement d'une loi d'estimation de la concentration des polluants par télédétection. Ce présent article traite des relations existants entre les mesures satellitaires et les mesures par les stations de surveillance. Des corrélations multidates sont calculées entre les réflectances mesurées par le satellite Landsat et les mesures, intégrées dans le temps, de concentrations de polluants. Les résultats montrent la possibilité d'estimer la pollution atmosphérique à l'aide des mesures satellitaires, non seulement dans les bandes spectrales du visible mais aussi celles dans l'infrarouge.
Mots-clefs : *télédétection, pollution de l'air, étalonnage, réflectance, corrélation.*

Abstract
The mapping of air quality over the city of Strasbourg and its vicinity requires an increase of the number of measurements aiming at spatializing information about air pollutants concentrations. A methodology based on a multisource approach for mapping air pollutants concentrations over the city was presented in previous communications. One step of the methodology is the estimation of pollutants concentrations by remote sensing techniques. This paper investigates the strength of linear relationship between satellite-made observations and air quality parameters. Multidate correlations were calculated between reflectances measured by Landsat satellite and measurements of the various pollutants. Those measurements are concentrations of pollutants on a daily average basis, or for the time of image acquisition, or on a basis of average of several hours before the image acquisition. The results add evidence on linear correlation between air quality parameters and satellite measurements not only in thermal infrared range but also in the infrared range.
Keys-words*: remote sensing, air pollution, radiometric calibration, reflectance, correlation.*

Introduction

Nowadays most large cities in Europe have acquired an air quality surveillance. Such a network is composed of a few static measuring stations, which allow a continuous surveillance of air pollution at the station locations. Pollution data are collected in near-real time and used to compute an air quality index (Garcia & Colosio, 2001) : the ATMO index. This index aims to inform local authorities, as well as the population, about air quality in the city. In answer to a high rate of pollution, public authorities are able to take restrictive measures on car traffic and on activities of some polluting companies.

However the real exposure of persons to ambient pollution cannot be estimated with the present network. The costs of a measuring station and its maintenance limit the knowledge to specific points of the town. Given the few measuring stations composing a standard air quality network, an accurate knowledge of the spatial distribution of the atmospheric pollutants over a city is currently impossible. To overcome this problem, a methodology based on a multisource approach for mapping pollutants concentrations over a city has been proposed by Ung *et al*. (2000, 2001). Sources related to air pollution and urban shapes and morphology are exploited to densify the number of potential stations for a mapping by interpolation. One step of the methodology is the estimation of pollutants concentrations at so-called pseudostations. In that case, this paper investigates the possibilities of satellite-made observations for mapping air quality. Some studies have been undertaken using such data. The first section offers a state-of-the-art summarizing the different studies and the results obtained. But such approaches were limited to the black particulates or sulphur dioxide pollutants. And they could not be applied to the studied area presented in the second section, due to the number of measuring stations. The problematic aspect is the establishment of mathematical relations between ground-based measurements of pollutants concentrations and satellite measurements. A multidate approach is presented through an intensive use of Landsat 5 imagery. Multidate satellite measurements are converted into reflectances as shown in the third section. Ground-based measurements of pollutants are concentrations of pollutants on a daily average basis, or for the time of image acquisition, or on a basis of average of several hours before the image acquisition. Multidate correlations were calculated between reflectances measured by Landsat satellite and various measurements of the pollutants.

1 – State-of-the-art

Only a few studies seek for a relationship between satellite data and ground-based measurements. They have been made on the correlation between satellite measurements in thermal infrared and air quality parameters (Finzi and Lechi 1991, Sifakis 1992, Poli *et al*. 1994, Brivio *et al*. 1995, Sifakis *et al*. 1998, Retalis *et al*. 1999, Wald & Baleynaud 1999, Basly 2000). These satellite data are radiances observed by the sensor in thermal infrared band(s). These radiances are a function of the temperature and emissivity of the surface and also of the optical properties of the atmospheric column above the pixel and its surroundings. Most of the bodies of interest have an emissivity larger than 0.8 (e.g. Gaussorgues 1989). In that case, for the spectral band of interest, the emission by the surface is the most important phenomenon. The radiance emitted by the atmosphere towards the sensor after its reflection on the surface accounts for approximately 10% of the total radiance and may be neglected. Accordingly in a first approximation the temperature T_{sat} observed by the space-borne sensor can be written:

$$T_{sat} = \tau \, e \, T_{surf} + T_{atm}$$

where T_{surf} is the surface temperature, e the surface emissivity, τ the transmission factor of the atmosphere, and T_{atm} a weighted-average temperature modelling the emission of the atmosphere itself. This equation should actually be written in radiances. However as long as a limited range of temperature is concerned, the Planck function can be approximated by a linear function and this equation holds. From this equation, it appears that a decrease in the atmospheric transmission factor as caused by the appearance of a pollution layer results in a decrease in T_{sat}. This decrease may be significant enough to be sensed by space-borne sensors such as Landsat TM, the sensitivity of which is 0.5 °C. This was experienced and discussed by Mc Lellan as early as 1973. Actually the change would also have an impact on the radiance emitted by the atmosphere (modelled by T_{atm}) but the impact is negligible in a first approximation because the pollution layer is usually of very limited vertical extension and T_{atm} results from an integration over the entire atmospheric column.

Table 1 (Basly 2000) summarizes all the linear correlation coefficients obtained for several cities between apparent temperatures and concentrations in particulates.

Studied area	Rome •	Naples •• 05/10/97	Naples •• 15/04/98	Naples •• 02/06/98	Nantes •• 20/05/92	Nantes •• 11/04/95	Nantes •• 27/01/00	Nantes •• 27/01/00
Number of values	5	4	6	6	12	10	3	3
Satellite channel	TM6	TM6	TM6	TM6	TM6	TM6	ETM6	ETM9
Pollutant	PTS	PTS	PTS	PTS	FN	FN	PM_{10}	PM_{10}
Concentration average ($\mu g/m^3$)	120,0	79,51	63,96	57,82	16,17	15,30	70,00	70,00
Correlation coefficient	-0,97	-0,87	-0,83	0,06	0,57	0,57	-1	-1
Confidence level %	99	87	96	9	95	91	100	100

Table 1: Correlation coefficients between the particulate measurements and the brightness temperatures measured in TM6. • : Poli et al. 1994. ••: Basly 2000.

Tableau 1 : Coefficients de corrélation entre les mesures de concentrations en particules et la température de surface TM6. • : Poli *et al.* 1994. ••: Basly 2000.

It brings out the high correlation between Landsat satellite measurements in thermal infrared band and air quality parameters for high concentration levels. Wald and Baleynaud (1999) discussed about the relationship between the suspended particulates (PM_{10}) measurements and the apparent temperature. Nevertheless if we assume that the pollution plays a major role in the pattern of temperature, two processes occur simultaneously which explain the relationship between the particulates measurements and the apparent temperature. The appearance of a pollution layer (more absorption and scattering) results in a decrease of the atmospheric transmission factor. On the one hand, this decay leads to a decrease of the solar radiation impinging on ground. The solar heating is thus decreased as well as the resulting temperature of the surface. Hence the emitted radiance is lower, and the signal sensed by the satellite is lower. On the other hand, this pollution layer absorbs as well the emitted radiance, causing a depletion of the upward radiance. This is the second process explaining the relationship. Both processes contribute to the decrease of the apparent temperature as the pollution increases. But the authors are aware of the limitations of the discussion, which is not a demonstration. The authors concluded that the mapping of the black particulates is possible using TM6 image but positive correlations are not explained yet.

On the contrary, the authors are partly conflict regarding sulphur dioxide (SO_2). Finzi and Lechi (1991) analysed two Landsat images of Milan. For the polluted day, the correlation coefficient is -0.84. For the unpolluted day, the correlation coefficient is very low (0.48). Even weaker correlation with SO_2 was observed by Brivio *et al*. (1995) for Milan. Poli *et al*. (1994) found weak and negative correlation for Roma. As for Brivio *et al*. (1995), Basly (2000) found no significant relationship except for one date, and stressed that the results depend on the number of values.

Those studies add evidence on the correlation between satellite measurements in thermal infrared and air quality parameters. It has been shown that particulates concentrations are correlated to apparent temperature. But the number of values is too small to be conclusive (Basly 2000). Though of limited extension the present study investigates multidate data allowing to increase the number of values and to measure changes in aerosols between several images of Landsat. Since this depletion of visibility is caused by scattering and not by gaseous absorption (Wald and Baleynaud 1999, Sifakis *et al*. 1992, Carnahan *et al*. 1984, Richards 1986) a major consequence is that the pollutants should affect visible and infrared bands and not only the thermal infrared band. Hence our study investigates whether pollutants can also be observed in these channels.

2 – Description of the area of interest

The city of Strasbourg is located in Eastern France at the border of Germany. A set of eight Landsat 5 Thematic Mapper (TM) quarter scene images was acquired on March 31, 1998, August 15, 1998, September 10, 1999, June 8, 2000, April 1, 2001, May 10, 2001, July 22, 2001 and August 14, 2001. Landsat TM images are acquired at 1030 mean solar time, in clear sky conditions. The Landsat TM sensor provides images with a 30 m pixel and seven spectral bands from the blue band TM1 to the thermal infrared spectral band TM6 (table 2). The thermal infrared band presents a spatial resolution of 120 m but interpolated to a pixel size of 30 m.

Channel	TM1	TM2	TM3	TM4	TM5	TM6	TM7
Wavelength (_m)	0,45 - 0,52	0,52 - 0,60	0,60 - 0,69	0,76 - 0,90	1,55 - 1,75	10,40 - 12,50	2,08 - 2,35
Spectral bands	Blue	Green	Red	Near IR	Midle IR	Thermal IR	Midle IR
spatial resolution	30	30	30	30	30	120	30

(from Landsat 4 Data Users Handbook, 1984, USGS)

Table 2: Landsat TM bands.

Tableau 2 : Les bandes spectrales du satellite Landsat TM.

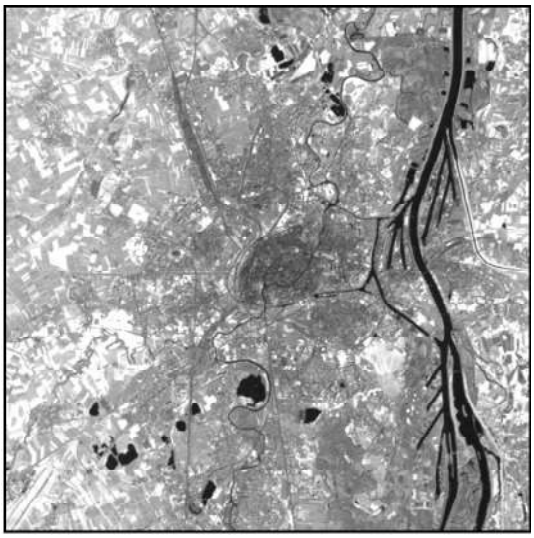

Figure 1 : Image de la ville de Strasbourg (Landsat TM4) du 31 mars 1998. © Eurimage

	SO2	NO2	NO	PM10	O3
31/03/1998	21	62	27	40	50
15/08/1998	17	39	4	27	88
10/09/1999	25	58	22	37	65
14/08/2001	14	56	25	36	80
22/07/2001	41	31	6	21	73
01/04/2001	12	48	24	28	57
08/06/2000	17	50	18	26	66
20/05/2001	12	44	23	33	71

Tableau 3 : Concentrations journalières de polluants pour les dates étudiées (en µg/m^3).

A sample of an image of the city of Strasbourg, acquired on 31 mars 1998, is presented in figure 1. The size is 15.36 km, with a pixel size of 30 m. The channel TM4 reveals the patterns of the streets and roads in the city (in dark tones). The airport is clearly seen in the South-West. Also appearing dark are the Rhin river and lakes. Light tones are mostly related to vegetation as several large parks are found in Strasbourg. The pollution data corresponding to the overpass of the satellite were acquired by the measuring network and archived by the ASPA team, the local organization in charge of the air quality measuring network in the city of Strasbourg and its vicinity. This network is composed of fourteen measuring stations in the city. The number of measuring stations per pollutant is about 6, which is too few to establish an accurate relationship. The measurements are concentrations of a pollutant every 15 minutes in near real-time. Table 3 shows that the pollution levels for the studied days were below critical levels.

3 – The processing of the Landsat data

The Landsat TM images are geometrically corrected and remapped to a same regular grid in a same

standard map projection. This is accomplished by constructing a mapping between pixel coordinates in the images and geographic coordinates on the BD TOPO® geographical database available over the area (Michel 2000, Veillet et Leconte 1995). Looking into the physics of the problem, a nearest-neighbour interpolation method is applied. This method does not modify the digital accounts of the images, so the representation of reality for measured radiances is conserved. This processing allows superimposition of Landsat images.

To allow comparisons of measurements of radiances, a radiometric calibration is then processed of concerting raw digital numbers observed by the TM sensors into physical units, except for the thermal band TM6. The radiometric calibration of the thermal band, is fundamentally different than the reflective bands as the instrument itself contributes a large part of the signal. The Landsat 5 TM was radiometrically calibrated prior to launch, and processing algorithms were developed that estimated detector gain based on the internal calibration lamp response. Even if the instrument were designed to maintain a constant bias level, the users may observe radiometric differences. Teillet *et al*. (2001) propose a lifetime radiometric calibration. According to the U.S. Geological Survey (USGS, 2003), the percentage difference observed in the gain between 1998 and 2002 didn't exceed 4%. We apply the resulting updated gains.

The radiance measured by the Landsat instrument at the top of the atmosphere is dependant of the solar irradiance at that level. To avoid variations of the radiance due to yearly variation of the solar irradiance one has to normalise the radiance measured by the satellite to reflectance. The values will then be comparable from one date to the other. This allows inter-date comparison of images. The obtained accuracy is just dependant on the calibration accuracy. The equation to be applied to each single pixel is the following :

$$r = \pi L / (I_0 \varepsilon \cos \theta_z)$$

$$r = \alpha L$$

with: r : reflectance at the top of the atmosphere
L : spectral calibrated radiance at the top of the atmosphere in $W/m^2/Sr/\mu m$
θ_z : solar zenith angle
I_0 : mean spectral solar irradiance at the top of the atmosphere in $W/m^2/\mu m$
ε : radius vector (ration of mean to actual sun-earth distance)
α : $\pi / (I_0 \varepsilon \cos \theta_z)$ conversion coefficients from radiance to reflectance in $Wm^2Sr\mu mW^{-1}$

canal	*31/03/1998*	*15/08/1998*	*10/09/1999*	*14/08/2001*	*22/07/2001*	*01/04/2001*	*08/06/2000*	*10/05/2001*
TM1	2,330	2,081	2,285	2,051	1,963	2,315	1,894	1,954
TM2	2,495	2,229	2,448	2,197	2,103	2,479	2,028	2,093
TM3	2,926	2,614	2,870	2,576	2,466	2,907	2,378	2,454
TM4	4,365	3,900	4,281	3,843	3,678	4,337	3,548	3,661
TM5	20,819	18,600	20,421	18,328	17,544	20,684	16,923	17,461
TM7	61,171	54,649	59,999	53,851	51,547	60,775	49,724	51,303

Table 4: Radiance - reflectance conversion coefficients for Landsat 5 images (10^{-3} $Wm^2Sr\mu mW^{-1}$).
Tableau 4 : Coefficients de conversion luminance - réflectance pour Landsat5 (10^{-3} $Wm^2Sr\mu mW^{-1}$).

Spectral solar irradiances are unique for each spectral band (Markham and Barker, 1985). The radius vector and solar zenith angle are given by the project SoDa Service (Integration and exploitation of networked Solar radiation Databases for environment monitoring, supported by the EC, DG-XIII "INFSO", IST-1999-12245, web site: http://www.soda-is.com/). Table 4 shows the calculated conversion coefficients α from radiance to reflectance for each date.

4 – Air quality parameters

Most studies, presented in the state-of-the art, deal with the daily averages of pollutants concentrations. But Landsat TM images are acquired at 1030 mean solar time (around 10h UTC) and can hardly contain information about the daily pollution.

For the 8 studied dates and for each pollutant, we calculate the average concentration between the time of satellite image acquisition (10h UTC) and several time before. This parameter represents an integrated concentration of a pollutant on a basis of average of several time before the image acquisition. Figure 2 illustrates the resulting parameters for suspended particulates pollutants (PM_{10}). The surveillance network for suspended particulates pollutant was composed of five measuring stations (Illkirch, Centre, Nord, Clemenceau, Est) on August 14, 2001. The first parameter at coordinates (x = 10 h, y = 35 µg/m^3) in figure 2 represents the concentration measurement by the station "Centre" at 10h UTC. And the parameter at coordinates (x = 8h, y = 47.4 µg/m^3) represents the average concentration between 10h UTC and 8h UTC.

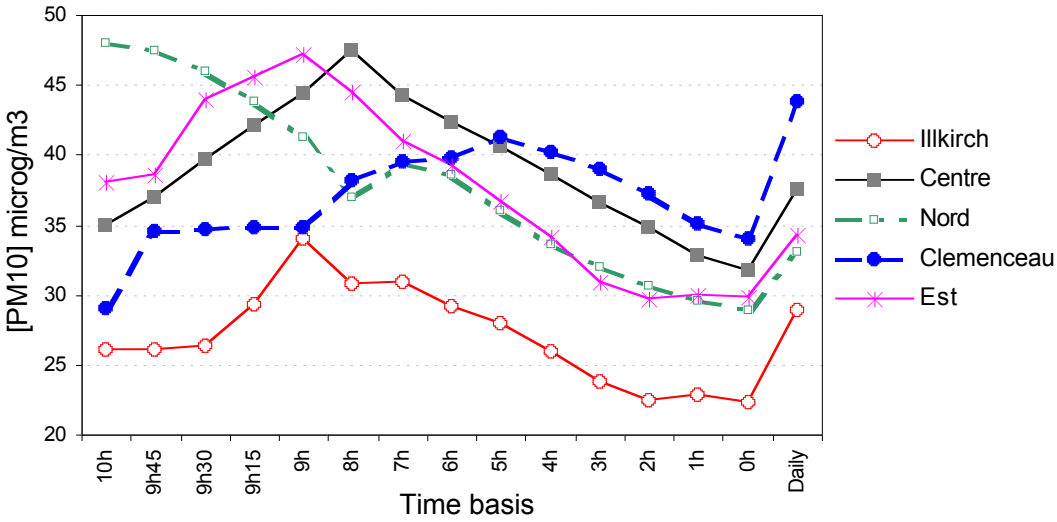

Figure 2: Average concentrations on a time basis for August 14, 2001. - the x-axis and y-axis refer to the time basis and the concentrations in particulates.

Figure 2 : Concentration moyennées sur une base de temps pour le 14 août 2001 – les axes x et y des ordonnées représentent la base de temps et les concentrations en particule.

5 – Comparison between air quality measurements and satellite observations

Locations of the fourteen measuring stations are reported onto a digital map of Strasbourg. This map is superimposed onto the Landsat images. The multidate radiances corresponding to the stations are extracted from the images for the 8 studied dates.

For each time basis and each pollutant, a linear correlation is calculated between integrated concentrations of the pollutant and reflectances of the measuring station places. Data from every dates are processed together. It results in an increase of the number of values for the correlation : 70 for SO_2, 56 for NO_2, 51 for NO, 33 for PM_{10} and 36 for O_3.

Analysis of the correlation coefficients reveals that the correlations between SO_2 and satellite data in all spectral bands are weak according to previous studies. It is likely that the concentration level of SO_2 is too low. For [NO_2], [NO], [PM_{10}] (primary pollutants), the sign of the correlation coefficients is negative according to previous studies. Figure 3 shows the correlation coefficients between suspended particulates concentrations PM_{10} and reflectances of the measuring stations places. An increase of those primary pollutants concentrations causes a depletion of the upward radiance measured in the visible and infrared spectral bands. Confidence levels are up to 95 %. Better correlation coefficients are observed for the three infrared spectral bands (TM4, TM5 and TM6). In the case of O_3 (secondary pollutant), the sign of the correlation coefficients is positive.

The results clearly indicate that the correlation coefficient depends on the time basis used for the average. Better levels of correlation are observed when using large time basis. When the time basis increases, the integrated concentration parameters better reflect the background pollution situations. It results that mapping background pollution by remote sensing is more accurate than a real-time

mapping by remote sensing. But the variation of correlation coefficients are not fully understand yet and might be related to the pollutants properties or emissions. For example, the abrupt decrease of correlation for PM_{10} occurs at 7 o'clock, when traffic pollution is high.

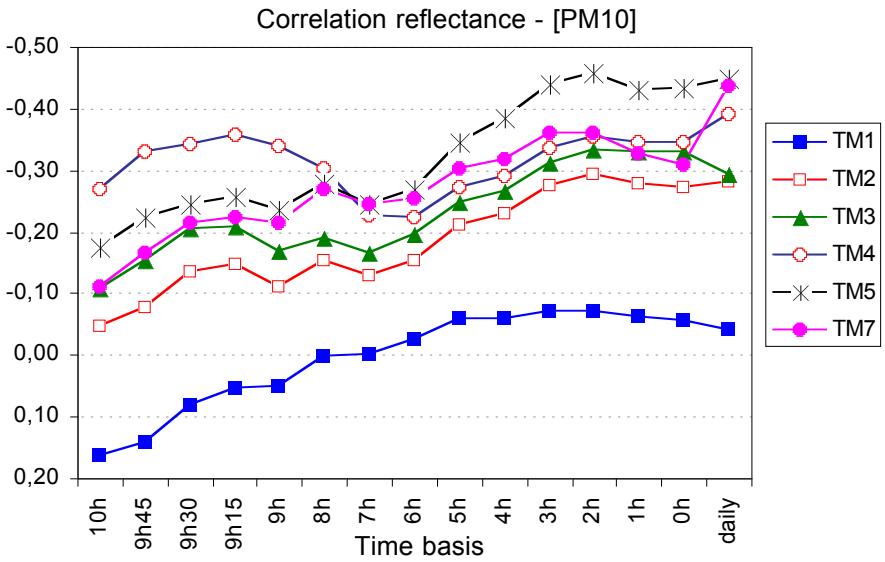

Figure 3: Linear correlation between integrated concentration of suspended particulates PM_{10} and reflectance derived from Landsat satellite- the x-axis and y-axis refer to the time basis and the correlation coefficients.

Figure 3 Corrélation linéaire entre les mesures intégrées dans le temps de concentrations de particules PM_{10} et les réflectances dérivées des mesures satellitaires – les axes x et y des ordonnées représentent respectivement la base de temps et les coefficients de corrélation.

Conclusion

This study adds evidence on the correlation between air quality parameters and satellite measurements in infrared range. The results demonstrate that satellite observations of upward radiance can be used to estimate the pollutant concentration levels, not only at the time of image acquisition but for an integrated time basis. The use of remotely sensed data for mapping of pollutant concentration in towns brings a better spatialization of the phenomena under study. Mapping background pollution by remote sensing is more accurate than a real-time mapping by remote sensing. Such results will be exploited for a better definition of virtual station presented in Ung et al. (2000, 2001). Further analysis related to the variation of correlations are needed to definitely assess its causes. And a relationship could be derived through a multi-regression analysis for example.

Acknowledgements

This project is supported by the French Ministry of Research through the research program Action Concertée Incitative Ville.

References

Basly L., 2000. Télédétection pour la qualité de l'air en milieu urbain. PhD thesis in « sciences de technologies de l'information et de la communication », University of Nice-Sophia Antipolis, France, 186 p.

Brivio P.A., G. Genovese, S. Massari, N. Mileo, G. Saura & E. Zilioli (1995) : Atmospheric pollution and satellite remotely sensed surface temperature in metropolitan areas. In EARSeL Advances in Remote Sensing 'pollution monitoring and geographical information systems', p 40-46, 2, avenue Rapp, Paris, France, 185 p.

Carnahan W.H., P.W. Mausel & G.P. Zhou (1984) : Evaluation of atmospheric particulate concentrations derived from analysis of ratio thematic mapper data. 10th Int. Symp. Machine Processing of Remotely Sensed data, p 235-243.

Finzi G. & G.M. Lechi (1991) : Landsat images of urban air pollution in stable meteorological conditions. Il Nuovo Cimento, 14C(5), p 433-443.

Garcia J. & Colosio J. (2001) : Les indices de qualité de l'air : élaboration, usages et comparaisons internationals. Collection - Sciences de la terre et de l'environnement. Presses de l'École des Mines, Paris, France, 120 pages.

Gaussorgues G. (1989) : La thermographie infrarouge. 3ème édition, Technique et Documentation Lavoisier, Paris, France, 560 p.

Le H.-Y. (1993) : An application of NOAA AVHRR thermal data to the study of urban heat islands. Atmospheric Environment, Part B, 27, 1, p 1-13.

McLellan A. (1973) : Remote sensing of atmospheric turbidity variations by satellite. J. Spacecrafts and Rockets, 10, 11, p 743-747.

Michel F. (2000). Le territoire vu du ciel. Pierre d'angle, 28, pp. 12- 19.

Poli U., F. Pignatoro, V. Rocchi & L. Bracco (1994) : Study of the heat island over the city of Rome from Landsat-TM satellite in relation with urban air pollution. In: Remote sensing - From research to operational applications in the new Europe, pp. 413-422, R. Vaughan Ed., Springer Hungarica, 442 p.

Retalis A., C. Cartalis and E. Athanassiou (1999) : Assesment of the distribution of aerosols in the area of Athens with the use of Landsat Thematic Mapper data. Int. J. Remote Sensing, 20, 5, p 939-945.

Richards J.A. (1986) : Remote sensing digital image analysis: an introduction, Ed. Springer-Verlag, Berlin-Heidelberg, Germany, 281 p.

Sifakis N. I., P. Bildgen & J.P. Gilg (1992) : Utilisation du canal 6 (thermique) de Thematic Mapper pour la localisation de nuages de pollution atmosphérique. Application à la région d'Athènes (Grèce). Pollution Atmosphérique, 34, 133, p 96-107.

Sifakis N., N.A. Soulakellis & D.K. Paronis (1998) : Quantitative mapping of air pollution density using Earth observations : a new processing method and application to an urban area. Int. J. Remote Sensing, 19, 17, p 3289-3300.

Teillet P.M., D.L. Helder, B.L. Markham, J.L. Barker, K.J. Thome, R. Morfitt, J.R. Schott & F.D. Palluconi (August 2001) : A lifetime radiometric calibration record for the Landsat Thematic Mapper. Proceedings of the 23rd Canadian Symposium on Remote Sensing, Ste. Foy, Quebec, August 20 - 24 , CASI , 2001 , p 17-25.

Ung A., L. Wald, T. Ranchin, C. Weber, J. Hirsch, G. Perron & J. Kleinpeter (2001) : Air pollution mapping over a city – virtual stations and morphological indicators. Proc. 10th Int. Symposium "Transport and Air Pollution", Colorado (CD-Rom), USA.

Ung A., T. Ranchin L. Wald, C. Weber, J. Hirsch, G. Perron & J. Kleinpeter (2002) : Air pollution mapping : a new approach based on remote sensing and geographical databases. Application to the city of Strasbourg. Photo-Interpretation 2000 / 3-4, 38, p 53-63.

USGC U.S. Geological Survey (2003). Technical Documentation (Landsat 5) : Landsat 5 TM Level 1 Product - Radiometry Status. http://landsat7.usgs.gov/documents/L5_radiometry.pdf .

Veillet I., Leconte G. (1995). Evaluer la qualité de la BD TOPO : l'approche de l'IGN. Bulletin de la S.F.P.T., n.137 (1995-1), pp.119-123.

Wald L. & J.M. Baleynaud (1999) : Observing air quality over the city of Nantes by means of Landsat thermal infrared data. Int. J. Remote Sensing, 20, 5, p 947-959.

12th International Symposium "Transport and Air Pollution" / 12e Colloque international "Transports et pollution de l'air", Avignon, 16 -18 *June* / juin 2003
proceedings / actes, n°92, tome / Vol. 1, Inrets ed., Arcueil, France, 2003, p. 113-120

Impact of EcoDriving on emissions

Håkan Johansson*, Pär Gustafsson*, Magnus Henke, Mattias Rosengren****
*Swedish National Road Administration, SE-781 87 Borlänge, Sweden –
Fax +46 243 750 89, email: hakan.johansson@vv.se
**AVL-MTC, P.O. Box 223, SE-136 23 Stockholm, Sweden

Abstract
This paper presents results from a study conducted between 2000 and 2002 by the Swedish National Road Administration, MTC and later also TFK to improve the knowledge of the impact the economical driving concept EcoDriving has on emissions. In the study 86 persons, half of these earlier trained in EcoDriving, drove on a route in real traffic with two instrumented cars. Driving patterns and fuel consumption were measured on road. Emissions were measured on dynamometer for complete cycles. The results show no significant differences in emissions between trained and untrained drivers except for CO2. Drivers trained in EcoDriving who in the enquiry stated that they regularly check their fuel consumption and therefore have a motivation for driving economically had lower fuel consumption compared to other trained and untrained drivers. This result shows that both training and motivation is needed to achieve low fuel consumption.
Keys-words*: ecodriving, ecodrive, driving style, emissions, fuel consumption*

Introduction

It has for long time been known that the driving style influence the fuel consumption. Some of the early recommendations how to drive economically are still valid but some have changed with engine technology. Above all it is the method how to accelerate and to decelerate that have changed. With older cars, that often had carburettors, acceleration should be done with throttle not as wide open as with modern cars with fuel injection. Modern cars with fuel injection also have fuel cut when braking via engine. An efficient deceleration with those cars should be done by engine braking on a high gear instead of disengaging the clutch, which often was most efficient for cars with carburettors. Other recommendations like planning the driving to avoid unnecessary stops are and will always be valid. Also the objective of economical driving style have changed from only fuel saving to also be an efficient measure to reduce the emissions of carbon dioxide.

In 1996 the Swedish National Road Administration (SNRA) started to work with economical driving style. At the end of 1998 the National Association of Swedish Driving Schools (STR) adopted the Finnish concept EcoDriving with support from SNRA and the Swedish National Energy Administration. From 1998 to 2002 13700 persons have been trained in EcoDriving in Sweden. Another 7200 have been trained in Heavy EcoDriving for HDV and buses. EcoDriving is the most common concept for economical driving styles in the Nordic countries. Another common concept in Europe is the Swiss concept ECO-DRIVE (Reinhardt, 1999) that later have been introduced and slightly adjusted in Netherlands in the New style driving concept (Wilbers, 1999).

The effects of EcoDriving and other concepts for economical driving style like New style driving on other emissions than carbon dioxide have until recently not been well known. Therefore in 1999 SNRA in collaboration with Rototest AB conducted a pre-study to improve the knowledge of the impact the economical driving concept EcoDriving has on the emissions. In the study a car with measurement equipment for driving style, a large number of engine parameters and position together

with an instantaneous emission model specially developed for the specific car was used during training of 16 students in EcoDriving. The results showed no significant differences in the emissions (except for CO2) between before and after training in EcoDriving (Johansson et.al., 1999). It was also shown that the recommendations of maximum half throttle and maximum 3000 rpm during acceleration are essential to keep the emissions at a low level. Somewhat later NOVEM in the Netherlands initiated a study conducted by TNO on the effects of New style driving on emissions (Gense, 2000). The results showed that the recommended 75 percent throttle level during acceleration caused higher emissions of carbon monoxide and hydrocarbons than normal driving. The recommendation was therefore changed to maximum 50 percent throttle during acceleration. A new study has later been conducted with the new recommendations that show no significant effects on the emissions (Burgwal and Gense, 2002).

To further improve the knowledge of EcoDriving and if possible to demonstrate statistically the impact on emission it was decided to follow up the pre-study by the present study.

1 – Trial design

Vehicles

In Sweden the total majority, about 95 percent, of the passenger cars are petrol-driven. The rest are diesel cars. The cars are also the largest and most powerful in EU. Two new common petrol-driven cars with manual transmission, one medium size car and one large were therefore chosen for the trial. The large car was a Volvo S80 2,4 l 125 kW and the medium size car was a Toyota Corolla 1,4 l 71 kW. Both were of model year 2000 but the Volvo met the Euro 4 standard and the Toyota Euro 3.

The cars were instrumented at MTC in Stockholm for measuring driving behaviour, gear position, fuel consumption, lambda and position on road. OBD signals were used for vehicle speed (from the ABS sensor), engine speed and mass flow. Throttle angle and brake use were measured from original sensor and contact respectively. Lambda was measured via an extra broadband lambda sensor. Position was measured with GPS. The data were collected in a data logger and sampled at 10 Hz except for GPS which was sampled at 1 Hz. Fuel consumption was calculated from mass flow and lambda and gear position from vehicle and engine speed.

Drivers

The idea of the trial was to compare emissions and fuel consumption from cars driven by EcoDrivers with cars driven by Normal drivers. Since EcoDriving was introduced in Sweden 1999 the number of people that had been trained in EcoDriving in the second half of 2000 was limited. Through contacts within the EcoDriving network in Sweden it was found out that Gothenburg with is surroundings had comparatively many EcoDrivers. These were contacted with the help of the EcoDriving instructors at the driving schools. The Normal drivers were collected from same or similar places of work through contacts with the employers. For example there were EcoDrivers from the local government in Gothenburg and Normal drivers from the local government in a suburb.

The persons that accepted to take part in the trial also had to answer an enquiry on their driving habits. Totally 109 persons accepted to take part in the study and of these 45 persons trained in EcoDriving and 45 Normal drivers were chosen. 45 EcoDrivers and 41 Normal drivers in the end drove the route. 57 of the drivers were men and 29 women. Both men and women were about equally distributed on EcoDrivers and Normal drivers. The drivers came from SNRA, local governments, a consulting firm and from driving schools (5 EcoDrivers and 5 Normal).

Route

The focus in the trial was the effects of EcoDriving on emissions on urban roads. The route should therefore include the most common road types in urban areas. If possible the percentage of the length of these road types on the route should reflect the percentage of traffic volume on these road

types in an average Swedish city.

Data for designing the route were taken from a study of driving patterns in urban areas in a Swedish city made in 1998 (Ericsson, 2000). In this 5 instrumented cars were lent to 30 randomly chosen car owners for two-week periods. The cars where equipped with instruments to log driving pattern, position and engine parameters. The GPS co-ordinates were matched to a digitised map of the road network of the city. A descriptive analysis was done on driving patterns on 21 road types. The percentage of driving on each road type was given, which is used in this study.

Gothenburg, which is the second largest city in Sweden, have some problems with congestion in central areas and on motorways at peak hours. To get as equal traffic situation as possible for all trips congestion during peak hours had to be avoided. The route was therefore located in a suburb of Gothenburg, Mölndal, where the impact of the traffic level was not so strong.

The driving on the route was conducted between 25 September and 6 October 2000. The route is described in table 1.

	Mölndal	Mölndal	Ericsson (2000)
Street type, speed limit	distance km	Share %	Share %
Motorway 90/110	5.1	25	23
Arterial 2/4 lanes 70	4.9	24	20
Arterial 2/4 lanes 50	4	20	15
Main CBD 2/4 lanes 50	0.3	1	1
Local CBD 2/4 lanes 30/50	0.3	1	1
Main industr. 2/4 lanes 50	0.8	4	7
Local industr. 2/4 lanes 50	0	0	3
Main resid. 4 lanes 50 and 70	0	0	4
Main resid. 2 lanes 50 and 70	2.9	14	12
Local resid. 2 lanes 50	2.2	11	15
Local resid. 2 lanes 30	0	0	1
Total	20.5	100	100

Table 1: Description of the route. The shares of the different street types are compared to the shares in the driving pattern study by Ericsson (2000) where 30 randomly chosen car owners borrowed instrumented cars for two-week periods.

Chassis dynamometer measurements

On total 86 trips were made on the route. Measurements of emissions and fuel consumption on chassis dynamometer were carried out at MTC in Stockholm for all the trips. Complete cycles without compression were used. The same vehicle that the actual trip was recorded for was also used on the chassis dynamometer. All tests were executed with hot engines only. Emissions of CO2, CO, HC and NOx were measured at 5 Hz. Fuel consumption were calculated using carbon balance.

The measurements on the chassis dynamometer cannot simulate topographical variations around the route. The route was therefore selected to minimise such variations.

2 – Results

Measurements on chassis dynamometer only exist for 73 trips due to measurement problems. Of these 3 outliers (1 EcoDriver and 2 Normal drivers) with large differences between fuel consumption on road and on chassis dynamometer have been excluded to get a more representative data material.

The Volvo is 33 percent heavier and has 76 percent more power than the Toyota. It is therefore likely that the effects of EcoDriving differ between the two cars. We therefore here choose to present the result separately for the Volvo and the Toyota. Another reason is that the shares of EcoDrivers not are the same for the two cars. It is then difficult to statistically compare EcoDrivers

with Normal drivers without grouping them into cars.

For the Volvo fuel consumption is available both on the route and on chassis dynamometer. There is a fairly good correlation between the fuel consumption on the route and on chassis dynamometer (r=0,86). This indicates that the test driver on chassis dynamometer succeeded in copying the driving behaviour of the drivers on the route.

The mean difference in fuel consumption between Normal drivers and EcoDrivers are statistical significant for the Volvo but not for the Toyota (table 2). The difference for the Volvo is about the size that we usually see from long-term follow-up of fuel consumption conducted on car fleets where EcoDriving have been implemented. For the emissions of NOx and HC there are, for both cars, only small and not significant differences between EcoDrivers and Normal drivers.

Volvo					
	Average speed (km/h)	Fuel dyna (l/10km)	Fuel road (l/10km)	HC (g/km)	NOx (g/km)
Mean Norm (N=10)	34±3	0.76±0.02	0.75±0.03	0.0011±0.0001	0.071±0.011
Mean Eco (N=22)	34±2	0.71±0.02	0.69±0.02	0.0011±0.0002	0.080±0.010
Mean difference (%)	1.2±8.9	-6.3±4.3	-8.1±4.7	4±25	13±22
T-test sign. lev	0.781	0.006	0.002	0.742	0.326
Toyota					
	Average speed (km/h)	Fuel dyna (l/10km)		HC (g/km)	NOx (g/km)
Mean Norm (N=24)	36±2	0.59±0.02		0.0066±0.0016	0.088±0.011
Mean Eco (N=14)	37±2	0.59±0.02		0.0057±0.0021	0.096±0.019
Mean difference (%)	2.8±7.1	-1.2±4.1		-14±46	9±21
T-test sign. lev.	0.44	0.56		0.50	0.45

Table 2: Emissions and fuel consumption for the trips on the route. For the Volvo fuel consumption was available both on the route and on chassis dynamometer. In the table the 95% confidence interval is given for means and differences. Independent samples T-test has been used to investigate if there are any significant differences between the means for Normal drivers and EcoDrivers. If $p<0.05$ there is a significant difference.

3 – Discussion

Why is it then no difference in fuel consumption between Normal drivers and EcoDrivers for the Toyota?

Below we investigate the reasons for the lack of difference in fuel consumption for the Toyota more in detail. We first start with exploring what driving behaviour parameters that influence the fuel consumption and emissions. We could of course use the instructions for EcoDriving directly but they would not be car specific.

To get the driving pattern parameters that are important for fuel consumption and emissions we do a correlation analysis. In this analysis we do not split the trips between EcoDrivers and Normal drivers but only between the cars.

From table 3 we can see that to keep low fuel consumption for the Volvo it is important to avoid unnecessary stops, keep a low deceleration level, drive as little as possible on first and second gear and as much as possible on fifth gear and also to jump over gears when possible. To get low emissions of NOx, driving on forth gear should also be avoided, probably the fifth gear should be used instead. For the Toyota almost the same is true for fuel consumption as for the Volvo. The average deceleration level and driving on second gear does not seem to be that important and instead of numbers of gear changes where gears have been jumped over the number of gear changes are most important. To keep the emissions of HC low for the Toyota strong accelerations with more

than 50 percent throttle and engine speeds above 3000 rpm should be avoided.

	Volvo				Toyota		
	Fuel dyna.	Fuel road	HC	NOx	Fuel dyna.	HC	NOx
Average speed (km/h)	(-0.321)	-0.463**			-0.395*		
Number stops	0.482**	0.538**			0.615**		
Average acc (m/s2)						0.442**	
Average dec (m/s2)	0.690**	0.720**					
Brake dist (%)							
Fuel cut dist (%)		0.377*					
F.cut/(brake+f.cut) dist (%)							
Gear 1 dist (%)	0.682**	0.687**			0.618**		
Gear 2 dist (%)	0.548*	0.691**		0.387*			
Gear 3 dist (%)							
Gear 4 dist (%)				0.432*			
Gear 5 dist (%)	-0.556**	-0.649**		-0.449*	-0.426**		
Gear ch. over jump (%)	(-0.325)	-0.349*					
Number gear ch.					0.647**		
>3000 rpm time %						0.388*	
Throttle pedal > 50% time %						0.505**	

*Table 3: Correlation (Pearson) between driving behaviour parameters, fuel consumption and emission. Only statistical significant correlations are included. ** means that correlation is significant at the 0.01 level (2-tailed). * means that correlation is significant at the 0.05 level. Within brackets means that correlations is nearly significant at 0.05-0.10 level. Modern cars have fuel cut during engine braking when engine speeds are above 1300 to 1500 rpm. This is something that is taking advantage of in EcoDriving.*

We now know the driving behaviour parameters that have influence on the fuel consumption and emissions. Most of these parameters are also included in the EcoDriving instructions. The question is now if the size of these parameters differs between the EcoDrivers and the Normal drivers.

In table 4 significant differences between EcoDrivers and Normal drivers are given for the driving behaviour parameters in table 3.

For the Volvo there are significant differences between EcoDrivers and Normal drivers for driving on the first, third and fifth gear and gear change over jump. There are also nearly significant differences for average deceleration and brake distance. All the differences of the parameters have a sign that gives lower fuel consumption. If we compare this with table 3 we can see that for the parameters identified as important for fuel consumption for the Volvo there are significant or nearly significant differences between EcoDrivers and Normal drivers for most of these. Of the parameters identified as important it is only the number of stops (and average speed) and fuel cut distance that there are no significant differences for.

For the Toyota there are significant differences between EcoDrivers and Normal drivers for distance with fuel cut (and fuel cut/(brake+fuel cut)) and gear change over jump. There are also nearly significant differences for driving at the second gear and gear change over jump. These parameters were not identified as significant for fuel consumption in table 3. They are however included in the EcoDriving instructions. For the parameters identified as significant for fuel consumption in table 3 there were no significant differences between EcoDrivers and Normal drivers for the Toyota.

		Volvo			Toyota	

	Mean Norm	Mean perc differ	Sig. (2-tailed)	Mean Norm	Mean perc differ	Sig. (2-tailed)
Average speed (km/h)	34±3		0.33	36±2		0.44
Number stops	10±4		0.94	10±3		0.53
Average acc (m/s2)	0.74±0.05		0.91	0.92±0.02		0.48
Average dec (m/s2)	0.75±0.03	-6.3%	0.009	0.91±0.02		0.23
Brake dist (%)	11±2	(-25%)	0.08	6.5±1.1		0.23
Fuel cut dist (%)	10±1		0.70	7.2±1.0	41%	0.001
F.cut/(brake+f.cut) dist (%)	47±7		0.16	55±7	20%	0.05
Gear 1 dist (%)	3.3±1.0	-42%	0.02	2.1±0.5		0.29
Gear 2 dist (%)	23±4		0.16	17±2	(27%)	0.07
Gear 3 dist (%)	22±5	-29%	0.01	26±2		0.13
Gear 4 dist (%)	20±4		0.63	14±3		0.26
Gear 5 dist (%)	30±9	47%	0.02	36±4		0.14
Gear ch. over jump (%)	4.4±4.4	372%	0.0002	6.3±3.0	159%	0.0001
Number gear ch.	96±7		0.79	78±6	(-12%)	0.06
>3000 rpm time %	0.23±0.18		0.85	0.25±0.15		0.58
Throttle pedal > 50% time %	0.15±0.19		0.79	0.25±0.16		0.25

Table 4: Driving pattern caracteristics for Normal drivers (means and 95 % confidence intervals) and statistical significant differences between Normal drivers and EcoDrivers (in %). Independent samples T-test has been used to investigate if differences in means are statistical significant. $p<0.05$ is a significant difference and $0.05<p<0.1$ a nearly significant difference. Parameters with statistical significant differences should be compared with the parameters that have been identified as important for fuel consumption and emissions in table 3.

We can then partly answer the question stated above. The reason for no differences in fuel consumption between EcoDrivers and Normal drivers for the Toyota is that there are no significant differences in the driving behaviour parameters significant for fuel consumption. This gives of course a new question. Why are there no significant differences in these driving pattern parameters? These are parameters that the EcoDrivers have knowledge on how to handle to keep low fuel consumption. Again there are different possible answers. First is that the Normal drivers actually performs quite well EcoDriving without having a training because the car encourage this kind of driving. One reason for this is that the interior noise from the engine is probably higher in the Toyota than in the premium class Volvo. This could encourage use of high gears to avoid high engine noise. Also the gear ratio differs between the Toyota and the Volvo. Another reason could be that the EcoDrivers were not fresh from their training, for some of them more than a year had gone since their training. Some of them may therefore have forgotten or not felt motivated to perform important parts of the EcoDriving. This should also influence the results for the Volvo.

In table 5 we investigate if there is any connection between answers and statements in the enquiry and fuel consumption, emissions and driving behaviour. A number of different questions have been analysed but here we only report the four most interesting. First is the gender of the drivers. Second is a question if they follow-up their fuel consumption regularly when they fill up or by the trip computer. The follow-up gives a feed back to the driver on how economically he or she drives and therefore could be a source of motivation. Third is the drivers' own interpretation if they drive economically. Fourth is a test of knowledge, where the drivers had to chose which 3 parameters of 8 that had the largest effect on fuel consumption. Only those who picked the three right parameters are here selected as persons with knowledge.

	Volvo	Toyota

	Normal	Eco.	Normal	Eco.
Fuel dyna.	(B-)	M-, F-, (K-)		
Fuel road		M-, (F-, B-, K-)		
HC	(M+)			
NOx	(M+)			
Average Speed		(M+, F+, K+)		
Number stops		B-, (F-, K-)		
Average acc		(B+)		
Average dec		(K-)	(K-)	
Gear 1 dist		(M-)		
Gear 2 dist		M-		
Gear 3 dist		(M+)		
Gear 4 dist				(M+)
Gear 5 dist				
Gear ch. over jump			B+, (M+)	

Table 5: Connection between answers in the enquiry, driving behaviour, fuel consumption and emissions. Significances have been tested for the same parameters as in table 2-4, but only those found significant are reported here. M = men relative to women, F = follow-up fuel consumption regularly relative to not, B = believe that they drive economical relative to not believe, K = knowledge on parameters what parameters that have the largest effect on fuel consumption relative to not knowing them so well. The signs indicate if the attribute influences the parameters negative or positive. Letters within brackets mean either that there are only a few observations or that that it is only nearly significant at the 0.05-0.10 level.

The results in table 5 shows that EcoDrivers who follow-up their fuel consumption regularly has lower fuel consumption than those who does not. The results also indicate that men drive more economically than women. This could maybe be a result of that they follow-up their fuel consumption more regularly than women. The knowledge is interesting, only 2 of the 22 EcoDrivers that drove the Volvo failed to pick the 3 correct parameters. These individuals also had the highest respectively the second to the fourth highest fuel consumption (depending on looking at dynamometer or road fuel consumption).

Conclusions

For the two tested vehicles in this study EcoDriving has no significant effect on the emissions of NOx and HC. Together with the results from the pre-study and results from the TNO studies it is likely that these results are valid for modern petrol cars in general.

For the large car tested here, a Volvo S80, EcoDrivers had 8 percent lower fuel consumption than Normal drivers. For the medium size car tested here, a Toyota Corolla, there was no significant difference in fuel consumption between EcoDrivers and Normal drivers. The size of fuel consumption important driving pattern parameters did not significantly differ between EcoDrivers and Normal drivers for this car. One reason could bee that the car it self encourage EcoDriving behaviour so that also Normal drivers for example chose high gears. The differences between their driving behaviour and EcoDrivers then become less. Another reason could be lack of motivation to drive economically. Motivation has here showed to have significant effect on EcoDrivers fuel consumption.

For the fuel consumption there however exists much more extensive data material from long-term follow-up of fuel consumption in car fleets where EcoDriving have been implemented. An analysis of these data will give a better figure for the actual effects of EcoDriving on fuel consumption.

Acknowledgements

The authors wish to thank Jörgen Ryding and Kajsa Holm at the Swedish National Road Administration Western Region who carried out the recruiting of the drivers.

References

van de Burgwal H.C. and Gense N.L.J. (2002) Interpretation of driving style tips, Application of the major driving style tips of 'New Style Driving' by passenger car drivers and the effects on fuel consumption and tail pipe emissions, TNO report 02.OR.VM.004.1/HVDB, Delft, The Netherlands, 51 p. + append.

Ericsson E. (2000) : Driving pattern in urban areas – descriptive analysis and initial prediction model Bulentin 185, Department of technology and society, Lund University, Sweden, 59 p. + append.

Gense N.L.J. (2000) Driving style, fuel consumption and tail pipe emissions, final report, TNO report 00.OR.VM.021.1/NG, Delft, The Netherlands 52 p.

Johansson H., Färnlund J and Engström C. Impact of EcoDriving on emissions and fuel consumption, a pre-study, Swedish National Road Administration report 1999:165E, Sweden 35 p. http://www.vv.se/publ_blank/bokhylla/miljo/ecodrive/ecodrive_e.pdf

Reinhardt E. (1999) Improving Fuel Efficiency in Road Transport/Eco-Drive™ in Switzerland – A success story of Energy 2000, Proceedings of ECODRIVE The Conference, Graz Austria 990916-990917

Wilbers P. (1999) The New Driving Force: A New Approach to Promote Energy-efficient Purchasing and Driving Behaviour, Proceedings of ECODRIVE The Conference, Graz Austria 990916-990917

12th International Symposium "Transport and Air Pollution" / 12e Colloque international "Transports et pollution de l'air", Avignon, 16 -18 *June* / juin 2003
proceedings / actes, n°92, tome / Vol. 1, Inrets ed., Arcueil, France, 2003, p. 121-128

Measurements and analysis of real-world driving behavior of urban buses

Leonid Tartakovsky*, Yoram Zvirin*, Michael Motzkau, Martine Van Poppel***, Iddo Riemersma****, Mark Veinblat*, Vladimir Baybikov*, Yuri Aleinikov* & Marcel Gutman***
*Technion – Israel Institute of Technology, Technion City, 32000 Haifa, Israel
Fax +972 4 83 24 533 - email: meryzlt@tx.technion.ac.il
**Institute for Vehicle Technology (RWTUV), Adlerstrasse 7, D-4300 Essen 13, Germany
***Flemish Institute for Technological Research (VITO), Boeretang 200, 2400 Mol, Belgium
****TNO Automotive, PO Box 6033, 2600 JA Delft, the Netherlands

Abstract
The present paper contains an analysis of driving behavior measurements of urban buses. The following parameters were measured and logged on a second-by-second basis: engine torque and speed, bus velocity, road gradient, number of passengers in the bus, coolant and oil temperatures and on/off switching of the air conditioning system. For part of the experiments, exhaust gas temperature and braking system activation were also recorded at the same frequency. Average driving behavior parameters, such as maximal and average bus velocities, accelerations, decelerations, relative time of stops, etc., were derived for various bus routes, as well as for available driving cycles, and an appropriate comparative analysis was performed. Based on the gained data, the effects of road gradient and air conditioning operation on engine power demand were evaluated.
Keys-words*: urban bus, driving behavior, power demand, road gradient, air conditioning.*

Introduction

Vehicle driving patterns have been studied worldwide for decades and serve for the development of various driving cycles, which are used for a great variety of purposes: from quantifying vehicle emissions and energy consumption at different levels to assessment of new vehicle technologies, Andre (1996). Driving patterns can be described by many parameters. Andre (1996) performed a comprehensive analysis and suggested parameters most extensively used for characterization of vehicle driving cycles. These are: duration; average duration of running periods; idle period; number of stops per kilometer; average speed; running speed; positive kinetic energy; average values of accelerations and decelerations; standard deviation of acceleration; number of acceleration-deceleration shifts; relative distributions of speeds, accelerations; joint distributions of speeds and accelerations.

Most driving patterns studies that have been performed are focused on the research of real world driving behavior of cars, Andre (1996), Esteves-Booth et al. (2001), Ericsson (2001). Compared to passenger cars, relatively few studies of driving behavior of heavy-duty vehicles, and in particular urban buses, have been carried out, Andre (1996). The most comprehensive European works, which dealt with a development of driving cycles for urban buses in various traffic situations, were carried out by Steven (1995) and van de Weijer et al. (1993 and 1997).

Following the recommendations of the COST 319 Action (1999), further research on driving behavior of heavy-duty vehicles "with extensive measurement campaigns of all vehicle types and usages" is needed, in order to close existing gaps in knowledge. It is noted in the COST 319 Action that measurement of driving behavior in different countries is of high priority, in order to have a

good geographical representation of driving behavior data. Part of the objectives of the on-going ARTEMIS project and COST 346 Action are to address the above-mentioned challenges.

1 - Objectives

A main objective of this work, which was carried out in the framework of the ARTEMIS project and the COST 346 Action, under the financial support of European Commission, was to check the possibility of using available driving cycles for the calculation of bus emissions in countries of the Mediterranean region. For this reason, measurements of real-world driving behavior of urban buses in Israel were performed and compared with gained data from Western Europe. Taking into account this region's typical climatic and topographical conditions, as well as the strong effect of air conditioning (AC) and road gradients on emissions, effects of these factors on power demand and average fuel consumption were also assessed.

2 - Methodology

Measurements of real-world driving behavior of urban buses were carried out in two Israeli cities: Haifa (over 270 thousands inhabitants) and Netania (about 165 thousands inhabitants). These cities were selected as typical average Mediterranean cities, differing mainly by their topography: hilly in Haifa with road gradients up to 16% compared to flat in Netania. Measurements were performed over about 30 various bus routes, which were classified using a method developed by INRETS, Andre & Villanova (2002). Table 1 presents some results of this characterization, with the routes that were selected together with the bus operator (Egged) as representing a wide variety of urban driving patterns. It is noted that the classification, which was performed, is rather approximate, because the required data on population and employment distributions over the routes tested were not completely available.

Route #	Length	Speed (average over a week)	Number of departures at rush hours	Average number of departures	Number of bus stops	Geograph. Area*	Class	Notes
	km	km/h	/hour	/hour	/km			
1a	14.4	16.3	4	3	2.6	9 ~ 20% 10 ~ 40% 11 ~ 30% other ~ 10%	5	ring
1b	18.0	18.9	4	3	2.3			
2a	33.4	19.1	6	4	2.5	9 ~ 30% 11 ~ 60% other ~ 10%	1	long segments with road gradients
2b	27.7	15.6	7	4	3.0			
3	5.0	11.1	3	2	3.4	11	5	ring
4a	15.1	23.9	15	7	1.9	8 ~ 45% 9 ~ 45% other ~ 10%	4	connects main bus terminals
4b	15.6	21.3	12	7	1.8			
5	12.0	20.0	13	7	1.4	1 ~ 30% 4 ~ 50% 11 ~ 20%	3	Netania, ring

* The percentages mean a relative part of the total route distance that was traveled by the bus in the specific geographical area, as classified by Andre & Villanova (2002): 1 - low population; 4 - isolated mixed housing; 8 - main roads, high traffic; 9 primary roads, high traffic and population; 10 - concentrated mixed housing; 11 - concentrated collective housing, high population and employment.

Table 1: Characteristics of representative Israeli urban bus routes, based on data of the bus operator.

As may be seen from Table 1, bus routes that were studied are run at rather different conditions, both geographical and operational, e.g. route 3 is run only in city center through areas with concentrated group housing compared to routes 4, which connect between main bus terminals in Haifa and are operated mainly on main and primary roads, with much higher average speeds.

The Israeli bus fleet is mainly composed of popular European makes (Mercedes, MAN and Volvo).

A Mercedes O-405 model was selected as a typical urban bus and instrumented for the experiments. The bus was driven by different drivers chosen by the bus operator according to its standard routine. No driving instructions were used. The following parameters were measured, logged and processed on a second-by-second basis: engine torque and speed, bus velocity, road gradient, number of passengers, coolant and oil temperatures, and on/off switching of the AC system. For part of the experiments, exhaust gas temperature and braking system activation were also recorded at the same frequency. Measurements of engine and bus speeds, coolant temperature and activation of bus AC & braking systems were performed by connection to appropriate on-board signals. The exhaust gas temperature was measured at about 0.5 m downstream of the turbocharger outlet. Counting of the passengers number was allowed by access to the database of a special counting system, installed by the bus operator. For measurements of road gradient a special device was developed.

Measurements of engine torque were based on recording of instantaneous position of the fuel injection pump lever, using an on-board available position sensor. The input data required for engine torque calculation are: full load torque curve as function of the engine speed; test bench results of torque and corresponding fuel injection pump lever position for a number of different operation modes. Alternatively, test results over ECE R49 or ESC cycles (torque and corresponding fuel consumption) may be used, if bench-testing the engine that will be instrumented is not available. However, this method will result in a less accurate engine torque signal. Also required are the on-board logged data of engine speed, injection pump lever position and on/off switching of the AC system, which are measured with a frequency of at least 1Hz during real-world bus driving. Two different calculation methods were developed. One for idle and traction operation modes (zero and positive torque values) and another for non-traction modes (negative torque values, also referred to as 'motoring'). Detailed description of this methodology will be presented in a separate publication. Our calculations were based on ECE R49 official approval test results of the OM-447hA diesel engine, because testing the engine, which was instrumented for driving behavior measurements, was impossible. For each operation mode the relative fuel consumption was assumed equal to the relative position of the injection pump lever, and this assumption was validated experimentally by bench tests.

For estimation of the AC system power demand, the mechanical power consumed by the engine-driven compressor and the electric power consumed by fans were taken into account. Power consumed by engine-driven compressor, as function of the engine speed, was estimated based on the appropriate manufacturer's performance for the condenser and evaporator temperatures of 55 ºC and 5 ºC, respectively. These assumptions are justified because day-to-day variations of ambient temperatures during Israeli summer are usually low. Power consumed from the engine for operation of fans was evaluated by measurements of current and voltage supplied to the fans and based on the hot alternator efficiency performance (as function of the engine speed), as was supplied by the alternator manufacturer. Three basic modes of power consumption were defined for the case when the AC system is switched-on: power consumed from the engine is zero if the engine runs in the motoring mode; power consumed from the engine is equal to the measured engine's power if the latter is less than or equal to the AC power demand; power consumed from the engine is equal to the AC power demand if the latter is less than the measured engine's power.

3 – Results and analysis

Results with main parameters of bus driving patterns, as were measured in Israel, and data recorded by VITO in Belgium with its on-board system VOEM(Low), Pelkmans et al. (2001), Van Poppel (2003), ARTEMIS project, are presented in Table 2. These data are compared with the parameters of some available European bus driving cycles developed by Steven (1995) and van de Weijer et al (1993), which were kindly supplied by the ARTEMIS partners from TNO, TUG and RWTUEV. The TNO approach suggested by van de Weijer (1997) was used for the calculation of driving pattern/cycle parameters. For the Israeli driving patterns, parameters of each measured run were calculated and their averages for various bus routes are presented in Table 2.

Cycle parameters	Perc. Stop Time [%]	Avg. Speed [km/hr]	Avg. Running Speed [km/hr]	Avg. acceleration [m/s2] Acc > 0.06	Max. acceleration [m/s2]	Perc. accelerating [%] Acc > 0.06	Avg. deceleration [m/s2] Acc < - 0.06	Max. deceleration [m/s2]	Perc. decelerating [%] Acc < -0.06	Perc. cruising [%]	Estimated perc. no brake [%]	RPA [m/s2] Relative Positive Acceleration	PKE [m/s2] Positive Kinetic Energy
DUBC	22.56	20.96	28.29	0.57	1.69	40.00	-0.69	-2.28	33.10	4.33	74.89	0.26	0.53
Braunschweig	22.01	22.50	30.13	0.55	2.13	37.99	-0.74	-3.11	28.62	11.38	79.54	0.21	0.44
Munich L661	25.49	17.54	24.70	0.6	1.65	33.29	-0.60	-2.16	33.43	7.80	77.86	0.24	0.49
9040	19.63	15.62	20.13	0.47	1.37	37.26	-0.48	-1.57	36.51	6.60	72.85	0.21	0.42
10040	18.75	21.46	27.29	0.45	1.34	38.72	-0.51	-1.65	34.61	7.93	77.39	0.19	0.38
11240up	4.57	27.66	29.67	0.37	1.32	46.14	-0.55	-2.32	31.50	17.80	80.16	0.14	0.28
11440down	9.54	30.97	35.65	0.63	1.85	43.34	-0.70	-2.15	38.77	8.35	72.56	0.24	0.48
Stuttgart	32.79	15.88	25.08	0.71	2.36	30.10	-0.66	-1.67	32.24	4.87	72.47	0.27	0.55
Munich L66	23.85	18.83	25.90	0.57	1.66	35.38	-0.63	-2.45	32.31	8.46	78.33	0.23	0.47
VITO 1A	4.39	18.64	20.01	0.43	1.54	45.70	-0.53	-2.07	36.40	13.52	76.78	0.19	0.39
VITO 1B	2.56	21.19	22.31	0.48	1.35	48.40	-0.59	-2.34	39.57	9.47	72.46	0.23	0.47
VITO 2	5.12	24.25	26.44	0.57	1.62	50.41	-0.76	-2.51	38.37	6.10	68.31	0.29	0.58
Pelkmans (2001)	21	17.9	22.8	0.62	1.32	39	-0.72	-1.88	33	7	N/A	0.28	N/A
Route 1a-1b	31.08	17.18	25.15	0.65	2.02	39.15	-0.75	-2.94	35.18	5.42	85.24	0.29	0.61
Route2a down	27.47	19.57	28.50	0.71	2.5	37.10	-0.83	-3.01	31.75	3.68	74.37	0.34	0.72
Route 2b-up	19.49	24.75	32.06	0.63	2.45	40.05	-0.72	-2.52	35.32	5.14	73.64	0.26	0.53
Route 3	36.10	9.58	15.90	0.56	1.97	30.65	-0.61	-2.16	28.51	4.74	78.61	0.25	0.54
Route 4a-4b	29.62	21.60	31.21	0.54	1.67	35.01	-0.63	-2.43	30.09	5.27	78.32	0.24	0.51
Route 5	24.79	21.97	30.59	0.67	1.98	37.87	-0.78	-2.61	32.56	4.77	74.52	0.28	0.58

Table 2: Main parameters of tested bus driving patterns compared to available driving cycles. In this table: DUBC – Dutch Urban Bus Cycle; 9040 – Handbook urban cycle, short stop distance; 10040 - Handbook urban cycle, long stop distance; N/A – not available.

$$PKE=\frac{\Sigma(V_{next}^2-V^2)}{distance} \text{ for } (V_{next}-V)>0 \quad RPA=\frac{\frac{1}{T}\int_0^T\left(V_i\cdot a_i^+\right)dt}{\bar{V}}=\frac{\int_0^T\left(V_i\cdot a_i^+\right)dt}{distance}$$

Comparison of driving patterns

Comparison of measured driving patterns with available driving cycles (see Table 2) shows that these cycles cover almost the whole range of traffic situations and measured driving patterns. Driving cycles that show better resemblance to the measured driving behavior of buses in Israel are: Dutch Urban Bus Cycle, both Munich and Stuttgart driving cycles – see Table 2 and example in Figure 1. It is noted that there is no available driving cycle, which could describe suitably a congested city center bus driving pattern, as was measured on route 3 – see Tables 1, 2. Driving patterns, as measured by VITO in Turnhout (city with about 40 thousands inhabitants), are described better by the Swiss-German Handbook driving cycles 9040 and 10040 – see example in Figure 1.

From a comparison of the Belgian (Turnhout) and Israeli bus driving patterns, the following observations can be made: much higher percentage of stop time 19.5 – 36.1% in Israel compared to only 2.6 – 5.1% in Belgium was measured, together with lower levels of average (0.43-0.57 compared to 0.54-0.71) and maximal (1.35-1.62 compared to 1.67-2.50) accelerations, and higher percentage of cruising (6.1-13.5% compared to 3.7-5.4%) in Belgian driving patterns. The driving pattern measured by Pelkmans et al. (2001) in Brussels – city with 950000 inhabitants (see Table 2), is closer to the Israeli measurements, but also here lower maximal acceleration/deceleration values and higher percentage of cruising were observed. The above-mentioned numbers illustrate the more aggressive driving style of Israeli bus drivers.

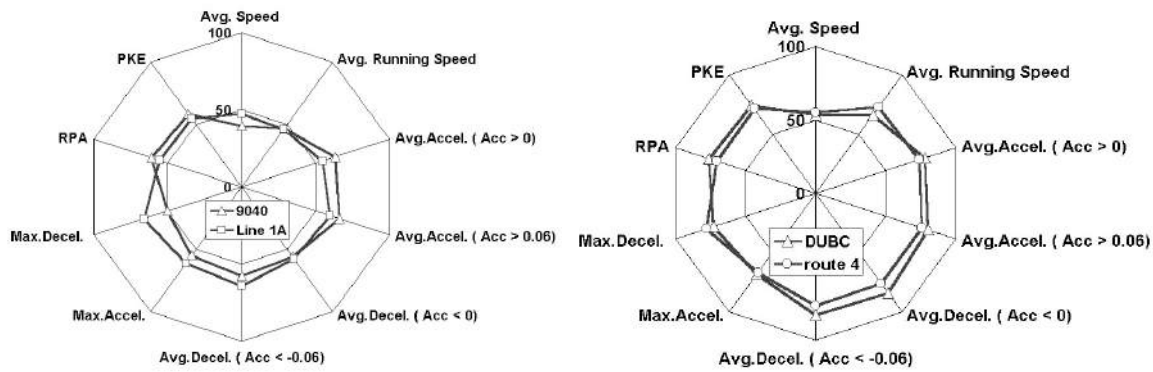

Figure 1: Comparison of measured driving patterns with available driving cycles – examples.

A 'driving dynamics factor' (DDF) is suggested, in order to describe driving dynamics effects on engine power demand. The DDF value was calculated according to the formula:

$$DDF = (TRT/PRT)*V_{PT} \text{ [km/h], where:}$$

TRT – total running time, sec;
PRT – running time with positive engine torque, sec;
V_{PT} – average bus speed of running with positive engine torque, km/h.

Figure 2 shows the dependence of average power demand on DDF values, for a variety of measured bus driving patterns. It can be seen that the average power demand varies remarkably within a given bus route, depending on the driving dynamics (governed by the driving style and road conditions). For example, for route 5 the power demand varies from 56 to 106 kW in accordance with DDF change from 41 to 77 km/h (about 88%); the corresponding change of average running speed for this route is only 48% (from 25.6 to 38 km/h). It was found that the DDF value gives a better measure of how much power is used compared to RPA or speed*accelerations values, Ericsson (2002). For example, the coefficients of correlation between average power demand and DDF, RPA and average running speed*RPA for routes 1a-1b were found to be 0.996, 0.647 and 0.818.

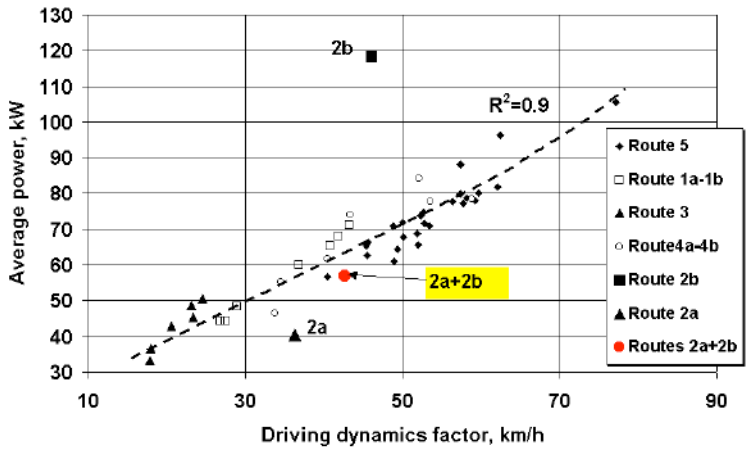

Figure 2: Dependence of the average power demand on the demand on the driving dynamics dynamics factor.

Figure 2 illustrates also that the dependence of the average power demand on the DDF changes dramatically with the road gradient (see points of routes 2b and 2a on the graph corresponding to uphill and downhill driving, accordingly).

Comparison of the average urban bus speeds in Israel (9.6-24.8 km/h) with those measured in Belgium (18.6-24.2 km/h), shows much lower speed values in city center driving. This results from highly congested traffic and high stop frequency in Israeli city centers. For reasons of comparison: data published by Andre & Hammarstrom (2000) show ranges of average bus speeds for Switzerland - from 6 (when traffic is congested) to 18 km/h and for Germany - from 16 to 21 km/h.

Figure 3 shows the influence of the bus driving pattern on the exhaust gas temperature (EGT), as was measured in the experiments carried out in Israel. These data may be useful for the purpose of decision-making concerning installation of exhaust aftertreatment devices in urban buses.

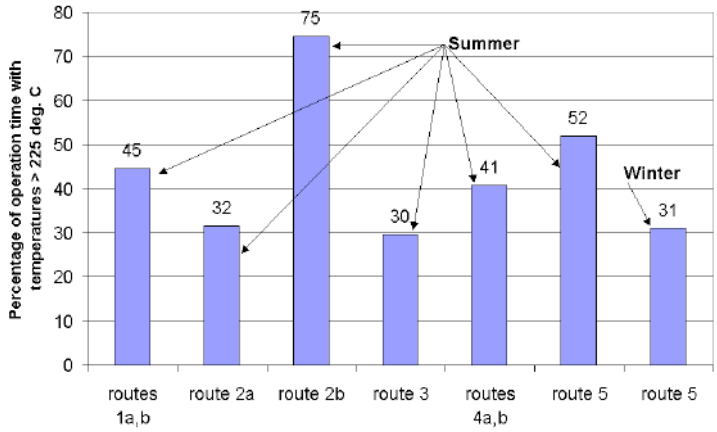

Figure 3: Influence of bus driving pattern on exhaust gas temperature.

As can be seen from Figure 3, for bus driving patterns in congested city centers, the problem of too low temperatures may arise. For example, in route 3 only at 30% of the total driving time the EGT is more than 225 ºC, which may result in problems of light-off or insufficient regeneration of aftertreatment devices. It is noted that the measurements on routes 1-4 were performed during the summer season, when the AC system was operated during almost all of the operation time. On route 5, the appropriate tests were carried out at both summer and winter months. The results show significant differences between measured EGTs (see Figure 3) that resulted mainly from the influence of AC operation on engine power demand. As may be seen from Figure 3, in the winter season the percentage of driving time with EGTs > 225 ºC is about 1.7 times lower compared to summer driving. This may cause severe problems when using exhaust aftertreatment devices. Analysis of measured engine oil and coolant temperatures has shown that only one really cold start per day occurs for all the studied urban bus patterns.

Effects of road gradients

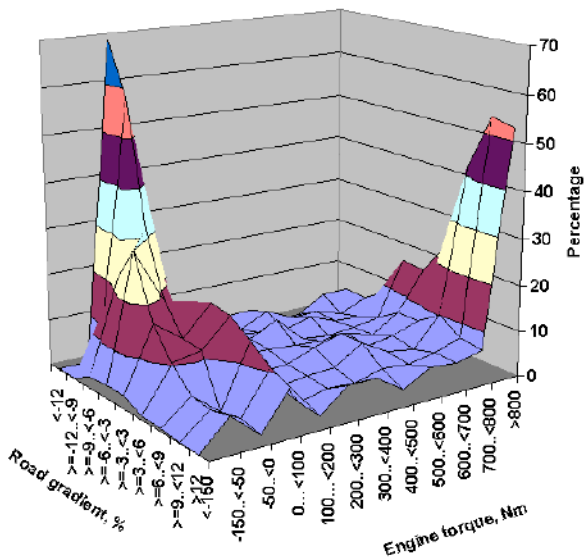

Figure 4: Share of bus engine torque utilization vs. road gradient.

As already noted, the topography of Haifa allowed the measurements of driving behavior on roads with steep gradients. For example, routes 2a & 2b were run on roads with gradients up to 12%. Gradients of more than 3% were measured at about 70% of the total route distance. Figure 4 illustrates the influence of the road gradient on the engine torque, as measured on routes 2a & 2b. It follows from this Figure that the share of maximal torque utilization rises from about 15 to about 55% with the increase of road gradient from the range –3…3% to values of more than 9%. It is interesting to note that even at downhill driving on roads with steep gradients of more than 9%, the share of maximal torque utilization is not zero, but around 3-4%. Figure 4 further illustrates that the most widespread engine operation regimes in Israeli driving patterns are at "motoring" and "full load" modes.

This fact validates the previously discussed finding about the aggressiveness of the local driving style.

Figure 5 demonstrates utilization of torque and engine speed values in the real-world bus driving on the hilly route (2a+2b). The areas, which were attributed as controlled by the ESC test cycle, are bounded by dotted lines (actual test points are marked by circles). Calculation results show that about 33% of the total operation time, the bus engine runs on modes, which are found outside of the ESC controlled areas. About 23% of the total operation time the engine runs in motoring mode.

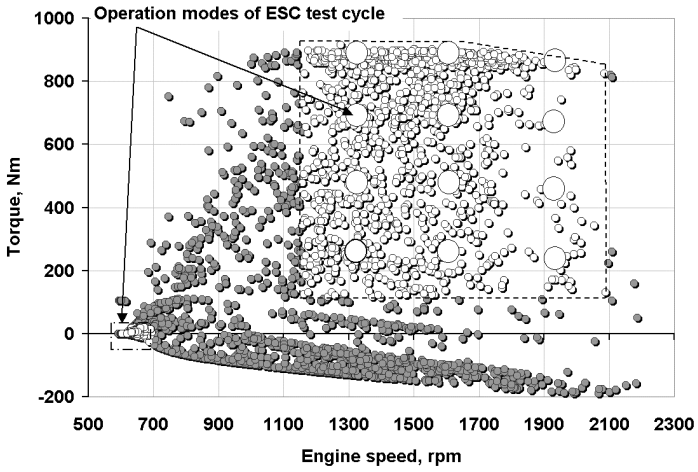

Figure 5: Example of torque values utilization versus engine speed.

Effects of air conditioning

Experiments aimed at estimation of AC effects were carried out on bus route 5. The driving behavior was studied during two summer months (July, August), when the AC system was almost permanently switched-on, and during two winter months (January, February), when it was not used. Data of bus fuel consumption (FC) were received from the bus operator and processed for the above-mentioned periods. Average FC values that were obtained for AC-on and AC-off periods are 65 and 59 l/100 km, respectively. The difference of 10% may be attributed mainly to the effects of AC system operation on engine power demand. It may be assumed that real effects of AC operation on urban bus FC is even greater, due to the negative influence on winter FC of longer lighting times, wet roads etc.

In order to estimate more accurately the AC influence on the bus engine power, the AC system power demand was evaluated according to the method described in chapter 2. Values of AC power were calculated on second-by-second basis for all measured driving patterns, when the AC system was switched-on. Then, weighted average values were calculated. It was found that the average power consumed by the AC system during urban bus driving on route 5 is about 11.5% of the average engine power demand. The mechanical power consumed by the AC at engine idle mode is more than 6.5 kW.

Conclusions

Comparison of measured driving patterns with available driving cycles shows that these cycles cover about the whole range of traffic situations and of the measured driving patterns. Driving cycles that show better resemblance to the measured driving behavior of buses in Israel are: Dutch Urban Bus Cycle, both Munich and Stuttgart driving cycles. There is no available driving cycle, which could describe suitably congested city center bus driving patterns. Development of an appropriate representative driving cycle for this traffic situation is certainly useful.

From comparison of the Belgian (Turnhout) and Israeli bus driving patterns, the following observations can be made: much higher percentage of stop time in Israel compared to Belgium was measured, together with lower levels of average and maximal accelerations, and higher percentage of cruising in Belgian driving patterns. The driving pattern measured in Brussels is closer to the Israeli measurements, but also here lower maximal acceleration/deceleration values and higher percentage of cruising were observed. This illustrates the more aggressive driving style of Israeli bus drivers. The results show that the most widespread engine operation regimes in Israeli driving patterns are at “motoring” and “full load” modes. A ‘driving dynamics factor’ was suggested, in order to describe the driving dynamics effects on engine power demand. It was found that the DDF value gives a better measure of how much power is used compared to RPA or speed*accelerations values.

For bus driving patterns in congested city centers, the problems of light-off or insufficient regeneration of aftertreatment devices may arise, due to the low exhaust gas temperatures. In the winter season the percentage of driving time with EGTs > 225 ºC is about 1.7 times lower compared to summer driving. The share of maximal torque utilization rises from about 15 to about 55% with the increase of road gradient from –3…3% to values of more than 9%.

It was found from a limited study of one urban bus equipped by one specific AC system, that the AC switching-on leads to rise of 11.5% in average power demand and about 10% in fuel consumption. The mechanical power consumed by the AC at engine-idle mode is over 6.5 kW. Detailed study of AC effects on driving behavior and emissions of buses and other heavy-duty vehicles, as also mentioned in the COST 319 Action, is needed.

Acknowledgments

Financial support of European Commission is highly appreciated. The authors wish to thank Israel and Belgium bus companies: Egged and De Lijn for their fruitful cooperation and technical support.

References

Andre M. (1996): Driving cycle development: characterization of the methods. SAE Technical Paper 961112, 13pp.

Andre M. and U. Hammarstrom (2000): Driving speeds in Europe for pollutant emissions estimation. Transportation Research Part D, vol. 5, p 321-335.

Andre M. and A. Villanova (2002): Characterisation of an urban bus network for environmental purposes. Presented at the 7th International Highway and Urban Pollution Symposium, Barcelona, Spain.

ARTEMIS Project: Assessment and Reliability of Transport Emission Models and Inventory Systems. Project funded by the European Commission within the 5th Framework Research Programme. http://www.trl.co.uk/artemis/index.html.

COST 319 (1999): Estimation of Pollutant Emissions from Transport. Final Report of the Action, edited by Robert Joumard, European Commission, Directorate General Transport, Brussels – Luxembourg.

COST 346 Action: Emissions and Fuel Consumption from Heavy-Duty Vehicles. http://www.cordis.lu/cost-transport/home.html

Ericsson E. (2001): Independent driving pattern factors and their influence on fuel-use and exhaust emission factors. Transportation Research Part D, vol. 6, p 325-345.

Ericsson E. (2002): Driving pattern, exhaust emission and fuel consumption over a street network. Proc. 11th Int. Symp. "Transport and air pollution", Graz, Austria, 19-21 June, p 331-340.

Esteves-Booth A., T. Muneer, H. Kirby, J. Kubie & J. Hunter (2001): The measurement of vehicular driving cycle within the city of Edinburgh. Transportation Research Part D, vol. 6, p 209-220.

Pelkmans L., D. de Keukeleere, H. Bruneel and G. Lenaers (2001): Influence of vehicle test cycle characteristics on fuel consumption and emissions of city buses. SAE Technical Paper 2001-01-2002, 11 pp.

Steven H. (1995): Auswertung des Fahrverhaltens von schweren Motorwagen, FE/BUWAL/310.92.53 "Auswertung von Fahrverleufen und Ermittlung von representativen Fahrkurven von schweren Motorwagen in der Schweiz", by order of Bundesamtes fur Umwelt, Wald und Landschaft (BUWAL), Bern.

Van de Weijer C. J. T., R. van der Graaf, P. Hendriksen and R. P. Verbeek (1993): Urban bus driving cycle. Presented at the 4th International EAEC Conference on Vehicle and Traffic Systems Safety, Strasbourg, France.

Van de Weijer C. J. T. (1997): Heavy-Duty Emission Factors – Development of Representative Driving Cycles and Prediction of Emissions in Real-Life. PhD Thesis, Technical University Graz, TNO, Delft.

Van Poppel M. and G. Lenaers (2003): Real Life Evaluation of the Emission Reduction Potential of a CRT Retrofitted City Bus. Proc 12th Int. Symp. "Transport and air pollution", Avignon, France, INRETS, to be published.

12th International Symposium "Transport and Air Pollution" / 12e Colloque international "Transports et pollution de l'air", Avignon, 16 -18 *June* / juin 2003
proceedings / actes, n°92, tome / Vol. 1, Inrets ed., Arcueil, France, 2003, p. 129-136

Regulated and Nonregulated Diesel and Gasoline Cold Start Emissions at different Temperatures

Martin Weilenmann, Patrik Soltic, Christian Saxer, Anna-Maria Forss
EMPA, Ueberlandstrasse 129, 8600 Duebendorf, Switzerland -
Fax: +41 1 823 40 12 – email: martin.weilenmann@empa.ch

Abstract
The emissions of modern cars are usually reduced in warm engine conditions by catalysts. Consequently emissions are significantly higher during the cold start, i.e. the warm-up phase of the car. The duration of this period and the emissions produced during it depend on the ambient temperature as well as on the initial temperature of the car's systems.
As part of the ARTEMIS project of the 5th EU FP, EMPA investigated the cold start emissions of Euro-3 gasoline cars, Euro-2 diesel cars and old pre-Euro-1 gasoline cars at cold ambient temperatures. Since the goal was to investigate real-world emissions, the measurements were done with cars belonging to private owners taken straight from the road with no maintenance. The chassis dynamometer tests were carried out at +23, -7 and -20 °C. The test cycle employed is a representative urban ride from a real-world driving behaviour study. Besides the regulated pollutants also methane, benzene and toluene were measured online by chemical ionisation mass spectrometry.
Key words*: cold start, cold ambient emissions, online emission measurement, real-world emissions, passenger cars, non regulated pollutants.*

Introduction

In central Europe, emission inventory calculations are performed by first dividing measurements from chassis dynamometer tests into cold start extra emissions (in g/start) and emissions from the warm engine (in g/km). Whereas "warm emissions" are multiplied by the size of the car fleet and the average yearly mileage, cold start emissions are multiplied by the number of cold starts. In previous campaigns, cold start emission data was taken from legislative cycles such as US FTP-75 and European ECE (Evéquoz et al. (1995a) and Laurikko (1998)).

Weilenmann (2001) confirmed that the cold start extra emissions of cars depend on three major parameters: First, the combustion principle (diesel/gasoline) and the legislative level (Euro-1,2,3...); second, the ambient temperature which is considered to be equal to the vehicle's temperature at test start; and third, the test cycle driven. Since cold start extra emissions vary by more than one order of magnitude between 23 ° and –20 °C, they need to be combined by meteorological data for emission inventories. The influence of the test cycles has been shown to be smaller and there is a debate about whether it should be taken into account for emission inventories, since it is assumed that most cold starts take place in urban situations.

Beside these main parameters for cold start extra emissions, it was highlighted that the methodology used to provide these emissions has a major influence on the results (Weilenmann 2001). Ideally a test to generate cold start extra emissions is based on a repetitive "real-world" cycle. Real-world means that the driving pattern is derived from studies of real-life traffic and that it is statistically representative. Repetitive means that the driving cycle consists of a short driving pattern (hereafter called "sub cycle") which is repeated several times. The overall duration must be such that at least

the last two patterns are driven with a hot stabilised engine. The cold start extra emissions are then derived from the difference between the emissions measured in the sub cycles where the engine is warming up and the emissions measured in the same number of sub cycles when the engine is warm.

This approach is absolutely identical with the following approach, which is based on instantaneous emission signals: The cumulated emissions are calculated from the instantaneous emission signal as the integral of the emissions from test start. This results in a monotonically increasing curve (Figure 1). In the warm phase, the cumulated emissions constitute an almost straight line and can be approximated by linear regression. The value at which this line crosses the ordinate, and thus the start time of the test, is exactly the cold start extra emission. For repetitive cycles, this method gives the same values as the above-mentioned approach. However, this regression model can also be applied to non-repetitive tests.

Thus it is helpful to compare the results of different cold start tests. In particular, it becomes possible to compare real world cold start tests with the huge number of tests performed with the legislative cycles (ECE and FTP-75). Both tests are not repetitive: The ECE test would be repetitive if there were not a 40 s idling period at the beginning; but in addition it is too short for some cars to warm up completely before the second but last sub cycle. The first and third parts of the FTP-75 test have an identical driving pattern and could be considered repetitive if the third part were not measured after a ten minute break, which means that the engine is not hot stabilised at the second start.

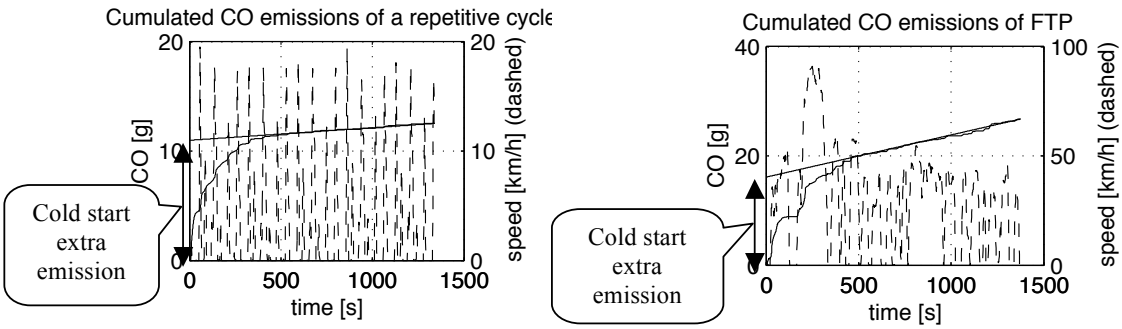

Figure 1: The regression model. Dashed: velocity diagram; solid: cumulated CO emissions.

Continuing on from Weilenmann (2001), who investigated the cold start emissions of Euro-2 gasoline passenger cars, the cold start emissions of Euro-3 gasoline cars, Euro-2 diesel cars and old pre-Euro-1 gasoline cars (hereafter called "Euro-0") are examined here. Section one of this paper focuses on the influence of the test cycle, section two on the results of cold ambient emission tests with gasoline cars and section three on the results with diesel cars.

In addition to the regulated pollutants – carbon monoxide (CO), hydrocarbons (HC), nitrogen oxides (NO_x) and carbon dioxide (CO_2) – emissions of benzene and methane from the gasoline cars) and toluene (from the diesel cars) were measured online by chemical ionisation mass spectrometry (CI-MS) (see Saxer (2003) for nonregulated emission measurements with warm engine).

For real-world emission inventories it is important to design tests that are as close as possible to real-world, on-road driving. In the case of cars, this means taking a random sample of vehicles from the road. The test fleet should be composed in such a way that it reflects sales figures for engine size, manufacturer, gearbox type, chassis type, etc. The test fleet's mileage should also be representative, as should its use and maintenance status. In the studies which EMPA carries out for both the Swiss Agency for the Environment, Forest and Landscape (SAEFL) and the ARTEMIS Project (5th EU framework programme), cars are obtained in this way from voluntary private owners. The cars are not serviced before the test (Soltic, 2002). Each group of cars (Euro-3 and Euro-0 gasoline, Euro-2 diesel) consists of six vehicles.

1 – Comparison of different test cycles at 23 °C

A cycle from André (1999) was chosen for the main investigations at different temperatures in the ARTEMIS project. The test consists of 15 repetitions of a 180-second sub cycle with urban driving. It is called "Inrets 15 x urbain fluide court" (IUFC15) and the basic part is displayed in Figure 2.

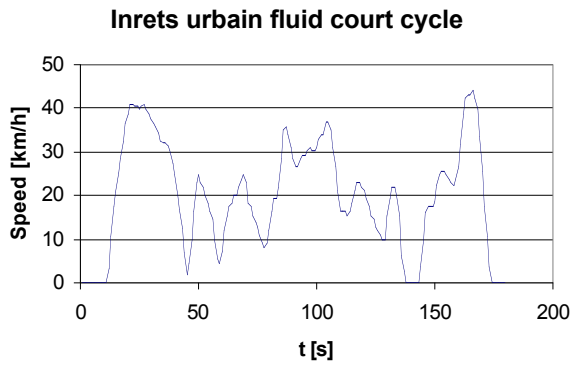

Figure 2: Test cycle "Inrets urbain fluide court".

In addition, all cars were measured at 23°C using the legislative ECE cycle, the FTP-75 cycle and another repetitive real-world cycle derived from extra urban data. The latter is called "Inrets 15x route court" (IRC15) (André 1999) and consists of 15 repetitions of a 120-s sub cycle.

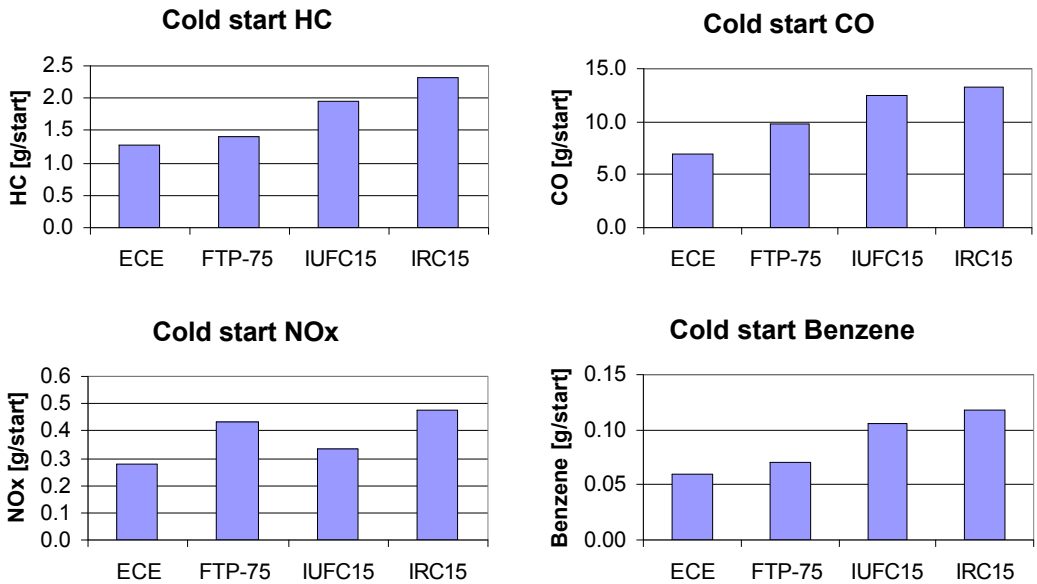

Figure 3: Comparing different cycles for cold start extra emission calculation.

Figure 3 shows the cold start extra emissions of the Euro-3 cars that were obtained in the different cycles. All calculations prior to this were made using the "regression model". These cars exhibit a trend similar to that already observed for Euro-2 cars in Weilenmann (2001): the ECE cycles exhibit lower cold start emissions than FTP-75 and IUFC15 and thus underestimate the real-world situation. In addition the rural cycle generates rather higher cold start emissions than the urban cycles, a fact which also corresponds closely to Weilenmann (2001).

As Figure 3 shows, the cold start extra emissions vary by not more than 30% for the real cycles and not more than a factor of two from ECE to rural driving.

2 – Results of cold ambient emission tests with gasoline cars

This section compares the cold start extra emissions of different vehicle generations at various

temperatures. Unfortunately not all vehicle generations were measured with the same test cycles. The results of the Euro-1 cars come from Laurikko (1998) and are based on the ECE test. They are therefore assumed to underestimate real-world cold start emissions. The values for the Euro-2 cars date from 2000 and were obtained with the C4 repetitive real-world urban cycle from the Handbook (Keller 1999). This cycle is similar to the IUFC15 cycle that was used here (Figure 4).

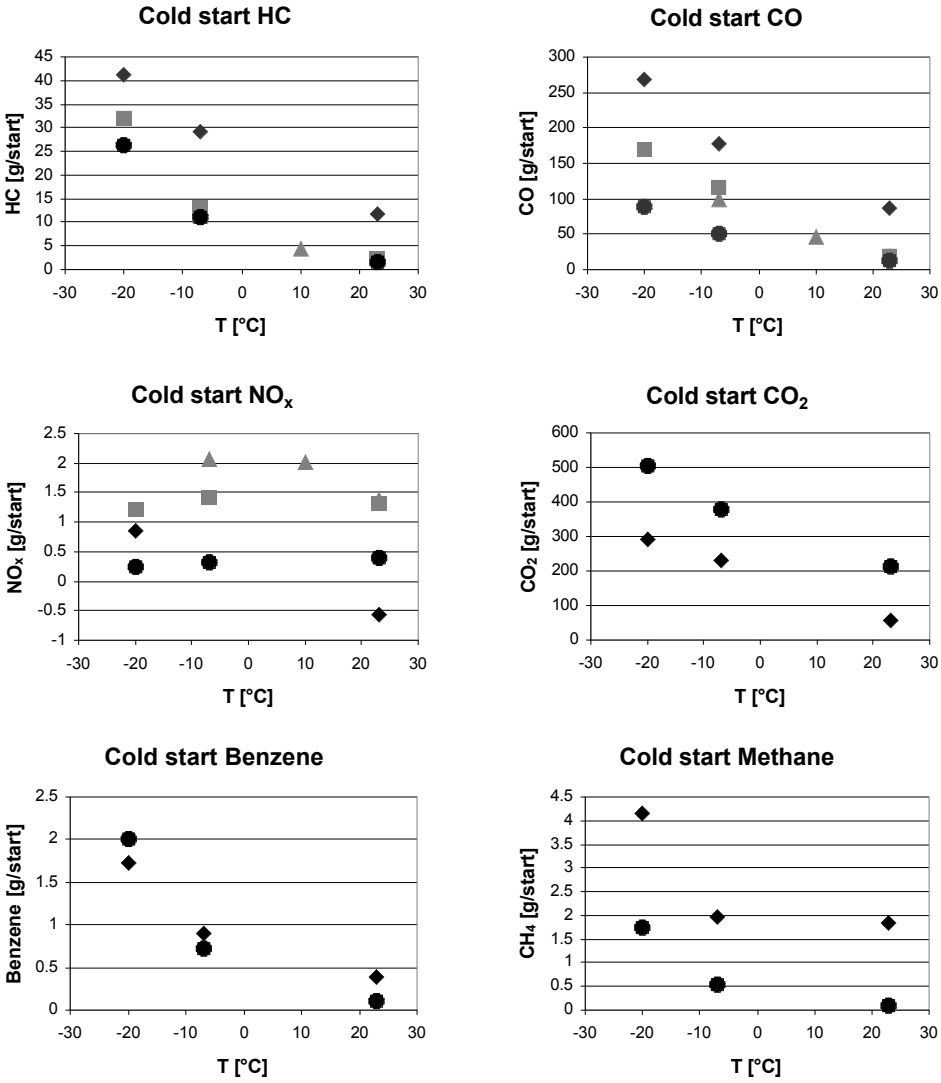

Figure 4: Cold start extra emissions from different generations of gasoline cars at different ambient temperatures: ◆Euro-0 IUFC15, ■ Euro-1 ECE, ▲ Euro-2 C4, ● Euro-3 IUFC15.

The hydrocarbon emissions of all car generations (HC) show a clear and disproportionately large trend at low temperatures. Keeping in mind that different cycles were used, Figure 4 shows a continuous 13 g/start reduction in cold start HC from Euro-0 to Euro-3 at all temperatures. The cold start emissions of all cars are 26 g/start higher at -20°C than at room temperature.

There is a slightly disproportionate rise in carbon monoxide (CO) emissions with lower ambient temperatures. The fall in emissions between Euro-0 and Euro-3 is about 180 g/start at -20°C and 72 g/start at 23 °C. The cold start CO emissions of Euro-0 cars are about 182 g/start higher at -20°C than at room temperature. For Euro-3 cars this difference is 76 g/start.

Cold start extra emissions of nitrogen oxides (NO_x) are very low for all car generations and show no relation to the ambient temperature.

The extra carbon dioxide (CO_2) generated during the cold start phase is 180 g/start higher for the

Euro-3 cars than for the Euro-0 cars, which is the compensation for the huge CO emissions of the latter. The increase for lower temperatures is linear and is approx. 250 g/start between -20 and 23°C.

Figures 3 and 4 show clearly that ambient temperature has a significantly larger influence on cold start extra emissions than driving style.

It is also apparent that benzene and methane follow a similar trend over temperature as the total hydrocarbons. However, considering the trend over the generations, methane displays a larger relative decrease than HC, while cold start extra benzene remains virtually constant!

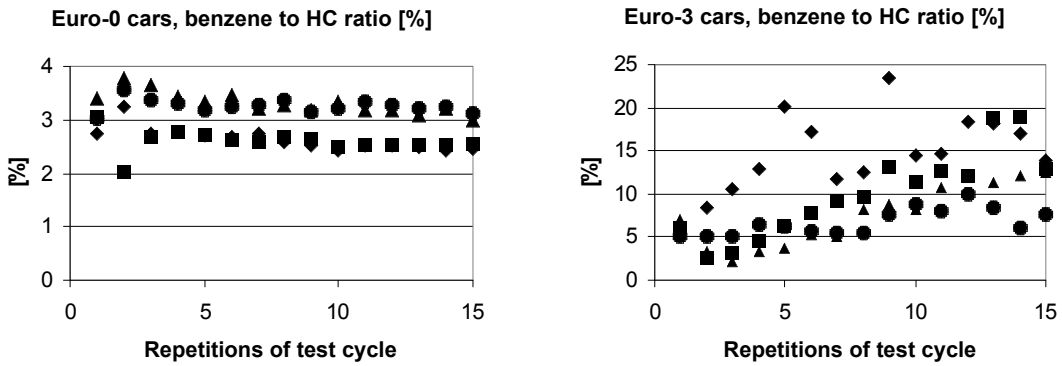

Figure 5: Ratio of benzene to HC for different generations of cars over the warm up phase: ◆ IUFC15 23°C, ■ IUFC15 -7°C, ▲ IUFC15 -20°C, ● IRC15 23°C.

Figure 5 shows the mass ratio of benzene to total hydrocarbons over the 15 periods of IUFC15 and IRC15 for the Euro-0 and Euro-3 car fleets. While this ratio remains at a more or less constant 3 % for the older cars, it rises significantly to an average of 15 % for the Euro-3 models as the catalyst starts to get hot.

3 – Results for the Euro-2 diesel cars

Figure 6 shows the cold start extra emissions from the diesel cars in different cycles. The situation is completely different to the gasoline cars for the following reasons: first, the ECE cycle is much too short for a complete warm up of the engine system. Even in the more aggressive IUFC15 it takes approx. 1000 seconds before CO and HC emissions stabilise. Thus, ECE data cannot be used to calculate cold start extra emissions for diesels. Secondly, the FTP-75 results obtained here using the regression model are even lower than the results of the bag 1 – bag 3 method. This can be explained by the time resolved emission data: the CO and HC emissions of the warm part of bag one are completely different to these of bag two, so the regression model cannot be applied to this non-repetitive test cycle for diesel cars. Thirdly, the cold start extra emissions from the urban IUFC15 cycles are higher than those from the rural IRC15 cycle. This is meaningful, since the warm up duration depends here on the engine temperature, while for gasoline cars just the much smaller catalyst needs to be warm to end cold start extra emissions. In contrast to gasoline cars, it seems appropriate to warm up diesels at high loads in order to minimise pollution.

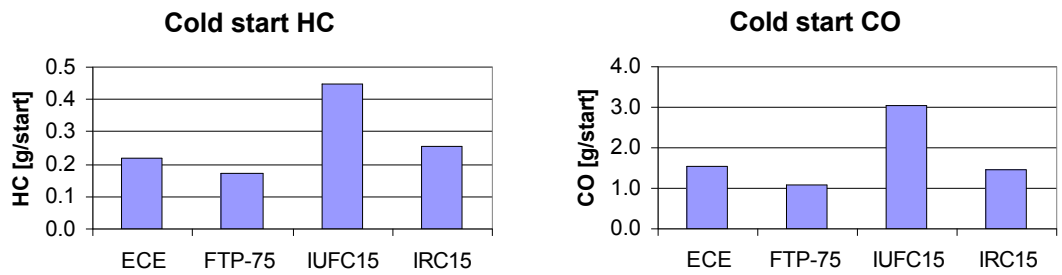

Figure 6: Comparing different methods and cycles for calculating cold start extra emissions.

Figure 7 shows the cold start emissions of the diesel cars as a function of ambient temperatures. The

results of the Euro-0 cars driven on the FTP-75 cycle are taken from Laurikko (1998). Cold start extra emissions of HC are five to ten times lower than for gasoline cars. However, they exhibit a similar, disproportionate trend for cold temperatures. The figure suggests that there has been no improvement between the Euro-0 and Euro-2 generations of cars. However, it must be remembered that the Euro-0 results originate from FTP-75 bag 1 – bag 3 data. Thus they underestimate the real situation.

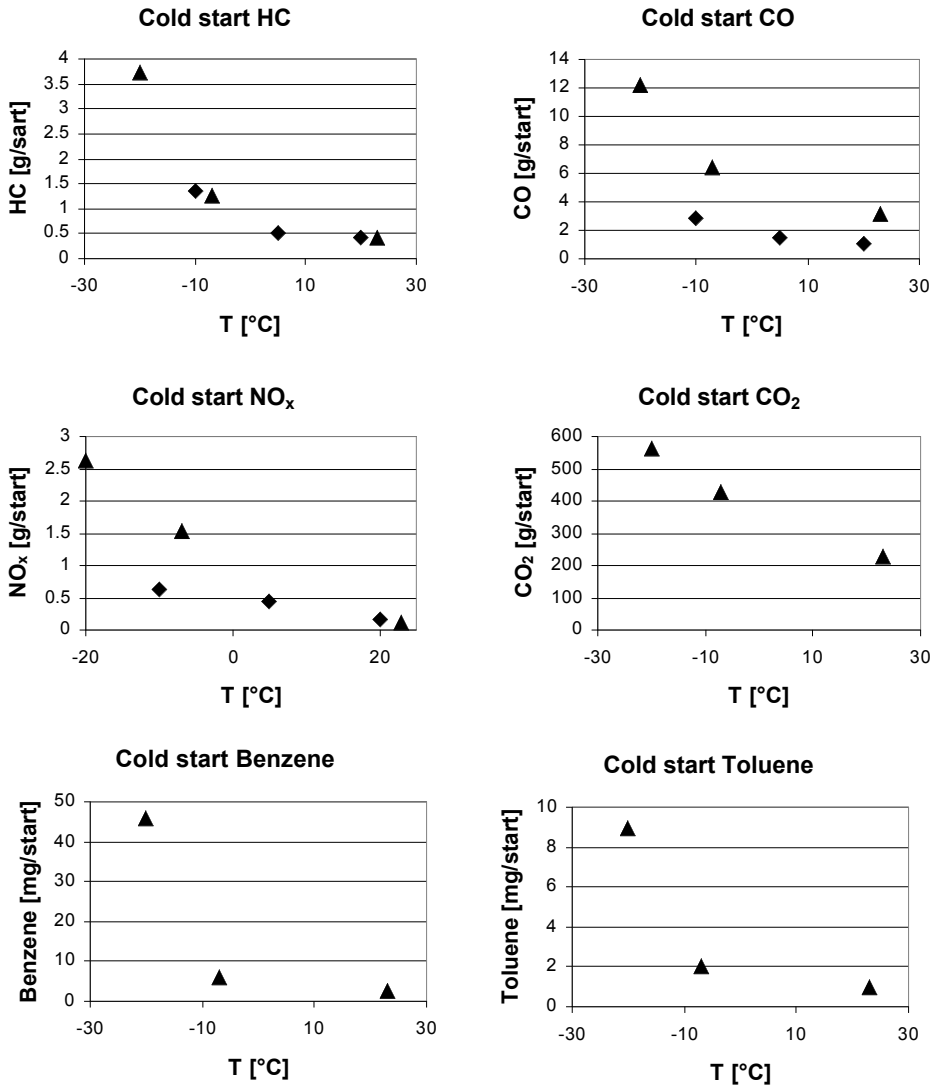

Figure 7: Cold start extra emissions from different generations of diesel cars: ◆Euro-0 FTP-75, ▲ Euro-2 IUFC15.

CO cold start extra emissions are also ten times lower than for gasoline cars. They also rise by a disproportionately large amount at cold temperatures. As in the case of HC, also the CO values of the Euro-0 vehicles are underestimated by an approximate factor of two. Thus the real-world CO cold start emissions of the two fleets of cars appear to be comparable.

Cold start NO_x emissions are comparably low for diesel cars and gasoline vehicles. Even so, NO_x emissions rise at low ambient temperatures. Because different cycles were used, the NO_x trend between the different car generations is not clear.

Diesel cars produce almost twice as much extra CO_2 during the cold start period than gasoline vehicles. The higher engine mass and higher fuel efficiencies cause a slower warm up and thus increased friction.

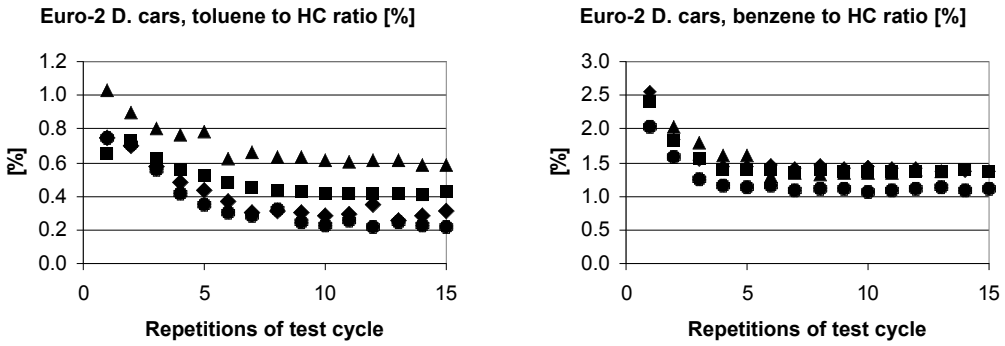

Figure 8: Ratios of benzene to HC and toluene to HC for diesel cars during the warm up phase: ◆ IUFC15 23°C, ■ IUFC15 -7°C, ▲ IUFC15 -20°C, ● IRC15 23°C.

The extra benzene and toluene emissions seem to behave similarly to total HC. However, the benzene/HC and toluene/HC ratios are not constant during warm up (Figure 8).

Conclusions

Cold start extra emissions are dependent on the driving situation. With gasoline cars they increase at higher loads, such as suburban or highway driving, while diesel cars seem to behave in the opposite fashion. However, the driving situation exerts a significantly smaller influence than the ambient temperature, and there is a debate about whether it has to be taken into account in emission inventories because most car journeys start in an urban environment. Repetitive urban real-life cycles should be used for cold start measurements. ECE measurements underestimate real-world cold start emissions.

The HC and CO cold start emissions of Euro-3 gasoline cars are significantly lower than those of Euro-0 cars. Both CO and HC are disproportionately high at cold ambient temperatures. The cold start emissions of Euro-3 gasoline cars are 15 times higher at –20°C than at 23°C. There is no appreciable reduction in the cold start benzene of Euro-3 gasoline cars compared to Euro-0 vehicles. In addition the benzene/HC ratio of the Euro-3 vehicles increases during warm up to about 20% but was constant at about 3% for Euro-0 cars.

For the application of such results for emission inventories, it is clear that the ambient temperature has to be taken into account. Moreover, the emissions of engines that are started before they have completely cooled down need to be modelled too. However, this is not the topic of this paper.

Overall cold start extra emission levels are significantly lower for diesel cars than for gasoline cars. Euro-0 and Euro-2 diesel cars emit comparable cold start CO and NO_x emissions, while HC emissions are somewhat decreased. In contrast to the gasoline cars, the diesels exhibit a relevant trend in cold start NO_x emissions for lower temperatures. Diesel and gasoline cars exhibit similar HC and CO emission trends over temperature. For diesels the benzene/HC and toluene/HC ratios display a slightly decreasing trend during engine warm up. Diesel cars emit significantly more extra CO_2 than gasoline cars during the warm um phase.

Acknowledgements

This work was conducted as part of both the national emission factor program and the ARTEMIS project of the 5th EU framework program. The authors wish to thank SAEFL, the BBW and all cofinancers for their support.

References

André M., Hammarström U., Reynaud I., (1999) Driving statistics for the assessment of air pollutant emissions from road transport. INRETS report, LTE9906, Bron, France.

Evéquoz R., Keller M., Heldstab J., Kessler H. (1995): Luftschadstoff-Emissionen des Strassenverkehrs 1950 – 2010, Schriftenreihe Umwelt No. 255, Swiss Agency for the Environment, Forest and Landscape (BUWAL), Bern, Switzerland.

Heeb N., Forss A.-M., Wilhelm P. (2001): Comparison of Methane, Benzene and Alkyl Benzenes Cold Start Emission data of EURO I and EURO II Three-Way Catalyst Passenger Cars and Light Duty Vehicles from Time Resolved Exhaust Gas Analysis, Proc. Int. Symp. "Transport and air pollution", Boulder Colorado USA, 17 – 19 Sept. 2001.

Keller M., Koch P., Heldstab J., Dähler Staub B., de Haan P., (1999) Handbook Emission Factors for Road Transport, UBA Berlin and BUWAL Bern, produced by INFRAS Bern.

Laurikko, J. (1998): On exhaust emissions from petrol-fuelled passenger cars at low ambient temperatures, dissertation, VTT publications 348, Espoo, Finland.

Lenner M. (1994): Pollutant emissions from passenger cars., VIT Report No 400a, VTI Swedish Road and Transport Research Institute.

Soltic P. (2002), Nachführung der Emissionsgrundlagen Strassenverkehr- Ergänzung der Messdaten auf das Bezugsjahr 2000, Benzin: Personen- und Lieferwagen, Teilbericht Standardprogramm, EMPA Untersuchungsbericht 201209, Dübendorf, Switzerland.

Weilenmann M. (2001), Cold Start and Cold Ambient Emissions of Euro II Cars, Proc. Int. Symp. "Transport and air pollution", Boulder Colorado USA, 17 – 19 Sept. 2001.

Saxer C. J., Forss A.-M., Weilenmann M., Heeb N. V. (2003): Benzene emission factors of the latest diesel- and gasoline-fuelled passenger cars within the common artemis driving cycle, Proc. Int. Symp. "Transport and air pollution", Avignon France, 16. – 18. June 2003.

12th International Symposium "Transport and Air Pollution" / 12e Colloque international "Transports et pollution de l'air", Avignon, 16 -18 *June* / juin 2003
proceedings / actes, n°92, tome / Vol. 1, Inrets ed., Arcueil, France, 2003, p. 137-144

Towards accurate instantaneous emission models

Delia Ajtay, Martin Weilenmann & Patrik Soltic
EMPA, Überlandstrasse 129, 8600 Dübendorf, Switzerland -
Fax +41 01 823 40 12 - email : delia.ajtay@empa.ch

Abstract
To address the needs of researchers and policy makers on local levels, a microscopic (i.e. at vehicle level) instantaneous emission model is being developed. This model aims to predict vehicle fuel consumption and emissions for a given speed profile, for various vehicle loads, slopes and gear shift scenarios.
Instantaneous emission modelling maps the emissions at a given time to their generating "engine state". To improve the existing models, an analysis of some preconditions must be made: owing to the frequency content of the engine and emission signals, they should be measured on a 10 Hz basis or faster.
Additionally, the emission signals measured in a test are delayed dynamically, owing to the transport from the engine to the analysers. This transport must be compensated for by time-varying approaches. The modelling and compensation for the gas transport in dilution systems is presented here.
With these preconditions fulfilled, new instantaneous emission models are developed and their improvement in quality is checked by comparing them with older models. Further improvements to describe the transient emissions of vehicles are sketched.
Keys-words*: vehicle, pollutant, instantaneous emission modelling, dynamic compensation, dynamic emission mapping.*

Introduction

During the past decades, the environmental impact of burning fossil fuel has become an important issue. Ozone, acid rain, the greenhouse effect, toxic gases and particles are a consequence of increasing traffic. Under stricter legislation, vehicle emissions per distance have been reduced. But the increased vehicle fleet and larger total distance covered yearly have counteracted these improvements.

For more than a decade, attempts have been made to map emission measurements of tests on chassis dynamometers or engine test benches in a neutral way, so that emissions of other driving conditions can be calculated from them.

There are two basic types of emission models, one based on bag measurements and the other on instantaneous measurements. While models based on bag measurements possibly allow interpolation for non-measured cycles, instantaneous models shall additionally make it possible to predict emissions for different vehicle loads, slopes or gear-shift scenarios.

In most instantaneous emission models, the emission signals and all other information from the tests are collected at a rate of one sample per second and the mapping of the emissions is performed by statically relating them to causative variables such as speed, acceleration, etc. The "BEFU" methodology of Jost, Hassel et ali (1992a) used in Keller (1999) and the corresponding publications of the Swiss Agency for the Environment, Forest and Landscape (Evéquoz 1995) are examples of such emission measurements for light-duty vehicles on chassis dynamometers. Examples of

instantaneous emission measurements on engine test benches for heavy-duty engines are to be found in Sams et ali (1992), Jost et ali (1992b) and Hausberger (2002). Nonetheless, the prediction quality of these models for modern gasoline vehicles is rather poor (Pritscher 1999).

On the way to new model approaches, first an analysis of some preconditions is made in Section One, concluding in pre-processing of the measured signals. Using these signals, in Section Two, the authors compare old and new static instantaneous emission models. The results show that these measures already improve the prediction quality of the emission models significantly. Section Three presents aspects for improving the model structure to take into account the transient generation of emissions.

1 – Preconditions for instantaneous emission models

From the analysis of emission signals measured with fast sensors (lambda sensors, NO_x sensors (NO_x = nitrogen oxides), fast FID sensors for hydrocarbons), it follows that many "emission peaks" last less than one second. Their frequency content is up to 5 Hz. Some engine-related signals such as torque or manifold pressure may also change remarkably within some tenths of a second. From the Shannon sampling theorem, which states that in a sampled signal no information above half of the sampling frequency is available, it follows that emissions and engine signals must be collected on a basis of 10 Hz or even faster (see Weilenmann et ali (2002a)).

In some laboratories, the exhaust gas is collected directly after the tailpipe and analysed at 10 Hz (raw gas analysis). Gas transport through the exhaust system of the car and the measurement line, as well as the analysers, causes the exhaust signal to be delayed by up to fifteen seconds and convoluted through mixing by up to ten seconds, i.e. an emission peak of one second duration is measured as a ten-times smaller hump of ten seconds duration (Weilenmann et ali (2001)).

If these dynamic aspects of the exhaust transport are neglected, the emission events are correlated to "the wrong second", resulting in incorrect engine status in emission modelling. For instantaneous emissions modelling, emission values can be correlated to the right engine state of the car only if they are at their correct location on the time scale. Therefore, these delays and mixing dynamics must be compensated for, i.e. the behaviour of the gas transport systems must be modelled and the developed models need to be invertible.

In Weilenmann et ali (2002a) it was shown that these delays and convolutions can be compensated satisfactorily by time-varying differential equations for the transport in the car and the raw gas system.

In a majority of laboratories the emissions are measured in a CVS (constant volume sampler) system; thus they are delayed even more (by up to twenty-five seconds) and mixed (by up to twenty seconds).

The compensation of these CVS dynamics is presented here. The same approach is applied as in Weilenmann et ali (2002a).

CVS gas transport model

For the dilution gas transport modelling, several aspects should be mentioned (see also Figure 2):

- In most of the CVS systems, the point where the raw exhaust gas is mixed with the dilution air is some metres away from the car's tailpipe.
- The transport of gas from the tailpipe to the mixing point goes with the volume flow of the exhaust gases. This volume flow varies between 3 l/s and 150 l/s for a typical 2000 cm^3 car. Thus, the transport lasts between 0.3 and 13 seconds (in our case, where the pipes from the tailpipe to the mixing point contain 50 l), depending on the volume flow.

In addition, the mass balance at the mixing point shows that the concentration after the mixing point is the product of the concentration values of the raw gas (in ppm) and the (time varying) mass flow of the car. Thus, the latter has to be measured accurately.

From these considerations, a model for the dilution system looks like the one shown in Figure 1 and Figure 2:

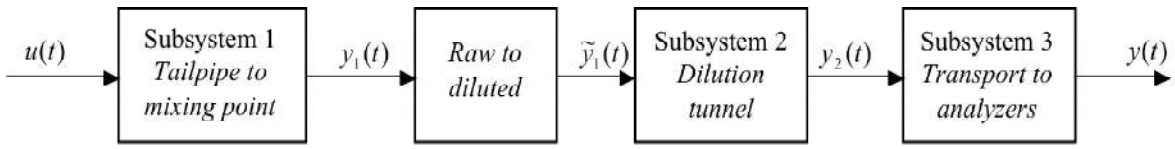

Figure 1: Diagram of the CVS model.

- A first subsystem describes the transport from the tailpipe to the mixing point. This transport is described by a time delay depending on the volume flow of the car and a turbulent mixing which is modelled as a linear time-variant system composed of two equal mixing volumes. They are described by two first-order systems whose time constants are also functions of the volume flow. Since the exhaust volume flow varies over time, it must be known.

  With *u(t)* denoting the input signal (gas concentration at the end of the exhaust system), $y_1(t)$ the output of the system (gas concentration at the mixing point), $T_{d,1}(t)$ the time delay and $T_{C,1}(t)$ the time constant of the system, the description of the first subsystem becomes:

$$T_{C,1}^{\ 2}(t)\,\ddot{y}_1(t) + 2T_{C,1}(t)\,\dot{y}_1(t) + y_1(t) = u(t - T_{d,1}(t)) \qquad (1)$$

- Since the exhaust signal is transformed at the mixing point, the mass balance gives:

$$\tilde{y}_1(t) = \frac{y_1(t)\overset{*}{V}_{raw}(t) + y_{dil}(t)(\overset{*}{V}_{CVS}(t) - \overset{*}{V}_{raw}(t))}{\overset{*}{V}_{CVS}(t)} \qquad (2)$$

  where $\tilde{y}_1$ is the gas concentration of the gas species after the mixing and y_{dil} is the concentration of the gas species in the dilution air. Again, the volume flow of the exhaust gases must be known.

- After this static non-linearity, the second subsystem describes the transport through the dilution tunnel. It is modelled as a time delay and a second-order dynamic for the turbulence. Since the volume flow is (almost) constant here, the parameters of the system are time-invariant. With $\tilde{y}_1(t)$ denoting the input of the system (diluted gas after the mixing point, obtained from equation (2)), $y_2(t)$ the output of the system (diluted gas at the end of the dilution tunnel), $T_{d,2}$ the time delay and $T_{C,2}$ the time constant of the system, we obtain:

$$T_{C,2}^{\ 2}\,\ddot{y}_2(t) + 2T_{C,2}\,\dot{y}_2(t) + y_2(t) = \tilde{y}_1(t - T_{d,2}) \qquad (3)$$

- Finally, the same approach is used for the transport in the small tubes carrying the gas from the CVS tunnel to the analysers and the analysers' dynamic is added. This is the third subsystem and it is again modelled as a time delay and a second-order linear system.

As a consequence, the model for the gas transport from the tailpipe to the dilution analyser becomes a bilinear time-varying system of order six.

Parameterisation of the model

For the parameterisation of the model, several gas bottle tests were carried out. The tests were run with a BMW 318 car (Euro-2 gasoline vehicle with TWC, displacement volume of 1.8 litres) connected to the system (as in Figure 2). The car was driven at a different steady-state point for each test.

For the identification of system's parameters, concentration step signals were generated by injecting calibration gases from bottles at the input of each of the CVS subsystems mentioned above and the

emission step responses were measured at the corresponding output by fast sensors (lambda sensor or NO_x sensor). Finally, the model parameters where identified by fitting the model output to the measured signal by least squares.

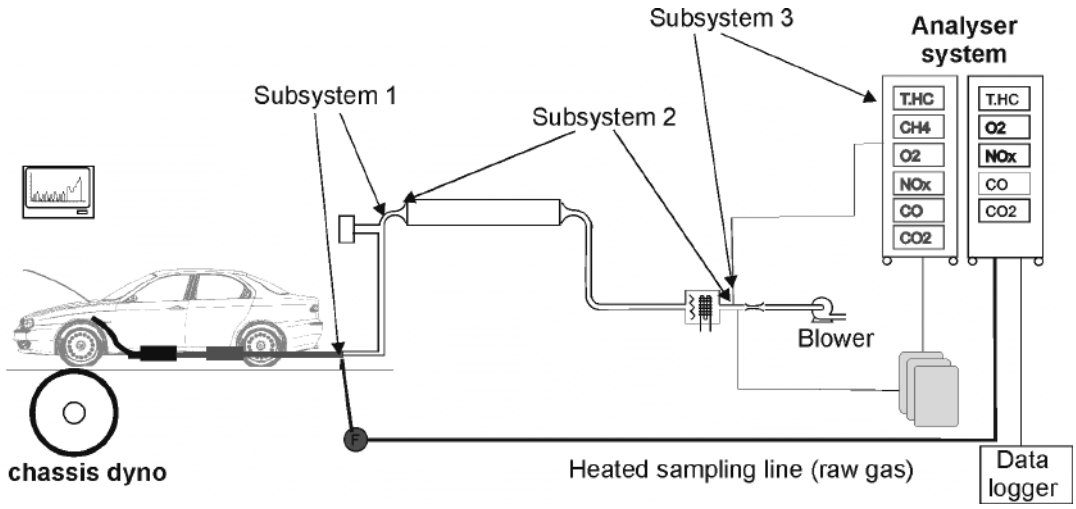

Figure 2: Set-up for the measurements.

Validation of the model

For the validation of the parameters obtained, an FTP cycle was used. No gas was injected, but the "natural" concentration signal of the car was measured at the tailpipe by fast sensors to log the input signal of the transport model. Figure 3 shows the quality of simulation compared to the measured signal at the analyser.

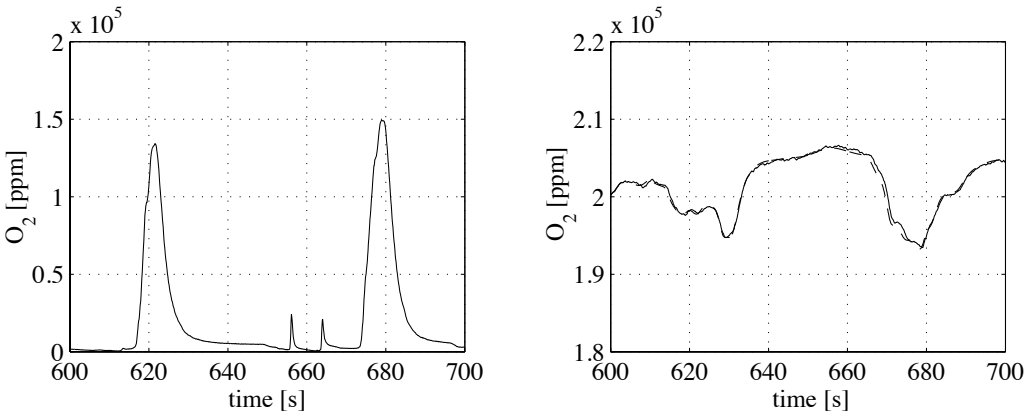

Figure 3: Result of model validation. Note: left: measured oxygen signal at the tailpipe, right: measured (solid) and simulated (dashed) oxygen signal at the analyser.

Inversion of the model

To achieve the reconstruction of the emission signal at the end of the car from the signal at the dilution analyser, this overall model must be inverted. This inversion is performed subsystem by subsystem. In each case, the input of the subsystem must be determined from the output of the subsystem. From the equations above, the solution becomes a linear function of the output's derivatives. However, since the output is a measured signal, its noise is amplified massively by building the derivatives. Therefore, the inversion has to be coupled to a low-pass filter (noise filter).

In addition, for signals such as oxygen, which is contained in both the exhaust gas and in dilution air, the reconstruction is not possible, because the signal-to-noise ratio of the measurement is too small, due to equation (2). The quality of the overall inversion is presented in Figure 4, for the NO_x signal.

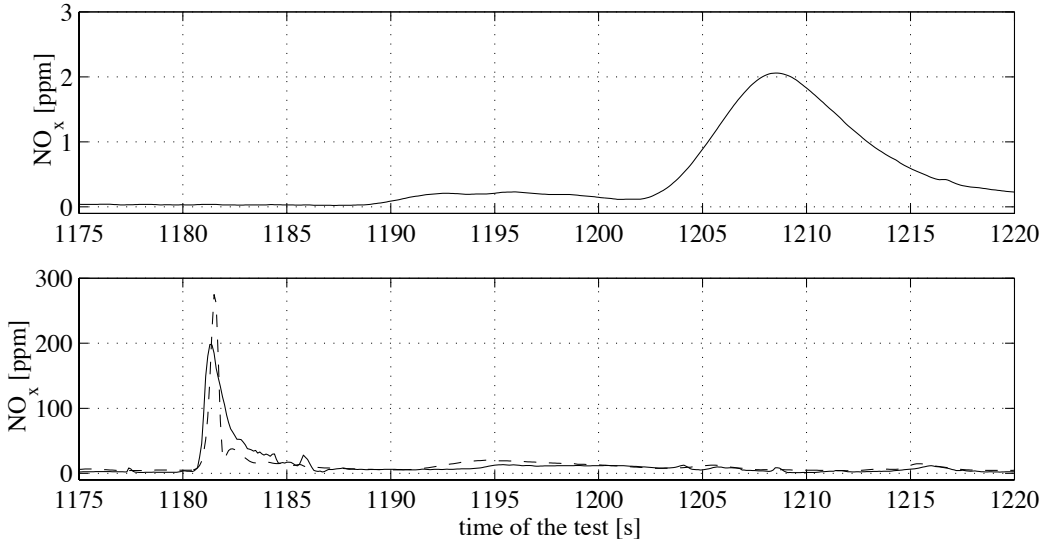

Figure 4: Result of the overall inversion. Top figure: NO_x signal at the analyser. Bottom figure: solid: reconstructed signal using the model of the dilution system, dashed: reference signal at tailpipe, obtained from raw gas measurement.

The original peak which lasts more than twelve seconds in the diluted measurements can be reconstructed to a peak of about 3.5 seconds duration. This is per se a very good result. However, the quality is roughly half as good as for the raw signal, whose peak lasts just 1.7 seconds.

2 – Static instantaneous emission model

The technologies applied in new vehicles have put the use of emission models under strain. The cars become cleaner and transient emission peaks become more and more important for the average emission factors. Therefore, the old emission models, without all the corrections described in Weilenmann et ali (2002a) and in Section One, exhibit a poor prediction quality and new approaches are needed.

A first step in improving the existing models, which allocate emissions to a speed - speed times acceleration map on 1 Hz measurements, is to fulfil the conditions of Section One. This is done by taking 10 Hz measurements and compensating for all the transport dynamics. In the next step, the mapping is changed to brake mean effective pressure and engine speed. Brake mean effective pressure (p_{me}) can be considered as "scaled" engine torque size since:

$$p_{me} = \frac{T_e \cdot 4\pi}{V_d}$$

where V_d denotes the displacement volume of the car and T_e is engine torque. Thus p_{me} is useful for the comparison of different cars.

Approach

As a first step, the emission signals were mapped on a classical speed – speed times acceleration map on 1 Hz data, as in most older models for passenger cars (Jost, Hassel et ali (1992a)).

Secondly, the emission signals, with the right time and dynamic correction, as described above, were mapped on a static basis onto speed and speed times vehicle acceleration, on a 10 Hz basis.

In a third step, the emission were mapped applying the same approach to brake mean effective pressure (p_{me}) and engine speed (n). The advantage of this new alternative of mapping derives from the fact that the influences of the vehicle loading and the gear-shift may be taken into account. The gear-shift strategies as well as the actual loading of the car have a considerable effect on emission

levels (Weilenmann 2002b, Gense 1999). This is why engine speed and mean effective pressure are more appropriate variables for the description of emissions behaviour. Additionally, the fuzziness of different gear settings at the same velocity is avoided.

To qualify the models' accuracy, the emissions calculated by the model for a certain cycle (not used for the model parameterisation) were compared with the measured emissions. This is done by choosing different cycles as verification cycles and for several cars. For the different models, the prediction quality is shown in Figure 5, for a classic, pre-Euro 1 gasoline vehicle (called hereafter "Euro-0"). The prediction quality is improved significantly from the first model to the third model.

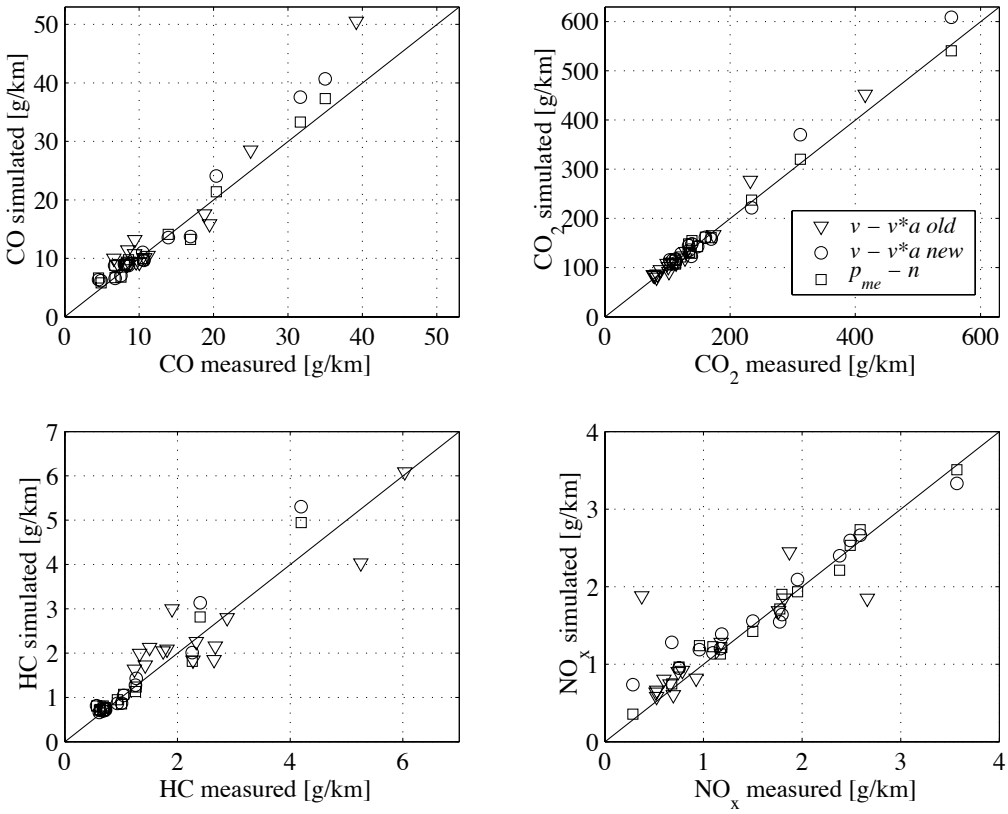

Figure 5: Emissions simulated with v - *v · a mapping without dynamic time correction (*v - *v · a* old*),* v - *v · a mapping with dynamic time correction (*v - *v · a* new*) and* p_{me} - n *mapping with dynamic time correction, compared with the measured emission values for a gasoline Euro-0 vehicle.*

The numeric qualification of the models is performed by calculating the correlation coefficient between the measured and simulated emission factors. The results for gasoline Euro-0 vehicles, diesel Euro-2 vehicles and gasoline Euro-3 vehicles are presented in Table 1.

As Figure 5 and Table 1 shows, the prediction quality improves significantly from the first to the third approach. For diesel Euro-2 cars and Euro-0 gasoline vehicles the prediction quality of the third model is near to being satisfactory. However, the prediction quality for the gasoline vehicles with a three-way catalyst is far from good. This was expected, since for these cars high emissions often arise during transient manoeuvres. Thus, since these static models do not include the dynamic behaviour of the engine, a dynamic emission model is needed.

Vehicle type	Map used	CO	CO_2	HC	NO_x
Euro-0 gasoline	v - $v \cdot a$ without time correction	0.95	0.994	0.94	*0.83*
	v - $v \cdot a$ with time correction	0.98	0.994	0.98	0.98
	p_{me} - n with time correction	0.99	0.991	0.99	1.00
Euro-3 gasoline	v - $v \cdot a$ without time correction	*0.24*	0.987	*0.32*	*0.05*
	v - $v \cdot a$ with time correction	*0.69*	0.994	*0.59*	*0.44*
	p_{me} - n with time correction	*0.73*	0.995	*0.64*	*0.50*
Euro-2 diesel	v - $v \cdot a$ without time correction	*0.73*	0.987	0.93	0.99
	v - $v \cdot a$ with time correction	*0.89*	0.992	0.95	0.99
	p_{me} - n with time correction	0.90	0.994	0.96	1.00

Table 1: The correlation coefficients for different categories of vehicles and mapping.

3 – Towards dynamic model

For the above reasons, it follows that the map should be extended by using a new variable expressing these dynamics. Such a dynamic variable might be the derivative of the manifold pressure or the derivative of torque. Figure 6 highlights the fact that emission peaks of HC are caused by peaks of derivative of manifold pressure. As it can be seen in the right part of the Figure 6, the two HC peaks cannot be drawn out of engine speed or vehicle velocity.

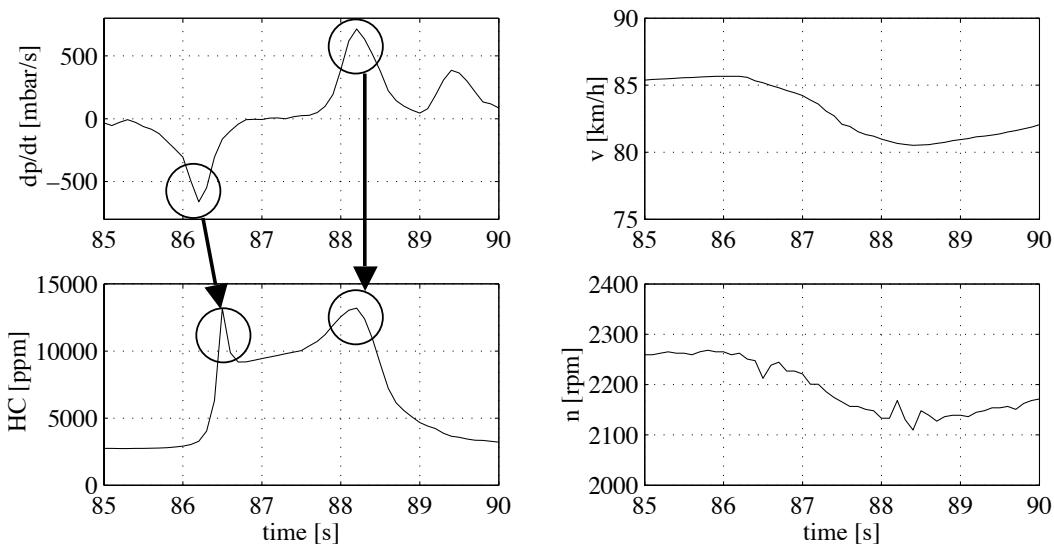

*Figure 6: Influence of derivative of manifold pressure (*dp/dt*) on emissions.*

Another element which is of great importance for the emissions level is the catalyst's behaviour. The maps used until now claim emissions to be engine output. But, it has to be taken into account that the catalyst has its own dynamics, i.e. oxygen storage dynamics. Thus, besides the engine model, a model for oxygen storage in the catalyst has to be added.

Conclusion

It has been shown that it is possible to reconstruct the emission signal at the car's tailpipe location with a time quality of about 2.5 seconds from the diluted gas emission signal, having an overall

delay of up to twenty-five seconds. This allows the emission data to be correlated with the state of their formation much better than before.

The emission maps based on engine speed and brake mean effective pressure and using 10 Hz corrected signals give better results than the classic speed and speed times acceleration map. For diesel and classic gasoline vehicles the prediction quality is near to being satisfactory, but for cars with emissions after-treatment systems the prediction is still not good enough. Extension of the model using a new dynamic variable and/or the inclusion of a catalyst model should represent new ways for the improvement of the existing model.

Acknowledgements

This work is being carried out within the Swiss emission inventory studies and within the ARTEMIS-Project (5th EU-FP). The authors wish to thank the BUWAL, the BBW and all the co-financers.

References

R. Evéquoz, M. Keller, J. Heldstab, H. Kessler (1995): Luftschadstoff-Emissionen des Strassenverkehrs 1950-2010, Schriftenreihe Umwelt Nr. 225, Swiss Agency for Environment, Forest and Landscape (BUWAL) , p 110-129.

N.L.J. Gense (2000): Driving style, fuel consumption and tailpipe emission, TNO Report oo.0R.VM.021.1/HG, TNO Automotive, Delft, Netherlands.

S. Hausberger, D. Engler, M. Ivanisin, M. Rexeis (2002): Update of the Emission Functions for Heavy Duty Vehicles in the Handbook Emission Factors for Road Traffic, elaborated on behalf of BMLFUW, BWIT, UBA, Graz, June 2002.

P. Jost, D. Hassel, F-J. Weber, K-S. Sonnborn (1992a): Emission and Fuel Consumption Modelling Based on Continuous Measurements. Deliverable No. 7 of the Drive Project V 1053 "Modelling of emissions and consumption in urban areas-MODEM", p 1-36.

P. Jost, D. Hassel, K-S. Sonnborn (1992b): Neuartige Methode zur Ermittlung von Emissionsfaktoren für NFZ. Tagungsband Abgasemissionen und Immissionen durch den Strassenverkehr, Mittelung des Institutes für VKM und Thermodynamik der TU-Graz, Heft Nr. 64.

M. Keller, P. Koch, J. Heldstab, B. Dähler Staub, P. de Haan (1999): Handbook Emission Factors for Road Transport, UBA Berlin und BUWAL Bern, produced by INFRAS Bern, CD.

L.Pritscher, W. Stahel, P. de Haan (1999): Emissionfaktoren im Strassenverkehr : Betrachtungen zu Prüfsatndmessungen der EMPA, BUWAL Arbeitsunterlage 9 zu Bericht-SRU NR. 255, Swiss Agency for Environment, Forest and Landscape (BUWAL), Bern.

Th. Sams, J. Tieber, G. Pretterhofer (1992): Verifizierung von hochgerechneten dynamischen NFZ-Emissionen, Tagungsband Abgasemissionen und Imissionen durch den Strassenverkehr, Mittelung des Institutes für VKM und Thermodynamik der TU-Graz, Heft Nr. 64.

M. Weilenmann, C. Bach, C. Rüdy (2001): Aspect of Instantaneous Emission Measurement, International Journal of Vehicle Design, vol. 27, p 94-104.

M. Weilenmann, P. Soltic, D. Ajtay (2002a): Describing and Compensating Gas Transport Dynamics for Accurate Instantaneous Emission Measurement, Int. Symp. "Transport and air pollution", Graz, Austria, vol. 1, p 155-162.

M. Weilenmann (2002b): Emissionen und Verbrauch bei Eco-Drive, EMPA Report, Nr. 201209e, Swiss Federal Laboratories for Materials testing and Research (EMPA), Switzerland.

12th International Symposium "Transport and Air Pollution" / 12e Colloque international "Transports et pollution de l'air", Avignon, 16 -18 *June* / juin 2003
proceedings / actes, n°92, tome / Vol. 1, Inrets ed., Arcueil, France, 2003, p. 145-152

PM regulation for 2-stroke two-wheelers: Necessity or haphazard legislation?

Rudolf Rijkeboer*, Dion Bremmers*, Zissis Samaras & Leonidas Ntziachristos****
*TNO-Automotive, postbox 6033, NL 2600 JA Delft, the Netherlands.
Fax +31-15-269 68 74 - email: rijkeboer@wt.tno.nl
**Lab. of Applied Thermodynamics, Aristotle University Thessaloniki, GR 54124 Thessaloniki, Greece.

Abstract
Although interest in particulate emissions has increased considerably during recent years, the subject of PM-emissions from small 2-stroke engines is still largely unexplored. This paper presents the results of an investigation, which examined the typical emission level and the typical characteristics of 2-stroke PM, as well as the possible impact on the (urban) environment, all in comparison to diesel engines. Attention was also paid to the possible problems concerning the measurement of 2-stroke PM and the possibilities to add a PM requirement to the moped type approval procedure.
***Key words**: particulate emission, two-stroke, moped, motorcycle, legislation*

Résumé
Malgré les efforts de recherche pendant les dernières années sur les émissions de particules, les émissions de particules des moteurs á deux temps sont encore un sujet largement inexploré. Ce papier présente les résultats d'une étude qui concerne les niveaux typiques d'émission et les caractéristiques physiques des particules des moteurs à deux temps, ainsi que leurs impacts sur l'environnement urbain, en les comparant aux particules diesel. De plus, les problèmes concernant la mesure des particules d' un moteur á deux temps et la possibilité d'ajouter une condition au regard des particules dans la réglementation des cyclomoteurs ont aussi été étudiés.

Introduction

The reduction of particulate emission levels from diesel vehicles has shifted the attention to emissions from other vehicles as well. At European level, this led to a desire on the part of the European Parliament and the EU Environment Council to introduce a particulate matter (PM) requirement into the emission legislation for mopeds. This legislation was introduced at a first stage in 1999, with a second stage in 2002. In this context, the main question was to indicate under what conditions a PM-requirement could be incorporated in the third step of the moped legislation, envisaged for 2006. This paper presents an overview of a study (Rijkeboer et al., 2003) sponsored by the European Commission, which had as main objective to map out the problem and to provide input for a possible answer to the above question. The authors made a literature survey, did experimental work on existing small 2-stroke engines, identified the possible and likely pitfalls concerning the measurement of such emissions, made expert judgments as to the likely future developments, and made overall calculations as to the urgency of such legislation. This resulted to a set of detailed conclusions and recommendations to the Commission, as regards the future emission legislation for small 2-stroke powered two-wheeled vehicles (PTWs).

1 - Quantifying the emissions

The typical PM-emission levels shown in Table 1 emerged from a literature survey. The diesel vehicle emission factor originates from COPERT III model (Ntziachristos and Samaras, 2000a), while motorcycle emission factors correspond to ECE-47 cycle tests for mopeds (Santino et al., 2001) and to ECE-40 or similar cycle for motorcycles (Palke and Tyo, 1999; Kojima et al., 2002). These figures suggest that in comparison to diesel engines the level of PM-emission of small 2-stroke engines does certainly justify further investigation. They also suggest that there may be ways to deal with the problem in an adequate manner: the emission levels of the catalyst equipped PTWs lie in the order of the Euro 3 and 4 diesel passenger car legislation (50 and 25 mg/km respectively).

Vehicle	Average speed (cycle) [km/h]	Emission factor [mg/km]
Diesel Passenger Car Euro 1	25	91
Non-catalyst moped	~30 (ECE-47)	172
Catalyst moped	~30 (ECE-47)	43
Non-catalyst motorcycle 100 cm³	~25 (ECE-40)	330 (190 – 470)[1]
Catalyst motorcycle 100 cm³	~25 (ECE-40)	10 - 20

[1] Kojima et al., 2002 report a range of 0,16-2,7 g/km but a more conservative range was adopted here to exclude some extreme situations reported in this particular paper.

Table 1: Typical PM-emission factors of mopeds in comparison to diesel engine passenger cars.

2 - Characterising the emissions

Practically all literature sources indicate that there is a significant difference between diesel PM and 2-stroke PM. While the first contains a large fraction of solid carbon (diesel "soot" – mainly elemental carbon), the latter consists mainly of condensed heavy hydrocarbons (organic carbon). Volatile fractions in the order of 90–99 % are frequently mentioned (e.g. Kojima et al., 2002). Several investigators indicate that the main source of this volatile fraction is the typical 2-stroke lubricating oil. The second major source is the scavenging of heavy hydrocarbons from the fuel; on a conventional 2-stroke about 30–40 % of the fuel supplied is passing straight through the engine.

In order to reveal the physical character of particulates, measurements of number concentrations, number based size distributions and diffusion-active surface were performed with two different dilution and sampling configurations, using both a mini-dilution system installed at the exhaust pipe outlet (more information can be found in Samaras et al., 2002 and Ntziachristos et al., 2003) and at the full dilution tunnel of the diesel legislation. Size distribution was measured using a TSI Scanning Particle Mobility Sizer (SMPS), number counts were performed with a TSI Condensation Particle Counter (CPC) and active surface was measured with a Dekati Diffusion Charger. Active surface is a measure of the particle surface which is available for diffusion of foreign species and is of significance for all processes involving adsorption and desorption (e.g. atmospheric reactions, desorption of materials after particle inhalation, etc.).The SMPS system classifies particles according to their mobility diameter in contrast to impactors which classify particles according to aerodynamic diameter.

The particle size distribution at low speeds was characterised by a log-normal distribution with a peak value at ~100 nm, which is commonly referred to as "accumulation mode" (Figure 1a). At higher speeds, the numbers of this accumulation mode tend to rise over one order of magnitude, but an additional mode develops at 20–30 nm, which is about one order of magnitude higher in number than the accumulation mode peak and is usually named as "nucleation mode". With this behaviour 2-stroke PM again differs significantly from diesel PM, as Table 2 shows. It appeared that this high nucleation mode consisted mainly or exclusively of condensed HC. Also, sulphates formed from fuel and lubricant sulphur contribute to the formation of nucleation mode. This is also common in diesel vehicle emissions.

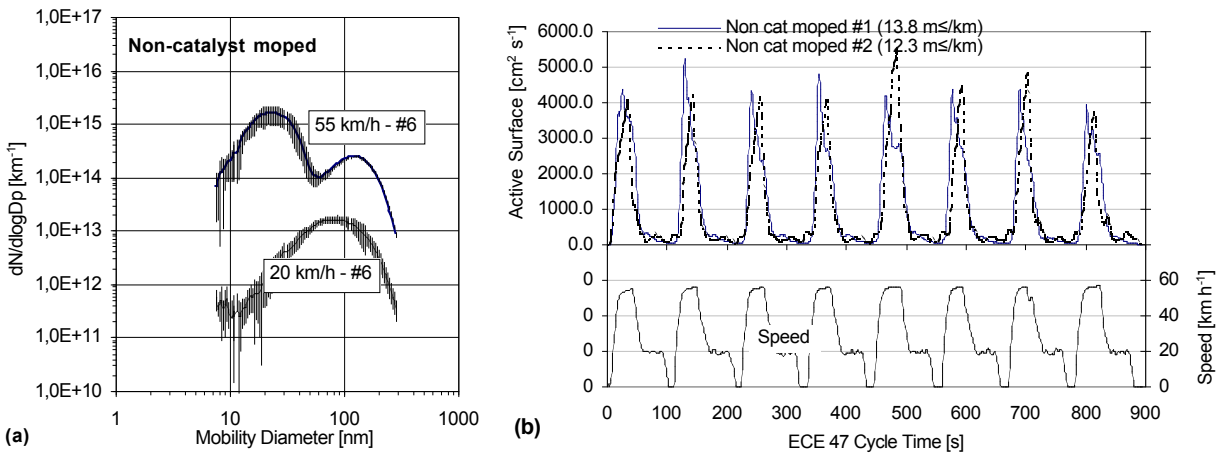

Figure 1: (a) Total particle distributions (in km^{-1}) for a moped, recorded with the SMPS. Means of six scans (#6). The range shows ± 1 standard deviation of the concentration for each particle size. (b) Active surface recorded with the diffusion charger over the ECE 47 for two mopeds. In both cases, sampling and dilution was performed with a mini-dilution system. Numbers in the legend correspond to mean active surface of particles over the cycle.

125 cm^3 2-stroke w/o aftertreatment	Operating condition or cycle	Significant diameter range [nm]	Peak occurs at [nm]	Number per km at peak(s) [dN/dlogD$_p$ 10^{14}·km^{-1})]
Steady state	Idle	20-200	80	-
	30 km/h	15-150	20[(1)] and 40	- and 1.9
	50 km/h	15-130	35	21
	70 km/h	15-120	30-35	11
	90 km/h	15-120	25-30	7.5
Transient cycle[(3)]	ECE-40	20-100[(2)]	20[(1)] and 60	6.6 and 3.2
	FHB urban	20-100[(2)]	20[(1)] and 60	5 and 4
	FHB suburban	20-100[(2)]	30	9.5
1.9 L TDI diesel car	50 km/h	15-600	90	0.44
	70 km/h	15-600	80	0.57
	100 km/h	15-600	80	1
	ECE-15 (UDC)	30-250[(4)]	80	1

(1) bimodal (2) measurements at 20, 30, 60 and 100 nm
(3) FHB cycles are real-world cycles: see Czerwinski, 1995
(4) measurements at 30, 60, 80, 100, 150 and 250 nm

Table 2: Summary of the particle size measurements with the SMPS. Sampling performed at the dilution tunnel.

Real time recordings of particle active surface (presented in Figure 1b) have shown that high surface concentrations occur mainly during accelerations and not at steady speed driving. Absolute levels of surface concentrations determined were 13,8 m²/km and 12,3 m²/km respectively for two non-catalyst mopeds over the ECE-47 cycle, for which the corresponding mass emissions rates were 135 and 172 mg/km. To provide a frame of reference, carbonaceous particles are associated with geometric surfaces in the order of 50–150 m²/g. Hence, a range of 6,5–28 m²/km should be expected if particles emitted were only carbonaceous. The values reported for our PTWs are within this range and differentiations occur because of the high volatile fraction and differences in the definitions of geometric and active surface. The high surface concentration per distance driven suggests that current PTWs may be significant contributors to atmospheric photochemical reactions and gas-to-particle transformations.

3 - The expected contribution in an urban inventory

Usually, urban emission inventories consider only exhaust PM emissions from four-wheel or larger vehicles, because only those emissions received focus in the past. In this section we attempt to approach the contribution of PM emissions from mopeds in an urban inventory. Two different sources are used comparatively. The first is the database of the "Co-ordinated European Programme on Particulate Matter Emission Inventories, Projections and Guidance" (CEPMEIP, 2002), an EMEP/EEA initiative aimed at establishing a consistent PM inventory for Europe. The second source is the combination of activity data used for the compilation of the European Environmental Agency's (EEA) central estimates for road transport air emissions (Ntziachristos et al., 2002) in combination with the PM emission levels established for mopeds in this project. Two countries were selected for the comparison. France with a large fraction of diesel passenger cars (~20 %) and a typical central European fraction of mopeds; and Greece where diesel vehicles are practically limited to taxis only (1–2 %) due to a diesel-ban legislation, and a large fraction of mopeds common in southern Europe.

	France		Greece	
	Diesel PCs	Mopeds	Diesel PCs	Mopeds
Annual activity rate [10^6 veh.km]	46200	9800	2500	6500
Emission factor [g/km]	0.085	0.120	0.90	0.120
Total annual emissions [t]	3905	1180	225	780
Moped emissions as a fraction of diesel PCs [%]	30.3		349	

Table 3: Estimation of moped contribution to exhaust PM_{10} emissions in urban inventories for the year 1995 according to CEPMEIP.

	France		Greece	
	Diesel PCs	Mopeds	Diesel PCs	Mopeds
Annual activity rate [10^6 veh.km]	28200	3080	1475	3270
Emission factor [g/km]	0.110	0.153	0.190	0.153
Total annual emissions [t]	3210	470	275	500
Moped emissions as a fraction of diesel PCs [%]	14.7		180	

Table 4: Estimation of moped contribution to exhaust PM_{10} emissions in urban inventories for the year 2002 according to EEA's data and emission factor data of this project.

Table 3 shows the data of CEPMEIP database in the year 1995. For the sake of this comparison, the results are limited to exhaust emissions and mopeds only, excluding non-exhaust emissions and other PTWs. Table 4 shows data for the year 2002, using the EEA's activity data and the moped emission factors presented in this project. Differences in activity data occur due to different estimations in each case. The last rows of both tables present the moped contribution to PM_{10} emissions, expressed as fraction of diesel passenger car PM emissions. The results indicate that despite the significant uncertainties in the estimation of activity data and emission factors, two independent sources show that urban PM contributions from mopeds cannot be neglected even for significantly dieselised countries like France and can exceed the diesel PC's contribution in special cases as in Greece.

4 - Typical measurement aspects

The measurement of particulate mass emissions or particle distribution characteristics from engine exhaust is prone to sampling artefacts because of the sensitivity of the exhaust aerosol to sampling conditions. The following phenomena can be indicated as the most important processes affecting aerosol characteristics (Ntziachristos and Samaras, 2000b):

- Thermophoresis. It may cause particle loss to the walls of the sampling line due to temperature gradient between the exhaust flow and the walls.

- Diffusiophoresis. It may cause particle loss to the walls of the sampling line due the Brownian motion of particles. It increases with decreasing particle size.
- Coagulation. It shifts the size distribution to larger diameters. It depends on concentration, temperature and particle size.
- Condensation. It causes particle growth, as volatile hydrocarbons or sulphuric acid may condense onto existing particles. It may cause particle formation, as volatiles may even condense to form droplets.

Due to the liquid nature of 2-stroke particle emissions, such phenomena are more important with mopeds than diesel engines and one needs to take their effect into account when sampling 2-stroke exhaust aerosol. All the processes mentioned here are promoted by longer sampling lines (i.e. longer residence time). Deposits on the exhaust pipes and sampling lines from former measurements ("hang-ups") pose an additional risk. Indeed our experiments showed that total particle concentration is the most variable of all metrics reported. The coefficients of variation reach values which would normally be unacceptable (>50%) to support repeatable measurements.

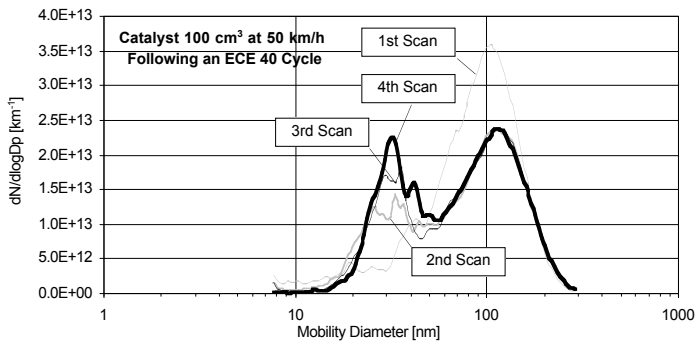

Figure 2: Shift of the particle size distribution with time, under 50 km/h steady state speed testing. All gaseous pollutant emission rates and exhaust gas temperatures were stabilised prior to recording the particle concentration.

The experiments also suggested that the operational history of the vehicle might be a significant additional factor (see also Czerwinski et al., 2002). Evaluation of our results showed that in general the nucleation mode (<50 nm) is more variable than the accumulation mode. Especially in the case of a catalyst equipped small bike (100 cm^3), where the accumulation mode is quite constant, the nucleation mode is so variable that it almost changes the shape of the distribution. Focusing on the total particle size distribution of this particular vehicle, Figure 2 presents the average of 4 SMPS scans, when the vehicle is driven at 50 km/h. Before the first scan, the vehicle was thermally stabilised for about 5 min at this speed. The scans in Figure 2 have been taken at 2 min time intervals. During the first scan, no nucleation mode is visible but only an accumulation mode with a peak at 101 nm. This gradually changes and the final scan presents a high nucleation mode and a much reduced accumulation mode with a peak at 102 nm. It is clear that, despite the stabilised conditions, particle emission follows a dynamic pattern. One may hypothesise an explanation: the actual size distribution shape is a function of the equilibrium conditions between the solid and vapour state of volatile substances present in the exhaust gases. Especially in the case of 2-stroke engines, a large concentration of lubrication oil hydrocarbons and sulphates is found in the exhaust gases. Hence, depending on the operational state of the engine and its operation history, such substances may adsorb or desorb from the walls and respectively suppress or promote the formation of nanoparticles. If this is true, then operation at 50 km/h can heat up the exhaust system, causing subsequent desorption of condensable species, which gradually form the nucleation mode as seen in Figure 2. Such transient phenomena, occurring under steady state vehicle and sampling conditions, originate from the volatility of PTW particle emissions and may bring complications to the definition and sampling of a representative PM measurement.

5 - Outlook to the future

PM emissions from conventional 2-stroke engines have been shown to consist mainly of unburned or partially oxidised heavy hydrocarbons and sulphates, either originating from the lubrication oil or from the fuel, due to the scavenging process. A modern trend is to apply the lubricant from a special tank by means of a pressure pump, in order to adapt the lubrication rate to the minimum required, depending on the engine load. In that respect, Sakai et al. (1999), Patschull and Roth (1994) and White et al. (1997) report that reducing the oil to fuel ratio can significantly reduce PM emissions, and also decrease the particle number concentration. Additionally, several studies revealed that emission reduction is possible with the use of synthetic lubrication oils rather than mineral-based ones (Yashiro, 1991; Sakai et al., 1999; Patschull and Roth, 1994; White et al., 1997). It is expected that in the near to midterm future a shift towards the use of synthetic oil will take place, enabling the usage of even lower dosages. In parallel, there is the reasonable expectation that in stage 3 legislation (foreseen for 2006, see "Introduction") there will be a widespread application of oxidation catalysts, which have good oxidation rates especially for synthetic lubricants.

From the engine side, the direct-injection (DI) 2-stroke has been developed, where the fuel is directly injected into the cylinder, after the closing of all ports. The fuel is then effectively trapped into the cylinder and cannot escape into the exhaust. In this case lubricant is not added in the fuel but is separately provided and also no fuel is present in the crankcase. Therefore, fuel does not dilute the lubricant, as in the case of conventional engines, allowing the use of lower lubricant dosages. In combination, this means a strongly reduced use of lubricant.

The above lead to the expectation that from legislative stage 1 (1999) onwards, the PM emission of small 2-stroke engines will be drastically reduced. There is also the likelihood that manufacturers will pursue this route even without a specific PM-requirement being added, in order to fulfil the stringent HC emission standards already set from legislation stage 2 (2002).

6 - The possibilities for a PM legislation

There is currently an on-going discussion on the evolution of type approval legislation with regard to particulate emissions of light and heavy-duty diesel vehicles, in the light of the continuously decreasing vehicle emission levels. Improvements in the existing legislation aim at increasing the sensitivity and repeatability of the measuring procedure in order to increase the accuracy of the measurement. At EU level this discussion is extended now to cover PM emissions from 2-stroke vehicles. The relevant legislative bodies were obviously hopeful that the existing equipment and procedure for the measurement of diesel particulates would be adequate for 2-stroke engines as well. Compared to the emissions of diesel vehicles, there are, however, two variables, which may force modifications of the procedure to accommodate 2-stroke emissions:

- The concentration of the PM in the exhaust of PTWs.
- The nature of the PM, and in particular their high volatile fraction.

With regard to the first point, the values reported in this paper show that the concentration is such that the actual emission rates of current PTWs can reach or even exceed the respective concentration of today's diesel passenger cars, even in the case of catalyst equipped PTWs. If this conclusion would be established over a larger sample of vehicles, this would mean that current CVS installations for passenger cars might provide the necessary sensitivity for PM emission recordings also from current PTWs. What our outlook for the future shows though, is that emission levels will significantly decrease. Under such circumstances the current CVS procedure may no longer be sufficiently sensitive.

In any case, measures need to be taken to obtain representative PM emission rates from current and future PTWs, given the volatility of the emitted aerosol. The main parameters, which may affect the emission result when using a CVS to sample PM were identified as:

- The CVS dilution factor and the CVS total flow rate.

- The dilution system designs (open or closed CVS; single stage or two-staged).
- The filter face velocity, filter material and filter loading, plus the use or not of a back-up filter.
- Filter temperature (highly important in view of the extended range in condensation points of the heavy HCs involved).
- Sample pre-treatment and CVS and sample line cleanliness.

In case that a CVS procedure is adopted for PTW PM sampling, a specific project aiming at a parametric study of the effect of these parameters would be strongly recommended. Although the existing equipment proved adequate to establish an order of magnitude of the PM-emissions of current 2-stroke PTWs, the requirements of a legal certification procedure demand greater accuracy, whereas the likely technologies of the near future may further complicate the issue. To this may be further added the fact that as yet there is no understanding of the importance of the volatile fraction, and more especially the nucleation mode, for the possible health effects of typical 2-stroke PM emissions.

Conclusions and recommendations

On the basis of all the above the authors came to the following conclusions and recommendations:

- Current CVS technique is likely not to be adequate for reproducible 2-stroke PM measurements in the future. But lacking further information no serious recommendation can be made at this moment as to the possible improvements needed to render this procedure suitable for use on 2-stroke engine PM emissions.
- The large variations observed are mainly caused by the dominant nucleation mode, which is very prone to artefacts. Therefore more understanding is needed about the reality of the observed nucleation mode and its behaviour under real-world circumstances. Only in that way meaningful conclusions can be drawn concerning the way sampling conditions should be optimised.
- Adequate understanding of the health effects of engine produced PM emission ought to be the basis of any legislative limitation of such emissions. Yet such understanding is still largely lacking, especially in the case of 2-stroke particulates. All we know is that 2-stroke particulates differ significantly from diesel particulate, inter alia in that they contain a dominant volatile fraction. In the absence of such understanding it is impossible to target the really relevant aspects of 2-stroke PM emissions. This could lead to a method that targets a possibly less harmful bulk with the unwanted secondary effect that the really harmful fraction gets lost in its variation.
- Since the major part of 2-stroke PM consists of (volatile) organic material, in the case of a legislation addressing particulates as well, this organic material is likely being measured twice: once as gaseous hydrocarbons, and another time in another sampling line, as 'particulates'. Such a situation also exists in diesel engines too, but the effect is more pronounced in the case of 2-stroke engines. This in turn means that the PM emission from 2-strokes is in fact already largely included in the NDIR measurement of HC emission. This statement is further supported by the fact that PTWs designed for compliance with future legislative steps also exhibit lower PM emissions. Hence a second, separate measurement as 'particulate matter' may be less urgent. It was therefore recommended that the best short-time solution would be to guarantee that the emission of heavy hydrocarbons is indeed measured in full. This could require the use of a heated sampling line and a heated FID, as in the case of diesel engine HC measurement.

Acknowledgments

The authors gratefully acknowledge the financial support to this work of the European Commission, Enterprise Directorate General, in the framework of the study contract No FIF.20010701. Special thanks go to Dr. Paul Greening (European Commission) for his valuable remarks and comments.

References

CEPMEIP (2002): Co-ordinated European Programme on Particulate Matter Emission Inventories, Projections and Guidance, 2002, http://www.air.sk/tno/cepmeip/.

Czerwinski J. (1995): Vorstudie zwecks besserer Erfassung der Fahrdynamik und Aktualisierung der Emissionsfaktoren von Zweirädern. BUWAL Arbeitsunterlagen Nr. 2, Bericht B026 z. Hd. BUWAL

Bern, Switzerland, 73 p.

Czerwinski J., P. Comte, S. Napoli & P. Wili (2002): Summer cold start and nanoparticulates of small scooters. SAE Technical Paper No. 2002-01-1096.

Kojima M., R.W. Bacon, J. Shah, M.S. Mainkar, M.K. Chaudhari, B. Bhanot, N.V. Iyer, A. Smith & W.D. Atkinson (2002): Measurement of mass emissions from in-use two-stroke engine three-wheelers in South Asia. SAE Technical Paper No. 2002-01-1681.

Ntziachristos L. & Z. Samaras (2000a): COPERT III - Computer {rogramme to calculate Emissions from Road Transport - Methodology and emissions factors (version. 2.1). Technical Report 49, European Environment Agency, Copenhagen, Denmark, 86 p.

Ntziachristos L. & Z. Samaras (2000b): Sampling conditions effects on real-time particle measurements from a light-duty vehicle. SAE Transactions 2000-01-2049, J. of Fuels and Lubricants, Vol. 109, pp. 2177–2189.

Ntziachristos L., P.M. Tourlou, Z. Samaras, S. Geivanidis & A. Andrias (2002): National and central estimates for air emissions from road transport. Technical Report 74, European Environment Agency, Copenhagen, Denmark, 60 p.

Ntziachristos L., B. Giechaskiel, P. Pistikopoulos, E. Fysikas & Z. Samaras (2003): Particle emissions characteristics of different on-road vehicles. SAE Technical Paper No. 2003-01-1888.

Palke D.R. & M.A. Tyo (1999): The impact of catalytic aftertreatment on particulate matter emissions from small motorcycles. SAE Technical Paper No. 1999-01-3299.

Patschull J. & P. Roth (1994): Measurement and reduction of particles emitted from a two-stroke engine. SAE Technical Paper No. 941683.

Sakai T., T. Nakajima & H. Yamazaki (1999): O-PM / emitted matters caused by two-stroke engine oil and its reduction. SAE Technical Paper No. 1999-01-3260.

Santino D., P. Picini & L. Martino (2001): Particulate matter emissions from two-stroke mopeds. SAE Technical Paper No. 2001-24-0068.

Rijkeboer R.C., D.A.C.M. Bremmers, Z. Samaras & L. Ntziachristos (2003): Emission regulation of PTWs. Final report to the European Commission under contract FIF.20010701. TNO report 03.OR.VM.004.1/RR (main report), Delft, the Netherlands, 105 p.

Samaras Z., L. Ntziachristos & B. Giehaskiel (2002): Characterisation of exhaust particulate emissions from road vehicles. Proc. Fisita 2002 Congress, 2–7 June, 2002, Helsinki, Finland.

Yashiro Y. and Takahashi K. (1999): Evaluation method of exhaust smoke of two-stroke engine oils. SAE Technical Paper No. 911280.

White J., J. Caroll & H. Haines (1997): Emissions from snowmobile engines using bio-based fuels and lubricants. SAE Technical Paper No.972108.

12th International Symposium "Transport and Air Pollution" / 12e Colloque international "Transports et pollution de l'air", Avignon, 16 -18 *June* / juin 2003
proceedings / actes, n°92, tome / Vol. 1, Inrets ed., Arcueil, France, 2003, p. 153-160

N_2O-emissions of LD and HD vehicles

Iddo Riemersma, Robin Vermeulen, Raymond Gense, Richard Smokers
TNO Automotive, P.O. Box 6033, 2600 JA Delft, the Netherlands
Fax +31 15 269 68 74 - email : riemersma@wt.tno.nl

Abstract
In an elaborate measurement programme, with 45 passenger cars and 33 trucks and buses, the N_2O-emissions of LD and HD vehicles have been measured and factors influencing these emissions have been assessed. The measured N_2O-emissions of LD vehicles are much smaller than the value used by the IPCC. N_2O-emissions of future LD vehicles are expected to be even lower. Catalyst ageing is found to have adverse effects on the N_2O-emissions of LD vehicles. The N_2O-emissions of Euro 1 to 3 HD vehicles are also much smaller than the value used by the IPCC. The use of aftertreatment systems such as SCR-deNOx and EGR with CRT filter in Euro 4 and 5 vehicles, however, is expected to cause a significant increase in N_2O-emissions. N_2O-emissions do not straightforwardly correlate with NO_x-emissions and can therefore not be estimated on the basis of measured NO_x-emissions.
Keys-words*: N_2O-emissions, greenhouse gases, LD vehicles, HD vehicles, emission factors*

Introduction

N_2O is known to be a greenhouse gas with a high global warming potential, approximately 296 times higher than that of CO_2. In road vehicles N_2O is mostly formed by reactions in the exhaust catalyst. The IPCC (Intergovernmental Panel on Climate Change) uses emission factors from research performed in the late 1980's and early 1990's to calculate the contribution of road traffic to the global emission of N_2O. However, in the last decades much has changed with respect to vehicle technology. Furthermore, the currently available N_2O-emission factors for LD vehicles are based on only a few measurements, while for HD vehicles they have been extrapolated from the LD emission factors by an assumed correlation with NO_x-emissions. Because of the high global warming potential, a clear need exists to derive reliable emission factors for N_2O that reflect the past, present and expected future contribution from traffic.

On behalf of the Dutch Ministry of VROM -responsible for environmental issues- TNO Automotive (in co-operation with TNO MEP) has performed a research project for LD-vehicles to address among other things the following issues:

- What are the typical values for N_2O-emission from passenger cars?
- What factors influence the temperature of a three-way catalyst and what is the resulting effect on N_2O-emissions?
- Is there a link between N_2O- and NO_x-emissions?
- Which influence does catalyst ageing have on N_2O-emissions?
- What is the influence of the sulphur content in petrol on the emission of N_2O?
- What is the influence of real-world driving?

Subsequently, a similar project has been executed to assess the N_2O-emissions of HD vehicles, with engine technologies meeting emission standards ranging from Euro 1 to Euro 5. Special interest was paid to vehicles with exhaust gas aftertreatment devices, such as urea SCR-deNOx systems and CRT. The platinum used in the catalysts of these systems is known to produce N_2O-emissions within

a certain temperature window.

This paper describes the set-up and testing details of both projects. Based on the measured N_2O levels, the identified issues for LD and HD vehicles are addressed. Finally, representative emission factors are derived for both vehicle categories.

1 – N_2O formation in vehicle catalysts

N_2O is not or hardly not formed in the combustion process in gasoline and diesel engines. The tailpipe emissions of vehicles equipped with catalysts, however, do generally show significant N_2O-concentration. A literature survey was performed by TNO to find relevant literature sources on this subject. The results can be found in Feijen-Jeurissen et al. (2001). In principle all platinum containing catalysts may produce N_2O under specific conditions. N_2O-formation, however, is most prominent in three-way catalysts of vehicles with stoichiometric otto engines.

Three-way catalysts

In a three-way catalyst (TWC) NO is reduced to N_2 by means of reactions with CO and HC. NO-conversion starts at catalyst temperatures above 200 ºC, and reaches over 90% conversion efficiency at temperatures above 350 ºC. In the same temperature window, however, also N_2O-formation is observed, with a maximum around 280 ºC. The formation of N_2O originates from the simultaneous presence of molecular NO and N-atoms adsorbed at the catalyst surface. Molecular NO-adsorption occurs only at low catalyst temperatures. At higher temperatures NO dissociates leading to a higher concentration of atomic N on the surface, resulting in a shift in selectivity from N_2O to N_2. At temperatures above 400 ºC the shift towards N_2-formation is further enhanced by decomposition reactions of N_2O to N_2 downstream in the catalyst bed. As the N_2O decomposition reactions are very sensitive to the concentrations of sulphur, oxygen, water, CO and NO, tailpipe N_2O-emissions are expected to increase as a result of catalyst ageing and the sulphur content of the fuel. Due to the temperature dependence N_2O-formation will mostly occur in the cold start phase when the catalyst is warming up. However, N_2O-formation is also possible at higher catalyst temperatures as a result of deviations from stoichiometric conditions. N_2O-emissions are therefore expected to increase under dynamic driving conditions.

Other catalysts

Direct-injection gasoline engines can not employ a TWC when operated under lean conditions. With the increased availability of low-sulphur fuel future DI-gasoline vehicles will be equipped with NO_x-storage catalysts. These catalysts may produce N_2O, both during the normal lean operating conditions and during regeneration. An additional disadvantage with respect to N_2O-formation is the relatively low temperature of exhaust gases of lean burn engines.

Diesel engines always operate under lean conditions and are characterised by high NO_x-emissions. Passenger car diesel engines are generally equipped with oxidation catalysts. Truck engines are expected to be equipped with exhaust aftertreatment systems in 2005 and beyond to meet Euro 4 emissions standards. Based on available research, oxidation catalysts for HD engines are expected to produce N_2O-emissions. Platinum catalysed particulate filters (e.g. CRT and CSF) are also expected to produce N_2O as a result of selective catalytic conversion of NO_x by hydrocarbons.

Based on experimental research, SCR-deNOx catalysts using urea or NH_3 with an active and selective catalyst, e.g. titania-vanadia, are not expected to produce N_2O at temperatures below 450 ºC. Above that temperature non-selective oxidation of NH_3 into N_2O and NO_x may occur. The use of an additional oxidation catalyst for removal of NH_3 is also a potential source of N_2O. In laboratory scale experiments high N_2O-formation is also observed in the platinum catalysts of prototype SCR-deNOx catalysts using hydrocarbons as reductant.

2 – N_2O-emissions of LD vehicles

The measurements on passenger cars were carried out in two consecutive measurement programs.

At first a "Screening Programme" was carried out on a large number of vehicles to investigate the nature and size of N_2O-emissions from passenger cars and their dependence on various vehicle and driving parameters. In a second "Extended Programme" more detailed measurements were performed on a limited number of vehicles to answer questions derived from the results of the "Screening Programme".

Measurement programme

In the "Screening Programme" 45 passenger cars (on petrol, diesel and LPG) and one hybrid electric vehicle were tested on the European Driving Cycle. N_2O was measured real-time, while regulated emissions were measured in bags. In the "Extended Programme" 10 passenger cars on petrol (with three-way catalyst) were driven over the European Driving Cycle as well as a real-world driving cycle, for which the Common Artemis Driving Cycle (CADC) was selected (ref. de Haan & Keller (2001)). The CADC consists of three specific parts, namely urban driving, rural road and motorway. Table 1 shows the vehicle selection for both the "Screening Programme" and the "Extended Programme".

		"Screening Programme"		"Extended Programme"		
Fuel	Legislative Category	Sample size [-]	Average mileage [km]	Sample size [-]	Average mileage [km]	Year of production
Petrol	Euro 1	24	88,700	5	1.1,570	1993...1996
	Euro 2	6	43,000	3	37,950	1996...2000
	Euro 3	2	20,000	2	16,040	2000...
Petrol hybrid	Euro 3	1	10,000			2000
Diesel	15-04	1	213,000			1993
	Euro 1	2	200,100			1993...1996
	Euro 2	4	60,600			1996...2000
	Euro 3	2	9,300			2000...
LPG	Euro 2	3	60,700			1996...2000

Table 1: The vehicle samples for the "Screening Programme" and "Extended Programme".

Tests were carried out with engine start temperatures of 9ºC, 20ºC and with a hot start. In all tests real-time measurements were made of N_2O, temperature, lambda and the regulated emissions before and after the catalyst. Also the effects of catalyst ageing and of low sulphur fuel were investigated. The influence of catalyst ageing was examined by measuring the emissions on 5 vehicles first with aged catalysts, and then with a new catalyst (after 3000 km of driving). The influence of fuel sulphur content was examined by comparing the results of initial tests on 5 vehicles with high sulphur petrol with the results of tests performed with low sulphur petrol after conditioning the catalyst by driving 2 tanks of low sulphur petrol.

For real-time sampling of N_2O before and after the catalyst a Thermo Environmental Instruments Model 46C N_2O chemoluminescent analyser was used. The measuring range used was 0,3 ppm to 1000 ppm.

Results

With a few exceptions the absolute levels of N_2O-emissions from passenger cars were found to be relatively small, especially in extra-urban driving situations. Results from the vehicles tested in the "Extended Programme" are shown in Figure 1.

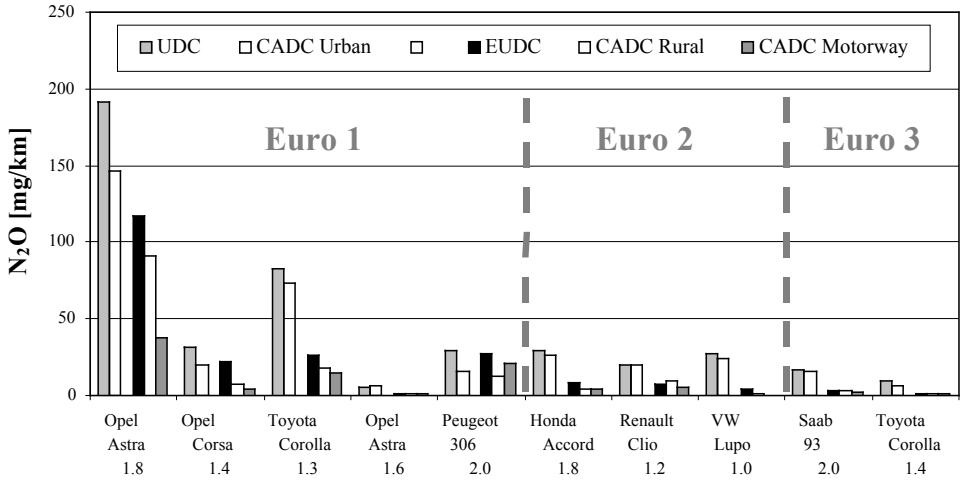

Figure 1: N_2O-emissions (post-catalyst) on the UDC and EUDC cycles compared to the CADC urban driving, rural road and motorway cycles (single measurements).

The measurements confirmed that in petrol passenger cars N_2O is not produced, or hardly produced, in the engine during combustion. Measured N_2O concentrations before catalyst were typically well below 1 ppm (at about the level of the background concentration), while after the catalyst concentrations in the range of 10 to about 250 ppm were observed (depending on the driving condition and catalyst temperature). The engine-out emission of N_2O can therefore be qualified as not significant compared to the N_2O produced in the three-way or oxidation catalyst.

The N_2O-emission of cars equipped with a three-way catalyst was found to be higher during a cold start than during a hot start. Over the hot started urban driving cycle on average 20 mg/km was emitted. After starts at 9ºC and 20ºC this increased to 35 mg/km and 41 mg/km respectively. The explanation of this phenomenon is that as a result of the longer warm-up time the catalyst remains longer in the temperature window favourable for N_2O-formation, which results in a higher N_2O-emission over the complete cycle.

For petrol cars the emission of N_2O during real-world driving are found to be clearly lower than those measured over the standardised European Driving Cycle. Driving more dynamically causes a three-way catalyst to warm-up more quickly and to reach a higher stabilised temperature. The catalyst remains shorter in the temperature window favourable for N_2O-formation (roughly between 200ºC and 350ºC), which results in a lower N_2O-emission over the cycle. On the real-world urban driving cycle the N_2O-emissions were 20% lower than on the standardised Urban Driving Cycle, with a stay of respectively 130 and 175 seconds (on average) in the N_2O-formation window. On the real-world rural road and motorway driving cycles the N_2O-emissions were 32% respectively 58% lower than measured over the standardised Extra Urban Driving Cycle.

For a small sample of 5 vehicles, it was established that in principle passenger cars equipped with aged three-way catalysts emit more N_2O than vehicles with fresh catalysts. Ageing causes a three-way catalyst to gradually deactivate. This deactivation enhances the formation of N_2O in the catalyst. The absolute effect of ageing is found to be the highest for cars that already have a relatively high N_2O-emission with a fresh catalyst. The increase of N_2O-emissions as a result of ageing varied between close to 0 and a factor of 2. However, statistically reliable deterioration factors could not be determined because of the relatively small vehicle sample of 5 cars. Additional research will be necessary to sustain these findings and to determine reliable deterioration factors.

Measurements did not show a significant difference in N_2O-emissions between driving on low sulphur petrol and driving on high sulphur petrol. From the theory, however, a decrease of N_2O-emission due to driving with low sulphur petrol could be expected. This would be caused by the effect that the catalysts are less contaminated and thus less deactivated by low sulphur petrol. It is

very likely that the variability of the measurement of N_2O, in combination with the low levels, has scattered the results and therefore neutralised the effect of low sulphur.

During the real-time measurement of N_2O and the regulated emissions some correlation between the tailpipe N_2O-concentration and the engine-out NO_x-concentration was observed in the sense that the N_2O-concentrations are only high when the engine-out NO_x-concentration are also high. The reverse is not found to be true. It can therefore be stated that the relation of N_2O with engine-out NO_x is only of secondary nature and that NO_x-emission values cannot be used for modelling N_2O-emissions.

It is found that three-way catalysts with a low NO_x-efficiency generally have a higher level of N_2O-emission, but in some cases the influence of the catalyst temperature is interfering with this correlation: a catalyst with a low NO_x-efficiency may actually produce less N_2O due to a higher catalyst operating temperature. For the future situation the results imply that with the increasing NO_x-efficiency in combination with the shortening of the warm-up period of new three-way catalysts, the N_2O-emissions are likely to decrease.

Emission factors for LD vehicles

Based on the results of this investigation new N_2O-emission factor have been estimated for European passenger cars of different emission legislation categories and with different fuels. Emission factors for petrol vehicles are based on the average emission results measured over the European Driving Cycle on the large sample tested in the "Screening Programme", corrected for the effects of real-world driving and ambient temperatures by means of correction factors derived from the measurement results of the "Extended Programme". Due to the absence of diesel vehicles in the "Extended Programme", the emission factors for diesel vehicles are solely based on the EDC test results of the "Screening Programme". The results indicated that emission factors for LPG and petrol vehicles are the same. An overview of the emission factors is presented in Table 2. The data from the "Extended Programme" were not sufficient to derive a correction factor to account for the effects of catalyst ageing.

	Test	Urban hot	Urban cold	Rural	Motorway
Fuel	Category	[mg/km]	[mg/km]	[mg/km]	[mg/km]
Petrol/LPG	15-04	0	0	0	0
	Euro 1	21	38	13	8
	Euro 2	13	24	4	2
	Euro 3	5	9	2	1
Diesel	15-04	0	0	0	0
	Euro 1	2	0	4	4
	Euro 2	4	3	6	6
	Euro 3	9	15	4	4

Table 2: Real-world emission factors of N_2O for passenger cars.

As can be seen from Table 2 there is a clear trend towards lower N_2O-emissions from petrol and LPG vehicles going from Euro 1 to Euro 3. The average emissions of passenger cars are thus found to be significantly lower than the default value of 50 mg/km as used by the IPCC (ref. IPCC (2001)). For Euro 3 vehicles the average values correspond to between 1 and 2 gCO_2-eq./km, which is about 1% of the average direct CO_2-emission of passenger cars (160 - 180 g/km). A more elaborate report of the research on LD vehicles can be found in Gense & Vermeulen (2002).

3 – N_2O-emissions of HD vehicles

The project for HD vehicles was set up to obtain reliable emission factors for the period 1988 – 2010. For this reason production vehicles of different Euro classes were tested as well as some demonstrator vehicles with exhaust aftertreatment technology that may be implemented in Euro 4 and Euro 5 vehicles.

Measurement program

In the measurement programme 13-mode engine tests were performed on a total of 33 HD vehicles using steady-state chassis dynamometer and a measurement method developed by TNO to simulate stationary tests on engines in vehicles (ref. van Gompel & Verbeek (1993)). 22 Euro 3 trucks, as well as two demonstrator vehicles with an experimental urea SCR-deNOx system and one demonstrator vehicle with EGR and CRT, were subjected to the simulated ESC 13-mode test. 3 Euro 1 trucks and 5 Euro 2 buses with CRT filters were subjected to the conventional ECE R49 13-mode test. Tests on two vehicles with CNG-engines (one lean-burn and one stoichiometric) are planned for the first half of 2003. The results will be presented at the conference.

During the 13 mode tests, the N_2O-concentrations were measured continuously, including the transitions from one mode to the next, using a Thermo Environmental Instruments Model 46C N_2O analyser. The regulated emission components (CO, HC, NO_x, and PM) were measured to assess the (maintenance) condition of the vehicles and to search for a correlation between N_2O and NO_x.

Results

The N_2O-concentration in the exhaust of all Euro 1 and Euro 3 vehicles was never higher than a few ppm and often close to the detection limit of the measurement set-up. N_2O-emissions in tests performed after a cold engine start (around 20 ºC) were of the same level as emissions after a hot start.

Also for the Euro 2 buses with CRT filter emissions of N_2O were quite low, on average 1 to 2 ppm, with occasional peaks of 4 to 12 ppm. When the official ESC weighting factors are applied (taking the average N_2O-emission level over the last 30 seconds of the mode points), the overall N_2O-emission result ranges from 0.01 to 0.02 g/kWh. Tests with a cold engine start did not affect the levels of measured N_2O. Upstream of the CRT filter the N_2O level was hardly above the minimum detection level. The latter measurements have been used to estimate N_2O-emission values for Euro 2 vehicles without exhaust aftertreatment.

The vehicles with SCR-deNOx systems produced the highest N_2O-emission levels within the measurement programme, even though both vehicles did not have a NH_3 clean-up catalyst in the after-treatment system. Over the test, an average emission level of 2.5 to 7.5 ppm was measured, and occasional peaks to 30 ppm were observed. Applying the official ESC weighting factors, the overall N_2O-emission result ranges from 0.03 to 0.07 g/kWh. To put this value in perspective: the Euro-3 limit for NO_x-emissions is 5 g/kWh.

The vehicle with EGR and CRT did not produce any noticeable N_2O-emissions, either in the 'warm' or the 'cold' test.

Real-time measurements of the N_2O levels of the 2 vehicles with SCR-deNOx systems and the vehicle with EGR and CRT did not show a straightforward correlation with the real-time NO_x-measurements apart from the obvious relation that N_2O-emissions are only high when NO_x-emissions are high. This relation is also observed in LD diesel vehicles.

In a static 13-mode test, emission levels will normally stabilise over the time that a mode is tested (2 resp. 6 minutes for the ESC and ECE R49 13-mode test). The emission level over the last 30 resp. 60 seconds is averaged to obtain a representative value for that mode. N_2O-emission levels, however, were often found to be rising constantly, and sometimes did not reach an equilibrium before the end of a mode. An example is given in Figure 2. The reason for this seems to be that N_2O is formed in the lower temperature range, but that it is not released until higher temperatures are reached. Taking the average emission level over the last 30 or 60 seconds can therefore not be considered as 'representative' for that mode. However, in contrast to the 13-mode test, in real-life situations the engine is operated more dynamically, and especially temperatures will not stabilise due to the engine's thermal inertia. Therefore it is safe to assume that the higher exhaust gas temperatures recorded during a 13-mode test (under which higher levels of N_2O are emitted) will not be seen easily in normal operation, simply because the engine will not be given sufficient time to

reach these levels. The emission levels for N_2O measured in this programme can therefore still be regarded as a good indication of the upper limit of N_2O-emissions in real life.

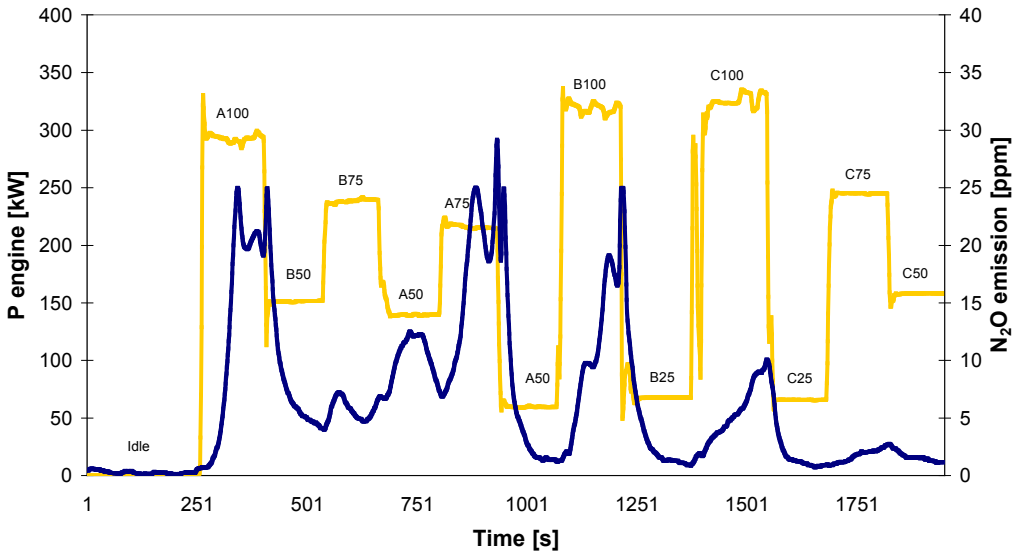

Figure 2: Real-time N_2O-emission of a demonstrator vehicle with SCR-deNOx over the ESC 13-mode test.

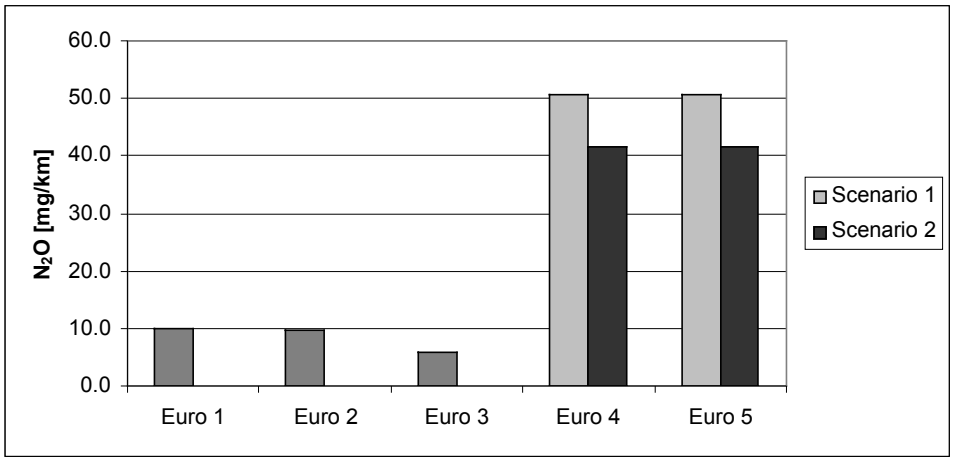

Figure 3: N_2O-emission factors for HD vehicles from 1988 - 2010 for 2 scenario's: (1) 100% SCRdeNOx aftertreatment, (2) 80 % SCRdeNOx and 20% cooled EGR with CRT.

Emission factors for HD vehicles

On the basis of the 13-mode emission results measured in this programme, N_2O-emission factors have been calculated, estimating the emissions of HD vehicles under representative real-world driving conditions. The calculation is based on the method of Adapted Weighting Factors developed by van de Weijer (1997), using a set of real-world driving cycles for HD vehicles (ref. Riemersma & Hendriksen (2001)). Emission factors for urban, rural and highway driving with different load factors have been derived for Euro 1 to Euro 3 vehicles of 5 different classes and for vehicles with SCR-deNOx and CRT filters separately. Detailed results can be found in Riemersma (2003). Figure 4 shows aggregate N_2O-emission factors, averaged over fleet composition and road types, for Euro 1 up to Euro 5 vehicles. For Euro 4 and 5 vehicles two scenarios are discerned with a different mix of exhaust aftertreatment technologies assumed to be applied. It should be noted that due to aspects of both the measurement method and the calculation method the values in Figure 4 should not be regarded as exact but rather as good indications of the upper limit.

As can be seen form Figure 3 the N_2O-emissions of present-day trucks (Euro 1 – 3) is well below the value of 30 mg/km assumed by the IPCC. Beyond 2005, when exhaust aftertreatment is expected to be used to meet the Euro 4 and 5 emission limits, the N_2O-emission of trucks and buses is expected to rise significantly to a value even higher than the IPCC value. However, expressed in CO_2-equivalents this value represents only 12 to 15 gCO_2-eq./km, which about 2% of the average direct CO_2-emission of trucks (820 g/km).

Conclusions

In an elaborate measurement programme the N_2O-emissions of LD and HD vehicles have been measured and factors influencing these emissions have been assessed. The N_2O-emissions of LD vehicles are found to be much smaller than the value used by the IPCC, and show a decline going from Euro 1 to Euro 3. N_2O-emissions are likely to decrease even further with the introduction of more advanced aftertreatment technology. Catalyst ageing is found to have adverse effects on the N_2O-emissions of LD vehicles.

The N_2O-emissions of HD vehicles of Euro 1 to 3 emission classes are also found to be much smaller than the value used by the IPCC. Euro 4 and 5 vehicles equipped with aftertreatment systems such as SCR-deNOx and EGR with CRT filter are expected to show a strong increase in N_2O-emissions. Expressed in CO_2-equivalents the resulting levels will still be relatively small.

N_2O-emissions do not correlate with NO_x-emissions and can therefore not be assessed on the basis of measured NO_x-emissions. Instead dedicated N_2O-measurements are necessary to assess these emissions.

Acknowledgments

The authors wish to thank Mrs. M. Feijen-Jeurissen and Mr. H. Oonk of TNO-MEP for providing state-of-the-art theoretical insight into the mechanisms of N_2O formation.

References

Feijen-Jeurissen M., H. Oonk & N. Gense (2001), N_2O-emissions form mobile sources: - Impact of technology development, TNO-report R 2001/113, March 2001.

de Haan P. & M. Keller (2001): Real-world driving cycles for emission measurements: Artemis and Swiss cycles, INFRAS-report, March 2001.

Gense N. & R.J. Vermeulen (2002), N_2O formation in vehicle catalysts, TNO-report 02.OR.VM.017.1/NG, February 2002.

van Gompel P. & R. Verbeek (1993): Final Report DCM; Procedure and accuracy of testing, according to 88/77/EEC and 72/306/EEC, carried out on a chassis dynamometer, TNO-report 93.OR.VM.023.1/PvG/RV, 1993.

van de Weijer C.J.T. (1997), Heavy-Duty Emission Factors, PhD-thesis Technical University of Graz, October 1997.

Riemersma I.J. & P. Hendriksen, (2001) Update and Evaluation of HD Testcycles, TNO-report 00.OR.VM.081.1/IJR, June 2001.

Riemersma I.J. (2003), N_2O-emissions of HD vehicles, TNO-report, to be published.

IPCC (2001), http://www.grida.no/climate/ipcc_tar/wg1/248.htm

12th International Symposium "Transport and Air Pollution" / 12e Colloque international "Transports et pollution de l'air", Avignon, 16 -18 *June* / juin 2003
proceedings / actes, n°92, tome / Vol. 1, Inrets ed., Arcueil, France, 2003, p. 161-168

Towards meaningful real-world emission factors for motorcycles: An evaluation of several recent TNO projects

Raymond Gense, Daniël Elst
TNO Automotive, P.O. Box 6033, 2600 JA Delft, the Netherlands
Fax +31 15 269 68 74 - email : gense@wt.tno.nl

Abstract
Representative testing of emissions from motorcycles requires much more care than in the case of passenger cars. Typical characteristics of bikes show a much wider range, and result in typical patterns of use that differ significantly from those of cars. Meaningful inventories should also take into account the typical motives of use, as they result in a predominant use of certain road types (depending on the 'class' of bike) that again differ significantly from those of typical car use. Further risks of misleading data acquisition originate from significantly greater sensitivities for laboratory and testing circumstances than in the case of cars. An evaluation of recently measured data on this basis serves to illustrate these effects.
Key-words: *Emission factors, motorcycles, real-world, test-cycles*

Résumé
Les tests d'émissions pour les motocycles demandent beaucoup plus d'attention que pour les voitures de tourisme. Les caractéristiques typiques des motos sont beaucoup plus variées et résultent de types d'utilisation qui diffèrent d'une façon marquée de ceux remarques pour les voitures. De bons inventaires devraient aussi prendre en compte les motifs typiques d'utilisation, vu qu'ils résultent de l'utilisation dominante de certains types de routes (dépends de la 'classe' de la moto) qui eux-mêmes diffèrent de façon significative de l'utilisation classique des voitures. De plus, les risques d'acquisition de mauvaises données s'expliquent par une sensibilité plus importante des laboratoires et des conditions de test pour les motos que pour les voitures. Une évaluation des données mesurées récemment faite sur ces bases illustre ces effets.

Introduction

Establishing typical exhaust emissions of motorcycles involves much more variation than in the case of e.g. cars: the total field is much wider. Motorcycles range in engine characteristics from less than 100 cm3 and less than 5 kW to 2000 cm3 and close to 150 kW, in ready to ride mass from less than 100 kg to nearly 400 kg, and in performance from less than 100 km/h to 300 km/h, even if you skip a few extravagancies. Technologies include conventional 2-stroke, DI 2-stroke and 4-stroke. This wide range in vehicle characteristics inevitably reflects in the characteristic patterns of use. This is best illustrated by considering the power to mass ratio for the bike on the road (that is: including rider and gear) as shown in Table 1 and comparing this with the typical values for passenger cars. Figure 1 further shows, by way of example, the percentage of models offered for sale in the Benelux a few years ago as a function of this power to mass ratio. It will be clear that characteristic riding styles will be heavily influenced by such variations in performance level. Inevitably this will have to be taken into account when establishing characteristic emission levels for powered two-wheelers (PTWs). The consequences of this statement will be further investigated in this paper.

Passenger cars		*Motorcycles*	
Vehicle class	*KW/tonne*	*Vehicle class*	*KW/tonne*
'Normal cars':			
nd butter cars	*35 - 60*	*Small utility & scooters*	*20 - 80*
cars	*60 - 80*	*Touring*	*80 - 180*
ars & sportscars	*80 - 120*	*Sports*	*180 - 300*
A few super sportscars	*150 - 200*	*Super sports*	*300 - >400*
Rare exotic sportscars	*240 - 260*		

Table 1: Characteristic power to mass ratios of cars and motorbikes (including rider and gear)

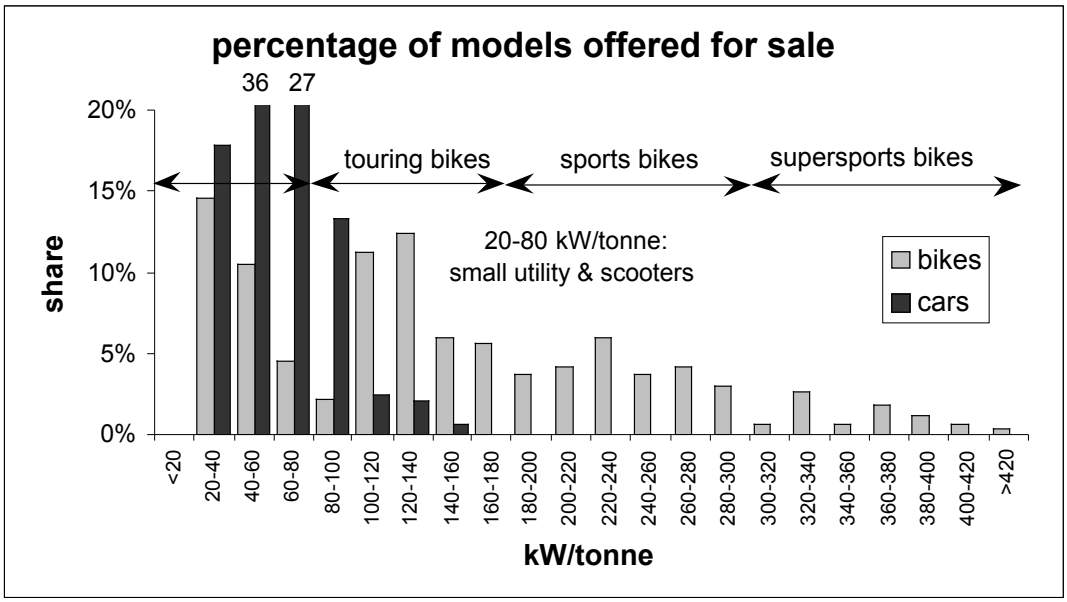

Figure 1: Typical on the road power to mass ratios of cars and bikes for the Benelux, 1999.

1 – Characteristic patterns of use

Because of the aspects mentioned in the introduction, in 1999 work was undertaken to develop a new 'real-world' driving cycle for use in certification of PTWs. This work was started by TNO on behalf of the Dutch Ministry of the Environment, and in co-operation with the International Motorcycle Manufacturers Association IMMA Rijkeboer (2001a). In a later stage it was adopted as a project of the UN, under the 1998 Agreement, under the acronym WMTC (World Motorcycle Test Cycle). In parallel a study was made for the European Commission Rijkeboer (2000). This latter study showed that the European vehicle fleet can be roughly characterised as a north-European fleet, predominantly consisting of larger bikes mainly used for recreational purposes, and a south-European fleet, predominantly consisting of smaller vehicles mainly used for daily transport. A country like Germany would be a typical representative of the first category; countries like Greece and Spain would be typical for the second. Countries like Italy and France possess a combination of both categories. Further investigation revealed typical circumstances of use (see Tab. 2).

It should be noted that the ECE-40 type approval test cycle in use at that time (dating from the very early days of car testing) only addressed the situation warm start/urban traffic. It will be clear that the data originating from this test have little to say about the actual emission behaviour of PTWs in the field. For the current Euro 2 a cold start has been included, but the urban character was maintained. Within the WMTC project this was a reason to set up the test cycle in 3 parts (roughly: urban, country road and motorway) and to weight them according to the considerations shown in Table 2. Based on the world-wide nature of the WMTC a world-wide weighting is needed, but a significant difference between Europe and the world only shows for class 3. The weighting factors

have not yet been finally established, but may turn out something like 50/50 urban cold/hot for bikes of class 1 (e.g. < 125 cc), 30/70 urban/country road for bikes of class 2 (e.g. 125-500 cm^3) and 15/65/20 urban/country road/motorway for bikes of class 3 (e.g. > 500 cm^3) in European traffic.

Type of bike	Type of road (and cold/warm started)			
	Urban – cold	Urban - warm	Country roads	Motorway
Scooters & Small utility	important	important		
Medium class & Touring	important	less important	very important	
	less important	important	very important	less important
Big and sporty	less important	less important	very important	less important

Table 2: Typical places and circumstances of use

But the main shortcoming of the ECE-40 test is that it has 'borrowed' the actual driving pattern from the car procedure. Investigation of the dynamics of this driving pattern showed that it already lacks sufficient dynamics to represent modern 'normally' driven cars, let alone bikes: see Figure 2.

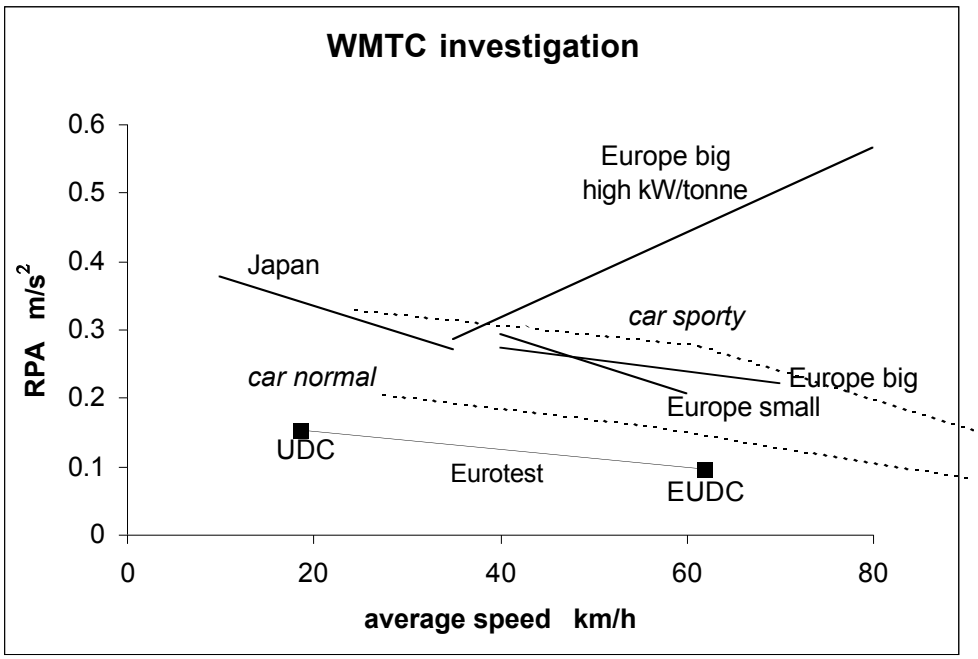

Figure 2: Typical 'dynamics' of car and bike use in real-world circumstances, compared to the European standard certification test cycle. UDC = urban driving cycle, EUDC = extraurban driving cycle.

The criterion used to judge the 'dynamics' used here is the RPA (relative positive acceleration); for an explanation of this parameter see van de Weijer (1997), or Rijkeboer et al. (2001b). Bikes, even small ones, show the dynamics of sportily driven cars. This turned out to be representative even for Japanese patterns of use, which are generally slower, but not less dynamic than European or American ones. Bikes with very high power to mass ratios (>200 kW/tonne) surprisingly showed increasing dynamics with increasing speeds, within the range of average speeds investigated. This was typical for European use only and did not show in American use (in the Japanese situation such bikes are not present). It is to be expected that all of this will have its influence on the emission behaviour, and it has. Figure 3 shows the emissions of a 600 cm^3 super sport bike measured over a number of driving cycles. The cycles are the warm started ECE-40 cycle, the cold started car type Eurotest as modified for typical motorbike acceleration rates by RW-TÜV on request of the German Umwelt Bundesamt, the US certification cycle (a real-world driving pattern as established for typical US passenger car traffic), a real-world motorbike driving pattern as established for Swiss

circumstances by the "Fachhochschule Biel" (FHB) comprising urban, suburban and country road riding (at that time the motorway section had to be omitted because of cooling problems on our chassis dynamometer), and finally the first version of the real-world based WMTC then under development (the current and probably final version is version 8). As can be seen all alternative cycles result in much less HC and CO_2, and much more CO, and in the case of the cycles with 'fiercer' acceleration rates also in considerably more NO_x in comparison to the 'standard' ECE-40 cycle. It is to be expected that such differences will increase for bikes with a more optimised fuelling than this rather uniformly rich adjusted, carburettor equipped one. As an example Figure 4 shows the CO-emission over different test cycles of a more modern, fuel injected (and catalyst equipped) 600 cm^3 super sport bike, as an indicator for the variability of its fuelling settings over different operational circumstances. As can be seen this one does not turn rich until it really has to perform, but even so the relative differences between the test cycles can be significant.

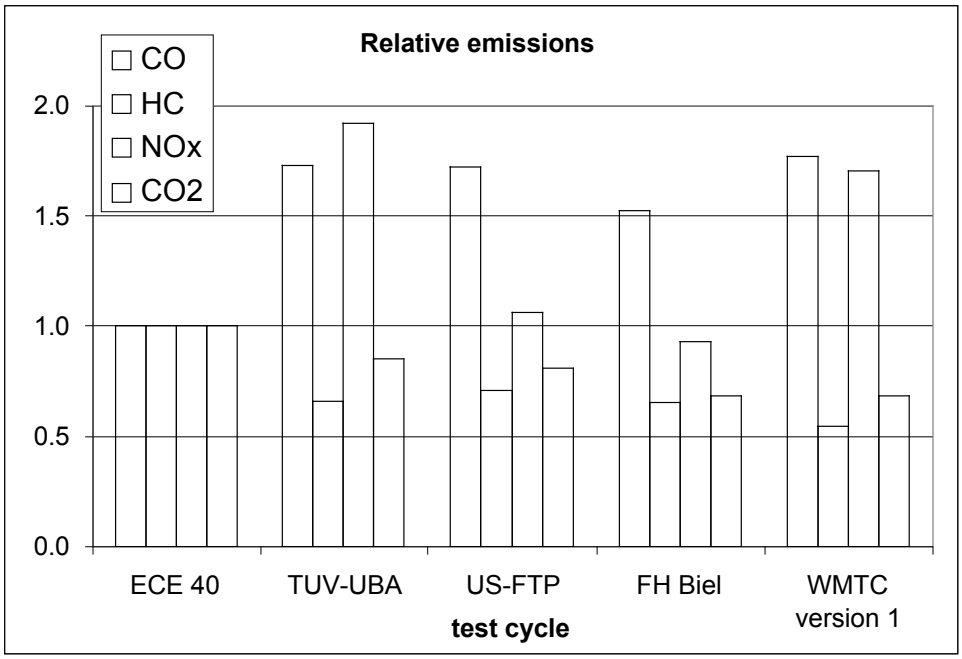

Figure 3: Relative emissions of a 600 cm^3 super sports bike with carburettor (no aftertreatment) in different test cycles. The results of the real-world cycles (FH Biel and WMTC) are unweighted.

2 – The database

For a further illustration of the influences of the parameters for motorbikes as presented in this paper, the data are used of a number of recent projects carried out by TNO, including the 5th framework project 'ARTEMIS', executed on behalf of the European Commission and counter financed, as far as TNO was concerned, by the Dutch Ministry of the Environment, the '2nd CITA Research Study Programme on Emissions', ordered by DG-TREN, and a study on urban two-wheeler emissions on behalf of the 'Netherlands Organisation For Energy and the Environment'.

3 – The influence of the testing parameters

The ARTEMIS project, of which TNO was project leader for the motorcycle part, included a round robin test between four representative laboratories, situated in the Netherlands, Germany, Switzerland and Hungary, aiming at an investigation as to the possible influences of typical laboratory characteristics on the emission test results of a PTW. Two motorbikes were selected to perform this round robin test:

- A 125 cc 2-stroke scootermodel with automatic transmission; no aftertreatment
- A 600 cc 4-stroke super sport bike with 6-speed manual gearbox; closed loop 3-way catalyst

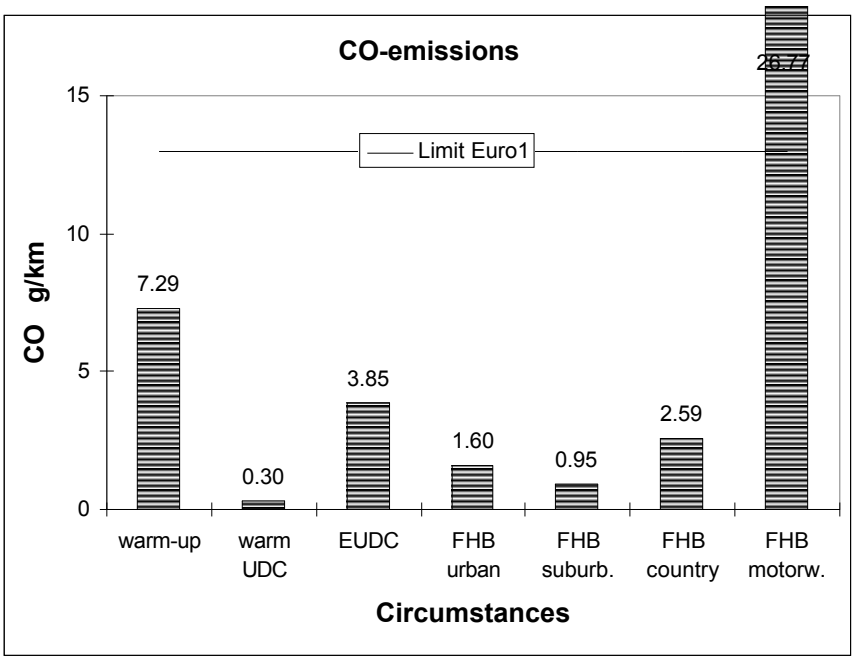

Figure 4: CO-emissions of a 600 cm^3 super sports bike with fuel injection and 3-way catalyst in different test cycles. Apart from the cold start test the CO-emission may be taken as an indication of the fuelling strategy. UDC = urban driving cycle (consisting of 4 identical subcycles) as originally devised for cars, warm-up means 2 UDC subcycles started from cold, EUDC = extraurban driving cycle as currently used for cars (additional to the UDC), FHB indicates the real-world driving patterns as developed by the Fachhochschule Biel. The emission in the 'warm UDC' is representative for the Euro 1 certification.

The parameters investigated were:

- Bench setting
- Chassis dynamometer reproducibility
- Drive wind simulation
- Analyser settings
- General operational aspects

The emissions were measured over the ECE-40/Euro-2 cycle (separately over the warming-up phase, not included in the ECE-40 version), the US certification cycle (warm start only) and the real-world cycles developed by the Fachhochschule Biel, including the motorway section. For confidentiality reasons the WMTC was not yet available for this project.

The general conclusions of this investigation were:

- The large range of emission values over the different cycles (e.g.: for CO two orders of magnitude in g/km between real-world urban traffic and motorway, in the case of the super sport bike as shown in Figure 4) made it difficult to accurately measure the different road types in one package of settings. Settings of sampling and analysing equipment should therefore as far as possible be adjusted to the emission level to be expected.
- The brake loads to be set for PTWs are relatively small in comparison to those for cars, making them difficult to set accurately. Internal frictions of the bench should be as low as possible or electrically compensated. This problem increases when a chassis dynamometer is used that was actually designed to test cars. 'Outdated' chassis dynamometers are unsuited for acceptable measurements of PTW emissions, especially in the case of small bikes.
- The load setting method as prescribed in the US legislation does simulate the actual road load better than the method described in the European Directive. Even so the method does not lead to

satisfactory settings for high speed test cycles such as the motorway cycle. Within the framework of the WMTC this aspect was looked into by an ISO working group.

- A highly dynamic driving cycle in combination with a high power to mass ratio of the vehicle tested can easily result in poor repeatability of the test. On the one hand this means that special attention should be paid to the response time of the brake load simulation device: this should be much faster than is acceptable for the ECE-40 (or the car type) test cycle. On the other hand it means that, preceding the test, the test rider should get himself sufficiently acquainted with the peculiarities of the driving cycle used and with the behaviour of the bike over this cycle. Especially in the case of 'nervous' bikes like the high performance super sport bike used in this round robin, this is an important requirement for repeatable, and hence representative, results.
- Many PTWs are essentially drive wind cooled, one way or another, even if they do possess a form of liquid cooling of the cylinders and cylinder head, as did both the bikes used in this round robin test. This puts more emphasis on the drive wind simulation than in the case of cars. There were sometimes considerable differences in the temperatures between labs, both of the coolant and as measured at the spark plug. And as a rule the temperatures were significantly higher than under comparable circumstances on the road. It is to be expected that especially the emissions of catalyst equipped vehicles during the warm-up may be affected by this aspect.

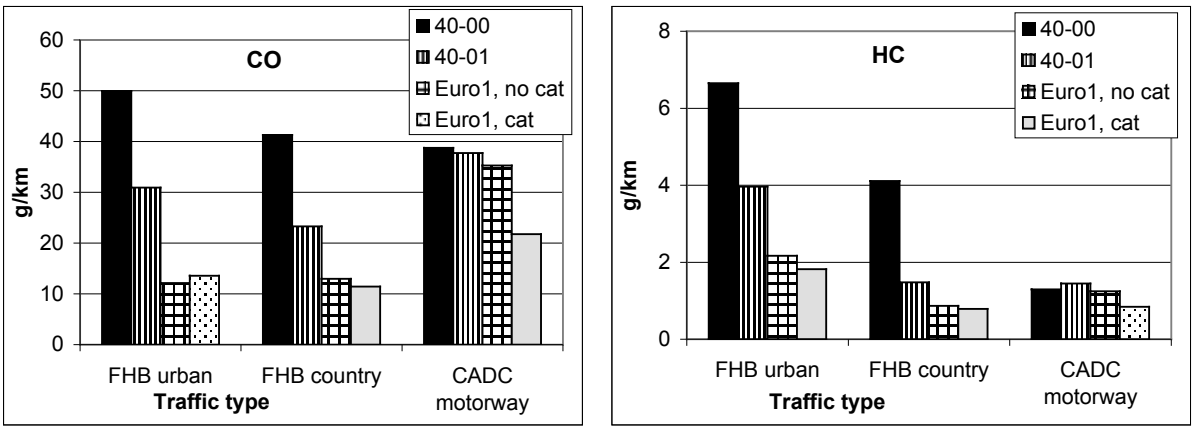

Figure 5: The emissions of CO and HC of a range of technologies (4-stroke bikes only) in different real-world driving circumstances. FHB indicates the real-world driving patterns as developed by the Fachhochschule Biel. CADC = common ARTEMIS driving cycle; this cycle actually represents car traffic. The category 'Euro 1, cat' actually contains one bike still certified under ECE 40-01.

4 – The influence of the technology

From the databases mentioned under section 2, representing nearly 100 bikes, a good picture can be derived as to the influence of the engine technology, both as regarding 2-stroke/4-stroke and as regarding the results of the steps in legislation. There are results for the legislative steps ECE 40-00, ECE 40-01 and Euro 1, all without catalyst, and for 40-01/Euro 1 with catalyst (> 500 cc only). The results for CO and HC are shown in Figure 5. As can be seen for Euro 1 the CO-emission has decreased most over the urban and country road parts, whereas the CO over the motorway part has decreased only for the catalyst equipped bikes. On the other hand the catalyst does not seem to contribute much to the non-motorway parts, where it is low already. For HC the urban situation is analogous to CO, but on the country road part most of the gain was already obtained in the ECE 40-01 step and in the motorway part the emission was low even in the ECE 40-00 situation and does not seem to have improved since, not even for the catalyst equipped bikes. The NO_x (not shown) roughly showed a doubling over the period 40-00 to Euro 1 w/o catalyst, both in urban traffic (0.13 to 0.28 g/km) and for country road situations (0.19 to 0.35 g/km), but not on the motorway (a stable 0.75 – 0.80 g/km).

5 – The influence of the test cycle

As stated before, the common test cycle used to be the ECE-40 cycle, which is the urban cycle as originally devised for passenger cars. This cycle consists of four identical subcycles. In the case of motorbikes two such subcycles are used for warming up, after which the four measured subcycles are driven. For Euro 2 it was decided to measure (without further weighting) all six subcycles, so as to include the cold start. Additionally two different real-world cycles have been measured: the set developed by FHB (but without the motorway part) and the so-called CADC (Common ARTEMIS Driving Cycle), which really was a real-world driving pattern developed for the passenger car section of ARTEMIS; this did include a motorway part and it had been found out that the emissions over the motorway parts of the FHB cycle and the CADC did not differ significantly. Table 3 shows the results for the ECE-40 test, the Euro 2 test and the (warm started) real-world FHB-tests (but with the CADC motorway part), in the latter case weighted as indicated in section 1, above.

Technology	*CO [g/km]*			*HC [g/km]*		
	ECE-40	*Euro 2*	*Real-world*	*ECE 40*	*Euro 2*	*Real-world*
2-stroke	23	23	21	12.7	14.0	11.1
4s < 125	12	13	12	1.2	1.4	1.5
125-500	15	17	14	1.5	1.7	1.1
> 500 no cat	17	23	27	2.9	3.6	2.0
> 500 + cat	8	12	12	1.0	1.6	1.0

Table 3: Emission results on the basis of three different test procedures

As can be seen the emissions of HC and (especially) CO for 2-strokes are relatively insensitive for the test procedure. For the class 1/ 4-stroke bikes and class 2 the results for HC tend to be sensitive for the inclusion of a cold start and the use of a real-world driving cycle (but the latter in different directions!). For class 3 w/o catalyst both the CO and the HC increase with the cold start, but react in very different ways to the drive cycle. For class 3 with catalyst the CO and HC tend to increase sharply for the cold start, whereas the CO also shows a significant increase for the real-world drive cycle, although the HC does not. The reason for the increase in emissions with the introduction of a cold start is obvious, whereas the decrease in HC for the weighted real-world results in the case of the classes 2 and 3 can be fully attributed to the high weighting of the country road part, which emits much less HC. This is also reflected in a 23-25 % decrease in fuel consumption over the weighted real-world test for class 3. The NO_x decreased from about 0.2 to 0.1 g/km from class 1 to class 3 under the old test cycle (both warm and cold start), but increases to between 0.25 and 0.30 g/km for all classes on the basis of the weighted real-world cycle. This may be attributed both to the higher dynamics of the test cycle and the influence of higher speeds in the weighting of the classes 2 and 3. So the results are very much dependant on the class of bike and on the question if they are needed for an overall national emission inventory, or for a local situation.

Conclusions

From a combined evaluation of the several projects the following conclusions can be drawn:

- The typical patterns of use of motorcycles differ significantly from those of passenger cars. The dynamics of a typical drive cycle are much higher than those of cars and even further removed from those of the original and current certification test cycles.
- Motorcycles show a much greater variation in characteristics than cars. These variations contribute even further to differences in the typical patterns of use.
- The typical motives of use vary per class of vehicle, and hence per typical, country specific, fleet composition. They in turn are determining the typical places (road types) and circumstances of use, which vary significantly, both between each other and in comparison to cars.
- The testing of motorcycles on a chassis dynamometer is much more dependant on the

characteristics of the specific test equipment and the test circumstances of the laboratory than the testing of cars. Special care has to be taken to avoid the risk of misleading test results.

- As a result of all of these aspects an inventory of different vehicles and engine technologies will result in significantly different conclusions depending on whether they are based on the emissions as produced over the type approval test cycle or on a programme that did take the above considerations into account.

References

Elst D.A.M.M., R.C. Rijkeboer, D.A.C.M. Bremmers, N.L.J. Gense, J. Czerwinski, A. Tamasi and T. Braun (2001), ARTEMIS deliverable D15 – Motorcycle round robin test. A common report by the partners. TNO report RAS-ID 3155, Delft, the Netherlands, 90 p.

Elst D.A.M.M., N.L.J. Gense and R.C.Rijkeboer (2002): 2nd CITA Research Study Programme on Emissions, Study 2 – Motorcycle Exhaust Emissions and Noise. TNO report 02.OR.VM.044.1/DE, Delft, the Netherlands, 92 p.

Rijkeboer R.C. (1999): The motorcycle emission situation – A report to the European Commission. TNO report 99.OR.VM.035.1/RR, Delft, the Netherlands, 53 p.

Rijkeboer R.C. (2001a): WMTC – Final report. TNO report 01.OR.VM.034.1/RR, Delft, the Netherlands, 68 p.

Rijkeboer R.C., P. Hendriksen and N.L.J. Gense (2001b): Real-world driving behaviour. 8th European Automotive Congress (EAEC 2001), paper SAITS 01037, Bratislava, Slovak Republic.

Rijkeboer R.C., R.J. Vermeulen and J.D. van der Toorn (2002): Inventariserend Onderzoek Gemotoriseerde Tweewielers (Inventory Powered Two-wheelers). TNO report 02.OR.VM.020.1/RR, Delft, the Netherlands, 23 p.

Van de Weijer C.J.T. (1997): Heavy Duty emission factors, development of representative driving cycles and prediction of emissions in real-life. PhD-thesis of the Technische Universität Graz, Austria. Delft, the Netherlands, 161 p.

12th International Symposium "Transport and Air Pollution" / 12e Colloque international "Transports et pollution de l'air", Avignon, 16 -18 *June* / juin 2003
proceedings / actes, n°92, tome / Vol. 1, Inrets ed., Arcueil, France, 2003, p. 169-175

Statistical analysis of road tunnel studies performed in the EU-project ARTEMIS

Johannes Staehelin*, Christian Sangiorgio, Bruno Tona**, Giovanni Catone**, Werner A. Stahel**, Christina A. Colberg* & Peter Sturm*****
* Institute for Atmospheric and Climate Science, Swiss Federal Institute of Technology Zurich, ETH-Hoenggerberg, CH-8093 Zurich, Switzerland - Fax + 41 1 633 10 58
- Email: staehelin@atmos.umnw.ethz.ch
** Seminar für Statistik, Swiss Federal Institute of Technology Zurich, ETH-Zentrum, CH-8092 Zurich, Switzerland
*** Institute for Internal Combustion Engines and Thermodynamics, Graz University of Technology, A-8010 Graz, Austria

Abstract
Tunnel measurements of nitrogen oxides (NO_x), carbon monoxide (CO), and total Non Methane Volatile Organic Compounds (t-NMVOC) were performed in spring 2001 in the Lundby tunnel (Sweden), in fall 2001 in the Plabutsch tunnel (Austria), and in fall 2002 in the Gubrist tunnel (Switzerland). In this paper we derive emission factors for light and heavy duty vehicles (LDV and HDV) by regression analysis. The results demonstrate the large effect of the tunnel road gradient for NO_x emissions of HDV, whereas the influence of the road gradient is less pronounced for LDV emissions of NO_x and CO. In the paper we show the strength and weaknesses of statistical analysis of road tunnel measurements.
Keys-words: *statistical modelling, road traffic emissions, tunnel measurements.*

Introduction

Road traffic is one of the largest emission sources of air pollutants. Road traffic emissions are calculated by emission models which are based on dynamometric test results for a number of single vehicles tested under appropriate driving conditions and on model calculations of mileages for these conditions. The accuracy of such calculations depends on the validity of the emission factors (EF) used. Road tunnel studies can be used to compare the EFs determined from dynamometric tests to field data for a real world collection of vehicles.

Earlier tunnel studies from the Gubrist tunnel in Switzerland (John et ali (1999) and the Plabutsch tunnel in Austria (Sturm et ali (2001), Hausberger et ali (2002)) showed acceptable agreement for carbon monoxide (CO) and total volatile organic compounds (t-NMVOC) with the emission model used in the "handbook" -- an emission model based on dynamometric tests of a large number of vehicles of the different types of engine and technology obtained in Germany, Austria and Switzerland (UBA, 1999). For nitrogen oxides the agreement was acceptable for light duty vehicles (LDV, including passenger cars and vans), but the emission model predicted much smaller EFs for heavy duty vehicles (HDV, diesel) than the tunnel studies. This discrepancy gave rise to extended dynamometric test measurements of HDV in the Cost initiative 346 and in the EU-project ARTEMIS (Assessment of Reliability of Transport Emission Models and Inventory Systems). In this paper we discuss the statistical analysis of three recent tunnel studies, performed in the Lunby tunnel in Sweden and the Plabutsch tunnel in Austria as part of ARTEMIS and in the Gubrist tunnel in Switzerland outside that project. The characteristics of these tunnels are displayed in Table 1.

Lundby tunnel, Goteborg, Sweden (ARTEMIS study): One tube, two lanes with traffic in one direction, passively ventilated. Between the measureing site 1 and 2 the tunnel tube decreases (slope of - 3.5 %, distance of 583 m) followed by a smaller part with a slightly increasing slope (+0.25%, 163 m); between the sites 2 and 3 the slope is first slightly ascending (+0.25%, 437 m) followed by a small distance with a slope of +4% for 38 m; the measurements were performed in spring 2001.
Plabutsch tunnel, near Graz, Austria (ARTEMIS study): One tube, two lanes with traffic in oposite direction, cross ventillation system (for more details see Sturm et ali (2001); the measurements were performed in fall 2001.
Gubist tunnel, near Zurich, Switzerland: One tube, two lanes with traffic in one direction, passively vetilated, with an averaghed slope of + 1.3% (for more details see Staehelin et ali (1995)). The measurements were performed in fall 2002.

Table 1: Summary of tunnel measurements used in this study. The measurements of the ARTEMIS tunnel studies were performed by the Bergische Universität-Gesamthochschule Wuppertal (Germany), Swedish Environmental Research Institute Ltd, Transport Research Laboratory (UK), and Technische Universität Graz (Austria), those of the Gubrist tunnel study by AWEL (Amt für Wasser, Energie und Luft des Kantons Zurich, Switzerland). The vehicle fleet composition was measured by loop detectors allowing to measure the number of vehicles passing the tunnel, a separation into LDV and HDV and the vehicle speed.

1 - Emission Factors

An emission factor (EF) is defined as the mass of a compound emitted per vehicle and distance. This definition can be used for individual vehicles as well as for averages over a fleet of vehicles. First, the mean EF of the entire vehicle fleet passing through the tunnel during appropriate time intervals i must be determined. In case of the passively ventilated tunnels and one-way traffic (Lundby and Gubrist tunnel), the air always moves in the same direction, and the following formula is used:

$$EF_i = \frac{\Delta c_i w_i s \Delta t_i}{n_i d} \qquad (1)$$

where:

Δc_i difference in concentrations of the compound between the measuring sites
w_i: wind speed
s: tunnel cross section
Δt_i: length of time interval (15 min in this evaluation)
n_i: number of vehicles driving through the tunnel
d: distance between the measuring sites
i: index of the measuring interval

The starting points of the time intervals used for the different measurements were adjusted to account for average transport times between locations of measurements.

In the Lunby tunnel wind speed was measured at the sites 2 and 3 (see Table 1). The measurements at site 3 sometimes showed negative values. This might be caused by the fact that the sensor was located in a niche. Wind speed for site 3 was determined using the measurements of site 2 after cross correlation with the measurements of site 3. However, the available wind speed measurements might not be representative for the air flow through the entire tunnel cross section. SF_6 data were used to test the validity of the wind measurements. A fixed amount of SF_6 was released at a constant amount at site 1 with a known amount during 11 periods of 2 hours. Measurements at site 3 are available from two teams. The measurements of team 1 were available for 6 periods and those of team 2, for 10 periods. The SF_6 measurements of the two groups showed very similar temporal evolution. However, systematic differences in the concentrations were found, which were attributed to the fact that the instrument of team 2 was not calibrated for SF_6 at the site. When the wind speed

measurements were compared with the information of the SF_6 measurements, significant differences were found, which led to a correction of wind speed by a factor of 1.3 in case of the measurements of team 2 and a correction factor of 1.6 for the measurements of team 1. The later value was used due to the lack of an on site instrument calibration of team 2. The inspection of the air pollutant measurements at sites 1 and 3 provides evidence for a travel time of the air pollutants in the order of 4 to 5 minutes. This value is in close agreement with the wind speed determination. However, in particular in the Lundby tunnel these uncertainties limit the precision of the results. The Plabutsch tunnel contains a cross ventilation system which needs measurements of the air pollutants in the air entering the ventilation system and the air leaving the tunnel ventilation.

2 - Statistical model description

Mean EFs for vehicle categories can be calculated by linear regression (see e.g. Staehelin et ali (1997)). We used in our analysis the two vehicle categories of light duty vehicles (LDV) and heavy duty vehicles (HDV). The basic regression model is

$$EF_i = \alpha + \beta\, pHDV_i + \varepsilon_i \qquad (2)$$

where:

α:	EF of the compound of light duty vehicles
$\alpha + \beta$:	EF of the compound of heavy duty vehicles
$pHDV_i$:	proportion of heavy duty vehicles
ε_i:	random error

In the studied tunnels HDV for goods transport are forbidden during weekends. Thus, the data sets contain periods with low *pHDV*. On the other hand, the amount of heavy duty vehicles never exceeded 30 %, which limits the accuracy of the calculated EF of HDV. Data analyses showed that the traffic volume during night is too small for the determination of accurate EF values, and those measurements were not included.

This simple model was extended in several aspects, mostly based on analyses of residuals of the considered models (i.e. the difference between the measured values and the respective values as predicted by the statistical model). Such analyses indicated (Catone (2002), Staehelin et ali (1997)) that the emission factors of LDV also depend on the day of the week, showing differences of the EF of LDV between workdays (Monday - Friday), Saturday and Sunday, probably caused by differences in the composition of the vehicle collectives (e.g. difference in the proportion of vehicles equipped with catalytic converters). The condition of the engine (acceleration, speed, etc.), which determines the emissions, depends on several factors including road gradient and driving cycle. Since no measurements of the driving behavior in the tunnels were available we introduced averaged vehicle speed as a further variable. In order to improve the statistical accuracy of the model, a logarithmic form is used, since the errors show a skewed distribution without this modification. The following statistical model turned out to be most appropriate to describe the measurements of the Lundby- and the Gubrist-tunnel (Catone (2002)):

$$log(EF) = log(\alpha + \beta\, pHDV) + \gamma\, (Sa) + \delta\, (Sun) + \eta\, veh.\ speed + \varepsilon \qquad (3)$$

where:

γ *and* δ:	constants for description of the differences between Saturday and Sunday and the other days of the week
η *veh. speed*:	description of the influence of the averaged vehicle speed

No vehicle speed measurements were available for the Plabutsch tunnel, and we used the number of vehicles driving through the tunnel as a surrogate:

$$log(EF) = log(\alpha + \beta\, pHDV) + \gamma\, (Sa) + \delta\, (Sun) + \eta\ \ veh.numb + \varepsilon \qquad (4)$$

where: η *veh.numb.*: term describing the influence of the vehicle number passing through the tunnel.

As an additional complication, time series correlations of the random errors had to be modeled in

order to obtain accurate confidence intervals for the estimated parameters. In order to check the consistency of the results, the models were fitted with and without the data for the weekend and the corresponding terms in the model. The model results were extracted for specific vehicle speeds (or specific vehicle numbers passing the tunnel).

3 - Results and Discussion

Figure 1 shows exemplarily for the statistical model results the EF of NO_x as function of vehicle speed for the measurements of the Gubrist tunnel.

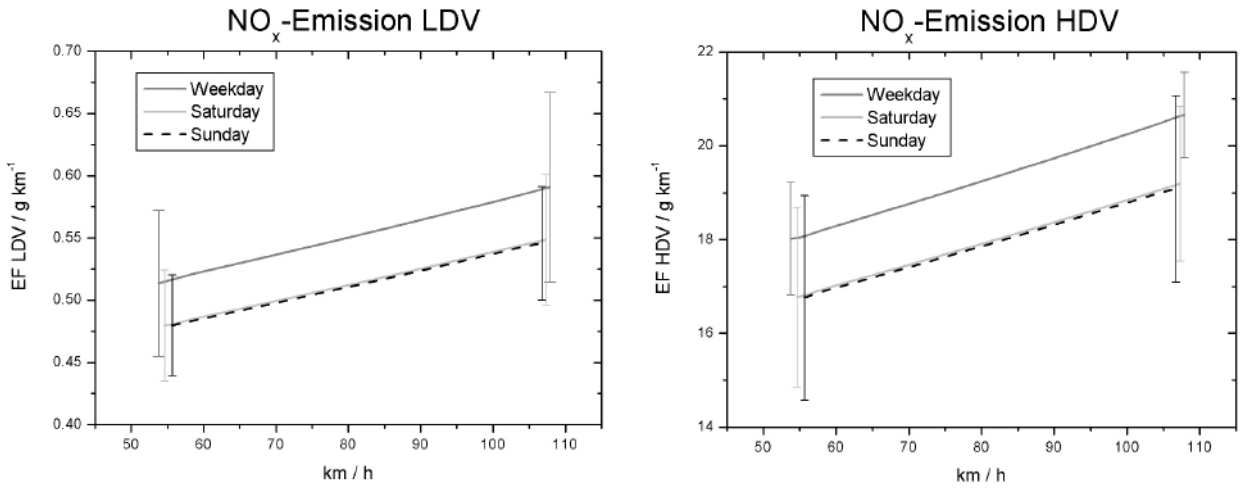

Figure 1. Statistical model results (see equation (3)) for the EF of NO_x *as function of averaged vehicle speed for the measurements of the Gubrist tunnel. Left side: LDV; right side: HDV.*

Nitrogen oxides ($NO+NO_2$)

Gubrist tunnel (road gradient: + 1.3%), 2002

vehicle speed: 60 km				90 km			
LDV		HDV		LDV		HDV	
workd.	sat./sun.	workd.	sat./sun.	workd.	sat./sun.	workd.	sat./sund.
0.52	0.48/0.48	18.3	17.0/16.9	0.56	0.54/0.53	19.7	18.4/18.3
(0.45	0.30/0.28	19.5		0.47	0.65/0.6 20.4)		

Gubrist tunnel, 1993 (aver. veh. speed: 92 km/h): 1.05±0.92 15.6±0.8)

Plabutsch tunnel (two lanes)

number of vehicles:300				number of vehicles: 500			
LDV		HDV		LDV		HDV	
workd.	sat./sun.	workd.	sat./sun.	workd.	sat./sun.	workd.	sat./sund.
0.86	0.56/0.43	11.51	7.41/5.67	0.75	0.48/0.37	10.3	6.45/4.94
(1.17	0.52/0.41	10.65		0.97	0.52/0.41	8.81)	

Lundby tunnel

road gradient: -3.5		road gradient: + 0.25	
LDV	HDV	LDV	HDV
0.36 (0.31-0.42)	1.16 (0.89-1.44)	0.69(0.58-0.81)	9.41 (8.82-9.99)

Carbon monoxide (CO)

Gubrist tunnel (road gradient: + 1.3%), 2002

vehicle speed: 60 km			90 km		
LDV		HDV	LDV		HDV
workd.	sat./sun.	not avail.	workd.	sat./sun.	not avail.
3.4	3.3/3.2		2.6	2.8/2.6	
(3.4	2.8/2.8				

Gubrist tunnel, 1993 (aver. veh. speed: 92 km/h): 4.17±0.37

Plabutsch tunnel

number of vehicles:300			number of vehicles: 500		
LDV		HDV	LDV		HDV
workd.	sat./sun.		workd.	sat./sun.	
1.12	0.75/0.75	not avail.	0.98	0.66/0.66	not avail.

(1.16	0.74/0.76	not avail.	0.99	0.74/0.69	not avail.)
Lundby tunnel					
road gradient: -3.5			road gradient: + 0.25		
LDV		HDV	LDV		HDV
2.68 (2.38-2.98)		not avail.	2.11 (1.79-2.43)		not avail.
Total Non-Methane volatile organic compounds (t-NMVOC)					
Gubrist tunnel (road gradient: + 1.3%), 2002					
vehicle speed: 60 km			90 km		
LDV		HDV	LDV		HDV
workd.	sat./sun.		workd.	sat./sun.	
0.28	0.23/0.20	not avail.	0.19	0.16/0.14	not avail.
(0.27	0.35/0.30	not avail.	0.19	0.16/0.14	not avail.)
Gubrist tunnel, 1993 (aver. veh. speed: 92 km/h):			0.46±.05		
Plabutsch tunnel					
number of vehicles:300			number of vehicles: 500		
LDV		HDV	LDV		HDV
workd.	sat./sun.		workd.	sat./sun.	
0.17	0.12/0.11	not avail.	0.15	0.11/0.09	not avail..
(0.19	0.11/0.10	not avail.	0.17	0.09/0.08)	

Table 2: Overview of the results of the statistical analysis of the tunnel studies (see text). In brackets are the confidence intervals of the statistical model for the Lundby tunnel measurements. The numbers in brackets on separate lines are the results of the statistical models obtained based on part of the measurements (e.g. only Monday to Friday or Saturday/Sunday). For the Gubrist tunnel the results of the measurements of 1993 are included for comparison (see Staehelin et ali (1997)).

Table 2 provides an overview of all model results. The EFs of NO_x of the Gubrist tunnel show an increase with vehicle speed and different results for the different days of the week. In addition a decrease for CO and t-NMVOC with vehicle speed was observed.

However, only preliminary results of the confidence intervals of these model results are presently available and the significance of these results needs to be tested further. Table 2 does not contain results of EF of CO and t-NMVOC for HDV. The proportion of HDV never exceeds 30% and therefore the EF of HDV obtained by extrapolation to 100% yields more reliable estimates for NO_x because its emission factor is much larger than for LDV which is not the case for the EF of CO and t-NMVOC.

For the Plabutsch tunnel the EFs were calculated by the new emission model PHEM (Passenger car and Heavy duty Emission model) developed by the University of Graz, yielding 8.79 g/km for NO_x emission of HDV. In the PHEM model new transient chassis dynamometer measurements of HDV were included (Hausberger et ali (2002)). This value is larger than the results of the "handbook" and still lower than the EF derived by the statistical model (see Table 2). However, for a conclusive statement of the significance of the differences the confidence intervals of the statistical model needs to be determined. The results of the analysis show in addition a considerable effect of the day of the week on the EFs of LDV of the Plabutsch tunnel, most pronounced for NO_x and CO. This suggests that the vehicle collective of LDV may be considerably different for weekends than during the week. The effect is weaker for the Gubrist tunnel. In an earlier study, when the effect was larger, the proportion of vehicles equipped with catalytic converters was lower (Staehelin et ali (1998)). The EFs determined for the same species for the different tunnels are different. Figure 2 provides evidence that at least a considerable part of this difference may be caused by the different road gradients of the tunnels. The dependence of the EF of NO_x on road gradient appears to be much larger for HDV than for LDV.

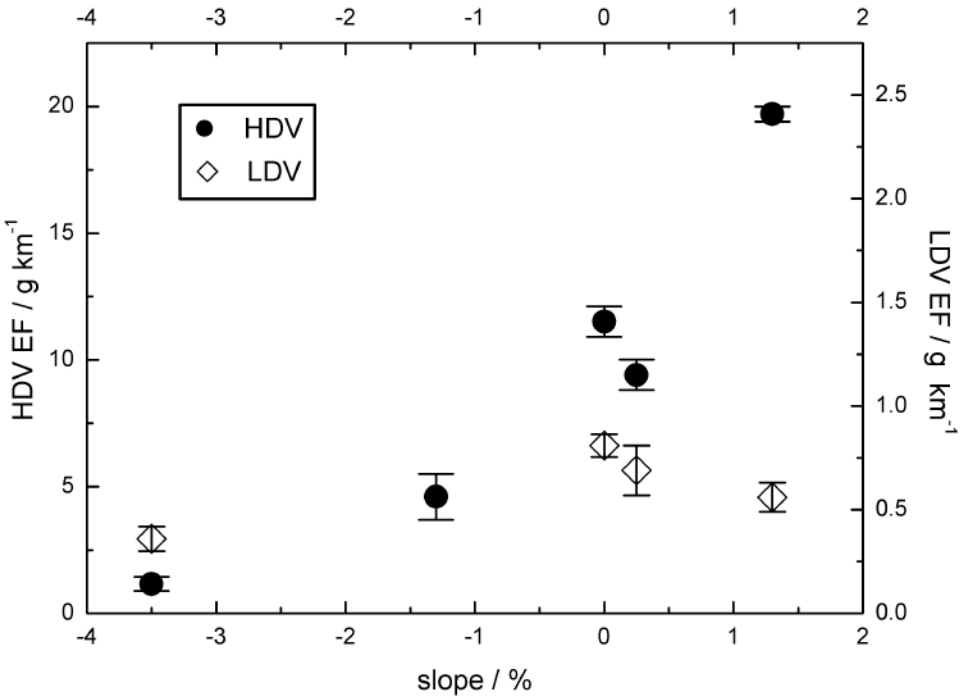

Figure 2. EF of NO_x for HDV and LDV as function of the road gradient derived from the measurements of the Lundby tunnel, the Plabutsch tunnel and the Gubrist tunnel (see text). The point of HDV at a slope of -1.3% was calculated from the Gubrist tunnel measurements of 1997 (from Steinemann and Zumsteg (2001)).

Large discrepancies between the tunnels were found for CO emission of LDV, resulting in a factor of almost 3, with the lowest value in the Plabutsch tunnel. Differences of the fleet composition, possibly different proportions of diesel passenger cars, could be important. This needs further investigation.

Conclusions

Road tunnel measurements allow for obtaining emission factors for a collective of vehicles ("real world emission"): This provides complementary information to dynamometric test measurements. In this presentation we attempted to show how statistical modeling can be used as tool to make best use of the measurements. A companion paper by Sturm et ali includes the comparison of NO_x measurements of the Plabutsch tunnel with recent dynamometric test results for NO_x of HDV. By such a comparison emission models can be validated by a collective of vehicles for a special condition. In the next step the results presented here will be compared with the numerical road traffic emission model which will be provided by the project ARTEMIS.

Repeated studies of emissions in the same tunnel offer the benefit of assessing the success of introducing new vehicle technologies. Measurements of the Tauern tunnel in Austria of the years 1988 and 1997 show a decrease in the LDV emissions of CO and t-NMVOC by approximately a factor of 10. This is mainly because of the successful introduction of catalytic converters, which increased from a share of virtually zero in 1988 to approximately 70% in 1997 in the collective of this tunnel (Schmid et ali (2001)). In the Gubrist tunnel, measurement campaigns took place 8 times between 1990 and 2002 and confirm the large decrease in the emissions of LDV (Steinemann and Zumsteg (2001)). We included the values of the EF of the Gubrist tunnel study of 1993 in Table 2 because the statistical models were similar in that study to those used here. While the emissions of LDV strongly decreased during these 9 years, the EF of NO_x for HDV increased by approximately 20%. This needs further attention.

Acknowledgments

The project was supported by the EU-project ARTEMIS and by AWEL (Amt für Wasser, Energie und Luft of the Kanton Zurich). We would like to thank our colleagues of AWEL who provided the data of the Gubrist tunnel study.

References

Catone G. (2002) Schätzung von Emissionsfaktoren für verschiedene Fahrezgkategorien, Diploma Thesis, Department of Mathematics, ETH Zurich.

John C., R. Friedrich, J. Staehelin, K. Schläpfer & W. A. Stahel (1999): Comparison of emission factors for road traffic from a tunnel study (Gubrist tunnel, Switzerland) and from emission modelling. Atmospheric Environment, vol. 33, 3367-3376.

Hausberger S., J. Rodler & P. Sturm (2002): Emission factors for HDV and validation by tunnel measurements. VKM-THD Mitteilungen, R. Pischinger (Ed.) , vol. 81, 93-100.

Kühlwein J. & R. Friedrich (2000): Uncertainties of modelling emissions from road transport. Atmospheric Environment, vol. 34, 4603-4610.

Schmid H., E. Pucher, R. Ellinger, P. Biebl & H. Puxbaum (2001): Decadal reductions of road traffic emissions on a transit route in Austria - results of the Tauerntunnel experiment 1997. Atmospheric Environment, vol. 35, 3585-3593.

Staehelin J., K. Schläpfer, T. Bürgin, U. Steinemann, S. Schneider, D. Brunner, M. Bäumle, M. Meier, C. Zahner, S. Keiser, W. Stahel & C. Keller (1995): Emission factors from road traffic from a tunnel study (Gubrist tunnel, Switzerland). Part I: Concept and first results, Sci. Tot. Env., vol. 169, 141-147.

Staehelin J., C. Keller, W. Stahel, K. Schläpfer, U. Steinemann, T. Bürgin & S. Schneider, (1997): Modelling emission factors of road traffic from a tunnel study. Environmetrics, vol. 8, 219-239.

Steinemann, U. & F. Zumsteg, 2001: Verkehrs- und Schadstoffmessungen 2000 im Gubristtunnel, Bericht US 89-16 für das Amt für Abfall, Wasser, Energie und Luft des Kantons Zürich (AWEL), Schweiz.

Sturm P.J., J. Rodler, B. Lechner & A. Almbauer (2001): Validation of emission factors for road vehicles based on street tunnel measurements. Intern. J. Vehicle Design, vol. 27, 65-75.

UBA, 1999: Handbuch für Emissionsfaktoren des Strassenverkehrs, Version 1.2, Umweltbundesamt Berlin, Bundesamt für Umwelt, Wald und Landschaft Bern, Infras AG Bern (published as software on CD-ROM).

12th International Symposium "Transport and Air Pollution" / 12e Colloque international "Transports et pollution de l'air", Avignon, 16 -18 *June* / juin 2003
proceedings / actes, n°92, tome / Vol. 1, Inrets ed., Arcueil, France, 2003, p. 177-183

The importance of the road transport sector in the global warming - the case of the city of Rio de Janeiro

Laura Bedeschi Rego de Mattos* & Suzana Kahn Ribeiro**
*Transport Engineering Program – COPPE, Federal University of Rio de Janeiro – e-mail: lauram@uol.com.br or laura@bndes.gov.br
**Transport Engineering Program – COPPE, Federal University of Rio de Janeiro – Centro de Tecnologia Bloco H sala H-111 – Ilha do Fundão, CEP 21945-970, Rio de Janeiro, RJ – Brasil – Fax +55 21 290 6626 – e-mail: skr@coppe.ufrj.br

Abstract
This paper intends to show the importance of the urban road transport sector on greenhouse gas emissions. With this purpose, Rio de Janeiro city was chosen for a case study. Emissions of carbon dioxide (CO_2) were considered as prime greenhouse gas. The carbon dioxide emitted by the transport sector is a consequence of the fossil fuel burning like gasoline and diesel oil. Therefore, highlighting the importance of the road transport sector in local emissions might enable actions of abatement and mitigation focused on the most significant sectors and not on diffused strategies. The paper also shows that, by itself, the road transport sector in Rio de Janeiro city is responsible for more than half of the CO_2 emissions from all the economy sectors in the use of fossil fuels.
Keys-words*: carbon dioxide emission, global warming, road transport.*

Introduction

The burning of fossil fuels throughout the world is the main cause of carbon dioxide (CO_2) emissions, the prime greenhouse gas. In a large city, among all sectors that consumes fossil fuels, road transport sector is one of the most important. Therefore, besides being the great responsible for local pollution, emitting gases like carbon monoxide, nitrogen oxides, sulphur oxides, aldehydes and particulate matter, this sector is responsible for the emission of a large amount of CO_2 as well.

Thus, comparing the importance of the road transport sector in greenhouse gase emissions with other sectors, highlights the relevance of choosing an abatement and mitigation strategy for the emissions in large cities. A quantitative analysis allows a definition of mitigation plans for the emissions in a qualitative and quantitative way. This paper intends to show the importance of road transport sector, represented by light vehicles (automobiles, motorcycles etc.) and heavy vehicles (buses and trucks), on the greenhouse gas emissions. With such purpose, the City of Rio de Janeiro was used as an example. Valuation was made based on the 90s available data. The main goal is to show the significance of the transport sector CO_2 emissions in Rio de Janeiro City along the mentioned decade.

1 - The transport sector in the city of Rio de Janeiro

Description of the transport matrix of the City of Rio de Janeiro

The City of Rio de Janeiro has currently about 5,595,578 inhabitants, with a population growth of 0.27% a year (CIDE, 1999). The most used modal in the passenger transport in the city is the road transport, represented by buses and automobiles. Table 1 shows the division of modals in the mass transport used in the city and Table 2 displays the evolution of the city vehicle fleet.

Modal	Percentage
Ferry boats	0.9%
Subway	5.7%
Trains	3.5%
Buses	89.9%
Total	100.0%

Table 1: Distribution of the passengers' demand per modal of transport in the Metropolitan Region of Rio de Janeiro, 1998.Source: Municipal City Hall of Rio de Janeiro (1999).

		Class of Vehicle					
Year	Type of Fuel	1.1.1.1.1.2 **assenger Car**	Commercial Cars	Transit Motor Bus	Freight Transport	Bicycles Tricycles	TOTAL
1996	Gasoline	801,152	161,693	386	3,902	60,127	1,027,260
	Ethanol	254,300	61,653	12	256	122	316,343
	Diesel	1,835	9,279	13,791	27,838	16	52,759
	Others	90	32	177	13	3	315
	Total	1,057,377	232,657	14,366	32,009	60,268	1,396,677
1997	Gasoline	860,383	152,270	260	2,391	62,473	1,077,777
	Ethanol	244,068	55,867	10	172	110	300,227
	Diesel	2,133	8,987	15,761	28,051	15	54,947
	Others	446	111	181	13	3	754
	Total	1,107,030	217,235	16,212	30,627	62,601	1,433,705
1998	Gasoline	933,768	159,917	257	2,342	68,526	1,164,810
	Ethanol	235,957	53,530	9	144	105	289,745
	Diesel	2,369	10,102	17,253	29,946	13	59,683
	Others	4,435	814	177	17	3	5,446
	Total	1,176,529	224,363	17,696	32,449	68,647	1,519,684

Table 2: Vehicle fleet in the City of Rio de Janeiro per class of vehicle and type of fuel in the years 1996, 1997 and 1998 (GEIPOT, 1999).

Use of fossil fuels and ethanol in the City of Rio de Janeiro

The city uses gaseous and liquid fossil fuels as a source of energy, the most representative being gasoline and diesel oil. The use of ethanol was also representative in the early 90s, but its use got into decline up to 1998. The data shown on Table 3 were directly provided by the National Oil Agency (ANP), the Gas Distribution Company of Rio de Janeiro (CEG), Petrobras S/A and the Refinery of Manguinhos. CEG provided the natural and manufactured gas consumption in the city, Petrobras informed the fuel consumption for non-energetic purposes (in the specific case of the city of Rio de Janeiro it was considered only the asphalt and the lubricants), the Refinery of Manguinhos sent the amount of oil barrels processed by them and the remaining data were provided by ANP. Table 3 shows the consumption of gaseous and liquid fossil fuels as well as ethanol in the city.

The bunker consumption is not accounted on table 3. Bunker is considered as the consumption of aviation kerosene, aviation gasoline, and fuel oil used in intercity, interstate and international aviation and navigation. In the case of the City of Rio de Janeiro, there is not bunker consumption of fuel oil, once the international navigation fleet is not fueled in the city. To the international bunker of the city it was also added aviation kerosene and aviation gasoline used in the air transport, considered as intercity/ interstate bunker, since almost all the trips by airplane are destined to areas outside the city. Only a part of the consumption of aviation gasoline was considered in the City of Rio de Janeiro for use in the air transport within the city limits.

	1990	1991	1992	1993	1994	1995	1996	1997	1998
Crude Oil (m^3)	16,912	14,453	16,744	18,182	16,712	17,751	17,091	16,933	17,239
Gasoline (m^3)	566,336	605,124	551,583	612,705	667,481	774,657	880,429	932,337	835,138
Aviation Gasoline (m^3)	4,114	1,848	1,307	1,094	790	835	889	1,616	1,213
Other Kerosene (m^3)	22,420	18,874	12,145	8,151	6,712	6,728	4,696	2,436	1,174
Diesel Oil (m^3)	632,309	586,744	506,672	551,032	587,512	529,933	532,601	650,439	674,484
Residual Fuel Oil (ton)	369,060	159,445	146,636	163,948	200,260	236,489	367,741	342,733	389,579
LPG (ton)	155,632	141,117	117,313	131,369	145,408	139,663	141,637	140,212	144,468
Asphalt (m^3)	21,419	18,465	26,589	22,650	29,790	25,358	35,058	27,626	nd*
Lubricants (m^3)	49,446	48,522	44,363	39,742	47,597	50,370	53,665	52,225	nd*
Natural Gas (Dry) (10^3 m^3)	274,016	304,594	297,980	302,632	303,367	326,987	329,220	362,541	418,813
Manufactured Gas (10^3 m^3)	155,870	154,865	141,760	127,164	121,278	112,543	109,863	104,334	106,026
Anhydrous Ethanol (m^3)	159,736	170,676	155,575	172,814	188,264	218,493	248,326	262,967	263,728
Hydrous Ethanol (m^3)	817,098	721,378	637,875	589,373	574,639	537,528	482,409	384,181	257,189

*Table 3: Consumption of Gaseous and Liquid Fossil Fuels and Ethanol in the City of Rio de Janeiro from 1990 to 1998. * data not available.*

2 - CO_2 Emissions in the road transport sector in the city

The CO_2 emissions were made in accordance with IPCC (Intergovernmental Panel on Climate Change) methodology, presented in the 1996 Guidelines for National Greenhouse Gas Inventories and officially adopted by the Brazilian government in order to develop the national inventory of greenhouse gases. IPCC is a panel of the United Nations gathering over 300 scientists from all around the world and it has the purpose of discussing and reporting the opinion of the different scientists of several fields, on issues involving global warming, the impact it may cause and the potential reply policies. Item 2.1 will show the simplified methodology and, on item 2.2, the emissions of the road transport sector.

Simplified methodology for counting the CO_2 emissions

The volume of CO_2 or carbon (C) contained in the CO_2 emitted from the oil products is determined in accordance with the following formula, considering the fuel consumption in energy unit and the emission factor.

$$ACO_2 = FC \times EF \qquad (1)$$

Whereas: ACO_2: amount of carbon (tC)
FC: Fuel Consumption (TJ)
EF: Emission Factor (tC/TJ)

So, the first action to obtain the emitted volumes of CO_2 from gaseous and liquid fossil fuels and ethanol is to transform the mass and volume unit into a common energy unit, in this case, tera-joule (10^9 joule). The conversion coefficients of mass and volume unit into energy unit were obtained in the Energy Balance of the Rio de Janeiro State (NUSEG, 1998) and the average energy value of the Brazilian toe (toe - ton of oil equivalent, where the energetic content of 1 toe is a function of the type of standard oil) used was 1 Brazilian toe = 10,800 Mcal = 45.2174 TJ. The emission factors shown in equation 1 were obtained with IPCC methodology (1996). Therefore, CO_2 emissions were estimated based on fuel data provided by Table 3 which was previously exhibited. In order to transform a ton of C into a ton of CO_2 stoichiometry was used by multiplying the value in tons of C by the factor (44/12), obtaining a result in tons of CO_2. The unit used by the inventories, to make easier the comparisons between the results, is the $GgCO_2$, i.e., Giga gram of CO_2 (1,000 tons of CO_2).

It is important to point out that, when using the ethanol originated from sugar cane, the final balance of CO_2 emission is considered null. That happens because, during the growth of sugar cane, the CO_2 released in the combustion process of the vehicles is reabsorbed through the photosynthesis process.

Total emissions and transport sector emissions in the City of Rio de Janeiro

In this section, greenhouse gas emissions originated from burning or non-energetic use (sources whose purpose is not to obtain energy) of the fuels presented on table 3 is shown. The resulting emissions can be seen in Table 4.

In accordance with the methodology used to raise the CO_2 emissions, asphalt does not emit CO_2, whereas lubricants emit 50% of the amount of carbon they have. In other words, to non-energetic purposes, a part, in case of lubricants, or the totality, in case of asphalt, of the existing carbon gets in stock or fixed. To the renewable and liquid biomass, the use of hydrous and anhydrous ethanol, such percentage of carbon in stock is of 100%, since all the carbon emitted in fuel burning is sequestered in biomass renewal, as previously mentioned. This fact justifies the zero emission for the hydrous and anhydrous ethanol.

	1990	1991	1992	1993	1994	1995	1996	1997	1998
Crude Oil	46	39	46	49	45	48	46	46	47
Gasoline	1,287	1,375	1,253	1,392	1,517	1,760	2,001	2,118	1,898
Aviation Gasoline	9	4	3	2	2	2	2	4	3
Other Kerosene	56	47	30	20	17	17	12	6	3
Diesel Oil	1,689	1,567	1,353	1,472	1,569	1,415	1,423	1,737	1,802
Residual Fuel Oil	1,134	490	451	504	615	727	1,130	1,053	1,197
LPG	454	412	343	384	425	408	414	409	422
Asphalt	0	0	0	0	0	0	0	0	nd*
Lubricants	67	66	60	54	65	68	73	71	nd*
Natural Gas (Dry)	533	593	580	589	591	637	641	706	815
Manufactured Gas	169	168	153	138	131	122	119	113	115
Anhydrous Ethanol	0	0	0	0	0	0	0	0	0
Hydrous Ethanol	0	0	0	0	0	0	0	0	0
Total Emissions	5,444	4,761	4,272	4,604	4,976	5,204	5,859	6,264	6,301

Table 4: CO_2 emissions ($GgCO_2$) per fuel from 1990 to 1998. data not available*

The role in the CO_2 emissions originated from gasoline and diesel oil, which are the main fuels used in the road transport sector, in the total of emissions is the most significant one, followed by the contribution of fuel oil. It is interesting to notice the effect of the economical crisis in the beginning of the decade, which caused a drop in the emissions. The economical recovery from 1994 on was followed by an increase in CO_2 emissions, lead by gasoline (from 1995 to 1998). Such fact originated a rapid expansion in the individual vehicle fleet, together with a drop in the use of ethanol, resulting in a huge increase in CO_2 emissions due to the gasoline used in individual transport between 1994 and 1996. From 1995 to 1998, the increase in CO_2 emissions began to be leaded by the gasoline used in individual transport, mostly represented by light vehicles. The CO_2 emissions due to fossil fuels burning and non-energetic use had an absolute increase between 1996 and 1998, equivalent to the raise occurred from 1990 to 1996.

The participation, in relation to the total of emissions, of each one of the utilized fuels, can be seen on Table 4. Therefore, the emissions of each fuel separately can be allocated according to the user sector, establishing the responsibility of each one.

In order to establish the responsibility of the several sectors which use of fossil fuels and biomass, a desegregation estimate of CO_2 emissions in the City of Rio de Janeiro was performed, in accordance

with the following large sectors of final use: Electric Generation, Industrial, Passenger Transport, Transit Bus and Freight Transport, Residential/ Commercial/ Services, Refinery of Manguinhos and Others. The allocation per large sectors of final use was performed considering the following standards:

Electric Generation – consumption of fuel oil and natural gas from the thermal power plant of Santa Cruz (the origin of the electric energy used in the City of Rio de Janeiro in 1998 was 81.9% hydro, 7.9% thermal and 10.2% thermonuclear); Industrial – consumption of fuel oil used in industrial boilers and ovens (less the residual fuel oil used for electric generation), consumption of natural and manufactured gas; Individual Transport - consumption of gasoline, hydrous ethanol, anhydrous ethanol and vehicle natural gas (in passenger vehicles and taxis); Transit Bus and Freight Transport – consumption of diesel oil (mostly used in buses, vans and trucks); Residential/ Commercial/ Services - all the consumption of LPG, other kerosene, natural gas and manufactured gas (cooking, water heating and lighting); Refinery of Manguinhos - total of energy spent in the refine process using equivalent crude oil; Others - remaining consumption of aviation gasoline which is not accounted in the bunkers (helicopters, etc.) and the consumption of lubricants and asphalt.

Figure 1 shows that the prime sector in CO_2 emission, among the sectors that consumes fossil fuels, is the transit bus and freight transport, responsible for 31% of the total emissions, presented on table 4.

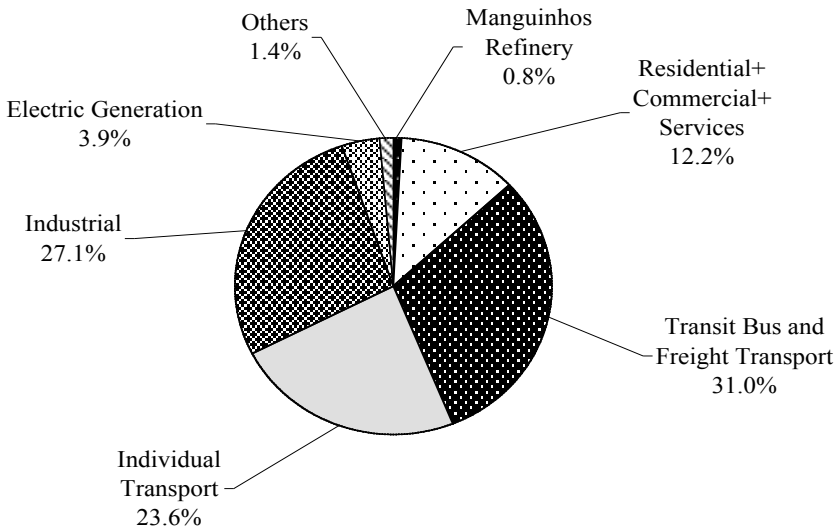

Figure 1: Percentage of the participation of each sector in CO_2 emission – 1990

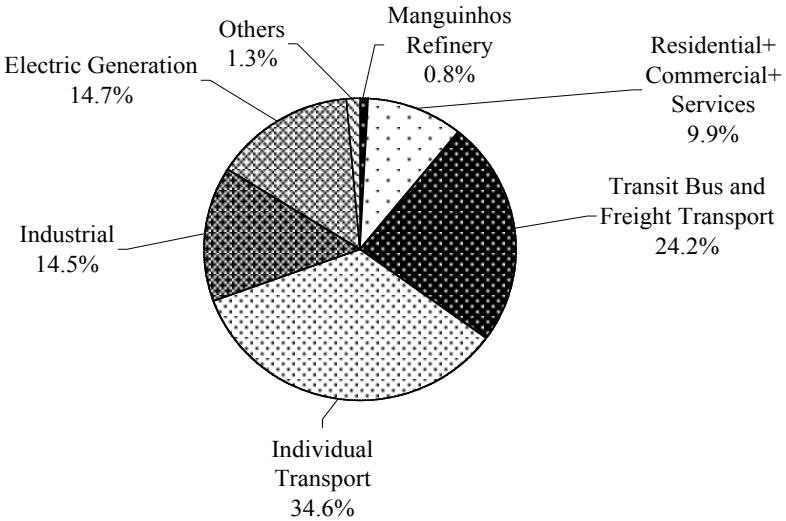

Figure 2: Percentage of the participation of each sector in CO_2 emissions – 1996

As previously mentioned, the individual transport sector uses anhydrous and hydrous ethanol, thus making the transit bus and freight transport sector the main responsible for the CO_2 emissions in the transport sector. Therefore, the road transport sector alone is responsible for about 54.6% of the CO_2 emissions originated from the use of fossil fuels in the City of Rio de Janeiro.

In 1996, the importance of the road transport sector in the CO_2 emissions was still high, with 58.8% of the total emission. The difference that can be seen in the period between 1990 to 1996 is that reduction in the role of ethanol in the fleet (see table 3), compared to the gasoline, caused the individual transport sector to increase its participation in the CO_2 emissions, being higher than the transit bus and freight transport.

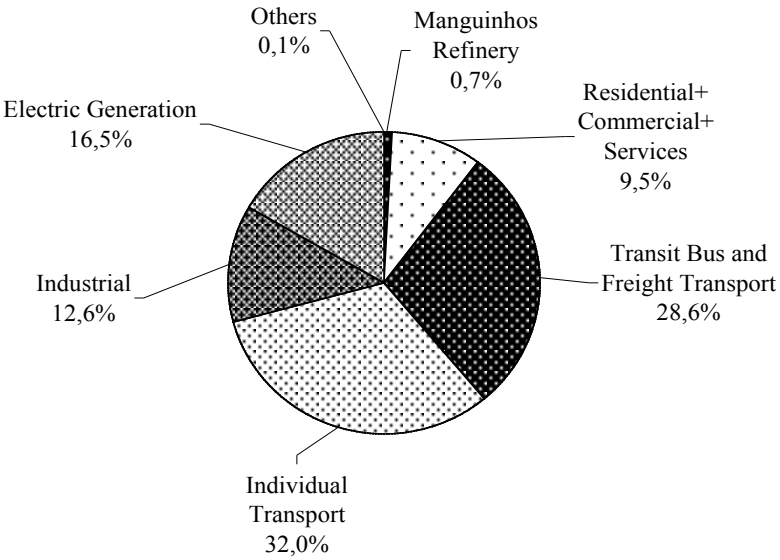

Figure 3: Percentage of the participation of each sector in CO_2 emissions – 1998

In 1998, there was a drop in the consumption of gasoline and an increase in the consumption of diesel oil, in relation to 1996, causing the CO_2 emissions of the transit bus and freight transport to be once more almost of the same magnitude as the individual transport emissions. It can be noticed on figure 3 that the road transport sector in 1998 is responsible for 60.6% of the CO_2 emissions.

Conclusions and General Comments

Considering the previously shown data, that the emissions of the road transport sector, in a large city as Rio de Janeiro, is the most impacting one. The CO_2 emissions of such sector varied from 54.6% to 60.6% of the total emissions of fossil fuels between 1990 and 1998. The country transport sector presents nowadays the same evolution presented before regarding CO_2 emissions, since the fossil fuels consumption in Brazil is still growing nowadays, maintaining the relevancy of the sector in the CO_2 emissions.

The factors to be taken into consideration to determine the level of consumption of the transport sector in a city are, among others, the variation in the sizes of the cities, the population density, the social and economical structure and the level of absorption of new technologies developed throughout the world. The use of energy and consequent greenhouse gases emissions depends on the following factors, among others:

- Type of modes.
- Demand for displacement
- Incentive to collective transport
- Technology – speed and amplitude of the use of new technologies. Considering that such new technologies can be basically separated in three categories:
  - Improvement in vehicle technology reducing carbon emissions. Periodic maintenance services, including tires, oil and engine adjustment can represent a fuel economy of 2 to 10%

(Davidson, 1992)

- Improvement in fuel technologies, including alternative fuels as compressed natural gas, liquefied petroleum gas, ethanol (that is a renewable fuel), and other renewable fuels.
- Changes in the infrastructure and in systems like smart signalling, as for example the automatic traffic control, improving the vehicle traffic flow, specially the collective ones.

In case Brazil is obliged, in the future, to reduce the greenhouses gas emissions, due to international agreements, the road transport sector will have to be the priority. The settlement of politic strategies as well as abatement/mitigation plans of greenhouse gases emissions for this sector are, therefore, extremely important. These measures, besides reducing the greenhouse gas emissions, can also result in a better energy utilization for the sector under focus.

References

CEG (1999) CEG abre o maior posto de gás natural do País. Cia. Distribuidora de Gás do Rio de Janeiro, http://www.ceg.com.br/noticias/n31.htm.

CIDE (1999) Anuário Estatístico do Estado do Rio de Janeiro - 1998. Centro de Informações e Dados do Rio de Janeiro, Rio de Janeiro RJ, p 87-106.

Davidson, O. R. (1992) Transport Energy in Sub-Saharan Africa: Options for a Low-Emission Future. Report No. 267, Princeton, NJ, USA.

GEIPOT (1999) Anuário Estatístico de Transportes - 1999. Empresa Brasileira de Planejamento de Transportes, Ministério dos Transportes, Brasília, DF, p 203-265.

IPCC (1996) Greenhouse Gas Inventory Reporting Instructions – IPCC Guidelines for National Greenhouse Gas Inventories, Vol. 1, 2, 3. Intergovernmental Panel on Climate Change, United Nations Environment Program, the Organization for Economic Co-operation and Development and the International Energy Agency, London, United Kingdom.

NUSEG (1998) Balanço Energético do Estado do Rio de Janeiro 1980 - 1997. Núcleo Superior de Estudos Governamentais, Universidade do Estado do Rio de Janeiro, Rio de Janeiro, p 53-55.

Pischinger, R. e Hausberger, S. (1993) Measures to Reduce Greenhouse Gas Emissions in the Transport Sector. Institute for Internal Combustion Engines and Thermodynamics, Technical University, Graz, Austria.

Prefeitura Municipal do Rio de Janeiro (1999) Plano Estratégico do Rio de Janeiro - Acessibilidade, Logística e Mobilidade na Cidade do Rio de Janeiro: Evolução e Desafios. Rio de Janeiro.

Ribeiro, S. K. (1995) Uso Energético dos Produtos da Cana-de-açúcar como Instrumento do Brasil em Negociações Internacionais para Redução de Emissão de Gases de Efeito Estufa. Tese (Doutorado) - Programa de Engenharia de Produção, COPPE/UFRJ, Rio de Janeiro, p 23-58; p 80-98.

12th International Symposium "Transport and Air Pollution" / 12e Colloque international "Transports et pollution de l'air", Avignon, 16 -18 *June* / juin 2003
proceedings / actes, n°92, tome / Vol. 1, Inrets ed., Arcueil, France, 2003, p. 185-192

Diesel vs. Gasoline Emissions: Does PM from Diesel or Gasoline Vehicles Dominate in the U.S.?

Alan W. Gertler
Desert Research Institute, 2215 Raggio Parkway, Reno, NV 89512, United States

Abstract
In the U.S., the majority of the on-road fleet and vehicle miles travelled are attributed to light-duty vehicles, which are fuelled almost entirely by gasoline. However, due to their significantly higher PM emission rates, emissions inventories have tended to attribute the majority of the mobile source PM to contributions to heavy-duty diesel vehicles and strategies to reduce mobile source PM have focused on the contribution from this source. A limited number of source attribution studies have implied that PM emission inventories over-estimate the diesel contribution and emissions from gasoline vehicles may be greater than previously believed. Other receptor-modelling studies have found diesel vehicles to be the dominant source of motor vehicle PM. The former conclusion is supported by recent on-road PM emission rate results obtained in a highway tunnel and crossroad series of experiments. This paper describes the often-conflicting results obtained from receptor modelling studies and emission inventories and attempts to reconcile the differences.
Keys-words*: emissions inventory, receptor models, emission factors, particulate matter.*

Introduction

The U.S. currently has National Ambient Air Quality Standards (NAAQS) for PM_{10} and $PM_{2.5}$. For PM_{10} the standard is 150 μg/m^3 for 24-hrs and 50 μg/m^3 for an annual average. The newly implemented $PM_{2.5}$ standard consists of a 65 μg/m^3 24-hr level and 15 μg/m^3 annual average. While nationwide measurements designed to characterize the levels of PM_{10} and sources contributing to the observed levels have been underway for many years, only recently has a national network for measurement of $PM_{2.5}$ been implemented. There have, however, been numerous intensive studies and local/regional monitoring efforts designed to characterize the levels and sources of $PM_{2.5}$.

Based on the ambient data and source characterization results, mobile sources are a significant source of ambient PM_{10} and $PM_{2.5}$ (Gertler et al., 2000) and control of PM emissions from this source category is crucial if the NAAQS are to be met. This is especially true for $PM_{2.5,}$ since a large fraction of mobile source PM emissions is in this size fraction. Figure 1 shows the results of an intensive monitoring study performed at a roadside location in New York City that had a significant impact from diesel buses (Wittorff et al., 1994). Average PM_{10} levels for this period exceeded the NAAQS 50 μg/m^3 level, although all loadings were below the 24-hr standard. Chemical analysis of the collected samples followed by application of receptor modelling methods determined that approximately 60% of the observed PM_{10} was attributable to diesel and gasoline powered vehicle emissions.

The longer duration and more extensive Northern Front Range Air Quality Study (NFRAQS) performed in the Denver area highlighted the importance of the mobile source contribution to ambient $PM_{2.5}$ (Fujita et al., 1998). In this study 38% of the observed wintertime $PM_{2.5}$ was attributed to mobile sources. One important finding of this work was the gasoline-fuelled vehicle $PM_{2.5}$ contribution exceeded the contribution from diesel vehicles by approximately a factor of 3. Compared with the European situation, this may not be unusual since there are very few light-duty

diesel cars and trucks in the U.S., while most heavy-duty vehicles are diesel powered.

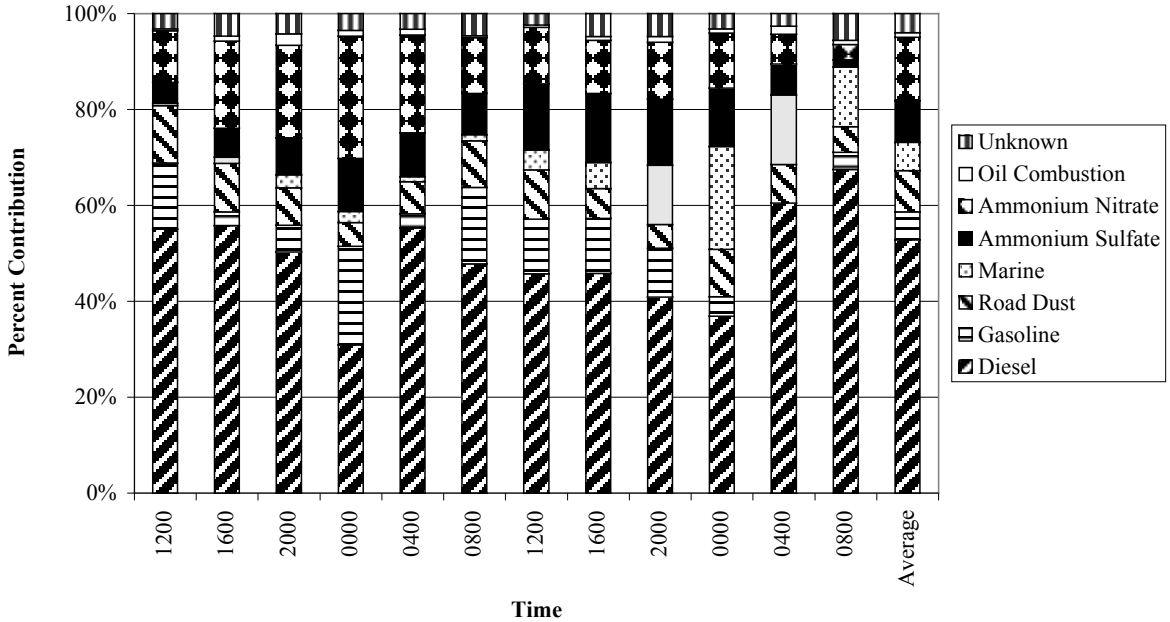

Figure 1: Results of a PM_{10} source apportionment study performed at a roadside location in New York City in April 1992. Emissions from diesel and gasoline powered vehicles contributed approximately 60% of the average observed PM_{10} levels (Wittorff et al., 1994).

Recently Clayton et al. (2003) reported the results of PM_{10} and $PM_{2.5}$ measurements performed at seven urban locations located across the U.S. The $PM_{2.5}$ source attribution results are presented in Figure 2. Primary mobile source emissions were an important contributor for all locations, although the relative contributions varied significantly from site to site. The Long Beach site had the highest observed ambient levels but the lowest percentage contribution from mobile sources. The authors noted that the major contributor to $PM_{2.5}$ was ammonium nitrate and this was likely due to the oxidation of NO_x emissions from motor vehicles.

Clearly motor vehicles are an important source of ambient PM in the U.S. but in order to effectively control the contribution from this source, it is necessary to quantify diesel and gasoline vehicle emissions and understand the mechanisms leading to mobile source related PM emissions. Primary PM emission sources from mobile sources include their exhaust (Mulawa et al., 1997, Gertler et al., 2002), the mechanical wear of tires and brakes (Pierson and Brachaczek, 1983), and the resuspension of particles from the pavement (Nicholson et al., 1989) and unpaved road shoulders (Moosmüller et al., 1998). Weingartner et al. (1997) found road dust and tire wear contributions to PM_3 to be very small, while Abu-Allaban et al. (2003a) found both PM_{10} and $PM_{2.5}$ tire and brake wear emission rates to be minimal or below their detection limit. Particulate matter in the vehicle-exhaust is dominated by particles smaller than PM_{10} (Sawyer and Johnson, 1995; Baumgard and Johnson 1996; Ristovski et al., 1998, Abu-Allaban et al, 2002). Mobile sources also contribute to atmospheric PM through the oxidation of emissions of gaseous precursors of PM from tailpipe and evaporative losses (e.g., ammonium nitrate in Figure 2).

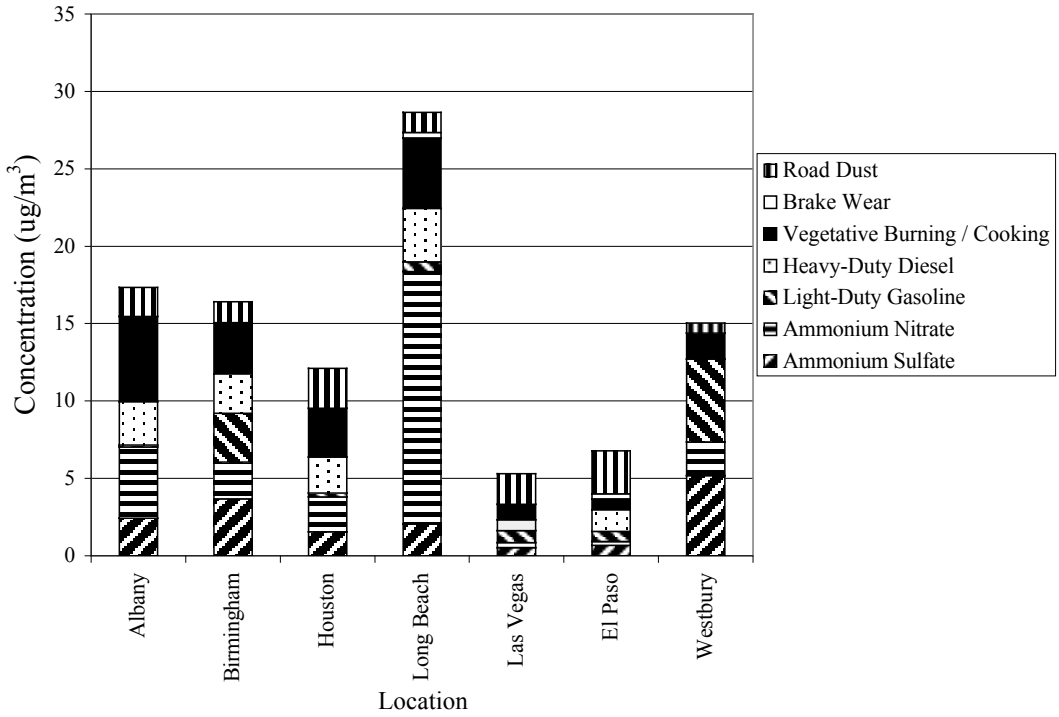

Figure 2: $PM_{2.5}$ source attribution results for seven urban sites in the U.S. (Clayton et al, 2003).

1 - Objectives

The primary objective of this paper is to assess the relative contributions of PM emissions from diesel and gasoline vehicles in the U.S. to ambient PM levels. Specific objectives include to:

- Compare emissions inventories in California and the U.S. to assess the influence of different mobile source emission factor models on the predicted contributions.
- Evaluate the results of ambient source attribution studies to compare the relative contributions from diesel and gasoline vehicles.
- Use on-road diesel and gasoline vehicle PM emission rates coupled with an estimate of vehicle miles travelled (VMT) to estimate the relative contributions from diesel and gasoline vehicles.

In presenting the results for the U.S. case, it is important to remember that the light-duty fleet is composed almost entirely of gasoline fuelled vehicles, while the heavy-duty fleet is composed primarily of diesel vehicles.

2 – Inventory Estimates

One of the most commonly applied approaches for evaluating the contribution of different sources to ambient pollutant levels is to prepare an emissions inventory that categorizes and sums the contributions from specific source groups. Inherent in this "bottom up" approach is a knowledge of the relevant emission factors (mass of pollutant per unit of activity) and the activity patterns of the sources. In the U.S. there are two models used to estimate emissions from mobile sources: the MOBILE series of models developed by the USEPA and used in 49 out of 50 states and the California Air Resources Board (CARB) EMFAC series of models used in California. Both rely on extensive dynamometer testing and fleet characterization to develop emission factors and correction algorithms (e.g., for different speeds, deterioration rates, etc.) for vehicle classes by model year. It should be noted that comparison of the emission model predictions with on-road observations have, in the past, raised doubts about the ability of EMFAC and MOBILE to accurately predict gaseous

emissions (Pierson et al., 1990, Gertler and Pierson, 1994) and the agreement has been even worse for PM (Gertler et al., 1997).

The U.S. national (USEPA, 2003) and California (CARB 2003) on-road PM_{10} emissions inventories by vehicle class and fuel type for 2000 are presented in Table 1. Comparing the fractions of emissions for both cases, we see that the USEPA predicted 62% and 38% of the on-road PM_{10} emissions were from diesel and gasoline vehicles, respectively. CARB predicted 33% and 67% of the PM_{10} as coming from these diesel and gasoline vehicles, respectively. There are a number of assumptions in this type of comparison. These include the fraction of vehicle miles travelled for each class is similar and fuels and technologies do not differ greatly and the basic emission rates in the models approximately the same. While emission factors used in the EPA model are know (6 mg/km for light-duty vehicles and 130 mg/km for heavy-duty vehicles), the emission factors used in the California model have not been published. Emissions standards for diesel vehicles are similar between California and the forty-nine states and stricter in California for light-duty vehicles. This should reduce the gasoline vehicle emission rate relative to the diesel vehicle emission rate in California, as opposed to the inventory prediction. Thus one might expect the CARB inventory to predict a higher fraction of PM from diesel vehicles than the USEPA inventory. Given the data in Table 1, the opposite is true.

	2000 U.S. (EPA)		**2000 California (CARB)**	
	tons/day	**% Total**	**tons/day**	**% Total**
Total On-Road	**273**		**53**	
Light-Duty Gas Vehicles & Motorcycles	**59**	**22%**	**18**	**34%**
light-duty gas vehicles	58		18	
motorcycles	0		0	
Light-Duty Gas Trucks	**36**	**13%**	**13**	**24%**
light-duty gas trucks 1	25		3	
light-duty gas trucks 2	11		10	
Heavy-Duty Gas Vehicles	**11**	**4%**	**5**	**9%**
Diesels	**168**	**62%**	**18**	**33%**
heavy-duty diesel vehicles	166		17	
light-duty diesel trucks	1		0	
light-duty diesel vehicles	1		0	

Table 1: Comparison between the U.S. (USEPA, 2003) and California (CARB, 2003) emissions inventories for on-road PM_{10}.

In 2000 CARB updated the EMFAC model, modifying the basic emission factors and algorithms. Following this change, they also adjusted past, present, and future emission inventory predictions. Table 2 contains the 1995 inventory using the old version of the model (CARB, 2000) and the revised data (CARB, 2002) for the South Coast Air Basin (Los Angeles). Under the new scenario the mobile source contribution is 42% diesel and 58% gasoline. This is not too different than the 2000 prediction for the whole state (Table 1). The prediction based on the older version of the model has 64% of the emissions coming from diesel vehicles and 36% from gasoline vehicles. This is similar to the U.S. national inventory results and is opposite the updated prediction. Given the primary modification was in the emission factor model, it is likely the differences are due to changes in this model. Further, the differences and changes in the inventories cast doubt on the accuracy of the mobile source emissions predictions contained in the inventories.

Emission Source	1995 (1999 Report)	1995 (2001 Report)
All Sources	496	339
Stationary Sources	33	23
Area-wide Sources	421	273
On-Road Mobile	28	25
Gasoline Vehicles	10	15
Diesel Vehicles	18	11
Other Mobile	14	18

Table2: 1995 South Coast Air Basin (Los Angeles, California) PM_{10} emissions inventory (tons/day, annual average) from two different California Air Resource Board documents (CARB 2000, 2002)

3 – Results of Source Attribution Studies

An alternative to the "bottom up" emissions inventory method to assess the impact of mobile source emissions on to ambient PM is the "top down" approach exemplified by the application of receptor modelling techniques. One source attribution technique involves the application of the chemical mass balance receptor model (CMB). In this approach, ambient samples are collected, chemically analysed, and the contributions from known source profiles used in a linear least squares regression model to provide a best fit to the ambient data (Watson et al., 1991). The coefficients fitting the source profiles provide a measure of contribution from the individual sources. The model fails when source profiles contain many of the same chemical species, as is the case with diesel and gasoline vehicle PM emissions. Recent advances using "enhanced" source profiles that incorporate additional species such as polyaromatic hydrocarbons (PAHs) can often resolve the colinearity problem (Gillies and Gertler, 2000, Fujita et al., 1998, Rykowski and Hrebenyk, 1997).

Two examples of source attribution studies using enhanced source profiles to separate diesel and gasoline PM contributions are the NRQAS study performed in Denver (Fujita et al., 1998) and Southern California Air Quality Study (SCAQS) performed in the Los Angeles Basin (Schauer et al., 1996). Results of the NFRAQS study, presented in Figure 3, indicate that gasoline vehicles contributed 28% of the observed $PM_{2.5}$, while diesel vehicles were responsible for 10% of the $PM_{2.5}$. Thus 74% of the mobile source contribution was due to gasoline vehicle emissions and 26% was attributed to diesel emissions. This contrasts with the Los Angeles result where 64% of the mobile source contribution was from diesel vehicles and 36% was from gasoline vehicle emissions Figure 4). Possible explanations for the difference between the studies include different seasons (NRAQS/winter, LA/summer), years, source profiles (chemical species comprising the profiles and inclusion of cold start and high-emitting vehicle profiles in NFRAQS), vehicle technology, and fuels. As with the discussion in the previous section, depending on the method it is possible to reach markedly different conclusions with respect to the contributions from diesel and gasoline vehicles.

4 – Contributions Based Developed from On-Road Emission Factors

One way to reconcile the differences observed in both the emissions inventory and source attribution approaches is to apply on-road emission rate data coupled with vehicle activity information to estimate the PM contributions from diesel and gasoline vehicles. Studies performed in roadway tunnel and crossroad experiments provide emission factors measured in a real-world setting. This approach also has a number of limitations such as limited speeds and accelerations and most of the vehicles are operating under hot-stabilized conditions. Still, it allows for the measurement of emissions from thousands of vehicles and avoids the difficulty of soliciting vehicles for dynamometer testing.

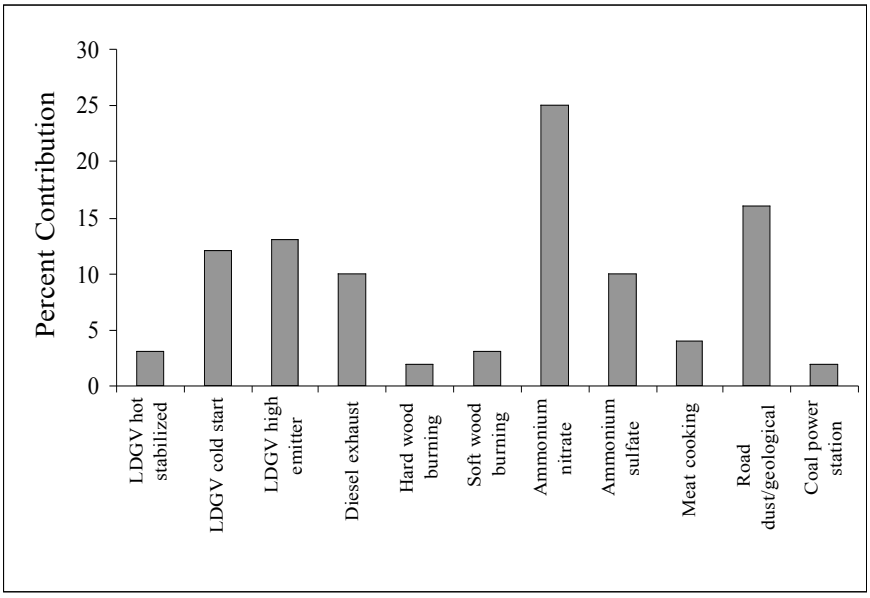

Figure 3: Results of the NFRAQS $PM_{2.5}$ source apportionment study (Fujita et al., 1998). Mobile sources contributed 38% of the observed $PM_{2.5}$, with most of the emissions coming from light-duty gasoline vehicles (LDGV).

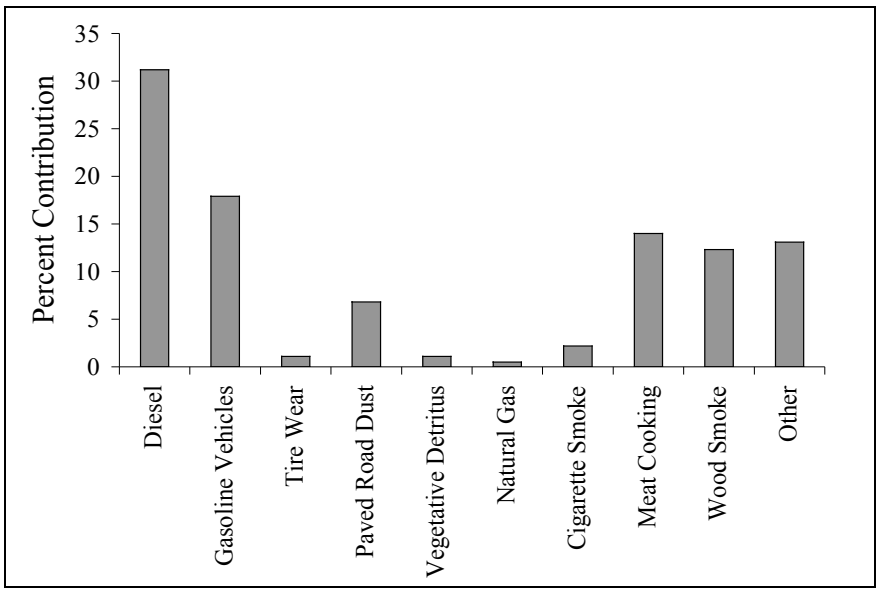

Figure 4: Results of the Schauer et al. (1996) $PM_{2.5}$ source apportionment for the Downtown Los Angeles site. Mobile sources contributed 49% of the observed $PM_{2.5}$, with most of the emissions coming from diesel vehicles.

In a tunnel study performed in the Tuscarora Mountain Tunnel along the Pennsylvania Turnpike in 1999 Gertler et al. (2002) reported $PM_{2.5}$ emission rates for light-duty vehicles (gasoline) and heavy-duty diesel vehicles of 10∀11 mg/km and 135∀18 mg/km, respectively. The large uncertainty in the light-duty emission rate raised doubts about its value; however, the indication is that the diesel emission rate may be approximately 14 times the gasoline emission rate. Recently Abu-Allaban et al. (2003) applied a multi-lag regression approach coupled with crossroad measurements to determine $PM_{2.5}$ emission factors for different vehicle classes. For a location with similar speed characteristics as was observed in the Gertler et al. (2002) tunnel study, they reported a light-duty emission rate of 10∀3 mg/km and heavy-duty rate of 97∀34 mg/km. These emission rates are not

too different than those used by EPA in the Part5/MOBILE6.1 model (6 mg/km for light-duty vehicles and 130 mg/km for heavy-duty vehicles). Based on the on-road data, the ratio of diesel to gasoline emissions is approximately 10. Using 2001 VMT data from the CARB, 94.7% of the VMT is from light-duty vehicles and 5.3% is due to heavy-duty vehicles. This estimate for percent VMT is similar to the national value used by the USEPA. Based on this VMT estimate, the diesel emission rate would have to be 15 times the gasoline emission rate for the two sources to contribute equally to the $PM_{2.5}$ loading. Given the ratio from the two on road studies is less than a factor of 15 and cold-start emissions have not been taken into account, it is likely that emissions from gasoline vehicles contribute more to the observed $PM_{2.5}$ than do emissions form diesel vehicles in the U.S.

Conclusion

The use of various methods to evaluate the relative contributions of diesel and gasoline powered vehicles to ambient PM in the U.S. yields inconsistent results. The 2000 USEPA inventory attributes 62% of mobile source contribution to diesel vehicles and 38% to gasoline vehicles. The California inventory predicts 33% of the emissions are from diesel vehicles and 68% are from gasoline vehicles. An opposite result was obtained with the previous version of the mobile source emission factor model. Similar discrepancies are observed in the results of ambient source attribution studies. A possible reason for the differences between the inventory estimates is the use of different mobile source emission factor models. For the source attribution studies, it is likely the inconsistency is due to differences in source profiles, season, and the year of the studies. Using emission factor measurements from on-road studies, it appears that gasoline vehicles comprise the majority of mobile source PM emissions in the U.S. Future studies need to be performed to resolve these inconsistencies; however, when developing strategies to reduce mobile source PM, emissions from gasoline vehicles will need to be considered.

Acknowledgements

The author would like to acknowledge Health Effects Institute for support of the Tuscarora Mountain Tunnel Study under RFA 98-3 and the National Cooperative Highway Research Program (NCHRP) for support of the for support of the cross-roadway measurements under project 25-18.

References

Abu-Allaban, M., W. Coulombe, A.W. Gertler, J. Gillies, W.R. Pierson, C.F. Rogers, J.C. Sagebiel, and L. Tarnay (2002): Exhaust particle size distribution measurements at the Tuscarora Mountain Tunnel. Aerosol Sci. & Technol, vol. 36, p 771-789.

Abu-Allaban, M., J.A., Gillies, A.W. Gertler, R. Clayton, and D. Proffitt (2003a): Tailpipe, resuspended road dust, and brake-wear emission factors from on-road vehicles. Atmos. Environ., submitted.

Abu-Allaban, M., J.A., Gillies and A.W. Gertler (2003b): Application of a multi-lag regression approach to determine on-road PM_{10} and $PM_{2.5}$ emission rates. Atmos. Environ., submitted.

Baumgard, K.J., Johnson, J.H. (1996): The effect of fuel and engine design on diesel exhaust particle size distributions. SAE Technical Paper 960131, SAE International, Warrendale, PA.

CARB (2000): "The 1999 California almanac of emissions and air quality", California Air Resources Board, Sacramento, California.

CARB (2002): "The 2001 California almanac of emissions and air quality" California Air Resources Board, Sacramento, California.

CARB (2003): "California emissions inventory data", www.arb.ca.gov/emisinv/emsmain/emsmain.htm.

Clayton, R., Gertler, A.W., Proffitt, D., Gillies, J.A., and M. Abu-Allaban (2003): Particulate Matter (PM2.5 and PM10) Apportionment for on-road mobile sources. Final Report, Project HR-25-18, Prepared for National Cooperative Research Program, Transportation Research Board, National Research Council, Washington, DC, January 2003.

Fujita, E., Watson, J.G., Chow, J.C., Robinson, N.F., Richards, L.W., Kumar N. (1998): Northern Front Range Air Quality Study, Volume C: Source Apportionment and Simulation Methods and Evaluation. Desert Research Institute final report, Reno, Nevada.

Gertler, A.W. and W.R. Pierson (1994): Motor vehicle emission modeling issues. Sci. Total Environ., vol. 146/147, p 333-338.

Gertler, A.W., J.C. Sagebiel, D.N. Wittorff, W.R. Pierson, W.A. Dippel, D. Freeman and L. Sheetz (1997): Vehicle emissions in five urban tunnels. Desert Research Institute report, Project No. E-5, Reno, Nevada,

March 1997.

Gertler, A.W., J.A. Gillies, and W.R. Pierson (2000): An assessment of the mobile source contributions to PM10 and PM2.5 in the United States. Water, Air and Soil Pollution, vol. 123, p 203-214.

Gertler, A.W. M. Abu-Allaban, W. Coulombe, J.A. Gillies, W. Pierson, C.F. Rogers, J.C. Sagebiel, L. Tarnay, and T.A. Cahill (2002): Measurements of mobile source particulate emissions in a highway tunnel. Int. J. of Vehicle Design, vol. 27, p 86-93.

Gillies, J.A. and A.W. Gertler (2000): Comparison and evaluation of chemically speciated mobile source $PM_{2.5}$ particulate matter profiles. J. Air & Waste Management Assoc., vol. 50, p 1459-1480.

Moosmüller, H., Gillies, J.A., Rogers, C.F., DuBois, D.W., Chow, J.C., Watson, J.G., Langston, R. (1998): Particulate emission rates for unpaved shoulders along paved roads. J. Air Waste Manage. Assoc., vol. 48, p 174-185.

Mulawa, P.A., Cadle, S.H., Knapp, K., Zweidinger, R., Snow, R., Lucas, R., Goldbach, J. (1997): Effect of ambient temperature and E-10 fuel on primary exhaust particulate matter emissions from light-duty vehicles. Environ. Sci. Technol., vol. 31, p 1302-1307.

Nicholson, K.W., Branson, J.R., Geiss, P., Cannell, R.J. (1989): The effects of vehicle activity on particle resuspension. J. Aerosol Sci., vol. 20, p 1425-1428.

Pierson, W.R., Brachaczek W.W. (1983): Particulate matter associated with vehicles on the road. II. Aerosol Sci. Technol., vol. 4, p 1-40.

Pierson, W.R., A.W. Gertler, and R.L. Bradow (1990): Comparison of the SCAQS tunnel study with other on-road vehicle emission data. J. Air & Waste Management Assoc., vol. 40, p 1495-1504.

Ristovski, Z.D., Morawksa, L., Bofinger, N.D., Hitchins, J. (1998): Submicrometer and supermicrometer particulate emissions from spark ignition vehicles. Environ. Sci. Technol., vol. 32, p 3845-3851.

Rykowski, R.A. and B. Hrebenyk (1997): Contribution of gasoline-fueled vehicles to ambient levels of fine particulate matter. AIR report, no. 071697, Novi, Michigan.

Sawyer, R.F., Johnson, J.H. (1995): Diesel emissions and control technology. In Diesel Exhaust, A Critical Analysis of Emissions, Exposure, and Health Effects. Health Effects Institute report, Cambridge, MA.

Schauer, J.J., Rogge, W.F., Mazurek, M.A., Hildemann, L.M., Cass, G.R., and Simoneit, B.R. (1996): Source apportionment of airborne particulate matter using organic compounds as tracers. Atmos. Environ., vol. 30, p 3837-3855.

USEPA (2003). "Clearinghouse for inventories and emission factors", www.epa.gov/ttn/chief/

Watson, J.G., J.C. Chow, and T.G. Pace (1991). Chemical mass balance - In "Receptor Modeling for Air Quality Management", Elsevier, New York, p 83-116.

Weingartner, E., Keller, C., Stahel, W.A., Burtscher, H., Baltensperger, U. (1997): Aerosol emission in a road tunnel. Atmos. Environ., vol. 31, p 451-461.

Wittorff, D.N., A.W. Gertler, and J.C. Chow (1994). The impact of diesel particle emissions on ambient particle loadings. Paper 94-WP91.01, Air & Waste Management Association 87th Annual Meeting, Cincinnati, OH, 19-24 June 1994.

12th International Symposium "Transport and Air Pollution" / 12e Colloque international "Transports et pollution de l'air", Avignon, 16 -18 *June* / juin 2003
proceedings / actes, n°92, tome / Vol. 1, Inrets ed., Arcueil, France, 2003, p. 193-200

Transport and Environment Database System (TRENDS): Maritime Air Pollutant Emission Modelling

Aliki Georgakaki [a*], Robert A. Coffey[a], Graham Lock [b] & Spencer C. Sorenson [a]**
[a] Section for Energy Engineering, Department of Mechanical Engineering, Technical University of Denmark (DTU), Building 403, 2800 Kgs. Lyngby, Denmark
[b] European Commission, Office BECH B4/459, L-2920 Luxembourg/Kirchberg, Luxembourg

Abstract
This paper reports the development of the maritime module within the framework of the Transport and Environment Database System (TRENDS) project. A detailed database has been constructed for the calculation of energy consumption and air pollutant emissions. The technical assumptions and factors incorporated in the database are presented, including changes from findings reported in Methodologies for Estimating air pollutant Emissions from Transport (MEET).
The database operates on statistical data provided by Eurostat. Data is at port to Maritime Coastal Area (MCA) level, so a bottom-up approach is used. This was the first attempt to use Eurostat maritime statistics for emission modelling, and the problems encountered, since the statistical data collection was not undertaken with a view to this purpose, are mentioned.
Examples of the results obtained by the database are presented. These include detailed air pollutant emission results per port and vessel type and aggregate results for different types of movements.
Key Words: Air Pollution, Maritime Transport, Air Pollutant Emissions

Introduction

The TRENDS study of maritime shipping has aimed to estimate the environmental pressures caused by the world's commercial shipping fleet attending EU15 countries. The study estimates emissions occurring during cruising from shipping movements calling into ports of the EU15 countries, which involve the delivery or receipt of goods. Other related activities such as loading, hotelling etc. are not examined. The datasets so far included in the database cover the years 1997 to 2000, but are not complete. The best dataset, for the year 2000, includes all EU15 member states except for Italy.

1 – Method

The fleet is divided into different categories, which demonstrate similar characteristics in terms of operation, goods carried, physical proportions and auxiliary machinery. The categories used are as defined in Lloyd's Register of Ships. Gross tonnage (GT) is chosen as the measure of a ship's size. However, links are also developed between the deadweight and GT of different types of ships, so these figures are interchangeable. The ship categories and respective relationships between GT and deadweight can be observed in table 1. The relationship is very strong for tankers, bulk carriers, general cargo and container vessels, while for Roll on/Roll off (RoRo) and passenger ships there is more variability. This may be attributed to the varied use of space on such ships. Often RoRo vessels carry passengers, and passenger vessels carry vehicles and cargo. The factors are based upon an in-house ship database, created and maintained at DTU in the Department of Naval Architecture and Offshore Engineering. The database contained around 2300 entries at that time.

*Corresponding author : Tel: +45 45254168, Fax: +45 45930663, E-mail: aliki@mek.dtu.dk (Georgakaki A.)
**Current address: Skt.Annae Gade 33, 1 tv, 1416 Copenhagen K, Denmark

Vessel type	Dead weight (tons)	Fuel Consumption (kg/km)
Tanker	1.87 * GT	$0,2283*GT^{0,5589}$
Bulk carrier	1.83 * GT	$0,3059*GT^{0,5241}$
General Cargo	1.39 * GT	$0,1637*GT^{0,6024}$
Container	1.09 * GT	$0,0489*GT^{0,7381}$
RoRo/Ferry/Cargo	0.54 * GT	$1,2324*GT^{0,3967}$
Passenger ship	0.18 * GT	$0,173*GT^{0,6134}$

Table 1: Relationship between Dead Weight and Fuel Consumption with Gross Tonnage

A second division is made based on propulsion machinery, as medium speed engines are found in smaller ships and slow speed engines in larger vessels. Although there is no definite size boundary that divides the engine types, several studies have indicated suitable assumptions, such as 2500 GT, Flodström (1997), and 2000 kW, Lloyd's (1995). Engines below this size are assumed to be medium speed and engines above this size are assumed to be slow speed.

A one-to-one relationship exists between average GT and installed power (kW) for ships within this range, and therefore, within the TRENDS project, it is assumed that all ships under 2000 GT have medium speed and those over 2000 GT have slow speed engines. It is also assumed that slow speed engines run on marine fuel oil (energy content 40.0-40.5 MJ/kg), while medium speed engines run on marine gas oil (energy content 42.0-42.5 MJ/kg).

Energy Consumption

The specific fuel consumption (SFC) of the marine diesel engine has decreased rapidly over the past thirty years. The SFC of a modern diesel engine can be 160 g/kWh compared to 220g/kWh for an older engine. The steam turbine on the contrary, which has not undergone the same development, offers a SFC of around 280 g/kWh, Hughes (1996).

The age distribution of 290 ships of different types, randomly chosen from the Lloyd's Register of Ships 1994-5 was examined, to provide an indication of the age of ships operating during the study period. The majority of ships were introduced to the fleet between 1970 and 1995, although significant numbers were introduced before 1970, which illustrates their relatively long working lives. The average launch date was 1987. This date varied for different types of ship. General cargo ships had an ageing population and container ships a young population as may be expected from the current trend towards container use. The weighted average SFC was calculated based upon slow speed engine test bed data and the age distribution. It was approximated at 187 g/kWh. A SFC of 200 g/kWh was used in the studies; Bouscaren (1993), Alexandersson et al. (1993) and Flodstrom (1997). Although not explicitly stated in the report by Lloyds Register Engineering Services (1995), carbon or sulphur balancing of the emission factors gave a SFC of 210 g/kWh. Considering that about 30% of the fleet runs on less efficient four-stroke and steam engines, and that the data used represented the engines running under ideal operating conditions on a test bed, an average SFC of 205 g/kWh is adopted in this study. This consumption is used with all engines, irrespective of engine load or age. It is also assumed that the main engine and auxiliary load generate a combined output equivalent to 85% of the main engine capacity. Of this, 5% accounts for auxiliary engine operation. It is also assumed that the auxiliary engine consumes gas oil.

From the assumptions described previously, the fuel consumption (FC) factors per kilometre seen in table 1 are derived for the different ship categories using the in-house DTU database. The factors of FC per unit distance include the influence of the speed of the vessel. The speed of ships tends to increase with size and this is taken into account when estimating the FC per unit distance. For this purpose the service speed is used, which is defined as, 'that which the ship is stated to be capable of maintaining at sea in normal weather and at normal service draught'.

The FC factors have been compared with those produced by MEET, Trozzi et al. (1998). A reasonable correlation is observed between the MEET and DTU factors as can be seen in figure 1,

with the exception of bulk carriers. As shown in figure 2, the DTU estimates are significantly greater than those produced by MEET. The MEET factors assume a linear relationship between GT and fuel consumption, as well as an average speed for each category of vessel. A power curve is used to estimate the FC of the ships within the DTU database. This is considered to give a better representation of the relationship with GT, especially for the smaller vessels, as seen in figure 2.

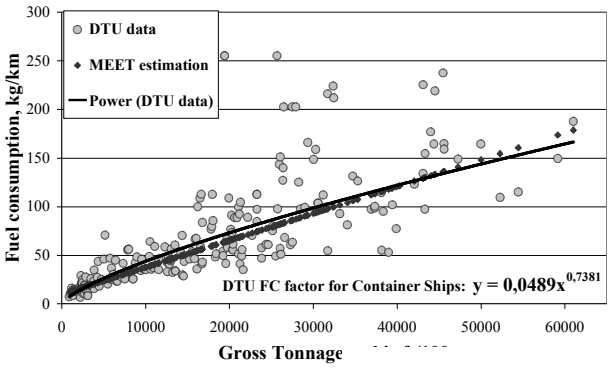

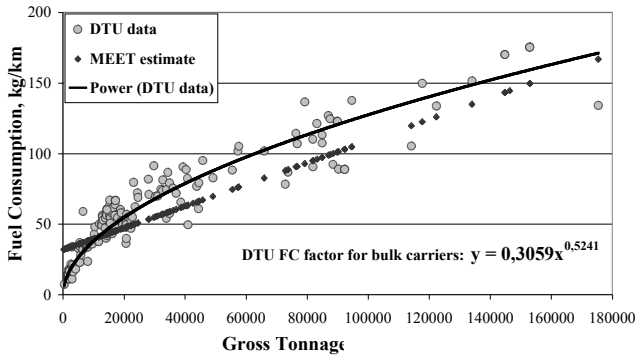

Figure 1: Fuel consumption for container ships *Figure 2: Fuel consumption for bulk carriers*

Emission Factors

The most extensive study into marine diesel engine emissions has been performed by Lloyd's Register Engineering Services Ltd, Lloyds (1995). The Lloyd's emission factors for slow and medium speed marine diesel engines are adopted for this calculation, with the exception of particulate matter. The emission factors for steam engines are quoted from the US Environmental Protection Agency (1985). As the relevance of European refinery estimates was limited, this study has adopted the EMEP/CORINAIR (1996) guidebook recommended sulphur content figures. The sulphur content of fuel oils is therefore assumed to be 2.99 and that of gas oils 0.73%. The user can redefine this assumption. As no information was available for the power plant mixture of the ships attending different ports a weighted average is assumed, based on the survey by Lloyd's Register Engineering Services. In the study it was observed that around 71% of the installed main engine power was accounted for by slow speed engines, around 23% was found to be medium speed engines and 6% steam. The balance between steam engines, medium speed and slow speed diesel engines can be modified by the user.

The particulate matter for the Lloyd's study was measured over just six engines, representing a range of marine vessel types. The emission factor does not take into account the effect of the fuel's sulphur content on particulate matter emission. Using the Lloyd's values as reference points, a correlation was developed to calculate the particulate matter emission as follows:

$$\frac{PM}{PM_{ref}} = 0.6\left(\frac{S - S_{ref}}{S_{ref}}\right) + 1$$

PM_{ref} and S_{ref} are the values given by Lloyd's, while S is the actual sulphur content of the fuel in question and PM the emission factor for this fuel. Table 2 displays the adopted emission factors along with the factors produced as a weighted average using all the assumptions mentioned.

Input Data

Traffic statistics for all shipping movements involving EU15 countries are supplied by the European Commission Statistical Office. This data is made available by the member states in accordance with the Council Directive 95/64/EC and 98/358/EC. Data sets A1, A2, F1, F2 and D1 as defined by the directive provide the database input. Due to the sensitivity of the data for port competition, dissemination is at this point only possible at a port-to-MCA level and not port-to-port as was originally intended. This restriction causes complications in estimating the distance travelled by

vessels, as certain MCAs cover a rather long coastline. The calculations are based on a Port-to-MCA distance table, which was provided by Eurostat.

Factor Kg/tonne fuel	Slow Speed Fuel Oil	Medium Speed Gas Oil	Steam Engine Fuel Oil	Steam Engine Gas Oil	Average Fuel Oil	Average Gas Oil
NOx	87	57	6.98	6.25	75.3	75.25
CO	7.4	7.4	0.43	0.6	6.98	6.99
HC	2.4	2.4	0.085	0.5	2.26	2.29
CO2	3170	3170	3170	3170	3170	3170
SO2	20*%S	20*%S	20*%S	20*%S	59.8	14.6
PM	7.6	1.2	2.5	2.08	7.75	1.56

Table 2: Emission factors used in the database. Source: Lloyd's Register Engineering Services Ltd and US Environmental Protection Agency

Two tables in each data set record the movement of goods between ports and maritime coastal areas, namely tables A1 and A2. While data set A2 has a more detailed account of the cargo carried, it does not register all types of freight so extracts from both tables are used in the calculation procedure. This data includes the reporting port, the maritime coastal area of the origin or destination port, the cargo type and mass.

Shipping movements by vessel type are recorded in data set F2. The data is specific to each port and gives information about the arriving vessels. It does not give the origin or destination MCA of the journey. The data indicates the tonnage category, number of vessels and gross tonnage of the vessels. The vessel types described in the directive are not the same as the categories defined by the study and therefore a correlation is used, as shown in table 3.

The goods traffic data registers the amount of each type of cargo arriving and leaving each port, and the origin or destination of the goods. The vessel data describes the number and size of vessels arriving at each port, but does not state the origin or destination MCA. As a result, while fuel consumption factors can be calculated for each port according to the type and size distribution of vessels calling, the total estimate of fuel consumption and consequently the emissions occurring has to be based on the goods traffic. For this reason the relationship between the goods transported and the different carriers has to be established.

Eurostat registers five main types of cargo: liquid bulk, dry bulk, containers, RoRo and other (not specified) cargo. The number of passengers is also registered. Problems are encountered mainly with attributing passengers and RoRo cargo. Table 3 shows that passengers may be allocated to general cargo (by Eurostat definition) vessels or to passenger vessels, or split between the two. The passengers are all attributed to passenger ships, in absence of a way to distinguish between RoRos that may carry them. This correlation is not successful. Passenger vessels produce occupancies that are not realistic by an order of magnitude or more, while RoRo vessels seem to consistently carry very small loads.

Eurostat	Ship categories included by Eurostat	TRENDS
Liquid Bulk	Oil tanker, Chemical tanker, LG tanker, Tanker barge, Other tanker	Tanker
Dry Bulk	Bulk/oil carrier, Bulk carrier	Bulk Carrier
Container	Full container	Container Ship
Specialised	Barge carrier, Chemical carrier, Irradiated fuel, Livestock carrier, Vehicle carrier, Other specialised	General Cargo
General Cargo, non specialised	Reefer, RoRo passenger, RoRo container, Other RoRo cargo, Combination carrier general cargo/passenger, Combination carrier general cargo/cargo, Single decker, Multi-decker	RoRo/Ferry/Cargo
Dry cargo barge	Deck barge, Hopper barge, Lash-Seabee barge, Open dry cargo barge, Covered dry cargo barge, Other dry cargo barge	Bulk Carrier
Passenger	Cruise, Other passenger only	Passenger ship

Table 3: Eurostat definition of ship types and correlation with the TRENDS categories

The explanation for this is obvious; the fact that passengers are carried in RoRo vessels is not accounted for, nor is the weight from such activities, including the weight of passenger vehicles, lorries etc. Note that the weight of vehicles carrying cargo is also not included by the directive. There is also a suspicion that goods travelling in RoRo vessels are registered according to their nature (e.g. dry bulk goods in lorries) and then falsely attributed to other types of carriers. This problem is inherent in the way the data is recorded, and while it depreciates any factors produced per unit of cargo or passenger carried, it should not influence the resulting emissions, assuming that there is consistency in the registration.

Port to MCA Distance Database

An estimation of the sailing distances was provided by Eurostat, in order to relate the origin and destination port and MCA descriptions to actual distances. The Veson Distance Tables from Fairplay were used to look up sailing distances. For missing ports an estimate was made based on neighbours along the same coastline and then the distances were adjusted on the basis of the unknown port's co-ordinates. In the majority of cases it was considered sufficient to take the shortest route. Only the most important inland ports were considered by calculating distances along the rivers or canals to a port at the mouth of the river, and then sea distances from there. It was decided not to estimate the average effect of weather. Up to date data were extracted on a port-to-MCA basis (11 950 pairs). The major ports for each MCA within the EU were identified from the raw data, covering at least 70% of the throughput for that MCA. For overseas MCA's, only one or two major ports were used. The results cover about 95% of the port-MCA pairs. In most cases, the missing records lack information on the partner MCA or refer to non-port locations. However, more than a third of the missing records are due to a lack of information on the location of minor Greek ports. Small numbers of minor ports from other countries could also not be located.

Port-MCA distances are inherently less precise than port-port distances, due to information lost in aggregation. This is especially true for ferries and bulk trades. It would be advisable to develop separate distance tables for different commodity groups and for passengers. The port-port flows of goods and passengers do not provide information on the route. A flow between two ports may involve a vessel calling at other ports along the way. There is thus an in-built underestimation of the real distance. This situation can only be rectified by collecting data on vessel movements, which include information on all ports of call for a particular journey. This would be a mammoth undertaking.

Allocation of Environmental Indicators

The environmental responsibility needs to be placed with those parties, which are directly gaining from the activity. This is not a straightforward decision because the beneficiaries are diverse and are generally distributed between different countries. The need for shipping is generated by the requirement for the import and export of goods. The allocation of environmental indicators to the importing or exporting countries is therefore well justified, especially if the allocation is made based on transported goods. It was decided to allocate the environmental indicators on the basis of import and export country. The responsibility for each route was divided equally between the origin and destination ports.

This method loses some substance in particular cases. For example, if a ship makes a long haul and then delivers to a cluster of several closely distributed ports, the emissions allocation to the first port of call will be higher than that of following ports for the same delivery of goods. This may also be observed when goods are delivered to a central port such as Rotterdam, only to be dispersed to smaller ports in neighbouring countries. Rotterdam will be receiving little financial benefits, but possibly a large allocation of emissions.

Fuel Consumption Calculation Method for Freight Vessels

The following describes the calculation of the fuel consumption to be allocated to each port. This

applies to all cargo vessels and RoRo ferries but not to passenger vessels for which a respective calculation method has been developed, attributing passengers instead of cargo.

Step 1. The FC factors for each type of vessel, as described in table 1, are applied to the vessels arriving at each port. A weighted average SFC is calculated for each vessel type based on the size distribution of ships attending each port, as shown in table 4. Data is not available detailing the sizes of vessels taking particular trips, so it is assumed that the same distribution of different sized vessels operates over each route.

Step 2. The aggregated fuel consumption per kilometre is calculated for all vessels of each type, attending each port.

Step 3. The aggregated fuel consumption for each vessel type is divided by the aggregated quantity of goods entering each port to calculate the average SFC per incoming tonne of goods transported one kilometre, as shown in table 5. The same is repeated using the aggregated outgoing cargo. It is assumed that the operating fleet is the same.

Step 4. The tonkm of incoming and outgoing goods transported over each route is calculated. The maritime distance of each route is obtained from the port to MCA database. This distance is divided by two, as only half of the route is allocated to the reporting port.

Step 5. From the SFC calculated for incoming and outgoing vessels and the respective goods traffic data the fuel consumed over a particular route in a given time period is produced.

Reporting port	Reference quarter	Tonnage Range	No. of vessels	Total GT	Average GT	FC kg/km	SFC g/GT km	Total FC kg/km
FIHEL	Q1	up to 499	25	4164	167	4.47	26.81	111.65
FIHEL	Q1	1000 - 1999	1	1102	1102	12.02	10.91	12.02
FIHEL	Q1	2000 - 2999	1	2163	2163	17.12	7.91	17.12
FIHEL	Q1	10000 - 19999	4	50148	12537	43.00	3.43	171.99
FIHEL	Q1	20000 - 29999	4	113320	28330	65.92	2.33	263.67

Table 4: Fuel consumption per kilometre for Bulk Carriers entering the port of Helsinki by tonnage range. First quarter of 2000.

Reporting port	Reference quarter	Cargo	Gross weight of goods, tonnes	Total FC kg/km	SFC g/ton km
FIHEL	Q1	Dry Bulk	232237	576.45	2.48
FIHEL	Q2	Dry Bulk	112656	396.32	3.52
FIHEL	Q3	Dry Bulk	191837	737.68	3.58
FIHEL	Q4	Dry Bulk	338642	1141.85	3.37

Table 5: Specific fuel consumption of Bulk Carriers entering the port of Helsinki with respect to goods weight. Year 2000.

Emissions Estimation Method

The following section describes the calculation of the emissions to be allocated to each port.

- *Step 1.* The fuel consumption of vessels under 2000 GT is calculated.
- *Step 2.* The average fraction of gas oil used by each type of ship at each port is calculated. This includes the fuel consumption of vessels under 2000GT and the 5% used by auxiliary engines.
- *Step 3.* The total fuel consumption is split into gas and fuel oil components.
- *Step 4.* Emission factors are applied to the gas and fuel oil components to obtain the total emissions from each route that should be allocated to each reporting port.

Except for the total emission allocated to each port, subtotals may be calculated for emissions occurring due to short sea shipping (SSS), deep sea shipping (DSS), national or European (EU) destinations, as seen in table 6. The MCA relative for each type of activity can be defined by the user for each country. The definition incorporated in the database at the moment is provided by

Eurostat.

2 – Results

These results are shown as an example of the database capabilities, with certain reservations as to their accuracy, due to the problems encountered with the data. Figure 3 shows SOx emission for France according to vessel type and destination. There is a factor 10 difference between emission results for container vessels and the remaining types. Even though these vessels have higher energy consumption, only 12% of the carriage of goods is attributed to them. RoRo emissions are also high, while they have a 10% share of the traffic. Examining the average load per vessel, this appears too low for RoRo vessels at 305 tonnes, as does the average distance travelled at 109 nautical miles. However, 67% of vessels calling at French ports are indeed RoRos. Containers account for only 8% but the distance they travel is 30 times greater at an average of 3137 nautical miles.

Country	Vessel type	Activity	CO2	SOx	CO	HC	PM	NOx
Finland	Dry bulk	EU	103876	1742	229	75	224	2467
Finland	Dry bulk	DSS	161466	2743	356	115	354	3836
Finland	Dry bulk	SSS	144630	2439	319	103	314	3435

Table 6: Air pollutant emissions of Dry Bulk Carriers calling at Finland for the year 2000, according to their destination (tonnes).

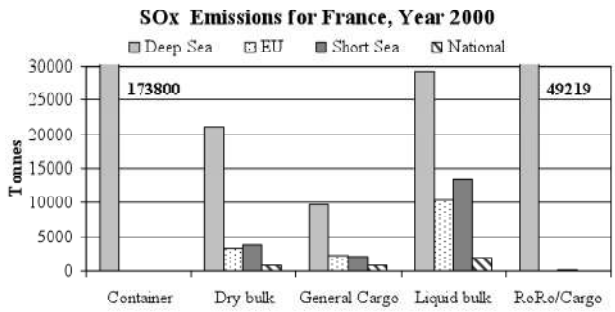

Figure 3: Calculated SOx emission for France

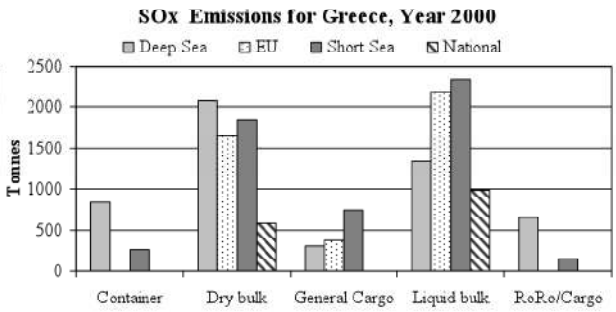

Figure 4: Calculated SOx emission for Greece

Figure 4 plots the same result for Greece, in this case no extremes are observed. One would expect more contribution from RoRo vessels in this case, especially for national destinations. RoRos are again predominant at 44% of the total number of vessels and 19% of the total cargo is attributed to them. The load factor is again low at 374 tonnes and so is the distance travelled at a mere 15 nautical miles. What is surprising is that no tonnage is attributed to such vessels at a national level. Calculated SOx emission from passenger vessels in Greece is 16089 tons for the same year, higher that any other contributor. This also amounts to 55% of the passenger emission in all member states. Passenger vessel movements amount to 78% of the total for Greece.

3 – Discussion

It is recommended that the actual tonnage of goods carried on a ship, regardless of type of goods, be made available as a statistic. If, when vessel movement is registered the amount of cargo and the destination of the ship are recorded, then there is sufficient information to calculate the environmental indicators from the different types and sizes of ships.

Since most other groups work with the RoRo as a vessel type, it is strongly recommended that EUROSTAT adapt its definitions and data collection procedures to accommodate this type of ship. As a minimum, one class of vessel called a RoRo should be established. Consideration should be given to separate passenger and cargo RoRo, though it is recognized that there may be instances where these are mixed.

The use of different average MCA distance for passengers and goods should be considered.

It is recommended that an evaluation be performed to compare the results of environmental indicators obtained from using average MCA distances to those resulting from the use of actual port-to-port distances with a calculation performed on detailed confidential data. This appears to be possible only internally within Eurostat.

Conclusion

A methodology has been developed for the calculation of air pollutant emissions arising from maritime transport. A detailed database providing results at port level for each vessel type has been constructed, using detailed maritime statistics provided by Eurostat. Results can be obtained on an aggregate level for the whole EU or according to destination (DSS, SSS, EU, and National). Though the uncertainties in the data do not allow for useful aggregations or conclusions regarding the actual air pollutant emissions at the moment, valuable information can be obtained by examining the calculation performed for each member state, especially with regard to short sea shipping or EU destinations.

A more interdisciplinary approach is needed to tackle the problems encountered, and this will only be done effectively in close collaboration with Eurostat.

Acknowledgments

The TRENDS project was funded by the European Commission, DG VII / DG TREN.

References

Alexandersson, A, Flodstrom E, Oberg R, Stålberg P. (1993): Exhaust Gas Emissions from Sea Transportation, Mariterm AB

Bouscaren R (1990): Emissions of SO2 and NOx in the British Channel by ship traffic, CITEPA, EMEP Workshop on Emissions from Ships Oslo, Norway 7-8th June, 1990. p 14 – 21

European Commission (1995): Council Directive 95/64/EC on statistical returns in respect of carriage of goods and passengers by sea, Official Journal of the European Communities

European Commission (1998): Council Directive 98/385/EC on rules for implementing Council Directive 95/64/EC on statistical returns in respect of carriage of goods and passengers by sea, Official Journal of the European Communities

EMEP/CORINAIR (1996): Atmospheric Emission Inventory Guidebook, First Edition, Published by EEA, Copenhagen

Flodström E. (1997): Energy and Emission Factors for Ships in Operation, KFB report 1997:24, The Swedish Transport and Communications Research Board, Stockholm, Sweden, p.5

Georgakaki A., Coffey R., Sorenson S.C. (2002): Development of a Database System for the Calculation of Indicators of Environmental Pressure Caused by Maritime and Inland Shipping Transport, TRENDS Project Final Report to the European Commission – DG TREN, Report No. MEK–ET–2002–04, DTU, Lyngby, Denmark

Georgakaki A., Sorenson S.C. (2002): Improving methods of estimating environmental indicators from Ocean-going ships, Report to Eurostat, Report no. MEK–ET–2002–05, DTU, Lyngby, Denmark

Hughes C. (1996): Ship Performance – Technical, Safety, Environmental and Commercial Aspects, Second Edition, LLP, London

Lloyd's Register Engineering Services (1995): Marine Exhaust Emissions Research Programme, Lloyd's Register Engineering Services, Croydon, UK. p 17

Lloyd's Register of Shipping (1994): Register of Ships 1994-1995, Lloyd's Register of Shipping, London

Trozzi C, Vaccaro R (1998): Methodologies for Estimating Air Pollutant Emissions from Ships, MEET, Deliverable No 19, Techne report MEET RF98

United States Environmental Protection Agency (1985): Compilation of Air Pollutant Emission Factors, AP42, 4th Edition.

12th International Symposium "Transport and Air Pollution" / 12e Colloque international "Transports et pollution de l'air", Avignon, 16 -18 *June* / juin 2003
proceedings / actes, n°92, tome / Vol. 1, Inrets ed., Arcueil, France, 2003, p. 201-208

Estimation of the Cost due to Air Pollution of Transport in Sweden.

Lena Nerhagen* & Håkan Johansson**
*Swedish National Road and Transport Institute, Box 760, 781 27 Borlänge, Sweden-
fax:-46 243 73671 - email:lena.nerhagen@du.se
**Swedish National Road Administration, 781 87 Borlänge, Sweden

Abstract
This paper presents results of the calculation of the costs due to the air pollution of transport in Sweden in 2000. The approach used is the Impact pathway approach developed within the EU funded ExternE Core/Transport project. Costs have been calculated for all transport modes based on detailed traffic data. The paper discusses the collection of data; there are uncertainties both related to traffic data and to the calculation of emissions from each transport mode. It also discusses the causes of the variability in the cost estimates. Finally it discusses the transferability of the models used. The knowledge gained through this project can be used to develop control instruments, including fees, that in a more efficient way can regulate the emissions of the transport sectors.
Key-words: *transport, air-pollution, external costs, impact pathway approach*

Introduction

In recent years large efforts have been devoted in EU-funded research projects, i.e. the ExternE-projects, to the development of an approach that can be used to calculate the external costs of transport air pollution. The valuation is based on the so called Impact pathway approach (Friedrich and Bickel, 2001). This approach has now been used to estimate the total cost of air pollution of transport in Sweden for the year 2000[2]. Since these estimates can be used for marginal cost pricing, in this project, cost estimates have been calculated for different transport modes in different circumstances and at different levels of detail. This paper presents and discusses the results from this project regarding air pollutants with a local and regional dispersion. The focus is on how the estimates vary and the reasons behind these variations.

The advantage with the Impact pathway approach is that the cost estimates are based on where the actual emissions take place, a so-called "bottom-up" approach. The problem with this for practical implementation is that the cost estimates are case specific and dependent upon a number of case specific factors ; metorological conditions, population density, traffic situation, vehicle technologies etc. The implication of this is that the estimations of costs would have to be made in each special case unless generalizations of results are possible. The first option would be too costly and cannot be justified in economic terms. Therefore the question of the practicability of the second option is of great interest. The investigation into this issue has recently begun (Friedrich R., & Ricci A., 1999; Bickel et al., 2002). This is an issue that deserves attention since generalisations are increasingly used in practice (Nääs & Lindberg, 2002; Hämekoski et al., 2002; Otterström et al., 2003; Holland and Watkiss, 2002).

[2] The calculations were done by IER, University of Stuttgart (see Bickel et al., 2003). They are based on the same assumption as the calculations in the EU funded UNITE-project (Bickel and Schmid, 2001).

In the first part of the paper we will shortly describe the content of the study and the data used in the calculations. Then we will present a short summary of the cost estimates with a focus on the variations in the cost estimates and the explanatory factors behind these variations. We will also discuss some of the assumptions used in the calculations and if these should be modified to account for Swedish conditions. Finally, in section four, we will discuss the problems related to these types of calculations and our conclusions about the policy implications of the results.

1 - The study

Content of the study

The calculations in the study have been performed for all transport modes but at varying levels of detail. For road and rail, costs have been estimated for the following categories; diesel trains (passenger and freight), HDV, bus, diesel car, gasoline car and two-wheelers. For road transport, costs were calculated for the different vehicle categories in extra urban and urban areas. For aviation costs have been estimated for the emissions from airports. For maritime transport the emissions considered are those at open sea. All the calculations are based on average yearly emissions. As far as possible, the spatial distribution of the emissions are accounted for.

The costs for emissions on urban roads have been calculated for every urban area in Sweden, i.e. accounting for geographical distribution of the emissions. The cost for each area and each vehicle category are then added to obtain the total cost for all urban areas. We use this figure to calculate the average cost per km in urban areas in Sweden, hence a weighted average of the costs in all urban areas[3]. Moreover, we have estimated the costs for two different "cases". These are the urban areas of Stockholm and Skellefteå. Stockholm was included since this is the city in Sweden with the most problematic traffic situation. Skellefteå was chosen in order to explore differences in regional costs. This is a town located in the northern part of Sweden where the population density in the extra urban areas are low. This is also an area that is farther located from the densely populated areas in Europe. Hence the expectation is that the costs for regional impacts will be lower for this case. Some data on the differences between the average for all urban areas, Stockholm and Skellefteå are presented in Table 1. The kilometers driven by gasoline cars relative to diesel cars are the same for all cases because of our assumption regarding the emissions in urban areas.

	Population	Area	Population density	Km (gasolin)	Km (diesel)
All urban area	7462943	5235 km^2	1425 persons/km^2	20260 million	4130 million
Stockholm	1212196	375 km^2	3233 persons/km^2	3292 million	671 million
Skellefteå	31742	22 km^2	1462 persons/km^2	86 million	17,5 million

Table 1: Statistics for urban areas

The data

The data used in the calculation had to be presented in high spatial resolution on GIS maps. It was obtained from several sources (see Johansson and Ek, 2002). The starting point for the calculation of vehicle mileage in urban areas for road transport was an estimate of the total vehicle mileage in urban areas in Sweden given by the Swedish Institute For Transport and Communications Analysis (SIKA). This was then distributed proportionally to the population in urban areas. The vehicle mileage on rural roads was given by Swedish National Road Administrations road database (VDB). VDB does not include all rural roads. A residual that could not spatially distributed were given by

[3] Since there are a large number of small towns in Sweden the average population in urban areas is only 3839 inhabitants. The population in Stockholm amount to 16% of the population in urban areas. Since the total km (and emissions) in each urban area are related to the population, Stockholm also accounts for 16% of the total km driven in urban areas. Hence, the cost per km in Stockholm will strongly influence the average cost per km for urban areas.

comparing the sum of rural roads in VDB with an estimate given by SIKA. Emissions were calculated by using emission factors from COPERT III.

The activity data and emissions for railway were given by the Swedish National Rail Administration. The spatial distribution of the diesel railway traffic was based on the "timetable", data on which sections that are not electrified and data from SJ (the national railway company) on the passenger traffic. For aviation spatially distributed activity data and emissions were given by Swedish Civil Aviation Administration (SCAA) for airports administrated by them, which includes the majority of the flights. The emissions that are of importance for this purpose are those related to the so called LTO cycle, i.e. those that are emitted below the mixing height. For maritime, the emission data used are those in the EcoSense emission data base (Bickel et al., 2003).

For railway and road transport the methods used include all transports. The spatial distribution of the diesel railway traffic, especially the freight traffic, and the urban road traffic, is however somewhat uncertain. The total emissions from railway are the same as calculated by the Swedish National Rail Administration. For road transport there are differences between the total emissions calculated here with COPERT III and those calculated for the same total traffic by the Swedish National Road Administration with the EMV-model. The differences are largest for hydrocarbons. The emissions from road transport in individual urban areas are both underestimated and overestimated. For Stockholm the emissions are probably underestimated. For aviation, airports not administrated by the SCAA are not included and therefore the emissions are somewhat underestimated. The statistics on the activity and emissions for individual airports are probably quite good.

2 -The results

The costs for different modes

In this section we focus on two pollutants, SO_2 and NO_2, for which we have data for all transport modes. In Table 2 the costs for SO_2 emissions are reported. In the first column are presented the cost due to local effects. As expected, the cost is related to where the pollutant is emitted. Two effects are accounted for; mortality and morbidity and the cost for these depend upon exposure. Hence the population density in the area where the impact is influences the results. The cost is lower on extra urban roads and for diesel trains since they mainly travel outside the urban areas. The cost is higher for the scenario covering all airports than the urban roads scenario. This is due to the different shares of pollutants emitted in densely populated areas. 62% of the total emissions in the airport-scenario are from Arlanda and Bromma that are located in densely populated areas. To be noticed is that the local cost due to maritime transport is higher than for other transport that take place in more densely populated areas. The maritime estimate however, should only be considered as an approximation since the spatial resolution used in the calculation is low compared to the other modes. That costs are lower for buses and HDV than cars that are driven on extra urban roads is presumably because cars to a larger extent travel in more populated areas.

A somewhat counterintuitive result is found in the second column where the estimated costs for regional dispersed pollutants are presented. For all diesel vehicles we get a negative estimate. This is due to the chemical reactions that take place between NO_2, SO_2 and NH_3. The outcome of the chemical reactions depend upon the ratio between NO_x and SO_2 emitted. For diesel vehicles this ratio is much higher than for gasoline vehicles. The negative cost occurs because, compared to the reference scenario used in the calculations, less amount of ammonium sulfates is formed and hence the damage due to this pollutant is reduced (see Bickel et al 2003, for details). That the negative cost is lower on extra urban roads is because the ratio between NO_x and SO_2 is different.

For diesel trains it is interesting to compare the results for passenger transport with those for freight since most of this traffic occurs in extra-urban areas but where the actual emissions occur and the composition of the emissions is somewhat different. What we find is that both the local and the regional cost estimates differ. Diesel freight trains have slightly lower costs for local effects but a considerably lower negative cost for regional effects than do passenger trains. At least part of the

explanation for this is the geographical location of the emissions. For diesel passenger trains 7% of the emissions are in the north of Stockholm while the same figure for freight trains is 57%.

	Local	Regional	Total	Emitted	Total cost	Mileage	Cost/km
	(Eur/tonne)			(Tonne)	(Eur)	(Million km)	(Eur/km)
Urban roads							
Gasoline cars	522	2113	2635	182	478871	19920	0,00002
Diesel cars	522	-1880	-1358	12	-15992	2640	-0,00001
Buses	522	-5858	-5336	8	-43647	490	-0,00009
HDV	522	-4928	-4406	18	-78938	1000	-0,00008
Extra-urban roads							
Gasoline cars	255	4147	4402	127	558437	35250	0,00002
Diesel cars	255	-1568	-1314	12	-15742	4650	0,00000
Buses	202	-4102	-3900	6	-23672	680	-0,00003
HDV	202	-3891	-3689	69	-254835	4500	-0,00006
Other modes							
Diesel freight trains	126	-9072	-8946	0,7	-6252	3,5	-0,00179
Diesel passenger trains	142	-16308	-16166	0,4	-6504	9	-0,00072
Airports	840	1041	1881	94	176742	-	-
Maritime	366	659	1025	349	357452	-	-

Table 2: Cost for SO_2 emissions

Turning to the third column in the table we find rather large differences in cost per tonne for the different modes. However, for practical purposes this difference is not that important since the amounts of SO_2 emitted for the different modes are small. Using the information in the fifth and sixth row we can calculate the cost per km for the different modes and it is almost negligible.

In Table 3 the result for NO_2 are presented. We have no local costs reported since no health effects have been verified on the local scale (Friedrich and Bickel, 2001). Regarding the regional effects we find that the cost is lower in extra urban areas. What can be noticed in this table is that the cost per tonne is higher for diesel passenger trains than for any of the other modes, even for urban traffic. Again this is related to the geographical distribution of the emissions. Regarding the cost for emissions on open sea is not much lower which is probably due to the larger part of these emissions occurring in the south of Sweden, close to populated areas. Concerning the cost per km we find that the cost is highest for diesel trains which implies that the amount of NO_2 emitted per km is comparatively high.

	Local	Regional	Total	Emitted	Total cost	Mileage	Cost/km
	(Eur/tonne)			(Tonne)	(Eur)	(Million km)	(Eur/km)
Urban roads							
Gasoline cars	0	1464	1464	18123,4	26537152	19920	0,0013
Diesel cars	0	1424	1424	3272	4661145	2640	0,0018
Buses	0	1424	1424	5085	7238990	490	0,015

HDV	0	1423	1423	9682	13774235	1000	0,014
Extra urban roads							
Gasoline cars	0	1453	1453	27720	40266598	35250	0,0011
Diesel cars	0	1391	1391	3126	4349260	4650	0,0009
Buses	0	1381	1381	3006	4151552	680	0,0061
HDV	0	1376	1376	32596	44860960	4500	0,0100
Other modes							
Diesel freight trains	0	1042	1042	948	988128	3,5	0,28
Diesel passenger trains	0	1681	1681	458	769412	9	0,085
Airports	0	1305	1305	1032	1346531	-	-
Maritime	0	1298	1298	18949	24604154	-	-

Table 3: Cost for NO_2 emissions

Costs on urban roads

In Table 4 the cost per km for local and regional effects for each pollutant are presented. The costs are highest for bus and HDV since they have larger specific emissions. Diesel vehicles in general have higher costs due to the larger amount of particles emitted. Two-wheelers on the other hand have relatively high costs that are related to the emissions of the cancerogenic substances of NMVOC considered (Benzene, BaP and 1-3-buta-diene).

Pollutant	Bus	HDV	Diesel cars	Gasoline cars	Two-wheelers
Local dispersion					
PM	0,00992	0,01135	0,00377	0,00041	0,00246
S02	0,000009	0,000009	0,000002	0,000005	0,000001
CO	0,0000005	0,0000003	0,0000001	0,000003	0,000003
Benzene, BaP,1,3-buta-diene	0,00021	0,00020	0,00001	0,00010	0,00032
Regional dispersion					
PM 2.5 + DME	0,0026	0,0030	0,0010	0,0001	0,0006
Ozone	0,0089	0,0083	0,0011	0,0016	0,0026
NO_2	0,0148	0,0138	0,0018	0,0013	0,0001
SO_2	-0,00009	-0,00008	-0,000008	0,00002	0,000003
Acid dep.	0,0007	0,0006	0,00008	0,00007	0,000005
CO	0,0000001	0,00000009	0,00000003	0,0000009	0,0000007
Benzene, BaP, 1-3-buta-diene	0,00005	0,00005	0,000003	0,00003	0,00009
Fuel prod	0,0011	0,0012	0,0003	0,0006	0,0002
Total cost/km	*0,0382*	*0,0385*	*0,0080*	*0,0042*	*0,0064*

Table 4: Costs due to regionally dispersed pollutants (Eur/km)

For Stockholm and Skellefteå the cost calculations where made for two vehicle categories; diesel

vehicles and gasoline vehicles. To be able to compare the estimates for the average cost per km in urban areas with these two cases we have used the cost estimates for the specific vehicle categories, summed them up and divided them by the kilometers driven for the whole category. To see how the cost for these categories change as we move from one area to another we have calculated the relative difference between the average estimates and the estimates for the case studies (in per cent). The results of these calculations for gasoline vehicles are presented in Table 5[4].

	PM2.5+ DME	Ozone	NO2	SO2	Acid deposition	CO	NMVOC	Fuel prod
Local (Stockholm)	186%			186%		186%	186%	
Local (Skellefteå)	78%			78%		78%	78%	
Regional (Stockholm)	57%	100%	91%	200%	89%	57%	57%	100%
Regional (Skellefteå)	41%	100%	29%	27%	24%	41%	41%	100%

Table 5: Comparison average cost urban areas and case specific costs.

A general result is that the costs for the (non-reactive) pollutants that have local impact change by the same amount. They increase for Stockholm and decrease for Skellefteå. The cost estimate decrease for Skellefteå although they have a slightly higher population density than the average for urban areas. This reveals that it is not straightforward to compare average cost estimates with cost estimates for specific studies. The average will be influenced by the geographical location of the emissions where meteorological conditions and population density will be different from those in the case study.

For the pollutants with regional dispersion we do not have the same result. For ozone the cost estimate is the same irrespective of where the emissions occur. The reason is that the calculation of ozone formation is based on EMEP country-to-grid matrices, so the results for a country are mainly the same. For particles, CO and the canceriogenic NMVOC, which do not involve in chemical reactions, the cost changes by the same amount. The costs decrease both for Stockholm and Skellefteå, which is probably due to the geographical location of these two cities, close to the Baltic Sea. The explanation for the lower cost estimates for regional impacts for NO_2 and acid deposition and the higher cost for SO_2 in Stockholm are related to a number of factors such as differences in geographical location, background concentrations, air chemistry etc. It would require a thorough analysis to fully understand the impact of each parameter.

The effect of these differences on the total cost per km are presented in Table 6. This table reveals that the cost varies for both locally and regionally dispersed pollutants. For local effects the cost is about twice as high in Stockholm as the average for urban areas and Skellefteå, while for regional effects the cost appears to be lower in the north of Sweden. The conclusion from this is that costs in urban areas should be differentiated according to local conditions but also based on the geographical location within Sweden.

	Gasoline	vehicles		Diesel	vehicles	
	Local	*Regional*	*Total*	*Local*	*Regional*	*Total*
Average urban area	0,0006	0,0037	0,0042	0,0064	0,0126	0,0190
Stockholm	0,0010	0,0035	0,0046	0,0120	0,0111	0,0231
Skellefteå	0,0004	0,0026	0,0030	0,0050	0,0068	0,0118

Table 6: Average km cost for urban areas and case specific km costs (Eur/km).

The Impact pathway approach and Swedish conditions

There are in every step of the Impact pathway approach, modifications that can be made to adapt the calculations to country specific conditions. Starting with the emission modeling there are a number

[4] Similar results are found for diesel vehicles.

of factors that can influence the amounts of pollutants emitted per vehicle kilometer. One obvious example accounted for in this study is the amount of cold starts for road vehicles. These increase the content of some pollutants in the emissions and hence increase the costs. Other aspects that have influenced the results in this study is the composition of the vehicle fleet and, for road transport, that the sulphur content differs between Sweden and Europe.

The second step of the chain is the dispersion and exposure modeling. In this study account have been taken to the meteorological conditions in Sweden. However, comparisons with cost estimates in other studies (Leksell, 1999; Hämekoski et al., 2002; Otterström et al., 2003) have raised the question of the influence of the level of detail used in the local dispersion modeling. The next step in the chain is to estimate the impact on the population, on crops and on materials. Here a predefined set of exposure-response functions are used. Regarding health effects, in some cases they apply to the whole population while in other cases they apply only to a fraction, elderly or asthmatics for example. To be correct, the calculations should be based on these groups share in the population where the calculations are performed. This has not been accounted for in this study. Furthermore, the generalization of ER-functions from one area to another is not obvious. According to Forsberg (2002) preliminary results from APHEA2 indicates that the ER-coefficient in some cases are higher for Stockholm than the average in the study. This might also be an issue in the estimation of impacts on crops. For ozone the ER-functions is based on a "critical loads" standard measure (the 40 AOT). The question has been raised if this is appropriate for Swedish conditions with our long summer days (Munthe et al., 2002).

The final step in the impact pathway chain is the valuation of the effects. In this study values derived from European studies, that are adjusted to account for the income level in Sweden, have been used. It would be more appropriate to use values from studies undertaken in Sweden. However, at present no comparable values to those used in this study are available.

3 - Discussion and Conclusions

This paper has presented estimates for the cost of air pollution of transport calculated with the Impact pathway approach. The focus in this paper has been on the reasons for why the costs calculated with the Impact pathway approach varies. One reason for investigating the variations in the estimated costs is because they are the basis for marginal cost pricing. That these costs should influence transport decisions is an established goal both in European and Swedish policy. Our conclusion from the results discussed in this report is that account needs to be taken to population density and wind speed (and possibly other meteorological conditions) when estimating costs for urban areas. Concerning the regionally dispersed pollutants, some regional differentiation should be used. At a minimum, the costs should be different between the south and the north of Sweden (this conclusion however is not valid for ozone). We have also found that since the costs for regional effects are mainly caused by secondary pollutants, formed by chemical reactions, it is problematic to use uniform costs on the pollutants participating in the chemical reactions.

Another conclusion from the work with this study is that it will not be possible to truly represent the variations in costs. The present Impact pathway approach used in this study is for example based on yearly averages for weather conditions. That this imposes limitations on marginal cost pricing is acknowledged in the literature. Friedrich and Ricci (1999) for example state that "as long it is not planned to implement weather-dependent prices, it is sufficient to estimate values that are average over the different weather conditions". We believe that the Impact pathway approach can be developed to achieve further differentiation. But we also believe that there is a limit to how well models can represent true variations. Another issue is that since these calculations trace a chain of events to obtain a value, the estimates will rely on how well this chain is represented. In some cases, simplifications are used and others are excluded due to lack of knowledge. Hence, it appears that what the present Impact pathway approach captures is only a fraction of the total effects of air pollution. Furthermore, at present, it only covers some of the variation in effects, and hence costs, that actually appears.

The implication of this for policy work is that there needs to be a focus in the discussion on when and how pricing can be used to internalize externalities of air pollution and what other measures that can be used as a complement. Implementation of true marginal cost pricing would require a collection of information that is currently practically and economically impossible. It would also require advanced simulations of the changes in the concentrations of pollutants that result from an additional vehicle which we also think are practically impossible at this point in time.

Acknowledgments

The authors wish to thank Peter Bickel , Stephan Schmid and Rainer Friedrich for performing the calculations and for providing valuable inputs to this paper. We also wish to thank Vinnova for financial support of this work.

References

Bickel P. and Schmid S. (2001) Approach for estimating costs due to air pollution, global warming and noise. Draft. Version1.1. UNITE (UNIfication of accounts and marginal costs for Transport Efficiency) Working Funded by the 5th Framework RTD Programme. ITS, University of Leeds, October 2001.

Bickel P., Schmid S., Tervonen J., Hämekoski K., Otterström T., Anton P., Enei R., Leone G., van Donselaar P and Carmigchelt H. (2002) Deliverable 11. Environmental Marginal Cost Case Studies. Draft. Version 1.0. UNITE (UNIfication of accounts and marginal costs for Transport Efficiency) Working Funded by the 5th Framework RTD Programme. ITS, University of Leeds, August 2002.

Bickel P., Schmid S. and Friedrich R (2003) Estimation of Environmental Costs of the Traffic Sector in Sweden. Draft 1.2. IER, University of Stuttgart, Germany.

Forsberg B. (2002) Översyn av beräkningarna av trafikemissioners hälsoeffekter – särskilt lokala effekter av partiklar och kvävedioxid. PM prepared for SIKA, draft version 2002-02-11. Insitutionen för folkhälsa och klinisk medicin, Umeå Universitet, Sweden.

Friedrich R. and Bickel P. (2001) Environmental External Costs of Transport. Springer-Verlag, Berlin Heidelberg, Germany.

Friedrich R. and Ricci A. (1999) Calculating Transport Environmental Costs. Final Report of the Expert Advisors to the High Level Group on Infrastructure Charging. http://europa.eu.int/comm/transport/infr-charging/library/env-cost.pdf

Holland M.R and Watkiss P. (2002) BeTa, Benefits Table database: Estimates of the marginal external costs of air pollution in Europé. Version E1.02a. Netcen. http://europa.eu.int/comm/environment/ enveco/air/betaec02aforprinting.pdf

Hämekoski K., Tervonen J., Otterström T. and Anton P. (2002) Estimation of Marginal Environmental Emission Costs of Maritime Transport – Pilot study based on the ExternE methodology. Final Report. 60K03130-Q090-003a. Electrowatt-Ekono Oy, Finland.

Johansson H., and Ek M. (2003) Emissions from transport in Sweden in 2000. TFK report 2003:5E, http://www.tfk.se/publik/2003_5E.pdf.

Leksell I. (1999) Ekonomisk värdering av luftföroreningar från trafiken. Del 1, Värdering av exponering samt sammanfattning. Underlagsrapport till ASEK. SIKA, Sweden.

Nääs O. and Lindberg G. (2002) Deliverable 5: The Pilot Accounts for UNITE, The Pilot Accounts for Sweden – Appendix Report. Draft version 4.6. UNITE (UNIfication of accounts and marginal costs for Transport Efficiency) Working Funded by the 5th Framework RTD Programme. ITS, University of Leeds

Munthe J, Grennfelt P-I., Sverdrup H., and Sundqvist G. (eds) (2002) ASTA. New concepts and methods for effect-based strategies on transboundary air pollution. Synthesis Report, April 2002. http://asta.ivl.se

Otterström T., Hämekoski K. and Anton P. (2003) Estimation of Marginal Environmental Emission Costs of Aircraft LTO Emissions – Pilot study. Draft Final Report. 60K04237-Q070-002b. Electrowatt-Ekono Oy, Finland.

12th International Symposium "Transport and Air Pollution" / 12e Colloque international "Transports et pollution de l'air", Avignon, 16 -18 *June* / juin 2003
proceedings / actes, n°92, tome / Vol. 1, Inrets ed., Arcueil, France, 2003, p. 209-216

10 ans de monétarisation des effets locaux de la pollution atmosphérique : des évaluations scientifiques aux décisions politiques

JP. Nicolas[1], F. Duprez[2], S. Durand[1], F. Poisson[3], PL. Aubert[1], M. Chiron[4], Y. Crozet[1], J. Lambert[3]
[1] Laboratoire d'Economie des Transports
ENTPE, rue Maurice Audin, 69 518 Vaulx-en-Velin Cedex – France
email : nicolas@entpe.fr, fax : 04 72 04 70 92
[2] CERTU, 9 rue Juliette Récamier, 69 456 Lyon Cedex 06 – France
[3] et [4], INRETS, Laboratoire Transport Environnement, et UMR Epidémiologie Transports Travail Environnement, 25 av. F. Mitterrand, 69675 Bron Cedex – France

Abstract
This paper is devoted to the economic valuation of local air pollution impacts. On the one hand, how these figures are built by economists and, on the other hand, how are they tackled and used to establish official values for public policies ? We highlight the gap between these two processes and we propose ways for working a better synergy.
Key-words : *local pollution, impacts, valuation, official values, public decision, international comparison*

Résumé
Cette communication s'intéresse à la valorisation monétaire des impacts environnementaux de la pollution atmosphérique locale. Comment, d'un côté, ces chiffres sont-ils construits par les économistes, et comment, de l'autre, sont-ils repris et utilisés pour établir des valeurs officielles dans le cadre des politiques publiques ? Nous mettons en lumière les écarts existant entre les deux et proposons des solutions pour les réduire.
Mots-clefs : *pollution locale, effets, monétarisation, actualisation, valeurs tutélaires, décision publique, comparaison internationale*

Introduction

En premier constat, les problèmes de pollution atmosphérique dans les grandes agglomérations françaises semblent en passe d'être résolus. Après les efforts dans l'industrie et le chauffage au cours des années 70-80, les progrès technologiques réalisés par les transports permettent d'enregistrer une amélioration continue de la qualité de l'air en ville[5].

Cependant plusieurs facteurs maintiennent cette question sur l'agenda politique. Tout d'abord il reste des incertitudes sur les évolutions de l'ozone de fond et des particules les plus fines. Ensuite, les exigences des populations urbaines vis-à-vis des problèmes d'environnement et de santé publique vont croissant. Enfin, les recherches épidémiologiques confirment de plus en plus que la pollution atmosphérique a un impact à long terme important sur la santé humaine. Ainsi, on a longtemps pensé que les décès provoqués par la pollution de l'air restaient limités (10 ou 20 000 années de vie perdues par an en France - Académie des Sciences, 1999). Or des travaux menés sous

[5] *cf*. le site du ministère de l'environnement, qui fournit les résultats des réseaux de mesure de la qualité de l'air des grandes villes françaises :
http://www.environnement.gouv.fr/dossiers/air/bilans/010116-bilan-air-91-2000.htm

l'égide de l'OMS (Künzli, 2000) estiment que les décès provoqués par une pollution moyenne équivalente à celle de 1996 pourraient correspondre à 316 000 années de vie perdues. Les impacts sont alors du même ordre de grandeur que ceux de l'alcool et du tabac (respectivement 500 et 750 000 années de vie perdues), changeant radicalement la hauteur des enjeux.

Comment l'approche économique, souvent utilisée pour justifier la mise en œuvre de politiques publiques, peut-elle prendre en compte ce type d'impacts, dans un contexte d'incertitude où existent de fortes divergences entre les différentes perceptions du problème ? Le propos de l'étude présentée ici (Nicolas et *alii*, 2002) a été de confronter les évaluations des coûts des impacts de la pollution atmosphérique, réalisées d'un point de vue scientifique (que mesure-t-on, comment, pourquoi ?) à celles retenues dans le cadre des politiques publiques (par quels mécanismes institutionnels les valeurs construites par les chercheurs -ingénieurs, économistes, épidémiologistes, etc.- vont aider à l'élaboration de valeurs officielles, qui fournissent une base aux prises de décision dans la gestion des affaires publiques ?).

1. Méthode : bilan bibliographique et comparaisons des pratiques européennes

L'objet du travail était donc de partir de cette double interrogation, sur la construction scientifique des chiffres d'abord, et sur l'usage institutionnel qui en est fait ensuite, pour mettre en lumière les écarts existants entre les deux et, éventuellement, proposer des solutions pour les réduire.

Même si la première phase de la réflexion s'inscrivait dans une logique de bilan et d'état des lieux, la méthodologie d'exploration a dû s'adapter aux différences existant entre les champs de la recherche académique et celui de l'action publique.

Du point de vue de la recherche en matière de valorisation des impacts locaux de la pollution de l'air, c'est une synthèse bibliographique qui a été privilégiée, reprenant de la manière la plus exhaustive possible les études et rapports publiés au cours des années 90 sur le sujet. Deux axes de recherche ont été distingués :

- De nombreux travaux sont consacrés à la mise en œuvre de méthodes de valorisation des impacts immédiats : quelles différences existe-t-il entre elles, quelles sont celles qui sont les mieux adaptées au cas de la pollution de l'air, y-a-t-il des complémentarités ? Une première étude réalisée au sein du « Programme national de recherche et d'innovation dans les transports terrestres » (Prédit 1996-2000) a fourni ici une première base bibliographique solide (Chanel et Vergnaud, 2001). Une vingtaine de recherches illustratives des différentes méthodes et des différents types d'impacts de la pollution de l'air ont ensuite été sélectionnées pour proposer des fiches de lecture détaillées. Le tableau 1 présente les 21 recherches retenues.
- Cependant une démarche de valorisation monétaire, notamment concernant des dommages environnementaux, ne prend de sens que si elle s'insère dans une vision dynamique de « longs » termes (10-20 ans, 30 ans et plus) de la situation. Il était donc nécessaire de tirer également un bilan des suggestions formulées en économie pour prendre en compte les dynamiques temporelles à travers les débats autour du taux d'actualisation.

Concernant l'usage de valeurs monétaires officielles pour prendre en compte les impacts de la pollution de l'air dans les politiques publiques, nous nous somme concentrés sur les nations européennes. Compte tenu des écarts existants entre les pays, nous avons privilégié trois pays, la France, la Suède et la Suisse, afin de mieux rendre compte des liens existants entre les valeurs proposées, les traditions institutionnelles et les pratiques nationales en matière environnementale. Ce travail a été réalisé en s'appuyant d'une part sur les synthèses internationales existantes et d'autre part, concernant l'étude des 3 pays, par le contact avec des experts nationaux et la consultation des sites web officiels consacrés à la question.

Méthode d'évaluation : *Type de dommages :*	***Dépenses de protection***	***Prix hédonistes***	***Evaluations contingentes***	***Réparation des dommages***	***Capital humain***	***Pertes de production***
Morbidité *Court terme*			Alberini al., 1997 Johnson al., 1997 Navrud, 1998	Deloraine al., 1995 Scott Voorhees al., 2000	Hansen al., 2000	
Mortalité-Morbidité *Court terme*			Ostro al., 1998 Chanel al., 1996 Rozan, 2000			
Court et long terme			Künzli al., 2000	Ecoplan, 1996		
Mortalité		Lannoie al., 1995				
Bâtiments			Grosclaude al. 94	Jeanrenaud al., 1993 Apsimon al., 1996		
Faune/Flore					Gregory al. 96	
Visibilité			McClelland al. 93			
Plusieurs impacts		Figueroa 96	Saelensminde, 99 Halvorsen 1996			
	Manière, 1999 - *toutes méthodes*					

Rq : on trouvera les références précises de ces travaux dans Nicolas et al. (2002)

Tableau 1 : Bilan et classification des études retenues

Table 1: List and classification of the selected studies

2. L'évaluation économique des coûts de la pollution atmosphérique

Quelles méthodes d'évaluation pour quels résultats ?

Lorsque l'on se penche pour la première fois sur les évaluations monétaires des impacts sur l'environnement et le cadre de vie, on est frappé par la diversité des méthodes de mesure, avec une dizaine de méthodes génériques, et la variabilité des résultats (qui peuvent aller de 1 à 15 concernant les impacts de la pollution de l'air - voir par exemple Chanel et Vergnaud, 2001).

De fait, l'extrême diversité des impacts nécessite des évaluations dans des domaines très différents, sur des biens qui ne sont pas du tout de même nature. Par exemple, les méthodes les plus proches d'une logique économique classique vont chercher à retrouver un marché des biens concernés par les impacts environnementaux. Soit, dans le cadre des *évaluations contingentes*, on fabrique de toute pièce ce marché et l'on demande à des personnes enquêtées de se positionner sur une échelle de valeur dans le cadre d'une ou plusieurs situations fictives ; soit on observe la manière dont les agents économiques se comportent sur des marchés concernés par ces impacts environnementaux (*méthode des prix hédonistes*, qui mesure les impacts sur les prix du marché de l'emploi ou de l'immobilier, *« coûts du voyage »* qui estime les dépenses que l'on est prêt à faire pour se rendre dans un lieu donné, *dépenses de protection* : mais ces 3 méthodes se sont révélées peu adaptées au cas de la pollution de l'air).

Mais il est également courant de chercher à d'abord mettre en évidence et à analyser la chaîne des impacts (*fonction des dommages* et mesure de courbes doses-réponses) avant d'en établir les coûts :

soit en en calculant les pertes de richesses induites (*pertes de production*, ou *méthodes du capital humain* en matière de risque et d'impacts sanitaires), soit en estimant les coûts de *réparation des dommages*, soit éventuellement en mesurant les coût des mesures de prévention (*coûts d'évitement* – cette dernière pratique ne mesure pas les coûts des dommages proprement dits et nous ne l'avons pas retenue comme pertinente par rapport à l'objet de notre étude).

Les méthodologies d'évaluation mises au point ne proposent donc pas forcément le même regard et n'apportent pas les mêmes résultats. Il importe dès lors de s'interroger sur les aires de pertinence des différentes méthodes, leurs complémentarités et leurs zones de "concurrence".

Trois distinctions apparaissent déterminantes pour établir l'intérêt d'une méthode par rapport à un objectif d'évaluation donné.

Le type de dommage que l'on veut évaluer tout d'abord (santé publique, bâtiments et matériaux, faune et flore, etc.), ainsi que leur localisation dans la chaîne des causalités (effets directs, comme la maladie, et effets indirects, comme l'absentéisme au travail qui en découle).

La nature individuelle ou collective de la prise en charge des coûts : certaines méthodes ne mesurent que les coûts ressentis par les individus (comme les prix hédonistes ou les évaluations contingentes) ; les coûts pris en charge par la collectivité, comme les dépenses médicales remboursées par la sécurité sociale, devront passer par d'autres méthodes, et notamment par l'estimation du coût de réparation des dommages.

Le type de valeur que l'on veut mesurer, d'usage ou d'existence, du bien qui se trouve dégradé[6]. Cette distinction permet de comprendre l'intérêt des évaluations contingentes qui peuvent envisager les valeurs de non-usage parfois importantes dans le cas des biens environnementaux et souvent difficile à prendre en compte dans les problèmes de santé publique, comme la douleur, l'isolement social ou le décès provoqués par les maladies.

De ce point de vue, les méthodes sont beaucoup plus complémentaires que concurrentes. Suivant les objectifs de l'évaluation on recourra de préférence à tel ou tel outil. A l'exemple de Rozan (2001), on peut ainsi évaluer les coûts sanitaires de la pollution atmosphérique en cumulant les dépenses médicales (coûts de réparation), les pertes liées à l'absentéisme (pertes de production) et les souffrances entraînées par la maladie (méthodes contingentes).

Cependant, le découpage des champs de pertinence n'est pas absolu, et de nombreuses zones sont susceptibles d'être couvertes par différentes méthodes. Et, sur ces points de recouvrement, une méta-analyse menée par Manière (1999) sur 49 études et 96 estimations souligne que chaque méthode fournit des coûts différents des impacts de la pollution atmosphérique. Ainsi, dans son échantillon, la méthode des dépenses de protection produit des coûts 1,5 à 1,9 fois plus élevés que l'évaluation contingente, elle-même 3 fois plus forte que la méthode des prix hédonistes. Les méthodes du surplus de production et des fonctions de dommages donnent des estimations encore inférieures. On constate aussi des différences importantes à l'intérieur d'une même famille de méthodes. Au sein des évaluations contingentes par exemple, les valeurs obtenues à partir d'un référendum sont en

[6] Pour effectuer leurs évaluations, les économistes de l'environnement ont été amenés à distinguer plusieurs natures de valeurs pour un bien. Ainsi par exemple Barde (1991) propose 4 grandes familles de valeurs : la *valeur d'usage* tout d'abord, liée à l'utilité directe du bien en question; la *valeur d'option* ensuite, liée à une utilité potentielle d'un bien, même si l'on ne sait pas encore de quoi il en retournera; un bien peut avoir une valeur que l'on veut transmettre à sa descendance ou aux générations futures, en dehors de l'usage que l'on en a sur le moment (*valeur de legs*); enfin, on peut aussi reconnaître une valeur en soi à une personne, une espèce rare, un écosystème, etc., indépendamment de toute utilité immédiate ou future. On aboutit à l'idée d'une *valeur d'existence*, qui ouvre une porte entre éthique et économie. Cette valeur d'existence rejoint la notion de *valeur de non-usage*, utilisée par de nombreux auteurs en opposition à la valeur d'usage évoquée précédemment. La *valeur économique totale* d'un bien est la somme de chacune de ces valeurs, qui pourront avoir un poids différent en fonction de la nature du bien considéré.

moyenne 3 fois supérieures à celles établies à partir d'un éventail de valeurs préétablies, les questions ouvertes fournissant des résultats intermédiaires. En matière de coûts des dommages, le procédé de comptabilisation des dommages (répertoire exhaustif *vs* extrapolation à partir de quelques cas) apparaît encore plus déterminant pour le résultat.

Le taux d'actualisation et les questions d'équité intergénérationnelle

La seconde variable clé dans l'évaluation socio-économique concerne la manière de prendre en compte les différents horizons temporels.

Le taux d'actualisation, qui est couramment utilisé en économie pour prendre en compte les avantages et inconvénients attendus d'un projet, est souvent conçu comme une expression des préférences pour le présent : 100 € disponibles immédiatement sont préférés à 100 € disponibles dans un an seulement et, si l'on considère un taux d'actualisation a, il faudrait se voir proposer $100.(1+a)$ € dans un an pour abandonner les 100 € immédiats. La valeur actuelle S_0 d'une somme S_n attendue pour l'année n sera dès lors $S_0 = S_n/(1+a)^n$. Ainsi, plus le taux d'actualisation n sera élevé, plus vite les valeurs futures seront effacées au fil des ans.

Cette préférence pour le présent est évidemment variable en fonction de chacun et de sa situation du moment, mais elle peut s'agréger à un niveau collectif, par le biais des marchés financiers ou à travers la valeur retenue par la puissance publique pour évaluer ses projets.

Initiées au début des années trente, les réflexions autour du taux d'actualisation se sont profondément renouvelées ces dernières années avec l'émergence des problèmes d'effet de serre. Tout d'abord, la notion de taux d'actualisation s'est enrichie par rapport à la première acception présentée plus haut. Trois grandes justifications peuvent être mises en avant pour son utilisation (Arrow, 1995) : *la préférence « pure » des agents économiques pour le présent* avec un taux estimé à 1 ou 2 % par an selon les auteurs (voire 0% pour les effets intergénérationnels) ; *« l'effet de richesse »* lié d'une part à l'accroissement du revenu moyen au cours du temps et d'autre part à la décroissance de l'utilité marginale de ce revenu ; il est de l'ordre de 2 à 3% par an dans les pays occidentaux ; et un « *coût d'opportunité de l'argent* » pour les agents économiques privés tels que les firmes et les entreprises. On peut prendre ici en référence le taux réel des obligations à long terme, qui est de l'ordre de 4% aujourd'hui, même si dans les faits, il existe toujours plusieurs taux, qui dépendent de la durée du prêt, du risque client, de la conjoncture économique et politique.

Dans l'absolu, du point de vue de la puissance publique représentante des intérêts collectifs, seuls les deux premiers éléments seraient à prendre en considération, hors profit dégagé sur la rémunération de l'argent. Cependant, et c'est tout le dilemme auquel se trouvent confrontées les nations aujourd'hui, le taux de 4% qu'il signifie entraîne l'acceptation d'un trop grand nombre de projets par rapport aux capacités de financement de la puissance publique.

Ainsi, la France préfère aujourd'hui un taux uniforme officiel de 8%, qui occulte les avantages et inconvénients générés à long terme. Pour pallier à ce défaut, plusieurs solutions sont envisagées :

- On peut distinguer des taux d'actualisation différents suivant l'horizon temporel considéré, notamment avec des taux faibles pour les effets attendus dans 20 ou 30 ans, permettant ainsi de mieux les prendre en compte dans l'analyse.
- Suivant les préconisations de Hotelling (1931), le coût des ressources non renouvelables comme le pétrole par exemple sera réévalué annuellement d'un taux équivalent au taux d'actualisation. D'une manière plus ponctuelle et statique, les valeurs de certains biens non marchands pris en compte par la puissance publique peuvent être réévaluées lorsque l'on considère qu'il y a un décalage trop grand entre les valeurs officielles et celles qui se dégagent des évolutions générales de la société (exemple en France de la valeur de la vie humaine qui vient de passer de 0,5 à 1,5 millions €).

Cependant d'autres pays ont choisi d'utiliser un taux d'actualisation de référence beaucoup plus bas. Ainsi l'Allemagne utilise-t-elle un taux officiel de 3% dans le domaine des transports. Pour éviter toute dérive du budget, les projets jugés rentables sont classés en fonction de leur bénéfice par euro

investi. La puissance publique se donne une enveloppe financière pour ses investissements et seuls les projets les plus rentables que peut contenir cette enveloppe sont réalisés. Comme dans le cas français d'un taux d'actualisation élevé, les projets les moins rentables sont donc éliminés, mais deux avantages peuvent être soulignés. D'une part les effets à long terme prévisibles, positifs comme négatifs, sont mieux pris en compte. D'autre part, en fixant au départ une enveloppe globale des dépenses d'investissement, la méthode allemande assure un choix plus transparent entre investissement et fonctionnement. Au lieu de polariser le débat sur la question, très technique, du taux d'actualisation, on revient à un choix politique sur la répartition des dépenses publiques.

Pour conclure cette partie, le champ de la recherche dans le domaine de l'évaluation en économie de l'environnement apparaît donc très ouvert. Ceci étant, il est peu probable que les enrichissements méthodologiques à venir conduisent à une convergence des résultats : il n'existe pas de coût en soi, unique et objectivable, des impacts de nos activités sur l'environnement et notre cadre de vie. Dans cette perspective, nous pensons qu'à côté des travaux scientifiques permettant de mieux évaluer ces impacts, il est aussi nécessaire de s'interroger sur les procédures qui font émerger des valeurs tutélaires de référence, qui vont aider la puissance publique dans ses choix d'investissements. La partie suivante est consacrée à cette réflexion, en comparant les manières de faire dans différents pays d'Europe et en proposant quelques lignes directrices en guise de conclusion.

3. De l'évaluation des coûts environnementaux à la décision politique

Dans le cadre des politique publiques, la valorisation monétaire des impacts environnementaux (comme des coûts externes en général) débouche sur deux applications pratiques distinctes. Elle peut tout d'abord permettre de les prendre en compte dans l'évaluation économique des projets publiques. Ainsi, à la fin des années 90, la moitié des pays européens monétarisent les effets de la pollution atmosphérique et du réchauffement climatique dans leur méthode officielle d'évaluation des projets de transport. Elle ouvre aussi sur la mise en œuvre du principe pollueur payeur, à travers des politiques de fiscalité environnementale de taxes et de subventions. Par exemple, tous les pays de l'OCDE ont introduit des taxes sur les carburants routiers, qui remplissent cette fonction et représentent près des deux tiers de leur fiscalité environnementale.

Cependant les synthèses internationales mettent aussi en évidence de fortes divergences entre les pays, avec des valeurs monétaires des effets externes très variables et une fiscalité environnementale très variables, de moins de 1% à plus de 4% du PIB selon les pays de l'OCDE. Dès lors qu'il s'agit d'analyser ces différences, ces études générales de comparaisons internationales s'avèrent insuffisantes. Elles ne permettent guère de comprendre les objectifs poursuivis dans chaque pays, les méthodes de valorisation retenues ou la manière dont sont réalisés les arbitrages. Il nous est donc apparu nécessaire de se pencher plus en détail sur le cas quelques pays, avec la France, la Suède et la Suisse qui ont chacune des pratiques bien marquées.

En France, les coûts environnementaux sont fixés par des groupes technico-administratifs

En France, l'évaluation socio-économique des projets de transport s'appuie sur une méthode d'analyse coûts/avantages (ACA) normalisée. Dès les années 60 des travaux proposaient déjà de prendre en compte des effets non marchands, conduisant à l'introduction des coûts de l'insécurité routière en 1970. Mais ce sont véritablement les réflexions menées par Marcel Boiteux en 1994 dans le cadre du Commissariat Général au Plan qui ont systématisé l'intégration des nuisances environnementales. Ce travail, reconduit en 2001, a permis de proposer des valeurs tutélaires pour le bruit, la pollution atmosphérique locale et l'effet de serre, en s'appuyant sur les connaissances scientifiques acquises et sur une concertation entre les ministères chargés des transports, de l'environnement, des finances et les entreprises ou établissements publics de transport (CGP, 2001).

Il existe donc, en France, un lien entre la recherche sur les coûts externes et les pratiques d'évaluation socio-économique des projets de transport. Mais face à la complexité des méthode de valorisation et à la variabilité des résultats proposés par les chercheurs, c'est un groupe technico-administratif (le "groupe Boiteux"), composé d'experts et de hauts fonctionnaires qui débat sur le

choix des valeurs tutélaires et les responsables politiques restent peu impliqués. Cette approche relativement technocratique explique sans doute en partie que l'évaluation socio-économique soit mal connue, voire déconsidérée par les décideurs locaux et par le public, alors même que cette démarche est rendue obligatoire par la loi. Les non spécialistes la considèrent le plus souvent comme une "boîte noire" produisant des résultats peu compréhensibles. Dans ces conditions, l'évaluation socio-économique est aujourd'hui plus vécue comme une obligation légale que comme une aide à la décision ou un élément de débat public.

En Suède, la fiscalité environnementale fait l'objet d'un véritable débat politique…

En Suède, les préoccupations environnementales comme la culture économique apparaissent très prégnantes pour guider la décision publique. Ceci s'est traduit par la mise en œuvre d'une politique fiscale orientée en faveur de la protection de l'environnement. De même, le principe d'une tarification des infrastructures au coût marginal social, prenant en compte les impacts environnementaux des transports, est clairement affirmé dans les textes (« Transport Policy Act », 1979 ; « Transport Policy Proposal for Sustainable Development », 1998).

L'existence d'une structure fiscale environnementale et d'un débat public sur l'environnement ouvert depuis près de quinze ans constitue un atout considérable pour la Suède : tous les éléments sont en place pour pouvoir réagir rapidement aux sollicitations de l'Europe ou aux accords internationaux sur l'effet de serre. La Suède qui exerce d'ailleurs des pressions sur l'Europe pour que des mesures communautaires plus favorables à l'environnement soient adoptées.

L'évaluation socio-économique des projets de transports reste, comme en France, un domaine privilégié de l'appareil technico-administratif. Le groupe de travail ASEK, composé de représentants des agences chargées de l'environnement et des différents modes de transport, auditionne des experts et des scientifiques, puis adopte, après débat, les valeurs de référence pour l'analyse coûts/avantages. En Suède comme en France, l'usage de l'évaluation socio-économique des projets de transport reste donc réservée aux seuls spécialistes, et les valeurs tutélaires sont le fruit d'un compromis entre les connaissances théoriques et les convictions ou intérêts, rarement explicitées, des participants aux groupes de travail. Notons cependant que les résultats et discussions à l'intérieur des groupes sont ensuite repris en commission parlementaire avant d'aboutir en proposition de texte validée au niveau du parlement. *In fine*, les valorisations monétaires de l'effet de serre et de la pollution atmosphérique locale retenues en Suède sont respectivement six et trois fois plus importantes qu'en France.

En Suisse, la volonté politique se conjugue avec une recherche pragmatique

L'un des principaux objectifs de la politique suisse de transport est de protéger les Alpes, véritable capital naturel du pays, contre les effets négatifs de la croissance du trafic routier. Pour y parvenir, la Suisse a choisi de favoriser le transport ferroviaire, en consentant d'importantes subventions publiques à ce mode et en limitant à 28 tonnes le poids total autorisé des véhicules lourds. Puis, face aux pressions européennes, les autorités suisses ont relâché cette contrainte réglementaire pour s'orienter vers une régulation économique : en 1998, une votation populaire a débouché sur l'acceptation d'une Redevance sur le trafic des Poids Lourds liée aux Prestations (RPLP). Sur le plan technique, cette redevance vise à internaliser les coûts externes du trafic poids lourds vers la sphère marchande : le tarif moyen de la RPLP correspond exactement à la somme des coûts externes et des coûts d'infrastructure non couverts par la fiscalité, rapportée au trafic des poids lourds en tonnes-km. Les deux tiers du produit de la RPLP sont destinés au financement des grands projets ferroviaires, en parfaite cohérence avec la volonté politique de développer le fer : ainsi les poids lourds paient aujourd'hui pour leur transfert futur sur le rail.

L'existence d'une recherche appliquée dynamique et bien insérée dans la vie sociale et économique du pays a permis aux autorités publiques d'animer une forte réflexion sur la monétarisation des coûts externes. D'importants progrès collectifs ont ainsi été réalisés en la matière dans les années 90. Le chiffrage précis des coûts externes imputables au trafic routier est venu quantifier les atteintes à l'environnement ressenties par les citoyens suisses ; il a alors constitué un argument technique et

politique très efficace en faveur de la RPLP. Par ailleurs, le débat national n'étant pas clos autour de cette redevance, il ne serait pas surprenant que la recherche suisse contribue encore à l'évolution des connaissances sur les externalités, comme ce fut le cas dans les années 80 et 90.

Conclusion

En conclusion, les coûts des impacts de la pollution de l'air peuvent être très variables d'une étude à l'autre, en fonction de ce que l'on a voulu mesurer et comment. La recherche en économie n'ayant pas pour vocation de converger sur la valeur unique d'un coût objectivable, cet éventail des valeurs, extrêmement ouvert aujourd'hui, n'a guère de raison de se réduire dans les prochaines années. Pour les pouvoirs publics désireux de rationaliser leurs choix en matière de projets publics ou de politique fiscale environnementale, l'exercice de détermination de valeurs officielles de référence reste et devrait rester problématique s'il attend des réponses définitives de la sphère scientifique. La tentation est alors grande d'enfermer le débat à un niveau technique, réservé aux seuls experts, alors que les enjeux relèvent de choix de société. A la lumière des expériences française, suédoise et suisse, deux grands axes nous semblent être déterminants pour aider à dépasser cet écueil et déboucher sur des choix plus transparents et plus opérationnels :

- Les groupes de travail devraient être plus ouverts à l'ensemble des acteurs concernés, avec notamment une implication plus forte des élus parlementaires nationaux dans la genèse et la validation des valeurs obtenues et une plus grande présence des décideurs et techniciens locaux lors de l'élaboration des méthodes d'évaluation des investissements.
- En amont, la recherche (ici en économie et en sociologie, compte tenu du sujet) doit être également mobilisée pour participer au débat public. Là encore, une meilleure association des décideurs politiques à la définition des programmes de recherche appliquée permettrait de déboucher sur des recommandations politiques concrètes. Un effort de diffusion des résultats des recherches financées sur fonds publics obligerait à dégager les principales conclusions scientifiques et aiderait également à tirer un message politique cohérent.

Références

Académie des Sciences (1999) : Pollution atmosphérique due aux transports et santé publique. Editions Tec & Doc, rapport commun n°12, Paris, 196 p.

Chanel O., Vergnaud J.-C. (2001) : Monétarisation des effets de la pollution atmosphérique : un état de l'art pluridisciplinaire. Rapport Greqam, Eurequa pour le compte de la DRAST et du PREDIT. 101+124 p.

Commissariat Général du Plan, groupe présidé par Marcel Boiteux (2001) : Transports : choix des investissements et coût des nuisances. La Documentation Française éd., Paris. 325 p.

Künzli N, Kaiser R, Medina S, Studnicka M, Chanel O, Filliger P, Herry M, Horak F Jr, Puybonnieux-Texier V, Quénel P, Schneider J, Seethaler R, Vergnaud J-C, Sommer H (2000): Public-health impact of outdoor and traffic-related air pollution: a European assessment. The Lancet, Vol 356, pp. 795–801.

Arrow K. (1995) : Effet de serre et actualisation, Revue de l'Energie, n°471, pp.631-636.

Hotelling H. (1931): The economics of exhaustible ressources, Journal of Political Economy, n°39, pp.137-175.

Nicolas J.-P., Duprez F., Durand S., Poisson F., Aubert P.-L., Chiron M., Crozet Y., Lambert J. (2002) : 10 ans de monétarisation des effets locaux de la pollution atmosphérique. Rapport LET, INRETS, CERTU, pour le compte de la DRAST. tome 1, 193 p.; tome 2, 156 p. http://www.ish-lyon.cnrs.fr/labo/let/francais/publications/rapports/couts-PA-t1.pdf

Manière D. (1999) : Méta-analyse de l'évaluation des coûts sociaux de la pollution atmosphérique. Thèse es Sciences Economiques, Université Paris X – Nanterre. 357 p.

Rozan A. (1999) : Evaluation contingente des bénéfices de santé d'une amélioration de la qualité de l'air : l'exemple de la région strasbourgeoise. Thèse es Sciences Economiques, Université Strasbourg. 251 p.

12th International Symposium "Transport and Air Pollution" / 12e Colloque international "Transports et pollution de l'air", Avignon, 16 -18 *June* / juin 2003
proceedings / actes, n°92, tome / Vol. 1, Inrets ed., Arcueil, France, 2003, p. 217-224

Real Life Evaluation of the Emission Reduction Potential of a City Bus Retrofitted with a Continuous Regenerating Trap

Martine Van Poppel and Guido Lenaers
VITO, Flemish Institute for Technological Research, Centre of Expertise 'ETE', Boeretang 200, 2400 Mol, Belgium - Fax +32 14 32 11 85 – email: martine.vanpoppel@vito.be

Abstract
A cost effective measure to reduce PM (Particulate Matter) emissions of city buses is retrofitting with a CRT (Continuous Regenerating Trap). This technology ensures continuous regeneration of the trap without using additives or supplemental heating if an exhaust temperature of at least 250 °C is reached during 10% of the operating time and the NOx/PM ratio is more than 15. In this paper the performance of the CRT is evaluated in real life conditions using VOEM (Vito's On-the-road Emission and energy Measurement system).
The CRT is found to reduce PM emissions to over 90% thereby also reducing CO and THC to at least 65%. No significant NO_x change is detected. The raise in fuel consumption is not significant. The exhaust gas temperature at the CRT is over 250°C for 70% of the time thus easily fulfilling the manufacturer's demand. The demand for a NO_x/PM ratio of 15 is at least realised during 70% of the time.
Follow up measurements after one year showed no deterioration of the CRT.
***Key-words**: CRT, particulate matter, emissions, on-board, real life, city, sulphur, retrofit, diesel.*

Introduction

Most city buses are propelled by a heavy duty diesel engine. These are durable and fuel-efficient but emit relatively high amounts of particulate matter (PM) and nitrogen oxides (NOx). A possible solution to reduce the PM emissions of existing buses is retrofitting with a Continuous Regenerating Trap (CRT).

The CRT consists of an oxidation catalyst and a soot filter (ceramic wall-flow filter) integrated into the silencer (Hawker et ali (1997)). HC, CO and NO are oxidised in the oxidation catalyst. The NO_2 formed, oxidises the soot that is trapped in the soot filter. This mechanism was uncovered by Cooper (1989). The technology ensures continuous regeneration without using additives or supplemental heating if an exhaust temperature of 250°C is reached during 10% of operating time and the NOx/PM ratio is more than 15. Although performance of the CRT is extensively tested in laboratory conditions (e.g. Hawker et ali (1997), Allanson et ali (2000), Liang et ali (2000)), buses operate under specific operating conditions, influencing exhaust temperature e.g., which can be critical for the performance of the aftertreatment device. Therefore, our main objective is to evaluate the performance of the CRT in representative real traffic conditions.

The Flemish Transport Company 'De Lijn' equipped 15 Van Hool A308 city buses (with Euro 2 MAN D0824 4.58L 114 kW engine) with a Eminox/Johnson Mattey CRT. Vito executes a real life performance evaluation on one of these buses by on-board emission measurements using its VOEM (Vito's On-the-road Emission and Energy Measurement system). These bus was fuelled with low sulphur fuel (< 50 ppm). The data presented in this paper are the result of a measurement campaign supported by the Flemish Region.

1 – Experimental Set-up

The performance of the CRT was evaluated in real traffic using an on-board emission measurement system. Emissions, fuel consumption and relevant engine and vehicle parameters are measured during real life driving. Measurements are performed on a bus before and after installation of the CRT. In addition the bus was measured one year after installing the CRT.

Measurement system

The measurement systems for gaseous emissions used in this study are VOEM (Vito 's On-the road Emission & energy Measurement system, Lenaers G. (1994)) and VOEMLow (Vito 's On-the road Emission & energy Measurement system for Low emitting vehicles, Lenaers G. et ali (2003)). Both are dedicated systems for on-board measurements of (ultra low) gaseous emissions and fuel consumption in vehicles. Both enable the analysis of dynamic emission behaviour under real life driving. VOEM and VOEMLow consist of an on-line sampling system for the exhaust gas, laboratory grade analysers, measuring equipment of fuel consumption, vehicle speed, engine speed and lambda value, the power supply and a data-acquisition system

The condensation of water and heavy hydrocarbons is prevented by heating transfer tubing and filter up to 190°C. In VOEM the exhaust gas sample is diluted to prevent condensation of water. In VOEMLow the exhaust gas sample is not diluted but the water in the sample is condensed at 3°C in the cooling unit. CO and CO_2 are measured by NDIR (Non Dispersive Infrared). THC is determined by a HFID (Heated Flame Ionisation Detector) and NOx by a CLA (Chemiluminescence Analyser). The data-acquisition enables the on-line collection and real-time processing of measurement data and automatic calculation of the results (in g/s and g/km).

Both systems were validated on LD and HD chasis dynamometers resulting in deviations below ±20% for VOEM and ±10% for VOEMLow. The major differences in methodology between the two systems are the absence of dilution in the VOEMLow system resulting in a higher sensitivity for low concentrations. Other differences are the special housing of the VOEMLow system, making it less sensible to vibrations and shocks present in the vehicle and protecting it against dust and splash water and the improved data acquisition by a user friendly Labview program. VOEM was used during the measurement campaign before and directly after installing the CRT. VOEMLow was used during the measurements one year after installing the CRT.

The mass of emitted particles is measured using an on-board real time PM mass emission measurement system as a module of VOEM and VOEMLow, Lenaers G. (2000). The basic layout of this module is shown in Figure 1. It consists of a TEOM (Tapered Element Oscillating Microbalance) and a sampling system, both computer controlled. The sampling system is an on-the-road version of a MDT (Micro Dilution Tunnel) from Horiba. The sampling system is heated at 190°C and dilutes exhaust gas at a constant ratio to prevent condenstion of water.

The TEOM measures PM mass per second (m_{TEOM}) in a constant sample flow F_{TEOM} through the instrument. PM exhaust emissions are calculated from the mass measured on the TEOM filter m_{TEOM} and the ratio of exhaust to TEOM flow $F_{exhaust}$ /F_{TEOM}. The TEOM mass readings are multiplied by 1.25, an average figure to account for the extra mass loss over the filter when comparing to the standard filter method, Whitby et ali (1985). $F_{exhaust}$ is calculated from fuel consumption and lambda both measured on a one second base. The integration over time delivers the total PM emission and combination with the travelled distance gives the PM emissions in g/km.

Validation on chassis dynamometer yielded accuracies of ±20%. For HD (Heavy Duty) the accuracy was ±30%.

Driving cycles

The CRT bus has been tested in real traffic on Line 2 in the city of Leuven and on a test circuit. Line 2 is the bus line were these buses operate. The route is situated partly insite the city centre and partly outsite the ring road. Figure 2 gives the speed profile as a function of distance driven. The

bus line is driven in 2 directions (there (Holsbeek – Heverlee) and back (Heverlee – Holsbeek)). The distance is approximately 15 km and the average speed is 18 – 23 km/h.

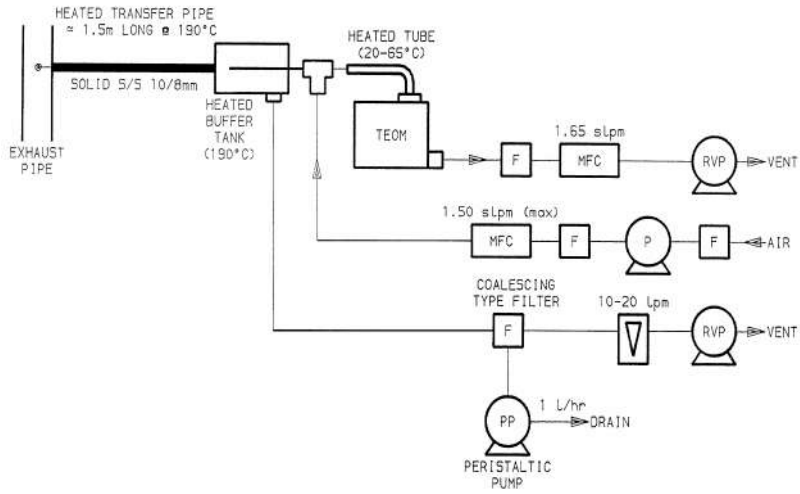

Figure 1: Schematic diagram of the particulate matter measurement system

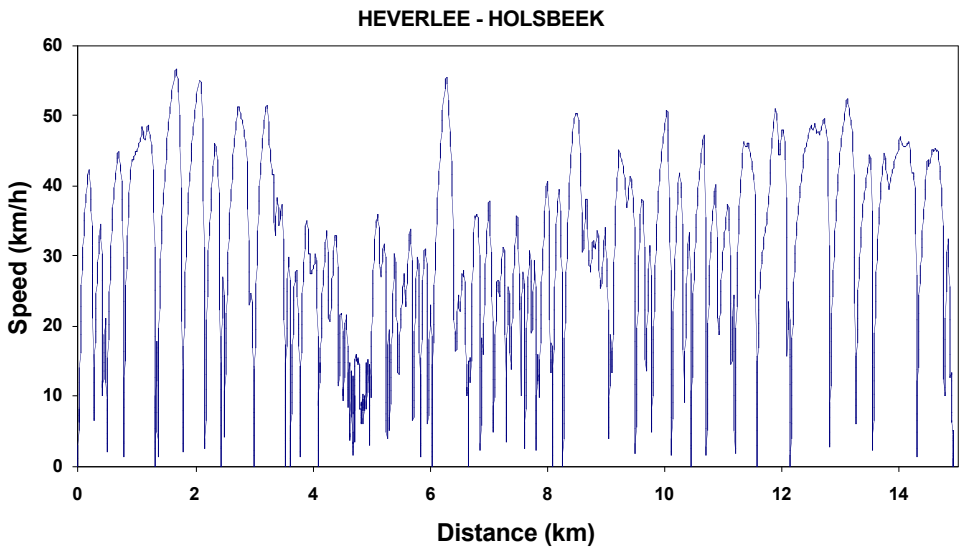

Figure 2 : Speed profile of the real traffic driving 'Line 2' (one way)

Measurements on the test circuit are performed on the city cycle 'De Lijn'. This is a distance based cycle of 5.8 km used by the Flemisch transport Company to compare fuel consumption, exhaust gas emissions and acceleration performance of new city buses. It comprises 25 full throttle accelerations up to a predefined speed. The speed profile is given in Figure 3.

2 – Results and discussion

Gaseous emission

Figure 4 and 5 show the emission results of the measurements carried out on a test circuit and in real traffic. The given values are the average of at least 2 measurements. The error bars give the standard deviation.

The CRT is found to reduce CO and THC to at least 65%. No significant NOx reduction was observed for both tests. The raise in fuel consumption is not significant. It must be remarked that differences observed in the results of the real traffic driving cycle 'Line 2' can be partly due to

differences in driving conditions, also resulting in somewhat higher error bars than the results of the test cycle on test circuit.

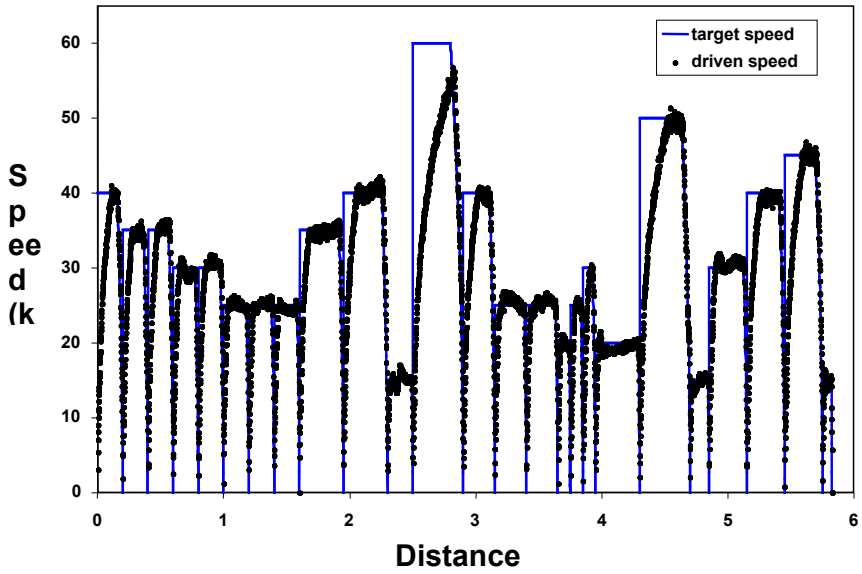

Figure 3 : Speed profile of the City Cycle 'De Lijn'

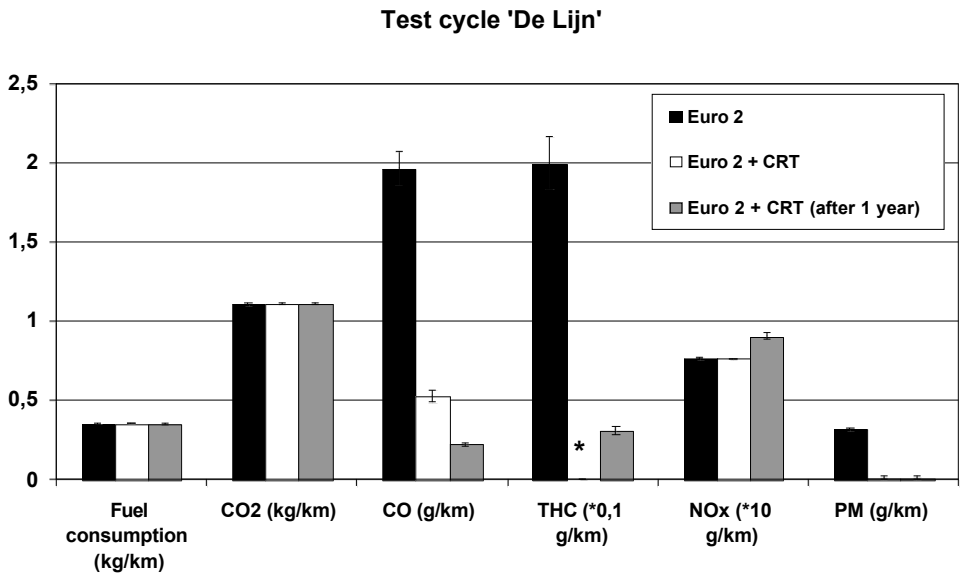

Figure 4 : Gaseous and PM emissions and fuel consumption measured on the 'De Lijn' cycle before, directly after and one year after installing the CRT. (no measurement value available)*

A follow-up measurement was performed after one year of operation. The results (also given in Figure 4 and 5) showed no deterioration of the CRT. CO and THC were even lower than measured directly after installation. The comparison of the measurements of the CRT bus without CRT and the CRT bus with CRT after one year of operation results in CO and THC reductions of 85 to 90%, on the assumption that the engine-out emissions are unchanged. This can be due to a real reduction of the emissions or – more likely – to the higher accuracy of the new measurement system VOEMLow at low emissions.

PM emissions

The PM emissions of the bus before installing the CRT were 0.32 g/km on the 'De Lijn' cycle and

0.58 g/km on Line 2. After installing the CRT the PM emissions were very low. The PM emissions of the CRT bus were calculated using a different methodology because the common methodology based on the absolute mass emissions per second (as explained above) was unsuited for these very low emissions. The CRT bus showed some particle mass emission peaks but also showed some 'negative' peaks of a similar size. This is due to adsorption of water and volatile organic compounds that are re-evaporated later resulting in negative TEOM mass readings. Therefore we calculated the PM emitted by the CRT bus based on the total PM on the TEOM filter at the end of the test. Figure 6 shows the total mass measured on the TEOM filter as a function of time during the 'De Lijn' cycle.

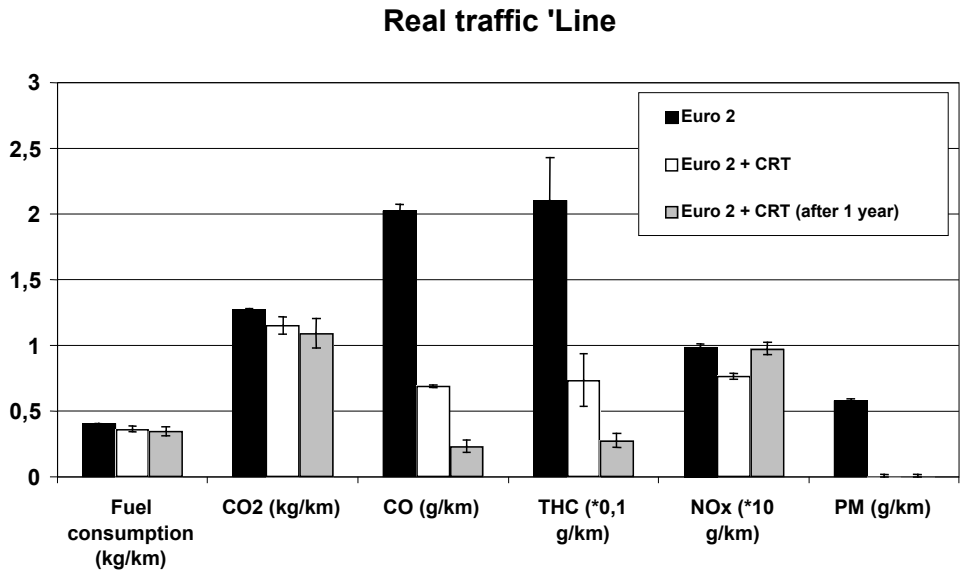

Figure 5 : Gaseous and PM emissions and fuel consumption measured in real traffic on Line 2 before, directly after and one year after installing the CRT

The measured PM on the TEOM filter must be scaled up by a good estimate of the 'average' exhaust to TEOM flow ratio to obtain the PM emitted by the vehicle. We calculated the exhaust PM emissions using the average and maximum exhaust flow measured. Using the maximum exhaust flow (200 g/s) resulted in an upper value of the PM emissions. The calculated PM emissions are given in Table 1.

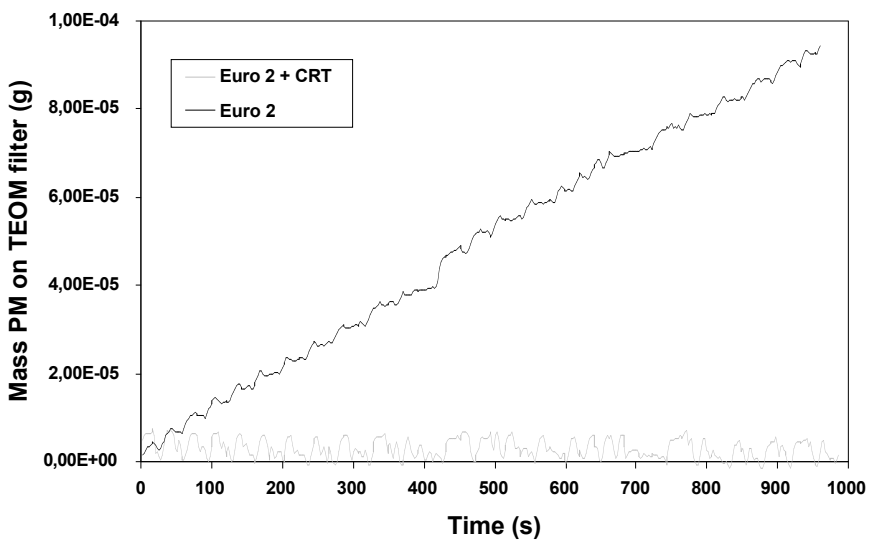

Figure 6: Total mass on the TEOM filter measured on the 'De Lijn' cycle before and after installing the CRT

Test cycle	Test run	Total m_{TEOM} (g)	Exhaust flow (g/s)	PM (g/km)
De Lijn	with CRT, test 1	$5\ 10^{-7}$	Average: 72	< 0.02
			Maximum: 200	< 0.02
	with CRT, test 2	$3.5\ 10^{-7}$	Average: 71	< 0.02
			Maximum: 200	< 0.02
Line 2	with CRT, test 1	$5\ 10^{-6}$	Average: 97	< 0.02
			Maximum: 200	< 0.02
	with CRT, test 2	$7\ 10^{-6}$	Average: 74	< 0.02
			Maximum: 200	0.02
De Lijn	**without CRT**	$9.4\ 10^{-5}$	Average: 77	0.26
	(0.32 g/km)		Maximum: 200	0.61

Table 1 : PM emissions calculated based on total mass on the TEOM filter

Using this methodology, the PM emissions of the bus with CRT were < 0.02 g/km which is the detection limit of the system. This methodology was compared to the common methodology for one of the results of the bus without CRT and gave a good correspondence. PM emissions obtained by the common methodology were 0.32 g/km compared to a 0.26 g/km and 0.61 g/km using the average and maximum exhaust flow respectively. This proves that using the maximum exhaust flow results in an upper limit for the PM emissions.

NOx/PM ratio

Since the working principle of the CRT is based on oxidation of soot by NO_2, sufficient NO_2 is required to oxidise the soot trapped in the filter. In the exhaust only a few percent of NOx is NO_2. In the CRT an oxidation catalyst is placed upstream the filter in order to raise the NO_2/NOx ratio. According to the manufacturer a NOx/PM ratio of 15 is needed to assure a continuous regeneration. Figure 7 gives the distribution of NOx/PM ratio of 2 different runs recorded in real traffic on Line 2 (there and back). We can conclude that on average during 70% of the operating time the NOx/PM ratio is at least 15. In the worst case (Line 2, there, test 1) this is at least 60%. It must be noted that the NOx/PM ratio is only calculated when PM emissions were not zero.

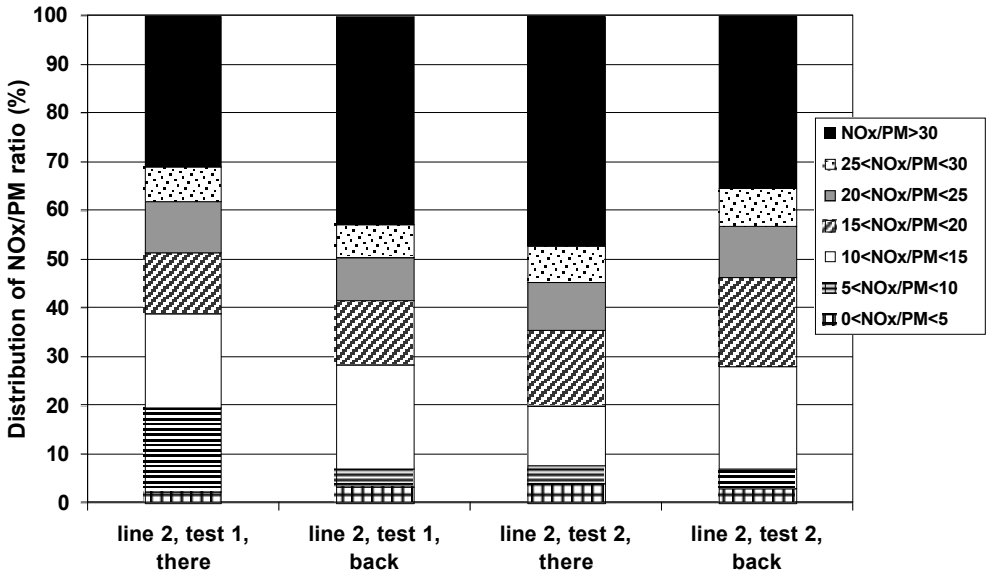

Figure 7 : Distribution of the NOx/PM ratio in real life operation (measured without CRT)

Temperature profile

The exhaust gas temperature was measured before and after the CRT during real life operation. The measured temperature variation after the CRT is smaller than before the CRT. This is due to the relative large thermal capacity of the CRT. The figure below shows the time distribution of the temperature measured before the CRT. The tests were performed with a fully loaded vehicle (12.9 tonnes) and a partly loaded (PL) vehicle (9.8 tonnes). The temperature during the tests on the partly loaded vehicle was somewhat lower.

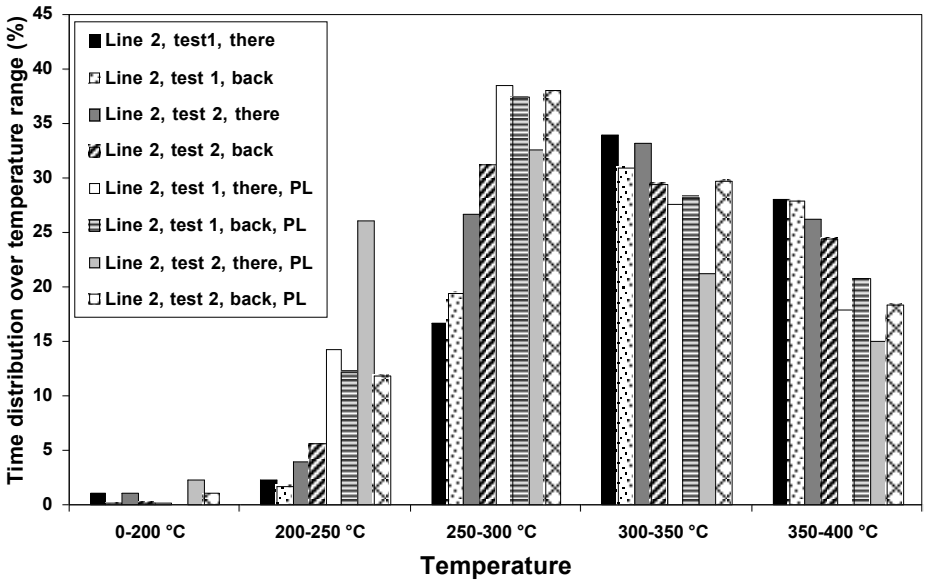

Figure 8 : Time distribution of the temperature for full loaded and partly loaded (PL) vehicle measured before the CRT in real traffic

Analysis of the time distribution of the temperature in the real traffic cycle 'Line 2' proved that the temperature of 250°C was reached at least 70% of the time. This is sufficient to assure a good regeneration of the CRT. According to the manufacturer, at least 10% of the operating time a temperature of minimum 250°C must be reached. Untill now no problems occurred due to the installation of the CRT.

Conclusion

In this study, the performance of a CRT was evaluated in real life operation. A Van Hool city bus was measured before and after installation of the CRT. Measurements showed a good performance of the CRT: PM is reduced by more than 90% and CO and THC by more than 65%. No significant reduction of NOx was observed and the raise in fuel consumption was less than 3%.

It was proved that in these real life operation the essential conditions for continuous regeneration as indicated by the manufacturer were met. An exhaust temperature of at least 250°C was reached during more than 70% of operating time and the NOx/PM ratio was at least 15 during 70% of operating time.

A fist follow-up measurement showed no indication of deterioration of the CRT. A final follow up measurement has to confirm these observations. This follow-up measurement campaign is planned at the end of 2003 i.e. after two years of operation.

It can be concluded that retrofitting of city buses with CRT can contribute to 'cleaner' city traffic.

Acknowledgments

The authors wish to thank all co-workers involved in this project. We are also grateful to the Public Transport Company 'De Lijn' for their support and the Flemish Region for their funding of the

project.

References

Allanson R., Cooper B. J., Thoss J. E., Uusimäki A., Walker A. P., Warren J. P. (2000): European Experience of High Mileage Durability of Continuous Regenerating Filter Technology, SAE Technical Paper Series n° 2000-01-0480, SAE.

Cooper B. J., Thoss J. E. (1989): Role of NO in Diesel Particulate Emission Control. SAE Technical Paper Series n° 890404, SAE.

Hawker P., Myers N., Hüthwohl, Vogel H. Th., Bates B., Magnusson L., Bronnenberg P. (1997): Experience with a New Particulate Trap Technology in Europe. SAE Technical Paper Series n° 970182, SAE.

Lenaers G. (1994): A Dedicated System for On-the-road Gas Emission Measurements on Vehicles. Proc 3th Int. Symp. "Transport and air pollution", Avignon, France, 1994, INRETS, Arcueil, pp. 179 – 184.

Lenaers G. (2000): Dynamic On-board Particulate Matter Mass Emission Measurements. Proc 9th Int. Symp. "Transport and air pollution", Avignon, France, 5-8 June 2000, INRETS, ISBN 2-85782-533-1, vol 2, pp. 431 – 436.

Lenaers G., Pelkmans L. & Debal P. (2003): The Realisation of an On-board Emission Measuring System Serving as a R&D Tool for Ultra Low Emitting Vehicles. Int. J. Veh. Design, accepted for publication.

Liang C. L., Baumgard K. J., Gorse R. A., Orban J. E., Storey J. M. E, Tan J. C., Thoss J. E., Clark W. (2000) : Effects of Diesel Fuel Sulfur Level on Performance of a Continuously Regenerating Diesel Particulate Filter and a Catalyzed Particulate Filter. SAE Technical Paper Series n° 2000-01-1876, SAE.

Whitby R., Johnson R., Gibbs R. (1985): Second Generation TEOM Filters – Diesel Particulate Mass Comparisons between TEOM and Conventional Filtration Techniques. SAE Technical Paper Series n° 850403, SAE.

12th International Symposium "Transport and Air Pollution" / 12e Colloque international "Transports et pollution de l'air", Avignon, 16 -18 *June* / juin 2003
proceedings / actes, n°92, tome / Vol. 1, Inrets ed., Arcueil, France, 2003, p. 225-232

Transport policies in Relation to Congestion and Air Quality in Seven European cities

Mervi Haakana[1], Mari Kauhaniemi[1], Jaakko Kukkonen[1], Suoma Sihto[2], Steve Neville[3], Ingrid Myrtveit[4], Blanca Martin[5], Paul Boulter[6], Peter Segaar[7], Thomas Maggos[8], John Bartzis[8], Lakhumal Luhana[9] & Ranjeet S. Sokhi[9]
[1] Air Quality Research, Finnish Meteorological Institute, Sahaajankatu 20 E, 00880 Helsinki, Finland – Fax: +358 9 1929 5403 - email: mervi.haakana@fmi.fi
[2] Helsinki Metropolitan Area Council, Opastinsilta 6 A, 00520 Helsinki, Finland
[3] Department of Community Protection, Westminster City Council, Westminster Council House, Marylebone Road, NW1 5PT, London, the United Kingdom
[4] Municipality of Oslo Department of Public Health, Maridalsveien 3, 0178 Oslo, Norway
[5] Technical Department, Sociedad Ibérica de Construcciones Eléctricas, S.A., 28108 Madrid, Spain
[6] Environment Group, TRL Limited, Old Wokingham Road, Crowthorne, Berkshire, England, RG456AU, the United Kingdom
[7] Town Development Division, Municipality of Utrecht, P.O. Box 8406, 3503 RK, Utrecht, the Netherlands
[8] Environmental Research Laboratory, NCSR 'Demokritos', 15310 Ag. Paraskevi, Athens, Greece
[9] Atmospheric Science Research Group, University of Hertfordshire, College Lane, AL10 9AB, Hatfield, Herts, the United Kingdom

Abstract
As a part of a major European collaborative project, OSCAR, this paper identifies and analyses transport policies in seven European cities: Athens, Gloucester, Helsinki, London, Madrid, Oslo, and Utrecht. Special interest is focused on methods aimed to decrease congestion and air pollution levels in urban areas.
Continuously increasing traffic volumes and the wide-spread use of private cars has led to a situation where streets are frequently congested in urban areas. The level of congestion varies but ring roads, outskirts of the city road networks, and the city centres are typical traffic bottlenecks in the studied cities. The primary focus in the transport policies was identified to be on the reduction of road traffic volume, especially on the reduction of the passenger car use. Improved public transport was generally seen as a key strategy to achieve this aim.
Key words: *transport, policy, congestion, air pollution, urban, regulatory, modelling*

Introduction

The European Union has set legally binding targets for seven air pollutants, including NO_2 and PM_{10}. These targets, together with national legislation, require city authorities to monitor, control and, if necessary, to take measures in order to reduce air pollution levels. Road transport is a significant source of air pollution, particularly within urban areas. Although, the introduction of catalytic converters, new generation fuels and improved engine technologies should help to reduce air pollution, further actions will be required. Moreover, the continuing growth in traffic volumes has led to increasing levels of traffic congestion, and the associated increase in the time that individual vehicles are operated under stop-and-go conditions.

This study is part of the work being undertaken under the European Union Fifth Framework Programme (EU FP5) project OSCAR, i.e., Optimised Expert System for Conducting

Environmental Assessment of Urban Road Traffic (2002-2005). The analysis contained in this study is part of a major work programme on identifying and prioritising key impact reduction policies in relation to traffic emissions and congestion levels.

1 – Methods

The OSCAR consortium involves academics, research institutions and end users from the participating cities. Each participant, as a city authority or in co-operation with city authorities, has gathered available information on transport policies in relation to traffic and air pollution in their city. Reports and data supplied by the local authorities (Haakana et al., 2003) were also utilised in this study. The local authorities are responsible for the quality of the supplied data, and we have not specifically evaluated their quality.

2 – Characteristics of the cities

Seven European cities are addressed in this study (Figure 1 and Table1).

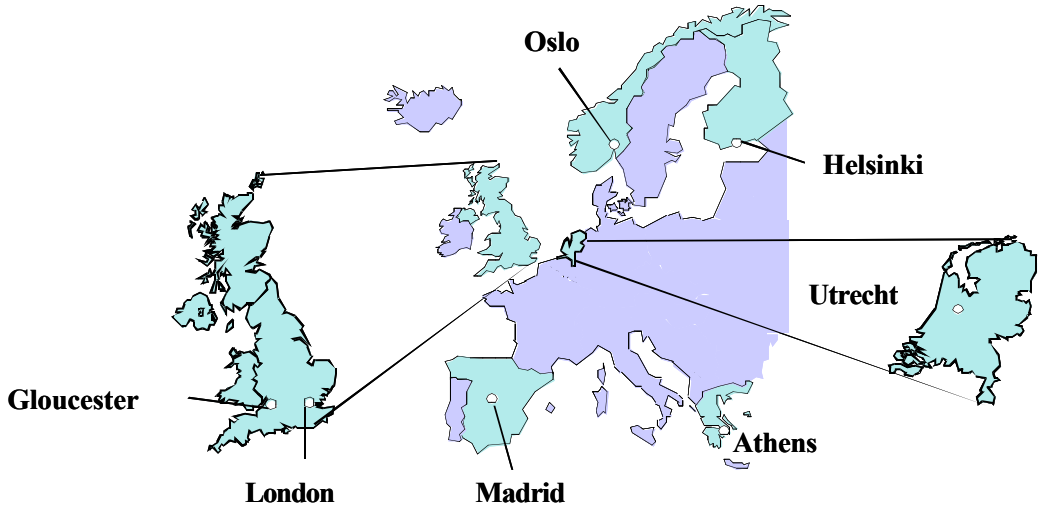

Figure 1: Location of the cities of Athens, Gloucester, Helsinki, London, Madrid, Oslo, and Utrecht.

	Athens	Gloucester	Helsinki	London	Madrid	Oslo	Utrecht
City population (10^6)	3.60	0.11	0.56/ 0.97[1]	7.40	2.90/ 4.50[1]	0.51	0.25
Predicted population growth in the next 10 years (%)	11	2	8	6	10	11	30
City land area (km^2)	450	41	186/764[1]	1 578	607	454	100
Average population density (persons/km^2)	8 000	2 700	3 000/ 1 300[1]	4 700	4 800	1 100	2 500

[1] Metropolitan area; Sources: Athens (2001), GLA (2002), Madrid Community Institute of Statistics (2002), Municipality of Utrecht (2003), ONS (2002), TfL (2001), YTV (2002d), The city of Oslo (2001)

Table 1: Compilation of some key characteristics of the studied cities (2000/2001).

Three of the studied cities each has a population of more than 2 million: London, Madrid, and Athens. The other four cities each has a population of between 110 000 and 560 000. Five of the cities are the capitals of their country: Athens, Helsinki, London, Madrid, and Oslo. Athens has the highest average population density, followed by Madrid and London. The population density can be considered as an important indicator of traffic density, and urban land use. However, the distribution of the population may vary significantly within a city. For instance, in London, population density

varies from less than 2 500 to 30 000 persons/km^2 (TfL, 2001).

The cities of Utrecht, Oslo, Athens, and Madrid can be classified as strongly growing areas. Steady growth of the population is also predicted to continue in other studied cities. A natural consequence of the continuous growth of population is increasing traffic volume, and measures are, therefore, required to prevent worsening of the present traffic congestion and air pollution levels.

3 – Transport

Passenger transport by road and rail, measured in person-kilometres, more than doubled between 1970 and 1997 in the 15 EU member states as a whole (EU, 2002). While passenger cars dominated the increase, some traffic modes, such as tram and metro remained at almost a constant level (+4% during the three decades).

This survey has confirmed that traffic volumes have an increasing trend in most of the studied cities. In Gloucester, the traffic volumes have not significantly changed in the last years and the levels of congestion are rather low compared to the major capital cities. In Oslo, the Helsinki metropolitan area, and Madrid, traffic volumes increased about 15-20% during the 1990s (The National Road Authority, 2002a; YTV, 2002a; Madrid City Council, 2001). The growth is not always uniformly distributed within a city. For instance, in the Helsinki metropolitan area and in London, traffic counts remained more or less steady in the city centre but increased in boundary areas in the 1990s (YTV, 2002d; TfL, 2001).

Comparison of traffic volumes between the cities is not a straightforward task because of differences in classification of the roads, definition of the total length of the roads and total kilometres travelled. Furthermore, the structure of the road network and distribution of the traffic varies between the cities. Thus, an average traffic volume does not necessarily describe the level of congestion in a city.

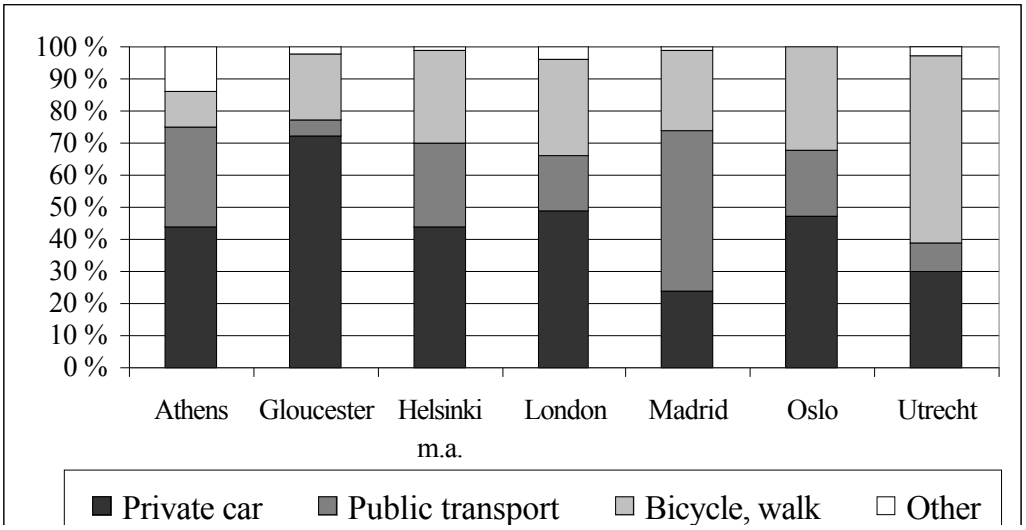

Sources: Attico metro s.a. (1996), Gloucester City Council (1996), Madrid Municipality (2002), Municipality of Utrecht (2001), Oslo Road Authority (2002), TfL (2001), TRL (2001), TØI (2001), YTV (2001)

Figure 2: Distribution of all journeys to the main transport categories (2000/2001).

The distribution of all journeys to the main transport categories have been presented in Figure 2. Private cars dominate the transport compared to the public transport, except in Madrid, where public transport has a clear leading position compared to private cars. In Utrecht, on the other hand, the share of public transport is minimal (9%), but bicycle and walk are common modes of transport (33% and 25%). In Gloucester, the use of private cars is clearly higher than in other cities.

The ownership of private cars has been presented in Figure 3. Interestingly, the highest fraction of car ownership is in the same city as the highest percentage of public transport use. In Madrid, the number of private cars per 1000 inhabitants was 450 in 2000/2001. This is somewhat lower than the

average of 469 vehicles/1000 inhabitants in the 15 EU member countries (EU, 2002). The lowest fraction of car ownership is in London.

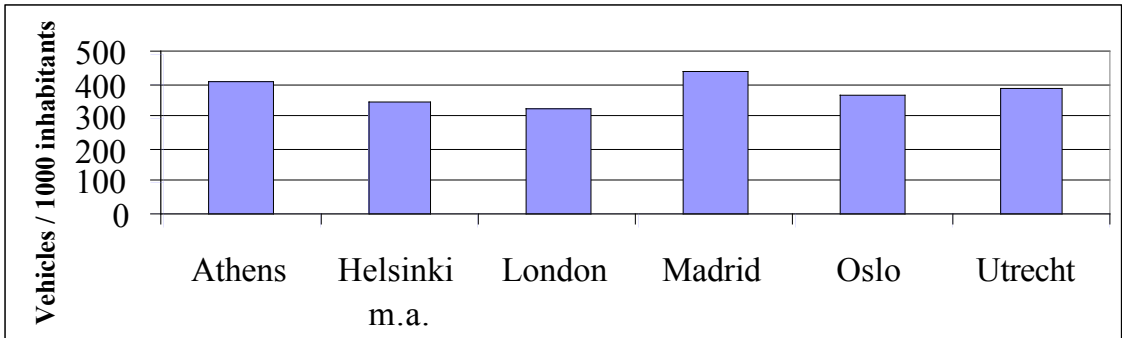

Sources: NTUA (2001), Municipality of Utrecht (2001/2003), Regional Transport Consortium (2002), TfL (2001), The National Road Authority (2002b), YTV (2001)

Figure 3: Number of private cars per 1000 inhabitants in the studied cities (2000/2001). Data from Gloucester were not available.

Typical bottlenecks of traffic in the studied cities are the ring roads, as the through traffic and the local traffic use the same roads. Typically, the highest traffic volumes are monitored on these ring roads. Other problematic areas are the outskirts of the city road network, because of large amount of commuter traffic. Especially, in the morning, several feeder roads bring in more traffic than the city road network is able to receive.

In the city centres of the studied cities, the traffic volumes are not as high as on the feeder and ring roads, but the streets are usually narrower, there are lot of junctions and traffic lights, and there are many different transport modes present. Therefore, travel speeds in the city centres are often low, and the frequency and duration of stops are high. For instance, in central London, half of the time is spent stationary, with the exception of cycles and motorcycles (GLA, 2002).

In all cities, except for London, there is a diurnal variation in levels of congestion caused by commuter traffic during morning and evening peak hours. The period of evening peak hours has gradually lengthened, because of increasing leisure activities. In central London, congestion is not limited to the peak hours but the travel speeds remain the same throughout the day (TfL, 2001).

According to the available information, average traffic speeds on the road networks of London, Madrid, and Helsinki are about the same, at 15-20 km/h (TfL, 2001; Madrid City Council, 2001; YTV, 2002c). As an example of the spatial distribution of average speeds, in Athens, the average speed is 18 km/h in the central area, 22 km/h within a 4 km radius of the central area, and 30 km/h in the rest of Greater Athens, and 48 km/h outside this area in the Attica Region (NTUA 2001).

4 – Transport Policies

The scope of the urban transport policies is wide, ranging from a master plan level, including, for example, plans regarding the structure of the whole city and location of services, to the local level with traffic-free zones and the provision of information to the public. All studied cities already have, or are currently working towards, municipal traffic and transport plans or strategies, which provide an overview and framework for the total short- and long-term transport policy for the city. This is exemplified by the Mayor's Transport Strategy in London (GLA, 2002) and the Helsinki metropolitan area transport system plan (YTV, 1999). Below, the transport policies, which are in use or under planning in the studied cities, are classified into five categories.

Reduction in travel overall

Where appropriate, an objective is to reduce overall travel. Land use may have a major influence on traffic volumes, and the use of public transport. For instance, by locating residential areas and work places near existing or feasible modes of public transportation, it is possible to decrease dependence on private cars. Furthermore, in a compact city structure, the services are better accessible by walking and cycling; this decreases the need for mobility in general (YTV, 1999).

However, the current socio-economic trend seems to be towards a more dispersed city structure. For instance, nowadays, every sixth worker in the Helsinki metropolitan area and in Madrid lives outside the area (YTV, 2002a; Madrid City Council, 2001). In Athens, in Utrecht and in Gloucester, even about 40-50% of the commuting originates from outside the city (Attico metro s.a., 1996; Municipality of Utrecht, 2001; TRL, 2001).

Favouring more sustainable transport modes

Development of more sustainable transport modes: walking, cycling, and public transport, as alternative modes of transport to private cars, is usually first on the list of possible measures to solve the congestion and air pollution problems in the studied cities. For instance, in London, the aim is that most of the increased demand for travel in the future will be accommodated by greatly expanded and improved public transport services (GLA 2002).

There are several ways to influence the travelling behaviour of the public:

1) Favouring public transport

   Policies that favour public transport aim to improve the attractiveness of this transport mode, and thereby hope to stop the trend of continuous traffic growth in the cities. For instance, in Madrid, significant investments in public transport have led to a 63% increase in number of passengers using public transport between 1986 and 2001 (Regional Transport Consortium, 2002). As the growth of the population in Madrid was moderate at the same time, this can be considered as a good indicator of the success of the investments and co-ordination efforts. In the Helsinki metropolitan area, the public transport share of all journeys declined continuously until the early 1990s, when the decline was brought to a stop by considerable improvements in public transport system (YTV, 2002b). The following methods are commonly used in the studied cities:

   a. Improvements in public transport infrastructure
   b. Improved accessibility
      i. Improvements in joint use of public transport and other transport modes
      ii. Easier and co-ordinated interchanges between public transport services
      iii. Improvements in access to public transport vehicles for disabled people
   c. Improved quality of transport
   d. Improvements in consistency of information, fares, and ticketing for public transport
   e. Financial support of public transport

2) Favouring cycling and walking

   Methods to encourage cycling and walking are rather similar in all studied cities; these aim to guarantee the rights of the pedestrians and cyclists to complete and free mobility in the reserved zones. Methods include the building of new cycle and pedestrian roads, improved bicycle parking facilities, and the planning of cycle and pedestrian roads in an environment with greater environmental quality (e.g. through parks).

3) Restrictions on road transport

Use of private cars is regulated in congested urban areas in order to improve air quality by:

   a. Directing traffic to alternative routes, e.g. via ring roads instead of city centre or

residential areas

b. Reducing motoring in a city through parking restrictions
c. Stricter traffic control
d; Traffic-free zones in city centres
e. Restricted use of private cars

Restrictions on the use of private cars do not always have the desired influence on traffic volumes. For instance, in Athens, only private vehicles with either odd or even plate numbers are allowed to enter a certain area in the city centre during specific times since 1982. There has not been any comprehensive evaluation in Athens, but the efficiency of this system has been severely reduced due to several factors: continuous traffic growth, increased double-car ownership, induced car use on allowed days, exemptions, violations, and increased use of motorcycles and taxis (unofficially shared). On the other hand, in London, congestion charges were introduced in February 2003 to deter unnecessary car journeys in the city centre. The first impression is that a reduction in the number of cars in the charging area will result (London www, 2003). However, detailed studies will be required to properly evaluate such schemes.

4) Education and sharing information

Sharing information about air quality, and the factors affecting it, seems to be a common approach to shape public attitudes and travelling habits. There are different media and methods to share information: local newspapers, reports, brochures, radio, internet, television, telephone services, traffic and air quality forecasts, campaigns, and street panels.

Improvements to road network capacity

Methods to reduce congestion by more efficient use of existing road capacity, and by increasing this capacity, are also considered in the studied cities. Reduced congestion and, thereby, more fluent traffic flow, is expected to lead to reduced emissions. In particular, traffic, which is running with constant speed, can be considered to be a better option than stop and go traffic (e.g. Rijkeboer et al., 2002). However, a general opinion in the studied cities is that increased supply will also increase demand. Thus, a new or improved route is not a long-lasting solution for congestion problems. The most commonly used or planned methods are:

- Leading traffic to alternative, less congested routes by dynamical traffic management systems
- Improving the road network by rerouting the traffic, repairing existing roads, and building new roads
- Classification of the roads and prioritising road users

Decreasing unit emissions

Clean technology can also be supported on local level. For instance, electric vehicles can be favoured by allowing them free parking in public parking zones (e.g. in Oslo) and traffic restrictions can be implemented in favour of clean technology vehicles. Furthermore, use of cleaner technology and alternative fuels can be encouraged through financial benefits. Unit emissions can also be decreased by sharing information about economic driving habits. Cities may also favour clean technology, for example electric or bio-fuel buses in public transportation.

Improvements on goods transportation

A significant proportion of urban traffic is commercial, including goods transportation. For instance, goods vehicles form about 15% of the average daily traffic flows on major roads in London (TfL, 2001). In Utrecht, it is expected that the volume of goods transportation will more than double in the next 20 years. The contribution of road freight to the overall traffic volume and the resulting emissions varies between different European regions and requires further study.

Improvements in the logistics of goods transportation are regularly stated in the transport plans. The

objectives for the development of commercial traffic are broadly similar to those for the development of car traffic: the creation of smoothly running transport conditions and the promotion of low emission vehicles. The transport of goods is of great importance for the city economies. Therefore, it is important to regulate flows of goods, as well as possible, while always balancing quality of life and accessibility.

Conclusions

During the last 30 years in the current 15 EU member states, passenger transport, measured in person-kilometres, has more than doubled. The majority of this increase was due to the increase in travel by passenger car and the proportion of travel by public transport decreased significantly. Similar trends were also observed in most of the cities studied here.

Athens, Madrid, and London have the highest average population density, which can be considered as an important indicator of traffic density. However, high rate of use of private cars and predicted population growth indicate likely congestion problems in other studied cities.

Congestion is not limited to the central areas in the studied cities. Ring roads and outskirts of the city road networks are also typical traffic bottlenecks. In particular, the highest traffic volumes are typically monitored on the ring roads. In the city centres, the traffic volumes are not as high as on the feeder and ring roads but the streets are usually narrower, there are a lot of junctions and traffic lights, and several traffic modes are present. Therefore, the traffic speeds in the city centres are often lower, and the frequency and duration of stops are relatively higher.

The primary focus in the transport policies of the studied cities is on the reduction of road traffic volumes, and especially on the reduction of the passenger car use, and the relocation of the traffic flows. Furthermore, the usage of clean technology is also supported on the local level.

An efficient transport policy starts from the planning of the socio-economic structure of the area. The use of the more sustainable transport modes: public transport, cycling, and walking, depends very much on the location and distances between the residential, business, and commercial areas. Possibilities to use this method to solve the congestion and air pollution problems in the cities are, however, often limited. There are also numerous other available transport policies; all of these aim to influence one or more of the traffic characteristics listed below:

- Emission per vehicle
- Share of different modes of transport in traffic
- Traffic volume
- The temporal variations of travel speed and driving patterns
- Spatial and temporal distribution of traffic

From the point of view of assessing the impact of transport policies, methods based on air quality modelling should be able to answer to the question: “What is the influence of changes in the above listed traffic characteristics on air quality in the city?” The final aim of the OSCAR project is to provide such an optimised system for assessing the impact of road traffic on urban environment, in particular vehicular emissions and air quality.

Acknowledgments

The OSCAR project has been financed within the European Union Fifth Framework Programme. Authorities in the cities addressed are acknowledged for providing valuable data and information.

References

Athens (2001): Athens 2001 census data, National Statistical Service of Greece.

Attico metro s.a. (1996): Athens, Internet : http://www.ametro.gr/cgi-bin/showdevelop.cgi

EU (2002): EU Energy and Transport in Figures 2002. European Commission Directorate General for Energy. Internet: http://europa.eu.int/comm/energy_transport/etif/list_of_tables.html

GLA (2002) : Cleaning London’s air – The Mayor’s Air Quality Strategy. Greater London Authority,

London.
Gloucester City Council (1996): Safer City Project - Record of all traffic surveys carried out between January 1993 and December 1995. NAT/S.128. Gloucester City Council Report, Herbert Warehouse, The Docks, Gloucester, GL1 2EQ.
Haakana M., M. Kauhaniemi, & J. Kukkonen (2003): Analysis of Transport Policies in Relation to Traffic Congestion in European Cities. Deliverable of EU OSCAR project, EVK4-CT-2002-00083. EESD: Energy, Environment and Sustainable Development, Public, 28 p.
London www (2003) : The official website for the Mayor of London. Internet : http://www.london.gov.uk/
Madrid City Council (2001): Direction of Services for Management and Information Infrastructure.
Madrid Community Institute of Statistics (2002): The region of Madrid in figures. Report.
Madrid Municipality (2002): Madrid Municipality City Government official web site, in English. Internet: http://www.munimadrid.es/Principal/ingles/portada.html
NTUA (2001) : Department of Rural Survey Engineering, Athens.
Municipality of Utrecht (2001): Commuter traffic in Utrecht 2001
Municipality of Utrecht (2003): The Municipal Traffic and Transport Plan (GVVP), Report
ONS (2002): Office of National Statistics, The United Kingdom. Internet : www.statistics.gov.uk
Oslo Road Authority, (2002) : Public transport in Oslo Year 2000 (Årsmeldinig Statens Vegvesen). Oslo vegkontor report.
Regional Transport Consortium (2002): Madrid public transport demand.
Rijkeboer R.C., N.L.J. Gense, E. van de Burgwal (2002): Real-world driving behaviour of cars the effects of different congestion levels on a motorway. In: Sturm, P., and Minarik, S. (ed.), Proceedings of the Int. Symp. "Transport and air pollution", Graz, Austria, 19-21 June, 2002. pp. 17-24.
TfL (2001) : Transport Statistics for London 2001. Transport for London publications. 2nd Edition http://www.londontransport.co.uk/tfl/pdfdocs/stats2001.pdf
The City of Oslo (2001): Chief commissioner's Department, Information section.
The National Road Authority (2002a): NTP 2006-2015. The traffic development on main roads in Oslo and Akershus. Report, Oslo.
The National Road Authority (2002b): The year reports 2002. National Road Authority reports, Oslo.
TRL (2001): UK town study: Gloucester Safer City Project. Deliverable from the EC DUMAS project.
TØI, (2001): National travel surveillance 2001, Transport Economic Institute, Oslo, Norway.
YTV (1999): Helsinki Metropolitan Area Transport System Plan PLJ 1998. Helsinki Metropolitan Area Council, Helsinki Metropolitan Area Series A1999:4, 25 p.
YTV (2001) : Liikkumisen nykytila (The Present-day Traffic Situation). Helsinki Metropolitan Area Council, Helsinki Metropolitan Area Series B2001:10, 24+3 p.
YTV (2002a) : Helsingin seudun nykytila (The Current State of the Helsinki Region). Helsinki Metropolitan Area Council, Helsinki Metropolitan Area Series B2002:1, 34 p.
YTV (2002b): Raide- ja ajoneuvoliikenteen verkkoselvitys (Network study of urban passenger transport) Helsinki Metropolitan Area Council, Helsinki Metropolitan Area Series B2002:5, 25 p.
YTV (2002c) : Matka-aikatutkimus v. 2001, (Travel time study 2001), Helsinki Metropolitan Area Council, Helsinki Metropolitan Area Series B2002:2, 42+8 p.
YTV (2002d): Pääkaupunkiseudun liikennejärjestelmäsuunnitelman vaikutusten arviointi (Impact Assessment of the Transport System Plan of Helsinki Metropolitan Area), Helsinki Metropolitan Area Council, Helsinki Metropolitan Area Series B2002:10 73+24 p.

12th International Symposium "Transport and Air Pollution" / 12e Colloque international "Transports et pollution de l'air", Avignon, 16 -18 *June* / juin 2003
proceedings / actes, n°92, tome / Vol. 1, Inrets ed., Arcueil, France, 2003, p. 233-240

Les enjeux de la pollution de l'air des transports

Robert Joumard
INRETS, case 24, 69765 Bron cedex, France. joumard@inrets.fr

Résumé
Au vu notamment de l'évolution de la qualité de l'air telle que mesurée en France et dans l'Union Européenne au cours des dix dernières années, de l'évolution des émissions de polluants atmosphériques des transports routiers en France, telle que calculée sur la période 1970-2020, et de l'évolution de la perception sociale du thème de la pollution de l'air, on évalue quels polluants sont les plus problématiques aujourd'hui et demain. Il s'agit en tout premier lieu du gaz carbonique et secondairement des oxydes d'azote et particules fines. On évalue ensuite les enjeux en termes de développement technologique et de gestion de la demande et de l'offre de transport. Ces enjeux sociétaux permettent de proposer des axes de recherche dans le champ de la pollution de l'air.
Mots-clefs : *pollution de l'air, transports, émissions, qualité de l'air, enjeux, technologie.*

Abstract
The stakes of air pollution in the transport sector.
According to the evolution of the air quality, as measured in France and in the European Union during the 90's, to the evolution of the pollutant emissions of the road transport in France, as calculated on the period 1970-2020, and to the evolution of the public concern regarding air pollution and environment, the main pollutants are listed for today and tomorrow. They are first the carbon dioxide, and then the nitrogen oxides and fine particulates. The stakes in terms of technology and transport demand/offer policy are assessed. These society stakes allow us to propose some research axes in the field of air pollution, which answer the present stakes and not the former ones.
Keys-words*: air pollution, transport, emissions, air quality, stake, technology.*

Introduction

Une spécificité de la recherche en pollution de l'air et plus généralement en environnement est que les thèmes traités dépendent fortement de la demande sociale. Il en a été ainsi pour la recherche sur les pluies acides puis sur l'effet de serre, ou sur la visibilité au dessus des agglomérations en Amérique du Nord. Aussi les axes proposés par les chercheurs ne peuvent-ils être déduits du seul questionnement scientifique (comprendre ce qu'on ne comprend pas), mais doivent tenir compte des enjeux publics du domaine. Dans celui de la pollution de l'air des transports, l'évolution de la qualité de l'air comme celle des émissions, qui a l'avantage de pouvoir être extrapollée de manière assez fiable à un horizon d'une vingtaine d'années, sont riches d'enseignements. Nous allons, essentiellement à partir du cas français, guère différent de celui de l'Union Européenne, tenter de pointer les enjeux actuels et futurs de la pollution de l'air, et par conséquent les thèmes de recherche prioritaires.

1 - Évolution de la qualité de l'air et des émissions routières

Qualité de l'air

Nous disposons maintenant d'une suite assez longue de mesures de la qualité de l'air dans des conditions comparables pour pouvoir apprécier de manière assez précise son évolution : plus de quatre décennies pour le dioxyde de soufre SO_2 et les fumées noires, une quinzaine d'années pour la

plupart des polluants, mais un peu moins pour l'ozone O_3 (Airparif, 1999, Fangeat et coll., 2003).

Ainsi dans la région parisienne le SO_2 a vu ses concentrations baisser d'un facteur proche de vingt depuis les années 50. Les teneurs en monoxyde de carbone CO et hydrocarbures totaux HC ont diminué d'un facteur proche de quatre depuis dix ans, tandis que les concentrations en fumées noires ont baissé de près de 80 % durant les années 50 à 80 avant de se stabiliser. Les teneurs en PM10 semblent avoir baissé aussi fortement. Les concentrations en dioxydes d'azote NO_2 sont restées assez stables au cours des années 90 et semblent diminuer depuis quelques années ; le phénomène semble plus marqué pour la pollution azotée urbaine de pointe. Le gaz carbonique CO_2 voit en revanche ses concentrations augmenter. Enfin les concentrations d'ozone ne connaissent pas d'évolution significative depuis dix ans ; cependant si les moyennes n'évoluent guère, la médiane des moyennes annuelles a tendance à augmenter. Cela pourrait traduire une extension géographique des épisodes de pollution photochimique dont les nuages s'étendent souvent sur des milliers de kilomètres.

On peut donc considérer que la qualité de l'air s'est globalement améliorée, mais pas systématiquement. Cette appréciation ne correspond toutefois pas à la perception du public, qui considère en majorité, tout au moins en France, que la qualité de l'air n'a jamais été aussi mauvaise et problématique. L'environnement est en effet essentiellement une construction personnelle, basée sur la perception personnelle de ses enjeux, au travers de notre perception par nos sens (la vue, l'odorat) à laquelle viennent s'ajouter des éléments intellectuels issus des informations techniques ou scientifiques que nous recevons par le biais du système éducatif et des média (van Staëvel, 2000).

Cette construction personnelle est ensuite structurée par la vision du long terme. Ainsi pour 65 % des Français au XXIe siècle le progrès technique sera mis au service d'un développement durable (Maresca & Hebel, 1999) qui consiste à transmettre aux générations futures un environnement viable et une nature qui ne soit pas un désert. La population étant beaucoup plus consciente aujourd'hui qu'hier des enjeux environnementaux et des risques de la pollution, la pollution de l'air considérée comme une préoccupation environnementale s'est donc détériorée, malgré une relative baisse des concentrations.

Émissions

Si les transports jouent un rôle mineur dans les émissions de SO_2, leur contribution est proche du tiers pour le gaz carbonique et proche des deux tiers pour CO, NOx et les précurseurs de la pollution photochimique, avec de fortes disparités régionales. Or globalement, le transport connaît une forte croissance (European Communities, 2002) : dans l'Union européenne, tous modes confondus, les transports de passagers – exprimés en passager-kilomètre – ont crû respectivement de 3,2 puis 1,8 % par an durant les années 70-80 puis 90, avec des chiffres très proches pour le seul transport routier. Et avec une progression de 6 % par an depuis 1970, l'augmentation du transport aérien est encore plus forte. Cela correspond au cours des années 90 à un doublement du trafic tous les 42 ans pour le transport routier et tous les 12 ans pour l'aérien.

Parallèlement, tous modes confondus, les transports de marchandises – exprimés en tonne-kilomètre – ont crû de 2,8 % par an au cours des trois dernières décennies du siècle, et de 3,5 % pour le seul transport routier, ce qui correspond respectivement à un doublement du trafic tous les 27 et 20 ans.

Évolution positive mais contrastée de la qualité de l'air, forte croissance simultanée des trafics et des préoccupations environnementales : il est utile de s'intéresser de près à l'évolution des émissions de polluants pour évaluer les conséquences de l'augmentation du trafic et des améliorations technologiques sur la qualité de l'air. Cette évaluation a été réalisée pour le cas français grâce au modèle européen d'inventaire Copert 3 (Hickman et coll., 1999). Ce modèle utilise des facteurs d'émissions issus de mesures jusqu'aux véhicules respectant la norme Euro 2 applicable jusqu'à fin 2000. Au-delà, les facteurs d'émissions tiennent compte des normes d'émissions Euro 3 et Euro 4, cette dernière s'appliquant à partir de 2006. En l'absence de projet solide plus lointain, aucune hypothèse de norme ultérieure n'a été introduite. Les technologies innovantes comme les filtres à particules, hybrides ou piles à combustibles n'ont pas été spécifiquement prises en compte, ni les auxiliaires comme la climatisation. Les projections du trafic routier à l'horizon 2020 sont issues du

scénario médian (B) du ministère français des transports (SES, 1998).

Les résultats (Lacour et Joumard, 2002 - cf. figure 1) montrent qu'après une quasi stagnation au cours des années 70 et 80, les émissions de CO et d'HC connaissent une chute d'un facteur proche de trois en dix ans. Cette tendance très positive devrait se poursuivre dans les années à venir. Elle est due à l'introduction des catalyseurs trois voies sur les véhicules à essence et à la diésélisation du parc des véhicules légers qui émettent moins de CO et d'HC. Rappelons que, depuis plusieurs années, près d'une voiture particulière sur deux vendue en France est une diesel.

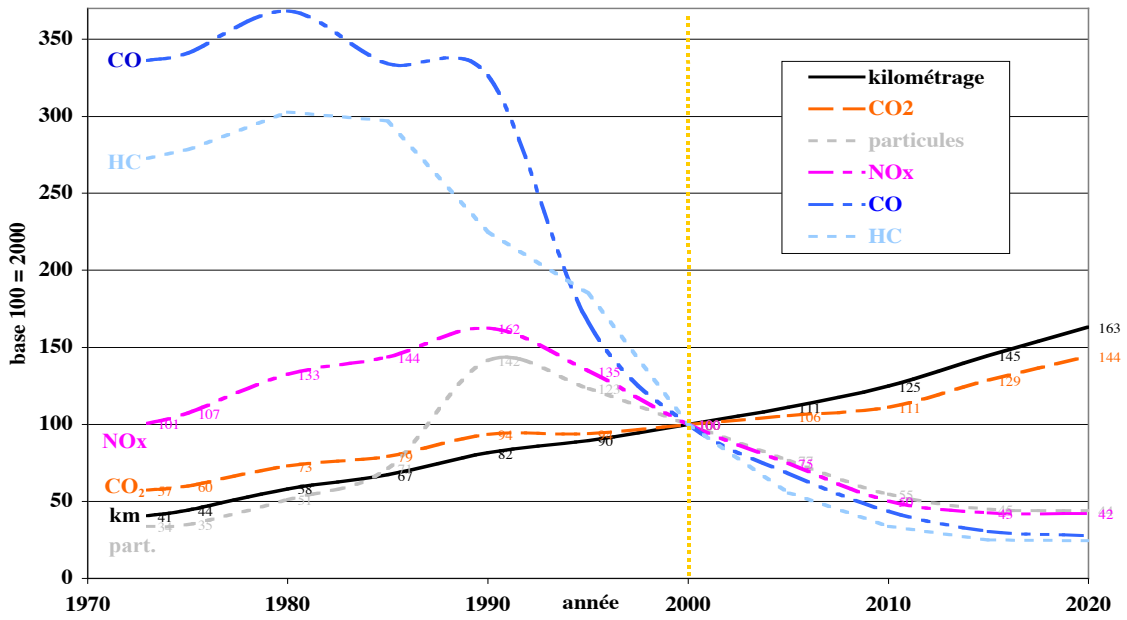

Figure 1 : Évolution relative par rapport à 2000 des émissions massiques de l'ensemble du trafic routier français de 1973 à 2020. Base 100 = année 2000.

Figure 1: Relative evolution according to 2000 figures of the emissions of the French road traffic from 1973 to 2020. Base 100 = year 2000.

Les NOx et les particules poursuivent une évolution quelque peu différente : ils augmentent jusqu'au milieu des années 1990 (les particules sont multipliées par quatre en vingt ans), puis ils diminuent de près d'un tiers, une tendance qui devrait se confirmer. Des effets s'exerçant en sens inverse se combinent pour expliquer cette configuration : croissance des trafics, diésélisation – un diesel émet trois fois plus de NOx qu'un véhicule à essence catalysé – et pots catalytiques très efficaces. L'évolution future devrait être encore plus marquée pour les particules, en raison de l'introduction progressive des filtres à l'efficacité très élevée, dont on n'a pas tenu compte. Pour ces deux polluants, les émissions des 2-roues sont tout à fait négligeables, et les poids lourds émettent respectivement 37 et 22 % du total en 2000.

La situation est en revanche particulièrement préoccupante pour le CO_2, principal gaz à effet de serre. Ses émissions ont progressé de 75 % de 1973 à 2000, et devraient croître de près de 50 % à l'horizon 2020. Cette prévision ne tient pas compte de l'introduction éventuelle de technologies peu consommatrices d'énergie fossile comme pourraient l'être les voitures hybrides ou les voitures à piles à combustible. Elle ne tient pas non plus compte de la climatisation qui équipe la plupart des véhicules vendus aujourd'hui et qui se traduit par 10 % de CO_2 supplémentaire, et jusqu'à deux fois plus d'émissions des autres polluants (Barbusse et coll., 1998 ; Ademe, 1999).

Si, mis à part le CO_2, les évolutions sont favorables pour tous les polluants, les émissions de l'ensemble des transports sont néanmoins encore très supérieures à leurs niveaux de la première moitié du XXe siècle : l'Office suisse de l'environnement (OFEFP, 1995) a montré que les émissions sont aujourd'hui près de cinq fois supérieures pour le CO et les HC, et respectivement dix et douze fois supérieures pour le CO_2 et les NOx que durant la première moitié du XXe siècle, ces facteurs

atteignant respectivement 50, 10 et 20 par rapport à 1900.

2 - Enjeux technologiques

Émissions unitaires

L'émission de CO_2 croissant légèrement moins que le trafic, cela signifie que les émissions unitaires diminuent en moyenne. On voit Figure 2 que c'est la cas pour les véhicules légers dont le facteur d'émission agrégé est passé de 273 g/km en 1973 à 215 en 2000 : cette évolution est la combinaison de l'amélioration bien plus significative de la technologie moteur et de l'accroissement parallèle des masse, puissance et éléments de confort des véhicules qui jouent en sens contraire. Les émissions et consommations unitaires moyennes ont en revanche augmenté pour les 2-roues motorisés, passant de 83 à 99 g/km en 27 ans grâce à l'extension des motos puissantes qui remplacent de fait partiellement les cyclomoteurs. De même les émissions des poids lourds augmentent, passant de 935 à 1002 g/km de 1973 à 2000, cette croissance devant se poursuivre à un rythme plus modéré dans l'avenir.

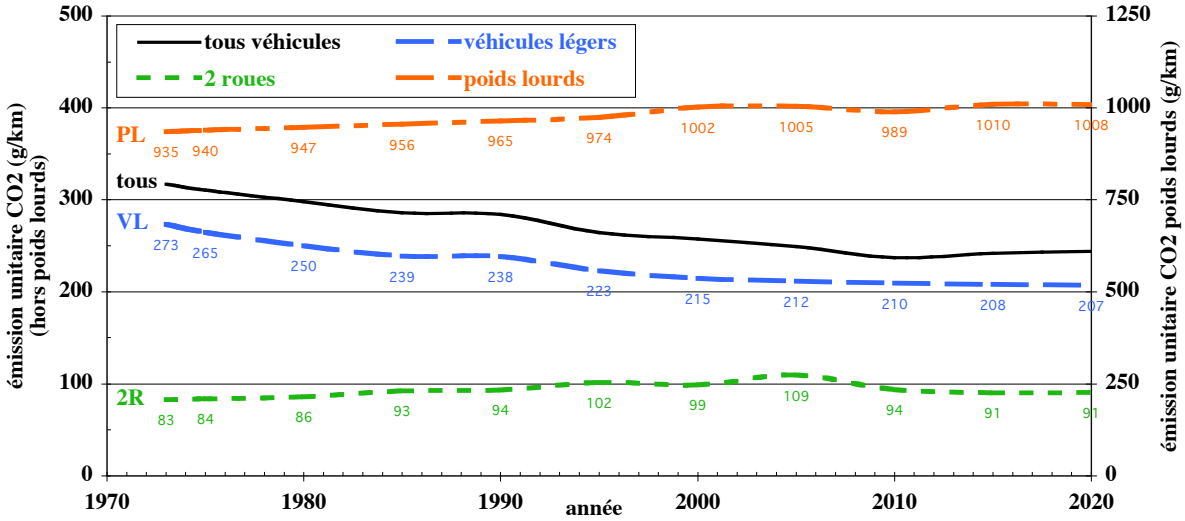

Figure 2 : Évolution des facteurs d'émission moyens de CO_2 par type de véhicule routier.

Figure 2: Evolution of the average CO_2 emission factors per vehicle type.

La situation est plus favorable pour les NOx, dont le facteur d'émission moyen des véhicules légers (essence et diesel confondus) a été divisé par plus de deux depuis les années 1970 et devrait l'être encore par un facteur proche de quatre d'ici 2020. Pour les poids lourds, bus et cars, le facteur d'émission n'a diminué que d'un tiers et devrait être encore divisé d'un facteur proche de trois dans les 20 prochaines années. Les 2-roues motorisés voient en revanche leur facteur d'émission augmenter : il a plus que doublé depuis 30 ans mais reste encore neuf fois inférieur à celui des voitures ; à l'horizon 2020 il devrait cependant leur être à peine inférieur.

Technologies

Le principal enjeu concerne la réduction des émissions unitaires de gaz carbonique des véhicules légers, des motos et des poids lourds, et la poursuite de la réduction des oxydes d'azote et des particules fines émises par les diesel légers et lourds, sans pour autant augmenter les émissions des autres polluants. Ces réductions sont à considérer sur l'ensemble du cycle de vie des véhicules, et même des infrastructures, à tout le moins en intégrant la chaîne de production énergétique et les usages réels des véhicules.

Les constructeurs européens d'automobiles se sont engagés à diminuer les consommations et les émissions unitaires moyennes de CO_2 des voitures particulières neuves de 21 % entre 1995 et 2008 (accord ACEA), essence et diesel confondus. Mais cet accord ne tient pas compte de la climatisation automobile. Outre ses effets négatifs sur les émissions de CO_2 et des autres gaz d'échappement, la

climatisation souffre de fuites de fluides frigorigènes qui sont de puissants gaz à effet de serre. Elle pourrait ruiner dix ans d'effort sur la réduction des consommations de carburant d'une part, et fortement modérer les évolutions positives ou très positives attendues pour les autres polluants. En prenant en compte les fuites de fluides frigorigène, l'Ademe estime que l'accord ACEA n'engendrera pas comme prévu une diminution de 2 % des émissions de gaz à effet de serre des voitures particulières, mais une augmentation de 8 % de 1995 à 2020 (Ademe, 1999). Les améliorations technologiques se doivent donc d'être majeures pour que cette demande de confort ne se traduise pas par une pollution locale et par une augmentation significative de l'effet de serre. Pour stimuler ces améliorations, sans doute serait-il efficace d'intégrer la climatisation aux normes d'émission et de consommation de carburant, ce qui n'est pas le cas aujourd'hui en Europe.

Plusieurs technologies sont ou seront en mesure de diminuer les émissions polluantes.

La substitution de carburants. La diésélisation de la gamme entraînerait une diminution probable du CO_2 de 10 à 20 %. L'utilisation de gaz de pétrole liquéfié (GPL) ou de gaz naturel permettrait une réduction en CO_2 de 10 à 25 % vis à vis de l'essence mais serait légèrement pénalisante par rapport au gazole (IEA, 1999).

Le filtre pour les véhicules diesel retient les particules en sortie d'échappement, mais se colmate progressivement. Il est donc indispensable de le régénérer périodiquement, ce qui semble enfin réglé de manière fiable (Barbusse & Plassat, 2002). Une grande partie des bus et poids lourds en circulation ainsi que les véhicules neufs peuvent ainsi être équipés de filtres dont la tenue est garantie dans le temps. Selon un nombre significatif d'études indépendantes, les réductions d'émissions touchent l'ensemble des particules, notamment les plus fines qui sont les plus dangereuses pour la santé, avec une efficacité allant de 90 à 99,9 %. Pour les voitures particulières, le seul système commercialisé aujourd'hui équipe progressivement les véhicules neufs du groupe Peugeot-Citroën. Il exige une injection directe avec une rampe commune et l'utilisation d'un additif à base de cérium. Lors de la courte régénération du filtre tous les 700 km environ, les émissions augmentent de 10 à 100 % pour les gaz et d'un facteur 30 pour les particules. Le bilan est donc très positif pour les émissions à l'échappement, ainsi que pour le cérium qui est entièrement récupéré sur le filtre. Les autres marques vont suivre : Ford et Renault l'annoncent pour 2003, le filtre de ce dernier n'utilisant pas d'additif mais un catalyseur, avec une efficacité équivalente. Les diesels équipés devraient donc émettre moins de particules que les véhicules essence.

L'injection directe essence vise à améliorer le rendement du moteur en injectant le carburant directement dans la chambre de combustion et non plus dans la tubulure d'admission du moteur essence ou dans la préchambre pour les diesel. Utilisée très largement pour les diesel, cette technologie semble prometteuse pour les moteurs essence bien que les premières mises sur le marché ne montrent qu'un gain modeste en consommation et une augmentation des émissions de particules. A terme, on en attend un gain en consommation de 10 à 15 %.

La *suralimentation par turbo-compression* consiste à comprimer l'air de combustion. Cela permet d'injecter un volume supérieur de carburant à volume de cylindre égal et donc d'augmenter la puissance du véhicule. Les développements futurs visent pour les véhicules essence à utiliser la turbo-suralimentation pour diminuer la cylindrée sans augmentation de puissance. En conditions urbaines la consommation étant pratiquement proportionnelle à la cylindrée, cela permet de diminuer la consommation.

La voiture électrique. Les moteurs électriques ont un rendement énergétique deux fois supérieur par rapport aux moteur thermiques : de l'ordre de 90% contre 35 à 40%. En outre, le rendement des moteurs thermiques dépend des conditions de conduite, ce qui n'est pas le cas des moteurs électriques. Deux voies principales sont actuellement en cours pour introduire la voiture électrique : les véhicules hybrides et les piles à combustible (Yonnet & Badin, 2002).

L'introduction de *véhicules hybrides* qui associent une chaîne de transmission essence et une chaîne de transmission électrique vise à compenser les défauts du moteur thermique. Le but est de stocker dans les batteries de la chaîne électrique l'énergie des freinages qui dans un moteur classique est

perdue. Il est aussi possible de charger les batteries en faisant tourner le moteur thermique à la vitesse qui garantit son meilleur rendement, ce qui est rarement le cas dans la circulation en ville. Gain de 30 % en ville, mais nul sur autoroute (Jeanneret et coll., 1999).

Les *piles à combustible* constituent une piste pour une voiture entièrement électrique. Elle convertit l'énergie chimique de l'hydrogène et de l'oxygène directement en électricité. Lorsque le véhicule consomme de l'hydrogène, les émissions locales sont nulles ; mais seul est significatif un bilan prenant en compte la filière de production de l'hydrogène, qui y joue un rôle majeur. Ce bilan du puits à la roue des voitures propulsées par pile à combustible fait apparaître aujourd'hui un gain proche de 30 % (si l'on considère de l'hydrogène comprimé obtenu à partir de gaz naturel en Union européenne), mais qui pourrait être annulé en une dizaine d'années par les progrès des technologies classiques (Antoine et coll., 2003).

3 - Enjeux de mobilité

Les gaz à effet de serre devraient rester un enjeu majeur, et même de plus en plus préoccupant, car les améliorations technologiques ne compensent pas la demande croissante de confort, fortement consommatrice d'énergie, combinée à la croissance des trafics. L'OCDE estime que même l'introduction accélérée des véhicules hybrides et des piles à combustible ne devrait pas suffire pour aller vers des transports écologiquement viables à l'horizon 2050 (Wiederkehr, 2000). Seuls 40 % de l'effort nécessaire devrait porter sur la technologie, les 60 % restants devant se concentrer sur la gestion de la demande de transport et l'adoption de modes de transports plus durables. Cela implique d'importants transferts modaux vers des modes moins polluants comme la marche, le vélo et les transports en commun terrestres et, surtout, une maîtrise de la demande de mobilité des personnes et des biens.

Certains considèrent que la demande de transport n'existe pas en elle-même et qu'elle découle des infrastructures ; en d'autres termes, c'est le trafic qui s'adapterait à l'offre en infrastructures. Au moins à moyen terme, l'effort devrait donc porter sur la maîtrise des infrastructures. Toutes ces orientations ne peuvent se réaliser sans une forte volonté politique.

Aussi la place de l'environnement et des problématiques de la pollution atmosphérique dans le processus de décision s'est-elle modifiée. La première prise en compte de l'environnement s'est faite au travers des études d'impact (EIA) qui avaient pour objectif d'évaluer l'impact sur l'environnement d'un projet, pour éventuellement introduire des mesures correctives, mais sans en remettre en cause la décision de principe. Les études environnementales stratégiques (SEA) interviennent maintenant dès la conception du projet et avant que la décision de principe ne soit prise. L'environnement acquiert ainsi un rôle stratégique car c'est un des éléments de la décision au même titre que les aspects techniques ou économiques. Dans la mesure où les aspects environnementaux et économiques (mais aussi sociaux) sont également pris en compte lors de la prise de décision, on peut alors réellement parler d'une approche intégrant le concept de développement durable. C'est aujourd'hui plus un objectif qu'une réalité car si les aspects environnementaux sont toujours pris en considération, les impacts à long terme ne sont guère qu'évoqués et la décision est le plus souvent prise en considérant prioritairement les arguments économiques.

4 - Enjeux de recherche

Au delà de la recherche fondamentale dont la nécessité demeure mais qui participe peu à la recherche en pollution de l'air dans le domaine des transports, l'essentiel de la recherche du domaine est finalisée, c'est à dire vise explicitement à contribuer à diminuer les impacts des transports par le biais de gaz ou particules atmosphériques. Cela demande de comprendre les mécanismes psycho-sociologiques qui sont à la base de la perception des nuisances, les mécanismes physiques, chimiques ou biologiques des impacts de la pollution sur différents milieux dont l'homme, ceux des émissions (de l'énergétique à l'économie des transports), et enfin les mécanismes politiques de la

décision. Les problématiques de cette recherche sont donc directement liées à la nature des impacts et à l'importance des enjeux.

La problématique de la pollution de l'air des transports n'est plus celle des années 70 ou des années 90 et le sera encore moins dans dix ou vingt ans, lorsque les résultats des recherches initiées aujourd'hui auront été appliqués. Nous devrions donc privilégier les polluants, les impacts et la mise au point des outils qui sont au coeur des enjeux majeurs et laisser progressivement de coté les autres thèmes, même si les incertitudes invitent à la prudence en menant une veille très active.

En termes de polluants, les gaz à effet de serre et notamment le gaz carbonique et donc la consommation d'énergie fossile devraient être prioritaires ; en second lieu les NOx et les précurseurs du smog photochimique car son évolution n'est guère positive ; en troisième lieu les particules fines en attendant la confirmation de la quasi disparition des émissions des diesels.

En termes d'impacts, l'effet de serre est sans conteste l'enjeu majeur. Il convient donc d'affiner nos connaissances, notamment quant à une prise en compte d'un nombre élargi de polluants dont l'effet peut varier selon leur lieu d'émission. Le second impact, en terme d'importance, est sans doute la pollution sensible (odeurs, fumées, salissures) qui fait l'objet de fort peu de recherches bien que toutes les enquêtes montrent que c'est une nuisance essentielle pour la population ; la décroissance des émissions de fumées vient cependant pondérer ce propos. Ensuite, on peut citer la pollution photochimique qui diminue moins que ses précurseurs, ce qui est quelque peu étonnant, puis les impacts sur la faune et la flore. Enfin le problème des synergies entre impacts n'est encore guère abordé, entre différents aspects de la pollution de l'air ou différents impacts sur l'environnement.

En termes d'outils, on peut distinguer les outils d'émissions et les outils d'aide à la décision. Pour les émissions, les aspects macroscopiques devraient être prioritaires en suivant une approche de type cycle de vie du service transport. Celle-ci doit intégrer les émissions issues de la production, de l'usage et de la destruction des infrastructures, des énergies et des véhicules. Les aspects socio-économiques sont essentiels car, à coté de la quasi stabilité des consommations unitaires, la croissance des trafics et sa relation avec la croissance économique posent problème.

Pour les outils d'aide à la décision, on ne peut se contenter d'une approche analytique, chère au monde scientifique, mais qui ne permet pas de répondre clairement et simplement, c'est à dire de manière agrégée, aux questions simples que se posent les décideurs comme les citoyens. Il est en particulier urgent d'agréger les différents impacts formant la pollution de l'air, de la pollution sensible à l'effet de serre en passant par le smog photochimique, et même souvent d'avoir une approche systémique de l'environnement, pour laquelle le concept de développement durable semble prometteur. Cette approche serait favorisée par une culture commune des chercheurs vis à vis de l'ensemble des aspects de la pollution de l'air des transports voire de l'environnement et des transports.

Conclusion

Les incertitudes quant aux évolutions des concentrations des différents polluants sont encore importantes car l'historique est encore limité, et même très limité pour les très nombreux polluants qui ne sont pas réglementés. Certains pourraient même se révéler bientôt, comme le gaz carbonique s'est transformé en quelques années de gaz inerte en polluant majeur. Les incertitudes sont au moins aussi grandes pour les inventaires d'émissions, pour les polluants non réglementés mais aussi parce que l'on a pu négliger une source importante d'émission, comme cela semble être le cas aujourd'hui pour la climatisation automobile.

Il convient donc d'être prudent quant aux conclusions et aux axes de recherche. En particulier il serait sûrement peu sage d'abandonner des thèmes de recherche qui pourraient s'avérer importants dans quelques années, contrairement à l'impression actuelle. Il reste cependant quelques axes forts, indubitables, qui tournent autour de la problématique de l'effet de serre, que l'on commence à comprendre mais que l'on ne sait régler. Au delà, les approches systémiques de la pollution de l'air et du couple environnement-transport semblent intéressantes. Elles devraient mieux répondre à la

problématique du développement durable que les approches actuelles essentiellement analytiques.

Cette analyse est basée sur les réalités ouest-européennes, qui peuvent être fort différentes en Europe de l'est et dans les pays émergents ou en développement. On ne peut donc en extrapoller les conclusions sans analyse.

Remerciements

Les auteurs remercient tout particulièrement le Ministère de l'environnement et du développement durable et l'Ademe pour leur soutien financier à une partie de cette recherche.

Références

Ademe (1999) : Impact comparé de la mise en place de l'accord ACEA et de pénétration de la climatisation automobile. Note Ademe, Paris, 27 mai 1999, 11 p.

Airparif (1999) : Les tendances de la pollution de l'air en Île-de-France. Airparif actualité, juin, Paris, 6p.

Antoine L., E. Martorana & F. Badin (2003) : Hydrogène : du puits à la roue. Rapport Inrets, Bron, France, n°LTE 03nn, 220 p.

Barbusse S, D. Clodic & J.P. Roumégoux (1998) : Climatisation automobile, énergie et environnement. Rech. Transp. Sécurité, n°60, p. 3-18.

Barbusse S. & G. Plassat (2002) : Les particules de combustion automobile et leurs dispositifs d'élimination. Rapport Ademe, Paris, 42 p.

European Communities (2002): EU energy and transport in figures, statistical pocketbook 2002. EC, Luxembourg, 207 p.

Fangeat E., J. Colosio & R. Stroebel (2003) : Évolution de la qualité de l'air. Poll. Atmos., à paraître.

Hickman J., D. Hassel, R. Joumard, Z. Samaras & S. Sorenson (1999): Meet - Methodology for calculating transport emissions and energy consumption. European Commission, DG VII, ISBN 92-828-6785-4, Luxembourg, 362 p.
http://vergina.eng.auth.gr/mech/lat/ ou www.inrets.fr/infos/cost319/index.html

IEA (1999): Automotive fuels for the future. Int. Energy Ag. report, Paris, 92 p.

Jeanneret B., F. Harel, F. Badin, R. Trigui, F. Damemme & J. Lavy (1999) : Évaluation des performances du véhicule Toyota Prius. 4e conf. C-VELEC, Grenoble, 3-4 nov. 1999, INPG, Grenoble, France, p. 168-178.

Lacour S. & R. Joumard (2002) : parc, usage et émissions des véhicules routiers en France de 1970 à 2020. Rapport Inrets, Bron, France, n°LTE 0208, 89 p.

Maresca B. & P. Hebel (1999) : L'environnement, ce qu'en disent les Français. Doc. Française, Paris, 218 p.

OFEFP (1995) : Émissions polluantes dues à l'activité humaine en Suisse de 1900 à 2010. Cahier de l'Environnement, n°256, 122 p.

SES (1998) : Les données détaillées du SES - le marché des véhicules. Ministère des transports, DAEI-SES, Paris, 1998.

van Staëvel E. (2000) : Cultures environnementales contemporaines et pollution. Rencontres européennes pour une histoire de l'environnement, Clermond-Ferrand, France, 4-6 mai 2000.

Wiederkehr P. (1999): Environmentally sustainable transport: report on phase II of the OECD EST project. OECD report, ENV/EPOC/PPC/T(97)1/final, Paris, 100 p.

Yonnet JP. & F. Badin (éd.) (2002) : Véhicules électriques et hybrides, enjeux technologiques et perspectives. 5e colloque C-VELEC, Grenoble, 25-26 juin 2002, actes Inrets, n°84, Bron, France, 200p.